

Fluorescence tagging of herpes simplex virus type 1 proteins by mutagenesis of a bacterial artificial chromosome

Von der naturwissenschaftlichen Fakultät der
Gottfried Wilhelm Leibniz Universität Hannover
zur Erlangung des Grades

Doktor der Naturwissenschaften
Dr. rer. nat.

genehmigte Dissertation

von

Claus-Henning Nagel
Diplom-Biochemiker

geboren am 13.02.1977 in Hannover

2006

Referentin: HD Dr. Beate Sodeik

Korreferent: PD Dr. Gert Zimmer

Tag der Promotion: 14.07.2006

„Die Einsicht oder Ansicht, daß das Vollkommene und die Wissenschaft Stückwerk ist, darf niemand daran hindern, doch stets weiterzubauen und eben doch das Mögliche zu erreichen.“

Hermann Hesse

(Lektüre für Minuten. Auswahl und zus. v. Volker Michels. Suhrkamp, Frankfurt/M., 1971, 1997)

Für Omi

Contents

| | |
|---|------------|
| Danksagung | 5 |
| Abbreviations | 6 |
| Abstract | 8 |
| Zusammenfassung | 9 |
| 1. Introduction | 10 |
| 1.1. Herpesviruses..... | 10 |
| 1.2. Herpes simplex virus type 1..... | 11 |
| 1.3. HSV1 replication..... | 17 |
| 1.4. Mutagenesis of herpesviruses..... | 24 |
| 1.5. Aim of the thesis..... | 40 |
| 2. Materials | 41 |
| 2.1. Laboratory equipment..... | 41 |
| 2.2. Microscopes | 42 |
| 2.3. Consumables..... | 42 |
| 2.4. Kits..... | 42 |
| 2.5. Chemicals..... | 43 |
| 2.6. Electrophoresis standards | 46 |
| 2.7. Enzymes..... | 46 |
| 2.8. Media and solutions..... | 47 |
| 2.9. Antibodies..... | 49 |
| 2.10. Oligonucleotides..... | 49 |
| 2.11. Organisms and plasmids | 51 |
| 3. Methods | 59 |
| 3.1. Eukaryotic cell culture..... | 59 |
| 3.2. Virological techniques..... | 59 |
| 3.3. Molecular biological techniques..... | 64 |
| 3.4. BAC mutagenesis..... | 70 |
| 3.5. Transfection of eukaryotic cells | 72 |
| 3.6. Light microscopy..... | 73 |
| 3.7. SDS-PAGE and Western-blotting | 73 |
| 4. Results | 75 |
| 4.1. Cloning of HSV1(17 ⁺) as a BAC | 75 |
| 4.2. Tagging of VP26 with a fluorescent protein | 95 |
| 4.3. Tagging of HSV1-gD with a fluorescent protein..... | 126 |
| 5. Discussion | 134 |
| 5.1. BAC-Cloning of HSV1 | 134 |
| 5.2. HSV1 encoding a fluorescence-tagged VP26 | 141 |
| 5.3. Dual coloured HSV1 virions..... | 147 |
| 5.4. Outlook | 149 |
| 6. Literature | 151 |
| Lebenslauf | 164 |
| Publikationen | 165 |
| Erklärung zur Dissertation | 166 |

Danksagung

Viele Personen haben zum Gelingen dieser Doktorarbeit maßgeblich beigetragen oder mir die Arbeit erleichtert. Allen, die diese Arbeit Korrektur gelesen haben, sei an dieser Stelle nochmals gedankt.

Ich danke PD Dr. Beate Sodeik für die Begutachtung dieser Arbeit und ihre professionelle Betreuung während dieses herausfordernden Projektes. Ihr persönlicher Einsatz, ihre Anerkennung von Erfolgen und ihr Ansporn bei Rückschlägen haben mir sehr geholfen, auch den einen oder anderen Fehler meinerseits als lehrreich hinzunehmen. In vielen Diskussionen konnte ich eine große Einsicht in wissenschaftliche Denk- und Arbeitsweisen erlangen.

Ich bedanke mich bei PD Dr. Gert Zimmer für die Übernahme des Korreferates dieser Arbeit.

Prof. Martin Messerle und Dr. Eva Borst waren und sind mir als Experte und Expertin auf dem Gebiet der BAC-Mutagenese stets zur Hilfe. In vielen Diskussionen konnte ich eine Menge lernen. Ihnen gilt mein Dank, ebenso Nadine Mütter, mit der ich die gemeinsamen Erfahrungen auf dem Gebiet der HSV1-BAC-Mutagenese austauschen konnte.

Ich habe im Jahre 2002 dieses Projekt von Dr. Tanja Strive übernommen und konnte nahtlos an ihre Vorarbeiten anknüpfen, somit trug auch sie einen erheblichen Anteil zum Gelingen dieser Arbeit bei.

Dank an alle Kollegen, die mir wertvolle Informationen und Reagenzien zur Verfügung gestellt haben.

Vielen Dank an Mojgan Fathollahy für ihre Hilfe bei der täglichen molekularbiologischen Routine- und Kniffelarbeit, ebenso an Heidi Pommer für den freundlichen Sequenzierungsservice. Danke an Ute Prank für ihre gewissenhafte Pflege der Zellkultur und ihre Hilfe im Laboralltag.

Meinen vielen Kolleginnen und den wenigen Kollegen aus dem Sodeik-Labor sei für die herzliche und erfrischende Arbeitsatmosphäre gedankt. Es macht Spaß, mit Euch zu arbeiten! In Zukunft gibt es auch wieder mehr Laborstammtische, versprochen!

Allen Kolleginnen und Kollegen des Instituts für Virologie der MHH danke ich für das kooperative und kollegiale Arbeitsklima.

Ich danke meinen lieben Eltern und meiner Familie für ihre stete Unterstützung, die ich während meines Studiums und meiner Doktorarbeit erfahren habe.

Danke Wibke, dass Du immer für mich da bist!

Abbreviations

Amino acids and nucleic acids are abbreviated as proposed by the IUPAC-IUB Joint Commission on Biochemical Nomenclature (JCBN).

| | |
|------------------|---|
| % (w/v) | weight per volume |
| % (v/v) | volume per volume |
| aa | amino acid |
| AdV | adenovirus |
| Amp ^R | ampicillin resistance |
| app. | approximately |
| ATP | adenosinetriphosphate |
| BAC | bacterial artificial chromosome |
| BHV | bovine herpesvirus |
| bla | β-lactamase (Amp ^R) |
| bp | basepair(s) |
| cat | chloramphenicol acetyl transferase (Cm ^R) |
| CFP | cyan fluorescent protein |
| Cm ^R | chloramphenicol resistance |
| (H)CMV | (human) cytomegalovirus |
| CPE | cytopathic effect |
| Da | Dalton |
| dATP | desoxyadenosinetriphosphate |
| dCTP | desoxycytidinetriphosphate |
| dGTP | desoxyguanosinetriphosphate |
| DIG | dioxygenin |
| DMSO | dimethyl sulfoxide |
| DNA | desoxyribonucleic acid |
| DR | direct repeat |
| dsDNA | double-stranded DNA |
| dTTP | desoxythymidinetriphosphate |
| e.g. | <i>exempli gratia</i> (for example) |
| EBV | Epstein-Barr virus |
| ER | endoplasmic reticulum |
| FCS | fetal calf serum |
| FITC | fluorescein thioisocyanate |
| FP | fluorescent protein |

Abbreviations

| | |
|-------------------|---|
| GFP | green fluorescent protein |
| gX | glycoprotein X |
| HHV | human herpesvirus |
| HIV | human immunodeficiency virus |
| HSV | herpes simplex virus |
| ICP | infected cell protein |
| i.e. | <i>id est</i> (that is to say) |
| Kan ^R | kanamycin resistance |
| kbp | kilobasepair(s) |
| kDa | Kilodalton |
| KSHV | Kaposi's sarcoma-associated herpesvirus |
| LRSC | lissamine-rhodamine sulfonyl chloride |
| Mbp | megabasepair(s) |
| MOI | multiplicity of infection |
| MT | microtubule(s) |
| MTOC | microtubule organising centre |
| MW _{app} | apparent molecular weight |
| nt | nucleotide(s) |
| ORF | open reading frame |
| PCR | polymerase chain reaction |
| pfu | plaque forming unit(s) |
| p.i. | post infection |
| PrV | pseudorabies virus |
| (m)RFP | (monomeric) red fluorescent protein |
| RNA | ribonucleic acid |
| RT | room temperature |
| Sm ^R | streptomycin resistance |
| ssDNA | single-stranded DNA |
| SV40 | simian virus 40 |
| Tet ^R | tetracyclin resistance |
| T _m | melting temperature |
| tk | thymidine kinase |
| UL | unique long region |
| US | unique short region |
| VP | viral protein |
| wt | wildtype |
| YFP | yellow fluorescent protein |

Abstract

Herpes simplex virus type 1 (HSV1) is a human pathogen, infects oral and perioral epithelia and establishes a life-long latency in the enervating neurons. Reactivation leads to recurrent infections of skin or mucosa.

In this study, the fully sequenced HSV1 strain 17⁺ was cloned as a bacterial artificial chromosome (BAC), providing a powerful tool to study virus-host interactions during the viral life cycle using HSV1 mutants constructed in *E. coli* by bacterial genetics.

Genes for the replication in *E. coli* as well as a eukaryotic β -galactosidase expression cassette and a single *loxP* site were introduced into the thymidine kinase locus (UL23) by homologous recombination in mammalian cells. After transferring circular replication intermediates into *E. coli* the BAC pHSV1(17⁺)blue was isolated. Restriction analyses revealed the integrity of the cloned viral genomes.

Next, a eukaryotic Cre recombinase expression cassette and a second *loxP* site were inserted into pHSV1(17⁺)blue in *E. coli* using the Red-recombination system of bacteriophage λ . After transfection of the resulting BAC pHSV1(17⁺)blueLox into eukaryotes, Cre excised the BAC sequences from the viral genome by site specific recombination. The efficiency of viral replication was reduced about fivefold in titer compared to HSV1(17⁺) wildtype.

The small capsid protein VP26 was N-terminally tagged with a fluorescent protein. However, most fluorescence tagged HSV1 variants constructed in *E. coli* by BAC mutagenesis were severely attenuated in growth or not viable. Marker rescue experiments and sequencing revealed that in a previously constructed HSV1-K26GFP, the four N-terminal amino acids of VP26 had been deleted. Fluorescence tagged VP26 BAC-mutants that were subsequently constructed without these amino acids were infectious and only slightly attenuated. Moreover, in immunofluorescence microscopy the fluorescence signal strongly colocalised with capsids, and GFPVP26 and RFPVP26 viruses were efficiently targeted to the nuclei of infected cells.

Furthermore the viral membrane protein gD was C-terminally labelled with a fluorescent protein, so the fate of capsids and the viral envelope during entry, assembly and egress of HSV1 can be monitored by fluorescence microscopy. The HSV1-BAC pHSV1(17⁺)blueLox will serve for the construction of specific HSV1 mutants for the study of virus-host interactions.

Keywords: herpes simplex virus, BAC mutagenesis, fluorescent proteins

Zusammenfassung

Das Humanpathogen Herpes-Simplex-Virus Typ 1 (HSV1) infiziert epitheliale Zellen der Mundschleimhaut oder der umgebenden Haut und ruft in den enervierenden Neuronen eine lebenslange latente Infektion hervor. Bei zeitweiser Reaktivierung kommt es zu erneuten Entzündungen der Mundgegend oder der Mundschleimhäute.

Im Rahmen dieser Doktorarbeit wurde der vollständig sequenzierte HSV1 Stamm 17⁺ als künstliches Bakterienchromosom (*bacterial artificial chromosome*, BAC) kloniert. So können Virusmutanten durch Anwendung bakteriengenetischer Methoden in *E. coli* konstruiert werden, um Virus-Wirts-Interaktionen im viralen Lebenszyklus zu untersuchen. Die für die Replikation des BACs in *E. coli* notwendigen Gene, eine eukaryotische Expressionskassette für β -Galaktosidase und eine *loxP* Sequenz wurden in den Genlocus der viralen Thymidinkinase UL23 durch homologe Rekombination in Säugerzellen eingebracht. Nach Transfer eines zirkulären Replikationsintermediates in *E. coli* wurde das BAC pHSV1(17⁺)blue isoliert. Restriktionsanalysen zeigten, dass das HSV1 Genom fast fehlerfrei kloniert wurde.

Eine eukaryotische Expressionskassette für die Rekombinase Cre und eine zweite *loxP*-Sequenz wurden mittels des Red-Rekombinationssystems des Phagen λ in pHSV1(17⁺)blue inseriert. Nach Transfektion des resultierenden BACs pHSV1(17⁺)blueLox in Säugerzellen schnitt Cre die von *loxP* Sequenzen flankierten BAC-Bereiche aus dem Virusgenom. Verglichen mit dem HSV1(17⁺) Wildtyp, hat durch die BAC-Klonierung eine fünffache Reduktion des Titers stattgefunden.

Das Kapsidprotein VP26 wurde N-terminal mit einem fluoreszierenden Protein fusioniert. Allerdings waren fast alle BAC-Mutanten mit dieser Modifikation nicht infektiös oder stark attenuiert. Durch *marker rescue* Experimente und Sequenzierung der schon existenten Mutante HSV1-K26GFP, wurde die Deletion der ersten vier N-terminalen Aminosäuren von VP26 festgestellt. Daraufhin konstruierte BAC-Viren mit einem GFPVP26 oder RFPVP26 Fusionsprotein ohne diese vier Aminosäuren waren infektiös und nur leicht attenuiert. Das Fluoreszenzsignal kolokalisierte mit einer Kapsidmarkierung, und die fluoreszenzmarkierten HSV1-Kapside wurden nach Zelleintritt effektiv zum Zellkern transportiert.

Darüberhinaus wurde das virale Membranprotein gD C-terminal fluoreszenzmarkiert, um die Lokalisation der Kapside und der viralen Hüllproteine während Zelleintritt, Zusammenbau und Ausschleusung fluoreszenzmikroskopisch zu untersuchen. Das HSV1-BAC pHSV1(17⁺)blueLox kann als Grundlage der Konstruktion spezifischer HSV1 Mutanten zur Untersuchung von Virus-Wirts-Interaktionen dienen.

Schlagworte: Herpes-Simplex-Virus, BAC-Mutagenese, fluoreszierende Proteine

1. Introduction

1.1. Herpesviruses

Within the DNA viruses the *Herpesviridae* form a large family of more than 130 species (Cleator and Klapper, 2004b). Most were found in mammalian hosts, but also in reptiles, amphibia and fish herpesviruses have been discovered. The *Ostreid herpesvirus 1* is the first herpesvirus isolated from an invertebrate, the Pacific oyster (Davison et al., 2005).

Herpesviruses contain a double-stranded linear DNA genome ranging from 108 to 241 kbp (Osterrieder et al., 2003) coding for up to 200 proteins, and are enveloped by a lipid bilayer membrane (Roizman and Knipe, 2001). Virion and genome size are amongst the largest of all viruses, together with the poxviruses. They are nevertheless exceeded by the 1.2 Mbp genome of the 400 nm large Mimivirus of amoebae (La Scola et al., 2003; Raoult et al., 2004). All herpesviruses establish a life-long latent infection in their host and the majority of humans will harbour at least one of the so far eight known human herpesvirus species in a latent state (Table 1).

The *Herpesviridae* are divided into the subfamilies of *Alpha-*, *Beta-* and *Gammaherpesvirinae*, according to their host range, tissue tropism and replication kinetics. The subfamily *Alphaherpesvirinae* is characterised by a variable host range, short reproductive cycles and rapid and efficient spread in cell culture, causing fulminant cytopathic effect (CPE; Cleator and Klapper, 2004b; Roizman and Knipe, 2001). The human alphaherpesviruses herpes simplex virus type 1 and 2 cause the well-known mouth and genital herpes, and varicella-zoster virus chickenpox and herpes zoster. Human Cytomegalovirus (HCMV), human herpesviruses 6A and 6B as well as human herpesvirus 7 are the human betaherpesviruses. HCMV is the most common and a severe threat in immunocompromised patients, where it causes pneumonia, retinitis or hepatitis. Moreover, when acquired via a congenital route, neurological disorders of the newborn can occur. The human gammaherpesviruses Epstein-Barr virus (EBV) and Kaposi's sarcoma-associated herpesvirus (KSHV) are associated with the induction of malignant neoplasia in immunocompromised patients, e.g. during the late phase of an human immunodeficiency virus 1 (HIV1) infection manifesting as the acquired immunodeficiency syndrome (AIDS). A primary infection with EBV causing infectious mononucleosis is prominent as "kissing disease" or "Pfeiffer's syndrome".

| Common Name | Abbreviation | Systematic Name | Subfamily |
|---|--------------|--------------------------------|-----------|
| Herpes simplex virus type 1 | HSV1 | <i>Human Herpesvirus 1</i> | α |
| Herpes simplex virus type 2 | HSV2 | <i>Human Herpesvirus 2</i> | α |
| Varicella-zoster virus | VZV | <i>Human Herpesvirus 3</i> | α |
| Epstein-Barr virus | EBV | <i>Human Herpesvirus 4</i> | γ |
| (Human) Cytomegalovirus | (H)CMV | <i>Human Herpesvirus 5</i> | β |
| Human Herpesvirus 6A/6B | HHV6A/6B | <i>Human Herpesvirus 6A/6B</i> | β |
| Human Herpesvirus 7 | HHV7 | <i>Human Herpesvirus 7</i> | β |
| Kaposi's sarcoma-associated herpesvirus | KSHV | <i>Human Herpesvirus 8</i> | γ |

Table 1: Systematics of human herpesviruses. Taken from Gärtner and Müller-Lantzsch (2002). The common names will be further used in this thesis.

1.2. Herpes simplex virus type 1

1.2.1. Pathology

The alphaherpesvirus HSV1 leads in most cases to the infection of oral and perioral skin and mucosa. The seroprevalence of HSV1 in the German population was about 85% in the year 1998 (Hellenbrand et al., 2005). Primary infection usually occurs during childhood and can manifest as a gingivo-stomatitis, which is sometimes misinterpreted as “teething”. Virus replicates in keratinocytes and epithelial cells and then enters efferent sensory and autonomous neurons, in which the virus is then transported retrogradely to the cell nuclei in cranial ganglia, very often the trigeminal ganglion (Vrabec and Alford, 2004; Figure 1). There, a life-long latent infection is established and only a subset of genes is expressed (Bloom, 2004). Upon stress or a weakened immunosurveillance, the virus escapes from latency, virions assemble and are transported anterogradely to the nerve termini from where a recurrent infection of the epithelium occurs. Primary and recurrent infection may be without symptoms, but often unpleasant lesions in the oral cavity or in the perioral region occur (Cleator and Klapper, 2004a; Wutzler, 2002).

During the course of a recurrent infection, the virus is spread from host to host by smear infection. In immunocompetent individuals, an HSV1 reactivation is rather benign and short-lasting. However, a systemic HSV1 infection in patients with a compromised immune system or HSV1 encephalitis are very severe threats with high mortalities. An infection of the eye can lead to keratoconjunctivitis, followed by a clouding of the cornea and ultimately, loss of eye sight. HSV1 infection is treated by the topic or systemic application of nucleoside analogs such as acyclovir, famcyclovir and valacyclovir. These prodrugs are phosphorylated by the viral thymidine kinase UL23 and then inhibit viral DNA replication catalysed by the

viral DNA-polymerase UL30. In thymidine kinase-negative HSV1 strains or in Aciclovir-resistant UL23 mutants, the DNA-polymerase inhibitor Foscarnet can be applied (Cleator and Klapper, 2004a; Wutzler, 2002).

Due to its neurotropism HSV1 is considered a promising vector for human gene therapy of neuronal disorders, e.g. Parkinson's or Alzheimer's disease as well as a selective agent for the treatment of brain tumors.

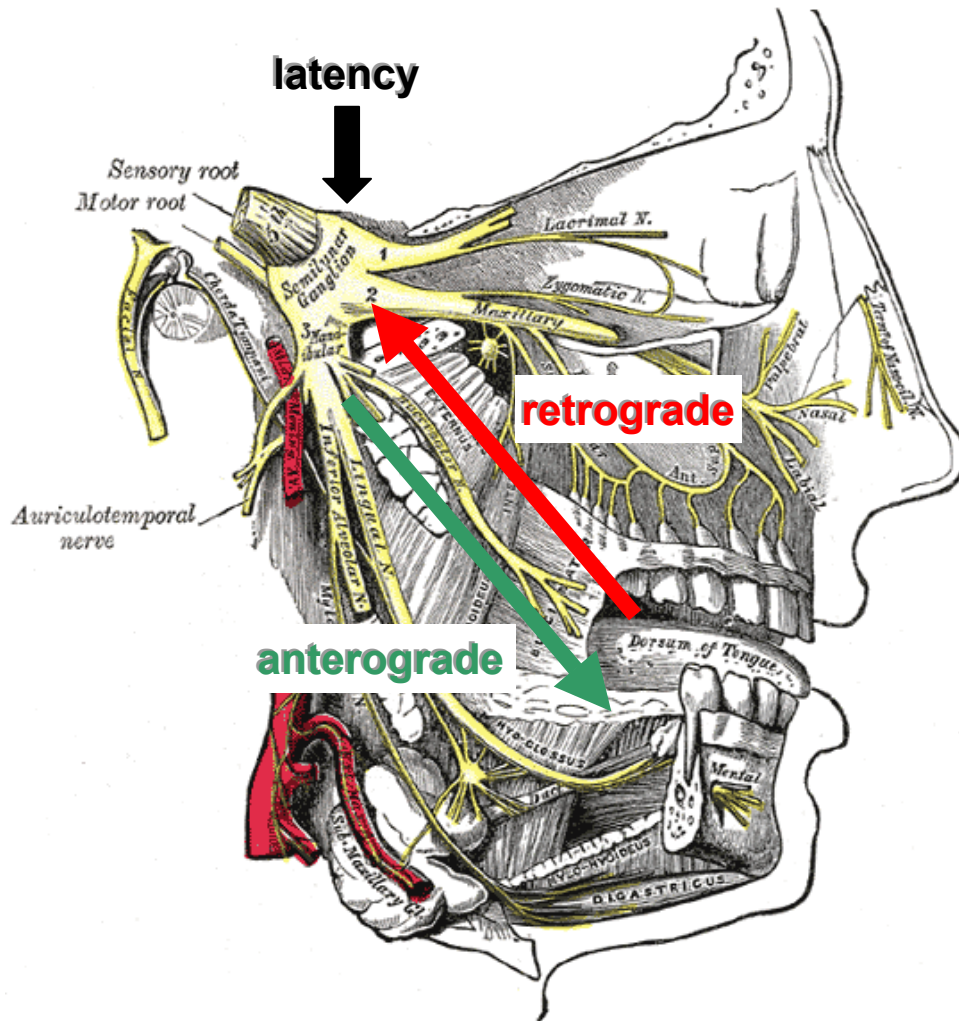


Figure 1: HSV1 infection of the trigeminal nerve. Drawing taken from (Gray, 1918; Fig. 778). HSV1 infects the host mainly via the oral and perioral region and enters the enervating sensory neurons after amplification in the epithelium. After retrograde transport, HSV1 can establish latency in cell nuclei of the cranial ganglia. Upon reactivation, virions are transported anterogradely to the initial site of infection, where they cause recurrent infection of the epithelium.

1.2.2. Structure

The HSV1 virion contains about 40 structural virus-encoded proteins, which are denominated either according to their molecular weight (e.g. VP1-3, MW_{app}=300 kDa; VP26, MW_{app}=12 kDa) or named after the position of their respective ORF on the HSV1 genome (e.g. UL37, US11; see chapter 1.2.3). Viral glycoproteins have a special nomenclature (e.g. gB, gC, gD), and several proteins are named after their function (e.g. vhs, virus-host-shutoff).

HSV1, as all members of the *Herpesviridae* family, is an enveloped virus with a virion diameter of about 225 nm (Figure 2). The lipid bilayer contains viral glycoproteins responsible for host cell binding and entry as well as immunomodulatory functions; they also play a role during virion assembly and egress.

The tegument is a layer of about 20 different proteins inside the virion; for many of these the functions are still unclear. Two of the best characterised are VP16 (UL48), a transactivator of immediate early viral transcription and UL41, the virus-host-shutoff factor (vhs), an RNase which degrades mRNAs and thus brings host protein synthesis to a halt in infected cells. Based on assembly studies, the tegument proteins were divided into an outer shell, to a major content consisting of VP11/12 (UL46), VP13/14 (UL47), and VP22 (UL49); and an inner shell with close contact to the capsid which encompasses VP1-3 (UL36), UL37 and the protein kinase US3 (Mettenleiter, 2002; Mettenleiter, 2004). The outer tegument dissociates after release of the capsid into the cytosol, while inner tegument proteins remain attached to the capsid (Granzow et al., 2005; Luxton et al., 2005; Sodeik et al., 1997). The two populations of tegument proteins are also separated by detergent lysis of extracellular virions in the presence of different salt concentrations (Wolfstein et al., 2006). VP16 (UL48) is considered as an adaptor protein between the inner and outer tegument layers, since it interacts with members of both, and has an untypical behaviour in the biochemical fractionation (Vittone et al., 2005; Wolfstein et al., 2006). Besides from the rather abundant proteins mentioned above, many additional minor proteins have been identified in the tegument.

The icosahedral viral capsid embedded in the tegument has a diameter of 125 nm. The 30 edges and 20 planes of the icosahedron are each built from three hexamers (hexons) of the 155 kDa protein VP5 (UL19) (Schrag et al., 1989). 11 vertices are built from VP5 pentamers (pentons). One vertex is thought to consist of a dodecamer of UL6 and is likely to be the portal for DNA packaging and uncoating (Newcomb et al., 2001; Trus et al., 2004). This “master portal” may be sealed by the UL25 protein, which is necessary to retain the viral DNA inside the capsid (McNab et al., 1998; Ogasawara et al., 2001). The capsomeres are linked by trimeric heterocomplexes of VP19c (UL38) and VP23 (UL18) (Trus et al., 1996). The small 12 kDa protein VP26 encoded by the UL35 gene decorates the hexons but not the

pentons with six copies each (Wingfield et al., 1997; Zhou et al., 1995). Cryo-electron microscopy revealed an eccentric position of the capsid inside the tegument (Grünewald et al., 2003; Figure 2).

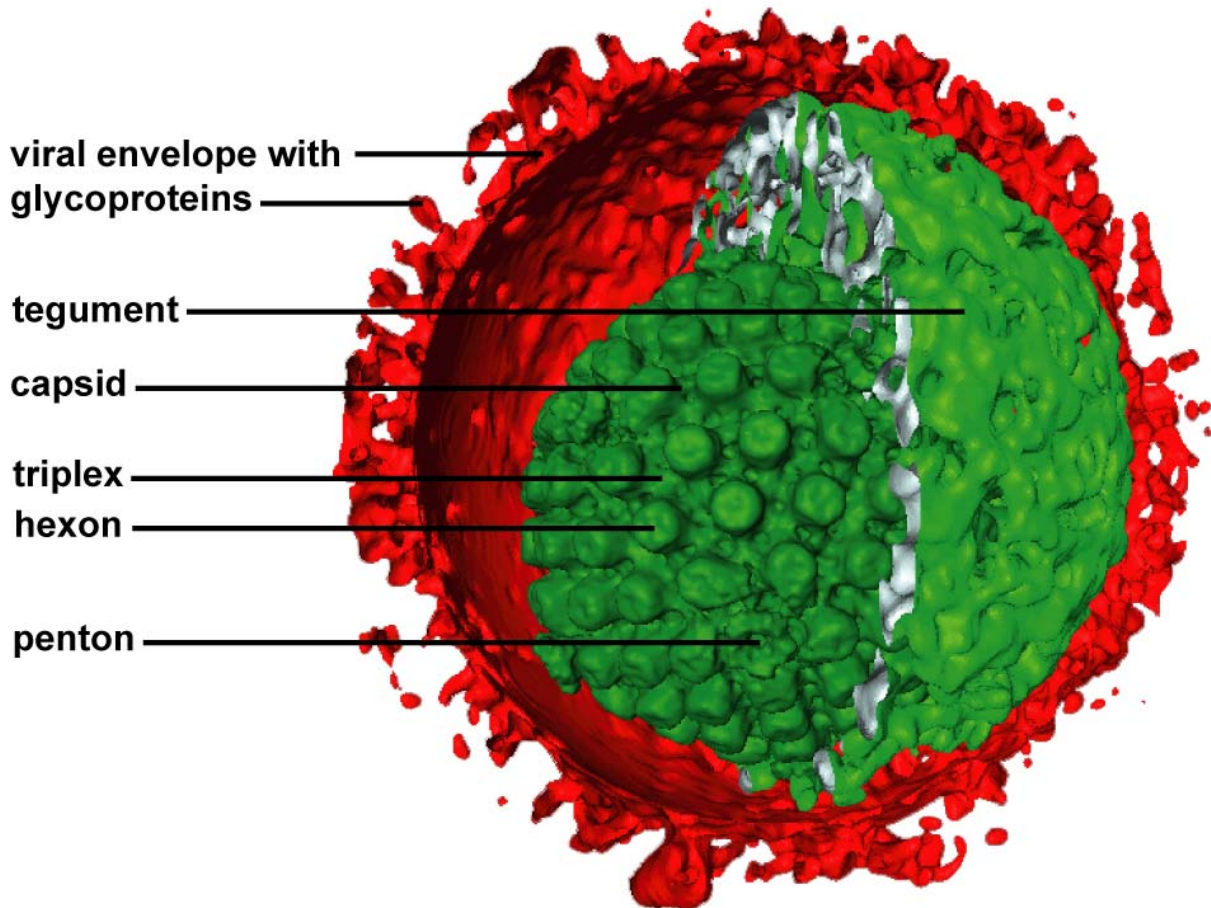


Figure 2: Cryo-Electron micrograph of HSV1. In this three-dimensional reconstruction, the viral envelope is depicted in red, the spikes can be assigned to as viral glycoproteins. The tegument (light green) shows an amorphous structure in which the capsid (dark green) is embedded in an eccentric position. The hexons and pentons, which are linked by the triplex complexes are clearly visible. Picture kindly provided by Kai Grünewald, Max-Planck-Institut für Biochemie, Martinsried, Germany (Grünewald et al., 2003).

Introduction

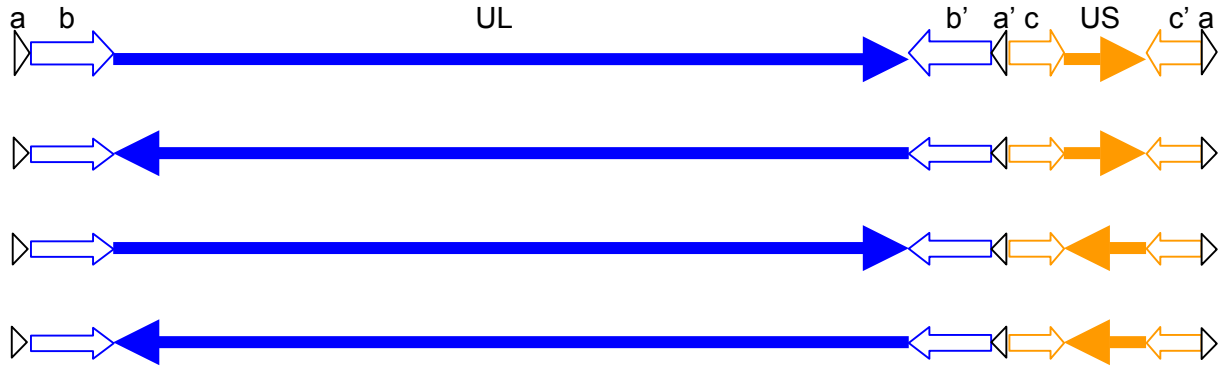


Figure 3: Genome arrangement of HSV1. The HSV1 genome contains unique sequences (UL and US) flanked by inverted repeats (b and c). The a-sequences are located at the termini and between the long and short region. During genome replication, four isoforms occur with regard to the relative orientation of the UL and US region. Depending on the enzyme used, these can differ in their restriction pattern (Roizman and Knipe, 2001).

1.2.3. Genome

Of the several strains of HSV1, strain 17⁺ (Brown et al., 1973) was the first, whose DNA sequence was fully sequenced and published (McGeoch et al., 1988; McGeoch et al., 1986; McGeoch et al., 1985; Perry and McGeoch, 1988; GenBank accession number X14112). The genome comprises 152,261 bp of a single, linear double-stranded DNA coding for more than 80 open reading frames (Rajcani et al., 2004). The genome is composed of a long and a short region, in which unique sequences (unique long, UL; unique short, US) are flanked by inverted repeats (Figure 3). During DNA replication, both genome parts isomerise, so that four equimolar isomeric viral DNAs can be isolated from virions (Roizman and Knipe, 2001). Between the long and short region and at the genome termini multiple copies of the a-sequence are arranged, which contains signals for the packaging of viral DNA into capsids. Inside the capsid the genome is packaged as a single linear molecule (Frenkel and Roizman, 1971), whereas during replication, circular-covalently-closed, concatemeric and even branched species are possible (see 1.3.3).

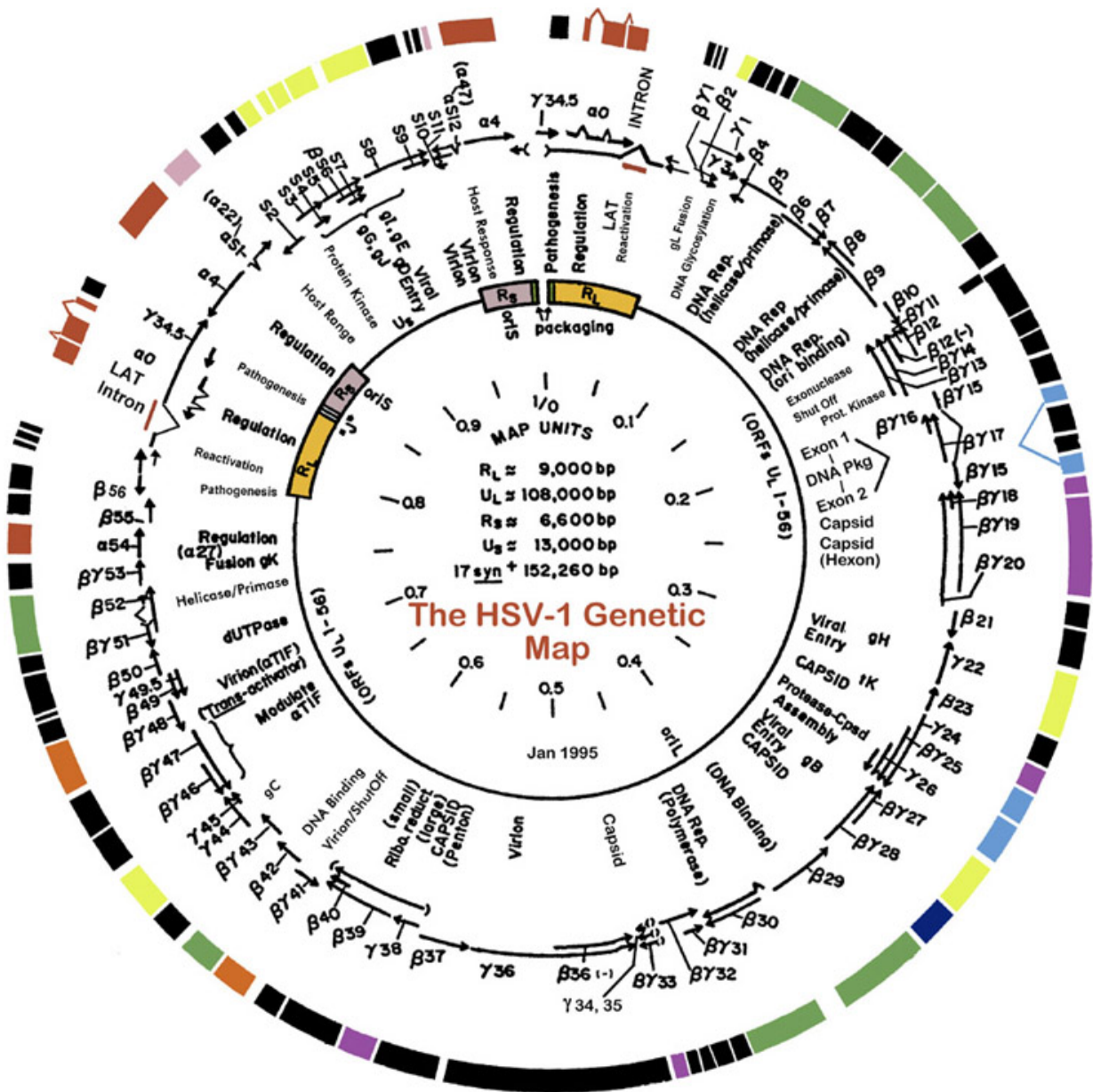


Figure 4: Genomic map of HSV1(17⁺) Outer ring: ORFs; violet: capsid, black: tegument; yellow: glycoproteins; green: DNA-replication; light and dark blue: capsid-maturation and DNA packaging; red and pink: immediate early proteins; orange: VP16 (UL48), α -transactivator, virus host shutoff (UL41); Middle ring: transcripts; α : immediate early; β : early; γ : late; Inner ring: genome organisation; from the homepage of Dr. Edward Wagner, University of California, Irvine, CA, USA; <http://www.dbc.uci.edu/~faculty/wagner/index.html>.

1.3. HSV1 replication

1.3.1. Attachment and entry

HSV1 infection commences with docking of the viral glycoproteins gB and gC to heparan sulfate moieties of cell surface proteoglycans (Spear, 2004; Spear et al., 2000; Spear and Longnecker, 2003). This reversible attachment is followed by an interaction of the glycoprotein gD with a coreceptor. These include HVEM, a TNF-receptor related protein, HveC or Nectin-1, a cell-cell adhesion molecule with several Ig-folds involved in the formation of synapses and adherens junctions, or specific residues in heparan sulfate modified by specific 3-O-sulfotransferases. Recently another human type II membrane protein, called B5 was identified as a potential receptor of HSV1 entry (Perez et al., 2005; Perez-Romero and Fuller, 2005). While the essential glycoprotein gH can bind to $\alpha\beta 3$ integrins, the role of this interaction is unclear, but it may trigger signalling events (Parry et al., 2005). In many cell types e.g. Vero or Hep-2 cells, the capsid together with the tegument enters the cytosol by fusion of the viral envelope with the host cell plasma membrane (Sodeik et al., 1997). The viral glycoproteins gB, gH and gL are essential for this process (Spear, 2004).

In some cell types, a productive infection can also be initiated by fusion of the viral envelope with an endocytic membrane. Endocytosis of virions has been observed earlier, but has been assumed to represent a dead-end route to degradation (Wittels and Spear, 1991). HeLa cells and chinese hamster ovary (CHO) cells expressing HSV1 entry receptors are entered by HSV1 via an endocytic pathway, which requires acidification of the endosome for the release of capsid and tegument into the cytosol (Nicola et al., 2003; Nicola and Straus, 2004), whereas in C10 murine melanoma cells fusion with the endocytic membrane is pH independent (Milne et al., 2005). Human keratinocytes, but not neurons are also productively infected by endocytosis (Nicola et al., 2005).

1.3.2. Capsid transport to the nucleus

To initiate replication, the HSV1 genome is delivered into the nucleus. Due to the high viscosity of the cytosol and the molecular crowding of vesicles, organelles and the cytoskeleton, mere diffusion cannot be the only means to reach the nucleus (Luby-Phelps, 2000; Sodeik, 2000), especially in neuronal cells, where capsids overcome macroscopic distances from their site of entry to their destination (Enquist et al., 1998; Smith and Enquist, 2002; Smith et al., 2001).

After entry, HSV1 capsids are transported to the cell centre along microtubules (Sodeik et al., 1997). In unpolarized cells, these polar filaments are arranged with their plus-ends in the cell periphery and their minus-ends attached to the microtubule-organising-centre (MTOC) near the nucleus; incoming capsids are transported by the motor protein dynein together with its cofactor dynactin (Döhner et al., 2002; Sodeik et al., 1997). Overexpression of dynamitin, a dynactin subunit, destroys the dynactin complex, and HSV1 nuclear targeting is diminished in dynamitin-overexpressing cells (Döhner et al., 2002). The viral proteins mediating the interaction with dynein are not identified, possible candidates are the inner tegument proteins VP1-3 (UL36) and UL37. After fusion with the plasma membrane, capsids lose parts of the tegument (Sodeik et al., 1997) and for the alphaherpesvirus pseudorabies virus it was shown using fluorescence-labelled mutants, that UL36 and UL37, but not VP16, VP13/14 and VP22 were bound to capsids during the retrograde transport in axons (Luxton et al., 2005) which was consistent with immunoelectron microscopic studies (Granzow et al., 2005). *In vitro*, HSV1 capsids can pull down dynein and dynactin from cytosol preparations (Wolfstein et al., 2006). However, inner tegument proteins have to be present and accessible on the capsid surface, as tegument-free capsids do neither bind dynein nor dynactin and capsids containing the full set of inner and outer tegument proteins also show less dynein binding. The inner tegument also is a prerequisite for the ATP- and dynactin-dependent motility of purified HSV1-GFPVP26 capsids along microtubules *in vitro* (Wolfstein et al., 2006). The dynein light chains DYNLT1 (Tctex1) and DYNLT3 (rp3; Pfister et al., 2005) can bind the small capsid protein VP26 in yeast-two hybrid and pull-down assays (Douglas et al., 2004). An HSV1- Δ VP26 mutant replicates to twofold reduced titers in cell culture, but is still able to induce infection and latency in a mouse infection model (Desai et al., 1998), for which retrograde long-distance transport is needed. Furthermore, capsids derived from this mutant bind dynein and dynactin subunits as efficiently as wildtype capsids *in vitro* (Wolfstein et al., 2006), and HSV1- Δ VP26 and HSV1-GFPVP26 capsids are efficiently transported to the nucleus in a microtubule and dynein-dependent manner (Döhner et al., 2006). Having arrived at the MTOC the further transport of the capsids is unclear. A plus-end directed microtubule motor, such as most kinesins, could move the capsids away from the MTOC towards the nucleus (Sodeik, 2002; J. Janus, K. Döhner & B. Sodeik; unpublished observations).

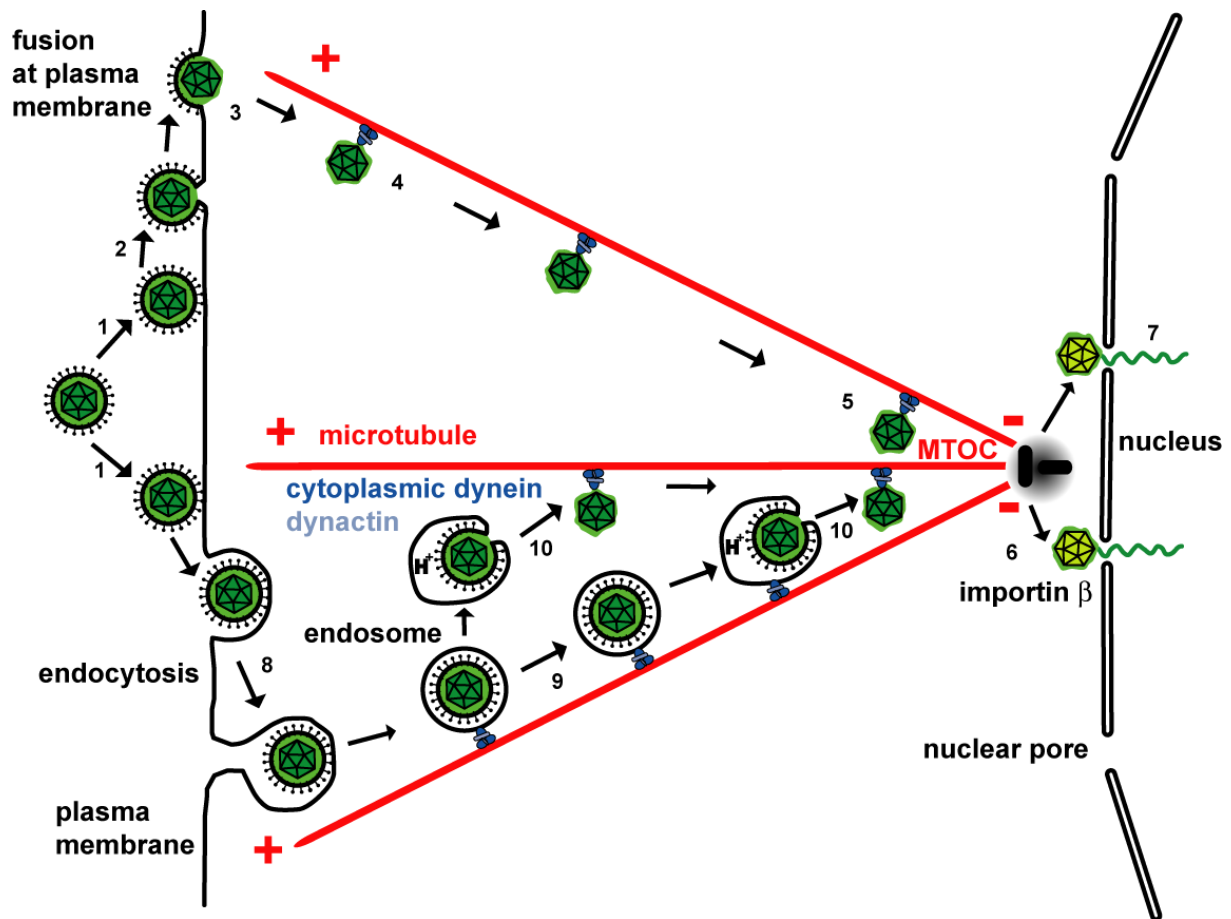


Figure 5: The entry of HSV1. HSV1 binds to the cell surface (1). In many cell types capsid and tegument enter the cytosol by fusion at the plasma membrane (2). The capsids pass through the actin cortex (3) and are transported along microtubules (MT, 4) towards the microtubule-organising centre (MTOC) utilizing the microtubule minus-end directed motor dynein with its cofactor dynactin (5). From the MTOC the capsids are transported further to the nucleus, where they bind to the nuclear pore complexes via importin β (6) and release their DNA into the nucleoplasm (7). In some cell types, the virus is taken up into the cell via endocytosis (8), and may then also be transported along MT inside endosomes (9) from which the capsids are released into the cytosol after fusion of the viral membrane with the endosomal membrane (10). (Diagram kindly provided by Katinka Döhner & Beate Sodeik, Institute of Virology, Hannover Medical School)

Having arrived at the nucleus, the capsids bind to the nuclear pore complexes (NPCs) and only there they release their DNA into the nucleoplasm. Capsids were observed docking to NPCs via a penton (Granzow et al., 2005; Ojala et al., 2000; Sodeik et al., 1997), which suggests a release of viral DNA from the portal complex consisting of UL6. Importin β is necessary for the binding to the NPCs (Ojala et al., 2000). Based on atomic force microscopy experiments, it has been suggested that the HSV1-DNA is injected into the nucleus as a condensed rod-like structure about 130 nm x 30 nm (Shahin et al., 2006). However, this largely exceeds the diameter of the UL6 portal channel (Newcomb et al., 2001; Trus et al., 2004). Moreover, after incubation of capsids with 0.5 M guanidinium chloride, which leads to the extraction of pentons, rather an expulsion of viral DNA as long filaments with a diameter

of 7 to 11 nm and a length of up to 500 nm was observed in electron micrographs (Newcomb and Brown, 1994).

1.3.3. Gene expression, DNA-replication and latency

After the viral DNA is released into the nucleus, viral gene expression commences. The tegument protein VP16 (UL48) which is released into the cytosol after viral entry binds to host transcription factors Oct-1 and HCF and transactivates the expression of the immediate early (α) genes ICP0, ICP4, ICP22, ICP27 and ICP47 by binding to TAATGARAT elements in their respective promoter (Weir, 2001). Concomitantly the virus-host-shutoff factor (vhs, UL41) which acts as an RNase, shuts down host protein synthesis (Roizman and Knipe, 2001). The immediate early protein ICP4 and the viral genomes form intranuclear replication foci localise near PML nuclear bodies or ND10, while ICP0 induces the degradation of PML, a main component of these structures by its E3-ubiquitin-ligase activity (Everett et al., 2003). This interplay between nucleoprotein complexes, formed by immediate early transcription of incoming viral genomes, and ND10 structures finally results in the formation of intranuclear replication compartments, which are devoid of PML (Everett and Murray, 2005).

HSV1 transcription is controlled in a cascade-like manner. The immediate early genes induce the expression of the early (β) genes which are largely responsible for the viral nucleotide metabolism and DNA-replication. Most of the late (γ) proteins, which are expressed concurrently with HSV1-DNA replication are structural proteins or mediate packaging of viral DNA into newly synthesised capsids (Rajcani et al., 2004; Roizman and Knipe, 2001; Weir, 2001; cf. Figure 4 for a map of the HSV1 genomic organisation).

The linear viral genome possibly circularises in the nucleus to a covalently closed form either by direct end ligation or by recombination of the terminal α -sequences (Yao et al., 1997). However, Jackson and DeLuca (2003) did not observe circularised genomes in cells lytically infected with HSV1 when ICP0 was present, and circular genomes may be restricted to latent infection in the absence of ICP0 expression. These observations were in turn challenged by Strang and Stow (2005), who provided evidence for end joining of incoming genomes by circularisation. In each case no terminal fragments of incoming HSV1 genomes were observed in the nucleus after uncoating. To initiate replication, the HSV1 origin-binding protein UL9 binds to one or more HSV1 replication origins and opens the double strand, then the HSV1 single-strand binding protein ICP8 (UL29) stabilises the single DNA strands. The helicase/primase complex of UL5, UL8 and UL52 mediates the formation of a replication fork and the viral DNA polymerase, consisting of the subunits UL30 and UL42 starts the synthesis of DNA daughter strands (Wilkinson and Weller, 2003). Originally, it was proposed that a circular viral genome is then replicated by a rolling circle mechanism, however, the rapid

increase in the number of genomes and the presence of branched DNA structures are not consistent with this model (Schildgen et al., 2005). Therefore, recombination may dominate at this stage of HSV1 DNA-replication. Cellular or viral factors may promote DNA-strand-invasion or strand-annealing reactions. The viral single-strand binding protein ICP8 (UL29) and a viral 5' to 3' exonuclease, UL12, share functional and structural homology to the λ phage recombination enzymes Bet (*red β*) and Exo (*red α*), respectively, and can mediate strand exchange *in vitro* (Reuven et al., 2003; Wilkinson and Weller, 2003). With this model, the occurrence of four isomeric HSV1 genome arrangements and the efficient recombination between two homologous coinfecting genomes can be described. Moreover, the observation that the origin-binding HSV1 protein UL9 is not required in later stages of DNA replication supports a two-stage model of HSV1 DNA-replication (Schildgen et al., 2005).

In neurons, HSV1 establishes latent infections, in which no progeny virus is produced, and the circular genomes remain quiescent in an episomal state. No virions can be detected within latently infected cells. The expression of lytic genes is not detectable, whereas a set of latency-associated transcripts (LATs) is expressed quite abundantly. Upon physiological or psychological stress, UV-light or hyperthermia, HSV1 reactivates, switches to lytic replication and starts to assemble new virions. In neurons, latency is probably induced by a block or impairment of immediate early gene expression (Preston, 2000). Reactivation is also blocked by CD8⁺ T-cells (Decman et al., 2005a; Decman et al., 2005b), which recognize the expression of lytic HSV1 genes and suppress reactivation by gamma interferone.

1.3.4. Assembly and egress

Viral capsids are assembled in the nucleus of infected cells (Gibson and Roizman, 1972). The capsid shell consisting of VP5 and the VP19c/VP23 complex is assembled around a UL26.5 scaffold, which is interacting with the portal complex of dodecameric UL6 (Newcomb et al., 2003; Singer et al., 2005). The viral protease UL26 cleaves itself into VP21 and VP24 as well as UL26.5 to VP22a. The internal cleaved scaffold is then removed upon DNA packaging. From the nuclei of infected cells three types of capsids can be isolated (Gibson and Roizman, 1972; Perdue et al., 1975). The A-capsids contain the full protein set of mature capsids, but are devoid of DNA, and thus considered as products of a defective assembly route or intermediate structures. B-capsids contain the internal scaffolding structure of VP22a, but no DNA. C-capsids contain the viral DNA and are the mature capsids which are assembled into virions. During replication concatameric DNA is produced which is packaged into newly synthesised capsids via the UL6 portal complex at a capsid vertex (Trus et al., 2004). The terminase complex UL15/UL28 cleaves the concatamers into unit-length genomes which are packaged into the capsids using ATP hydrolysis to power this process

(White et al., 2003a). UL25 is involved in sealing and retaining the DNA inside the capsid (McNab et al., 1998; Ogasawara et al., 2001; Stow, 2001).

After capsid assembly, the egress route of alphaherpesviruses involves several membrane budding and fusion events (Mettenleiter, 2002; Mettenleiter, 2004; Figure 6). Newly synthesised capsids bud through the inner nuclear membrane into the intermembrane space continuous with the lumen of the endoplasmic reticulum (ER). In this intermediate state the capsids have acquired a primary envelope containing UL34, and primary tegument containing UL31 and US3. The HSV1 tegument protein VP16 was observed bound to capsids in the perinuclear lumen (Naldinho-Souto et al., 2006). The primary envelope then fuses with the outer nuclear membrane, releasing the capsids into the cytosol. This model was recently challenged. It was proposed that progeny capsids either remain inside the ER lumen and are transported to the Golgi in vesicles, or that they leave the nucleus directly into the cytosol via impaired and dilated nuclear pores and then occasionally bud into the ER lumen (Leuzinger et al., 2005; Wild et al., 2005). However, these new ideas are very controversial since they do not fit to many previous electron microscopy studies (Mettenleiter and Minson, 2006). According to a current model the inner tegument proteins VP1-3 (UL36) and UL37 are attached to the capsids in the cytosol. In HSV1, deletion of either of these proteins leads to the accumulation of non-enveloped, non-tegumented capsids in the perinuclear cytosol as well as in the nucleus (Desai et al., 2001; Desai, 2000). The outer tegument proteins are assembled at cytosolic patches of trans-Golgi caverns or endosomes (Mettenleiter, 2004), where they are bound to the cytosolic domains of viral membrane proteins. During the secondary budding into the lumen of these organelles via an interaction of inner and outer tegument the virions become fully assembled and are then released into the extracellular space by fusion of virion-containing vesicles with the plasma membrane.

In neurons, virions are not only released at the cell body but also at the axon terminal (Figure 6). There is debate, whether enveloped virions are anterogradely transported along the axon in vesicles or whether unenveloped capsids are transported separately from vesicles containing viral envelope proteins (Enquist et al., 2002; Lavail et al., 2005; Miranda-Saksena et al., 2002). Tegument may be bound to the cytosolic face of these vesicles. Unenveloped capsids were observed in the distal axon and in growth cones and axon varicosities budding into vesicles with viral glycoproteins (Saksena et al., 2006). The mode of anterograde capsid transport along the axon is of importance regarding the interaction with anterograde motor proteins, which are likely to be kinesins. Either the virions take advantage of the cellular vesicle transport machinery, or the capsids must carry a receptor for a motor protein. Axonal capsids were observed to colocalise with kinesin-1 (Diefenbach et al., 2002)

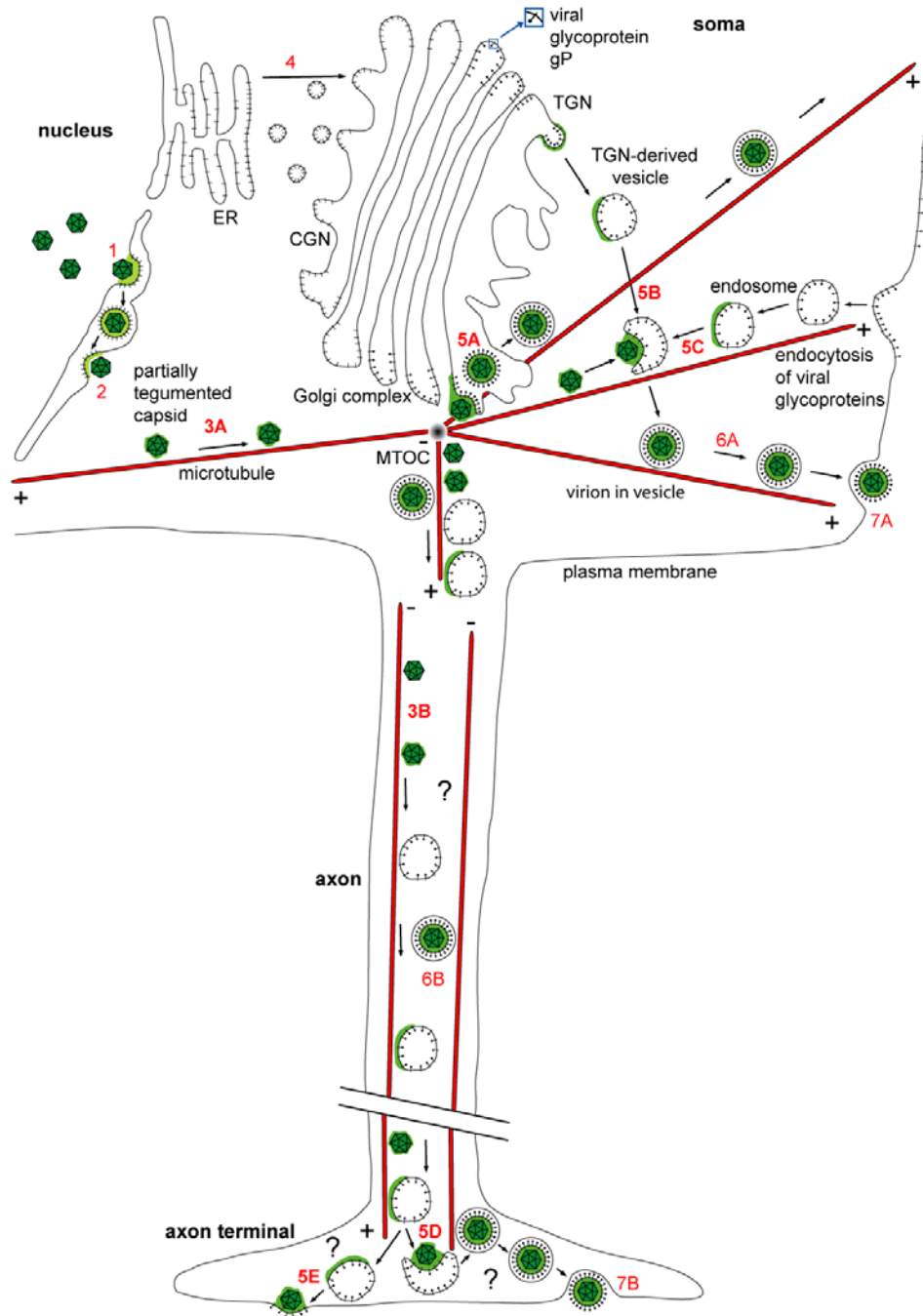


Figure 6: The egress of HSV1. After assembly, newly synthesised capsids bud into the intermembrane space of the nuclear envelope (1). After fusion with the outer membrane, naked capsids are delivered into the cytosol (2). The capsids are transported to the sites of secondary envelopment (3A). In neurons, secondary envelopment may take place at the presynapse (5D), so cytosolic capsids may be anterogradely transported within the axon (3B). Viral glycoproteins are synthesised in the endoplasmic reticulum (ER) and then processed via the secretory pathway (4). Capsids are believed to bud into the trans-Golgi network (TGN) where outer tegument proteins are bound to the cytosolic domains of viral glycoproteins (5A). Budding may also occur at TGN-derived vesicles exposing tegument on a cytosolic patch (5B). Alternatively or additionally, these vesicles may be of endosomal origin (5C). The vesicles, which contain virions are transported towards the plasma membrane (6A, 6B) and are released into the extracellular space after fusion (7A, 7B) (Diagram kindly provided by K. Döhner & B. Sodeik, Institute of Virology, Hannover Medical School).

and the tegument protein US11 interacts *in vitro* with kinesin-1 (Diefenbach et al., 2002) as well as with the protein PAT in a region which shares homology with kinesin light chain (Benboudjema et al., 2003). Whether these interactions have a functional role during egress, is unclear as the C-terminal basic region of US11 which mediates binding to kinesin-1 and PAT also binds several other host molecules, like several RNAs and protein kinase R (Mohr, 2004).

1.4. Mutagenesis of herpesviruses

1.4.1. Homologous recombination in eukaryotes

The function of the manifold viral proteins can be approached by the analysis of virus mutants. Due to the large size of a herpesviral genome, these were initially created by the use of mutagenic chemicals or irradiation. If a phenotype was observed, the causing mutations were mapped by cotransfecting infected cells with different viral DNA fragments identifying genomic regions which reconstituted the wildtype phenotype by homologous recombination (marker rescue; Stow et al., 1978; Figure 7A).

More specific mutations were generated by transfecting wildtype infected cells with a DNA construct, that is accompanied by a selection marker such as a fluorescent protein (GFP) or β -galactosidase (Desai and Person, 1998; Foster et al., 1998; Goldstein and Weller, 1988a; Goldstein and Weller, 1988b; Figure 7B). Also the viral thymidine kinase itself was used for selection of mutants (Mocarski et al., 1980; Post and Roizman, 1981). Occasionally, the mutant DNA together with the marker is incorporated into the viral genome by homologous recombination thereby replacing the wildtype counterpart. Recombinant virus is then purified against the wildtype virus background by plaque purification. Cells are inoculated with a diluted mixture of wildtype and recombinant virus under conditions, which restrict the free diffusion of secreted virions in the medium and only allow cell-to-cell spread, e.g. by overlaying the cells with agarose or neutralising antibodies. The infection of single cells results in a plaque in the cell lawn. By excision and passaging the infected cells of the plaques in which the selection marker is expressed, the recombinant virus is enriched and purified from contaminating wildtype virus.

This method has several drawbacks. If the introduced mutation leads to an attenuation in cell culture, the wildtype virus has a growth advantage, and the recombinant virus may be very difficult to purify. Furthermore, the introduction of lethal mutations into essential virus genes requires the use of complementing cell lines stably expressing the wildtype gene *in trans*. Moreover, this method is further hampered for certain herpesviruses with slow replication kinetics or low titers.

Introduction

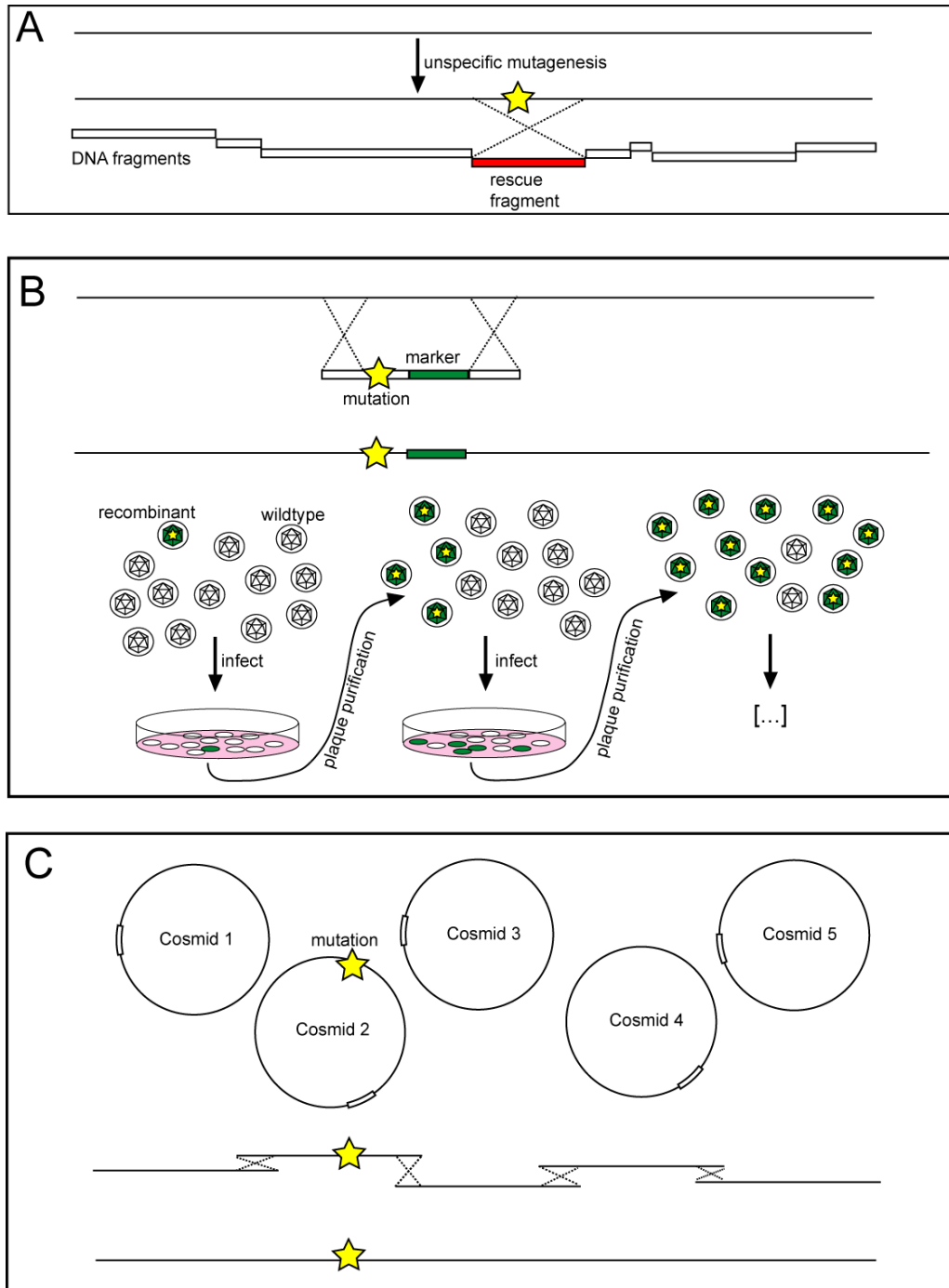


Figure 7: Mutagenesis of herpesviruses. (A) After undirected mutagenesis, a mutation leading to a certain phenotype can be mapped by cotransfecting fragments derived from wildtype virus-DNA, which recombine into the mutant genome and restore the wildtype phenotype. (B) A specific mutation is introduced by homologous recombination following cotransfection of a DNA fragment carrying the mutation together with an eukaryotic selection marker, e.g. GFP or β -galactosidase in permissive cells. The resulting mixture of recombinant and wildtype virus is then plaque purified several times under selection for plaques exhibiting expression of the selection marker. If an introduced mutation leads to an attenuation of the resulting virus, the wildtype growth advantage can hamper the purification of the mutant. (C) Cosmid based mutagenesis. The viral genome is cloned as a set of cosmids in *E. coli*, which reconstitute the complete virus genome after cotransfection into permissive cells. Thus, a mutation can be introduced by bacterial genetics.

1.4.2. Cosmids

Cosmids are bacterial vectors based on the *cos* packaging sequences of the bacteriophage λ (Hohn et al., 1988). Genome sequences of up to 40 kbp which are flanked by *cos* sequences can be packaged in λ phage heads and thus transmitted to bacterial hosts like *Escherichia coli*, where they are maintained extrachromosomally if they encode an antibiotic resistance gene, which is selected for during cultivation of the bacteria. The HSV1 genome was cloned as a set of cosmids in *E. coli* (Craig et al., 1990; Cunningham and Davison, 1993). Each of them contains overlapping viral sequences, so that after cotransfection of the cosmid set into permissive eukaryotic cells the complete viral genome reconstitutes by homologous recombination via the overlaps and progeny virus is produced (Cunningham and Davison, 1993; Figure 7C). Also HCMV (Kemble et al., 1996), VZV (Cohen and Seidel, 1993) and the simian varicella virus (Gray and Mahalingam, 2005) have been cloned as cosmids. This enabled the use of bacterial genetics to introduce mutations in viral genes without the need to purify mutants from wildtype virus. However, the reconstitution of a complete virus genome with a lethal mutation still required a complementing cell line. Moreover, the multiple recombination events requires after cotransfection are rare and can lead to unwanted alterations of the genome.

1.4.3. Bacterial artificial chromosomes (BAC)

A vector capable of maintaining a complete herpesviral genome is the bacterial artificial chromosome (BAC). These are F-factor derived plasmids with a cloning capacity of up to 1000 kbp, whose copy number and replication in *E. coli* is strictly controlled (O'Connor et al., 1989). They have been used for the cloning of large genome sequences and the establishment of genomic libraries of large DNA fragments. Cloning is performed in *E. coli* strains such as DH10B (Grant et al., 1990) which allow the precise maintenance and replication of large DNA sequences, due to the lack of the recombination function *recA*.

In 1997, the murine cytomegalovirus (MCMV) genome was cloned as a BAC (Messerle et al., 1997). For cloning a herpesviral genome as a BAC, the bacterial sequences required for maintenance and replication in *E. coli* are introduced together with a eukaryotic marker and a prokaryotic antibiotic resistance gene into the viral genome by classical homologous recombination in permissive host cells (Figure 8). Shortly after infection of eukaryotic cells with the purified recombinant virus, circular replication intermediates of the viral genome are isolated from the nuclei (Hirt, 1967) and used for the transformation of *E. coli* under selection for the provided resistance marker. Antibiotica resistant clones now carry the

Introduction

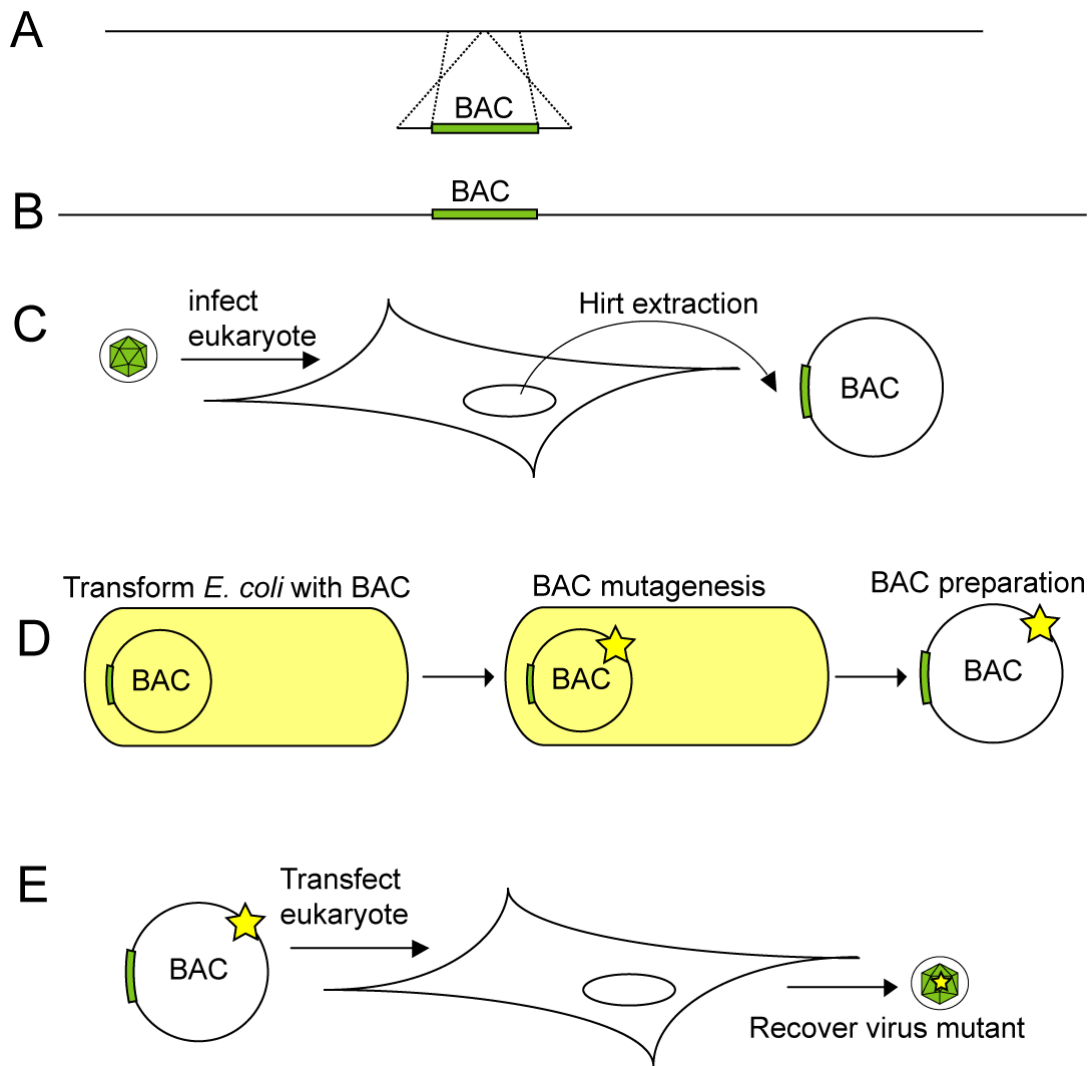


Figure 8: Cloning and mutagenesis of a herpesviral genome as a BAC. (A, B) Bacterial genes required for replication, maintenance and copy number control (BAC genes) are inserted into the viral genome by classical recombination in eukaryotic cells. (C) Recombinant virus is enriched by plaque purification and eukaryotic cells are infected at high MOI. Shortly after infection, circular DNA-replication intermediates are isolated from the infected cell nuclei by Hirt extraction. (D) *E. coli* are then transformed with the extract and selected for the antibiotic resistance encoded by the BAC genes. The viral genome has now been cloned as BAC and can be mutagenised in bacteria. (E) BACs can be prepared from bacteria and after transfection of permissive cells, virus is recovered.

complete viral genome as a BAC and the integrity of the genome can be confirmed by restriction analysis and Southern blotting. After preparation of the BAC-DNA and transfection of permissive eukaryotic cells, the virus is reconstituted.

A large number of other herpesviruses has been cloned as a BAC (Table 2) allowing the introduction of almost any mutation by the use of bacterial genetics. The methods for BAC-mutagenesis are based on homologous recombination in *E. coli* making use of clonal selection (cf. chapter 1.4.4). Thereby no wildtype contaminating virus is present and also

lethal mutations can be introduced into the viral genome (Adler et al., 2003; Brune et al., 2000; Wagner et al., 2002). Recently, the genome of the vaccinia virus, another DNA-virus with a very large genome was BAC-cloned and mutagenised (Domi and Moss, 2002; Domi and Moss, 2005).

| Species | Strain | Reference |
|---|--------------------|--|
| ALPHAHERPESVIRUSES | | |
| <i>Bovine Herpesvirus 1</i> | V155 Schonboken | (Mahony et al., 2002) (Trapp et al., 2003) |
| <i>Canid Herpesvirus 1</i> | | (Arii et al., 2006) (Strive et al., 2005) |
| <i>Equid Herpesvirus 1</i> | KyA racL11 | (Rudolph et al., 2002) |
| <i>Gallid Herpesvirus 2</i> (Marek's Disease Virus Type 1) | 584Ap80c | (Schumacher et al., 2000) |
| Herpes Simplex Virus Type 1 (<i>Human Herpesvirus 1</i>) | 17 ⁺ | (Saeki et al., 1998) (Stavropoulos and Strathdee, 1998) (Suter et al., 1999) |
| | F | (Tanaka et al., 2003) (Horsburgh et al., 1999) |
| Herpes Simplex Virus Type 2 (<i>Human Herpesvirus 2</i>) | MS | (Meseda et al., 2004) |
| Varicella-Zoster-Virus (<i>Human Herpesvirus 2</i>) | Oka | (Nagaike et al., 2004) |
| Pseudorabies virus (<i>Suid Herpesvirus 1</i>) | Ka Becker | (Fuchs et al., 2002) (Smith and Enquist, 2000) (Smith and Enquist, 1999) |
| BETAHERPESVIRUSES | | |
| <i>Cercopithecine herpesvirus 8</i> (Rhesus Cytomegalovirus) | 68-1 | (Chang and Barry, 2003) |
| Guinea Pig Cytomegalovirus | | (McGregor and Schleiss, 2001) |
| Human Cytomegalovirus (<i>Human Herpesvirus 5</i>) | AD169 | (Yu et al., 2002) (Borst et al., 1999) |
| Mouse Cytomegalovirus (<i>Murid herpesvirus 1</i>) | Smith | (Messerle et al., 1997) |
| GAMMAHERPESVIRUSES | | |
| <i>Bovine Herpesvirus 4</i> | V. test | (Gillet et al., 2005) |
| Epstein-Barr Virus (<i>Human Herpesvirus 4</i>) | AK B95.8 | (Kanda et al., 2004) (Delecluse et al., 1998) |
| Kaposi-Sarcoma Associated Herpesvirus (<i>Human Herpesvirus 8</i>) | | (Zhou et al., 2002) |
| <i>Murid herpesvirus 4</i> (Murine Gammaherpesvirus 68) | G2.4 | (Adler et al., 2000) |
| <i>Saimiriine herpesvirus 2</i> (Herpesvirus Saimirii) | | (White et al., 2003b) |

Table 2: Established herpesviral BAC-clones. Taken from Osterrieder et al. (2003); modified and updated

1.4.4. BAC mutagenesis

Mutagenesis of BAC-cloned herpesviral genomes is performed using recombination in *E. coli* under antibiotic selection. Due to the large size of the cloned genome, even rare-cutting restriction endonucleases may have multiple recognition sites, so BAC-mutagenesis by cutting and insertion of modified DNA by ligation is not applicable in most cases. As in the *E. coli* BAC-cloning strains the *recA* recombination is inactive, the recombinogenic enzymes are provided by helper plasmids or are expressed upon induction if they are integrated in the bacterial genome.

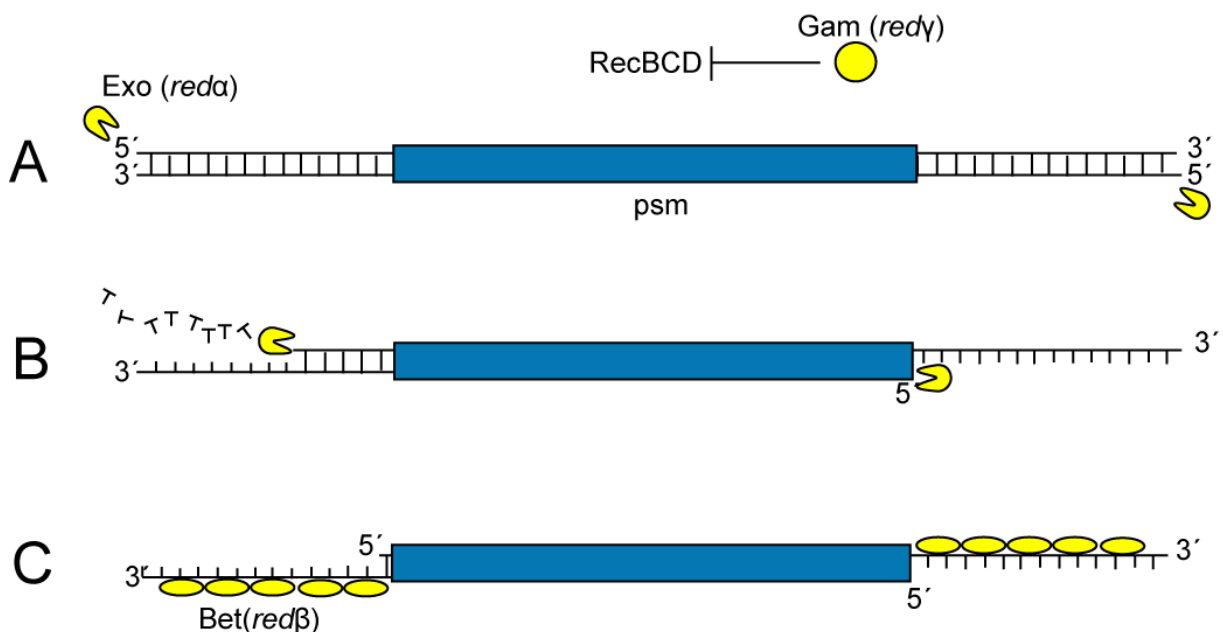
1.4.4.1. Red-recombination

Red-recombination is based on bacteriophage λ proteins (Court et al., 2002; Datsenko and Wanner, 2000; Muyrers et al., 2000; Muyrers et al., 1999; Zhang et al., 1998; Figure 9); Exo (*red α*) is a 5'-3' exonuclease that creates single-stranded 3'-overhangs on linear dsDNA, Bet (*red β*) binds and protects single stranded DNA (ssDNA) and mediates the annealing to a complementary ssDNA, thus being an essential protein for recombination. The degradation of linear dsDNA by bacterial nucleases like RecBCD is prevented by Gam (*red γ*). The method is also called "ET-cloning", named after the recombination proteins RecE and RecT of prophage *rac*, which have the same function as Exo and Bet, respectively. Interestingly, the HSV1 proteins UL12 and ICP8 (UL29) have structural and functional homology to Exo and Bet, respectively, and may play a role during recombination in HSV1 DNA replication (Reuven et al., 2003; Wilkinson and Weller, 2003; cf. chapter 1.3.3).

For recombination, a linear dsDNA fragment, which encodes a positive selection marker flanked by sequences homologous to the target sequence on the BAC, is introduced into *E. coli* harbouring the BAC and expressing the Red enzymes (Figure 9), either from a helper plasmid (e.g. pKD46; Datsenko and Wanner, 2000) or from a defective prophage inserted into their genome (Lee et al., 2001). Exo cleaves off nucleotides from the DNA double-strand thereby exposing a single-stranded 3' end. The large 3' single-stranded overhangs are then bound by Bet and can now anneal to their complementary single-stranded DNA, exposed in the DNA-replication fork, similar to a "large Okazaki fragment". Due to the noncomplementary region in the middle of the recombination fragment, the replication of the parental DNA strand stalls. A branched structure containing the parental wildtype-DNA strand and the strand with the positive selection marker insertion is formed, which is subsequently resolved, probably by RuvA or a topoisomerase. Bacteria containing the BAC with the inserted positive selection marker are able to grow under selection.

Since only short homology arms are needed, the recombination fragment can be synthesised by PCR using primers with 25-50 nt 5'-overhangs (Figure 10). Moreover, the positive selection marker can be flanked by *frt* sites allowing the subsequent removal of the resistance cassette by the recombinase Flp leaving only a short foreign sequence at the insertion site (Cherepanov and Wackernagel, 1995; Datsenko and Wanner, 2000; Wagner and Koszinowski, 2004). Red-recombination is used for knocking out viral genes or for the introduction of sequences, e.g. stop codons or epitope tags. Traceless mutations can be introduced by this method using a selection/counterselection cassette encoding a positive and a negative selection marker. This cassette is introduced by Red-recombination under positive selection as a “placeholder” at the mutation site and is then replaced in a second step with the mutant construct under negative selection (Figure 10).

The major risk of this method is the temporary presence of recombination enzymes with the ability to mediate homologous recombination over short sequences. Especially in herpesviral genomes containing short direct repeats, this can cause unwanted rearrangements and deletions, which make a thorough analysis of the mutant BACs indispensable. Furthermore, negative selection can lead to unspecific alteration of the BAC, because non-specific recombination as well as inactivation of the negative selection marker result in false positive clones.



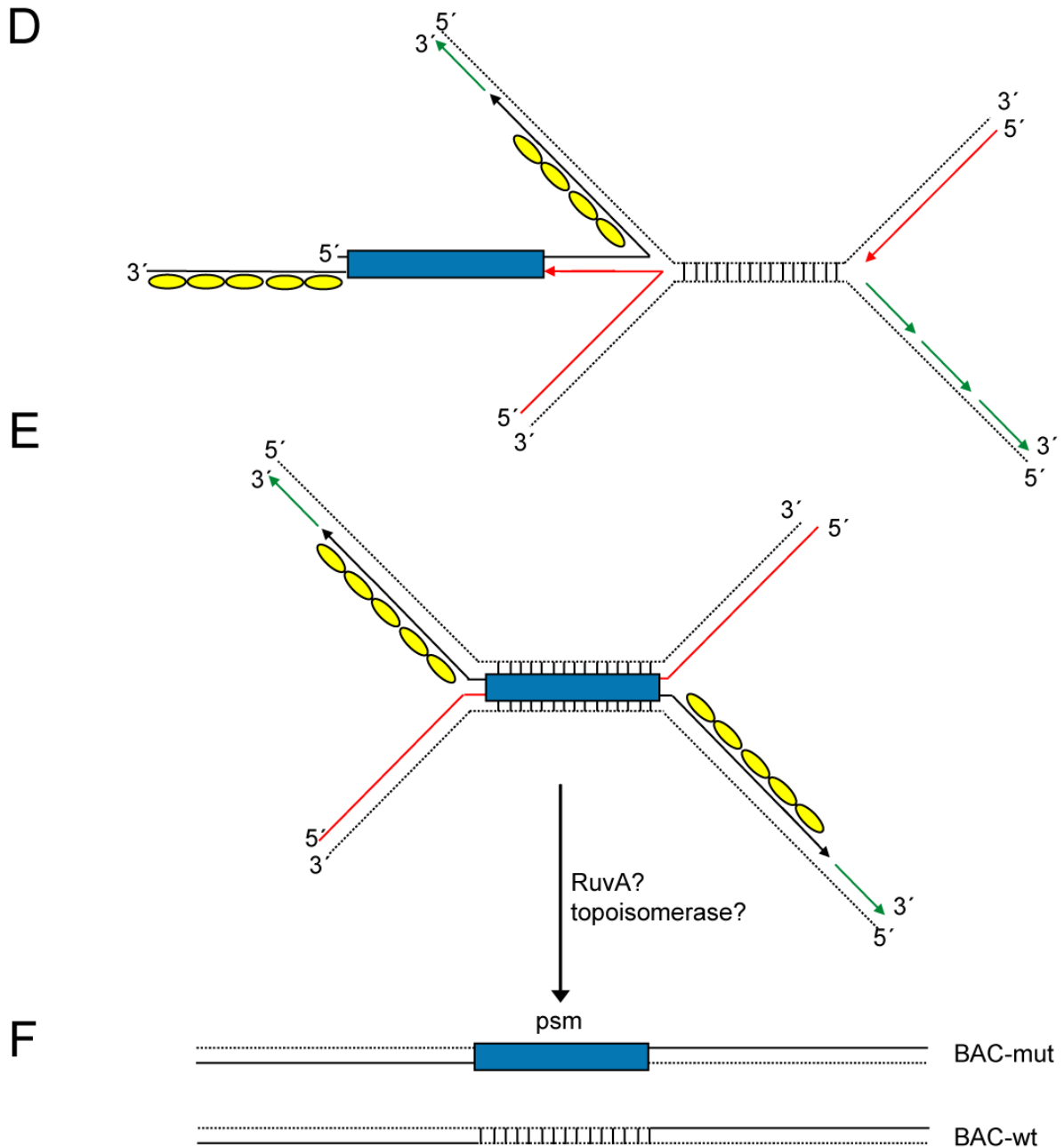


Figure 9: Red-recombination. (A) After induction of Exo (*redα*), Bet (*redβ*) and Gam (*redγ*), the bacteria are transformed with a linear double-stranded DNA encoding a positive selection marker (*psm*). The ends are homologous to the target sequence on the BAC. The RecBCD protein of *E. coli*, which would otherwise digest the linear DNA fragment by its nuclease function, is inhibited by Gam. (B) Exo is a 5'→3' exonuclease which starts removing nucleotides from the 5' ends of the DNA fragment leaving large 3' overhangs which are in turn bound and stabilized by Bet (C). (D,E) Also mediated by Bet, the 3' overhangs then anneal to their homologous single-stranded DNA in the lagging strand of a replication fork on the BAC, similar to a "large Okazaki-fragment". The parental DNA strands are depicted as dashed lines. No annealing occurs between non-complementary sequences. (E) The DNA strand with the parental sequence and the strand with the introduced selection marker are unwound by RuvA or a topoisomerase. (F) After recombination two BAC-copies are present, but under selection pressure only those BACs containing the selection marker will be propagated. Diagram modified after Court et al. (2002).

Introduction

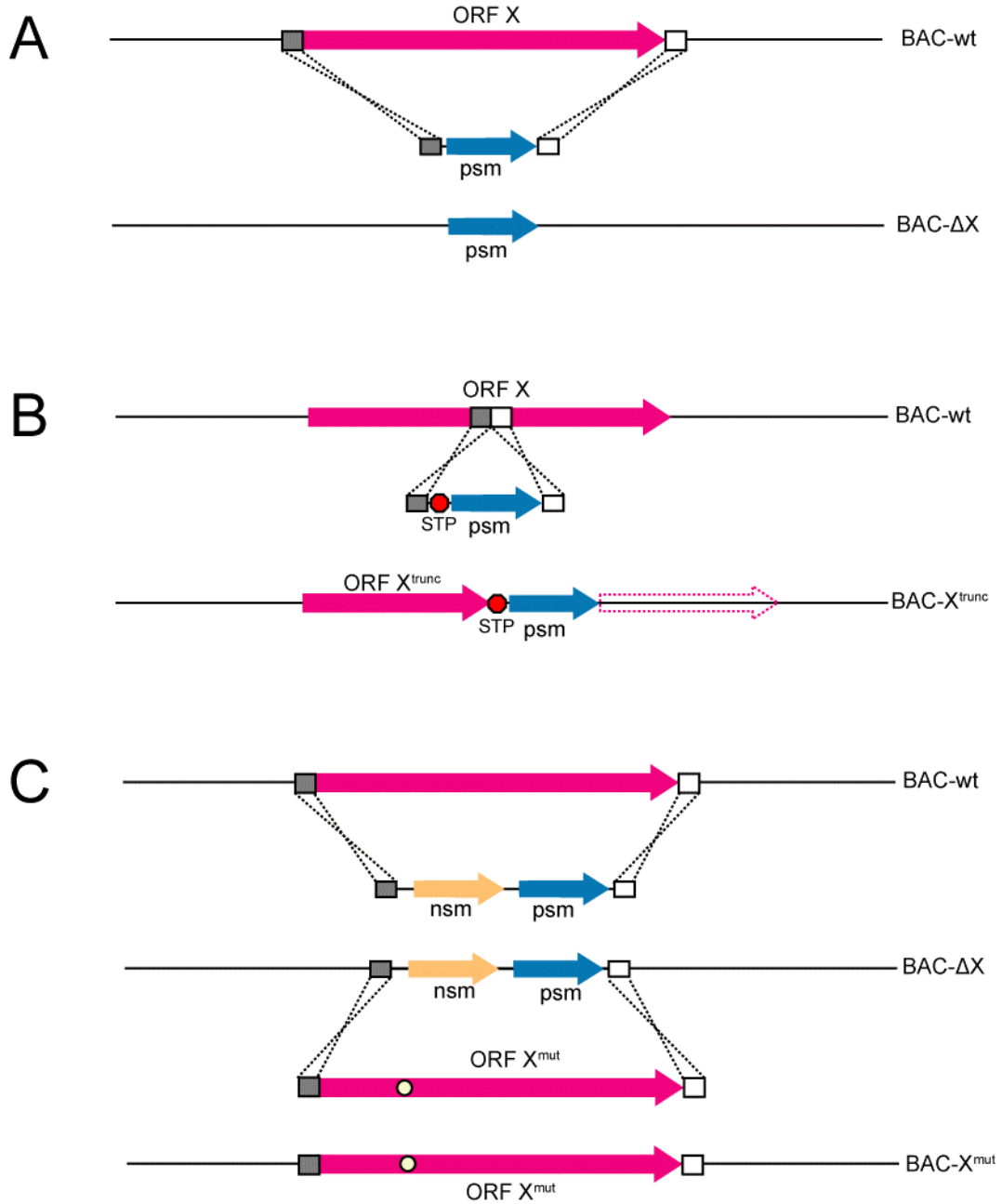


Figure 10: Applications for Red-recombination in BAC-mutagenesis. Using Red-recombination, different mutations can be introduced into a BAC. (A) For knocking out an ORF X, a positive selection marker (psm) is PCR-amplified with primers carrying 5' overhangs homologous to the sequences upstream and downstream of the target. After Red-recombination and selection for the psm, ORF X is completely deleted (BAC-ΔX). If flanked by *flp* sites, the psm can subsequently be removed from the BAC by Flp recombinase expression. (B) BAC-encoded proteins can be C-terminally truncated by premature translation stop of the ORF, if the psm is amplified together with a stop codon. (C) If an ORF is deleted by insertion of a cassette encoding a positive (psm) and a negative (nsm) selection marker, the cassette can in turn be replaced by a mutated version of the ORF under selection for loss of the negative selection marker.

1.4.4.2. Shuttle-mutagenesis

Another method for traceless allele replacement is a two-step recombination procedure, also called shuttle-mutagenesis, which is often used for the manipulation of BAC-clones and bacterial genomes (O'Connor et al., 1989; Posfai et al., 1997). The method was adapted for the targeted manipulation of BAC-cloned herpesviral genomes (Borst et al., 2004; Figure 11). The mutant allele is cloned into a shuttle vector together with 500-2000 bp of sequences flanking the mutation, which are homologous to the insertion site. If such a shuttle plasmid is introduced into bacteria harbouring the BAC, *recA*, which is non-functional in *E. coli* DH10B, but provided *in trans* on the shuttle plasmid, mediates a crossing-over event between a homologous sequences of the BAC and the shuttle plasmid, thus forming a cointegrate. Cointegrate formation is driven by selection for the antibiotic resistance encoded on the shuttle plasmid and growing the bacteria at a temperature which does not allow the replication of the non-integrated shuttle plasmid. The cointegrate spontaneously resolves by intramolecular recombination via a homologous sequence flanking the mutation site. Cointegrate resolution is driven by selection against a negative marker on the shuttle plasmid such as the *sacB* gene which codes for levansucrase, an enzyme converting sucrose into the toxic polysaccharide levan (Gay et al., 1983). Theoretically, this results in a mixture of 50% of both wildtype and mutant BAC, which can be differentiated by PCR or restriction screening of the obtained clones. However, the homologous sequences flanking the mutation may be differently prone to recombine, so in many cases, the formation of the cointegrate and resolution occurred via the same sequence part. After shuttle mutagenesis a thorough analysis is also required, due to the presence of *recA* recombination and the negative selection pressure applied by *sacB* (see above).

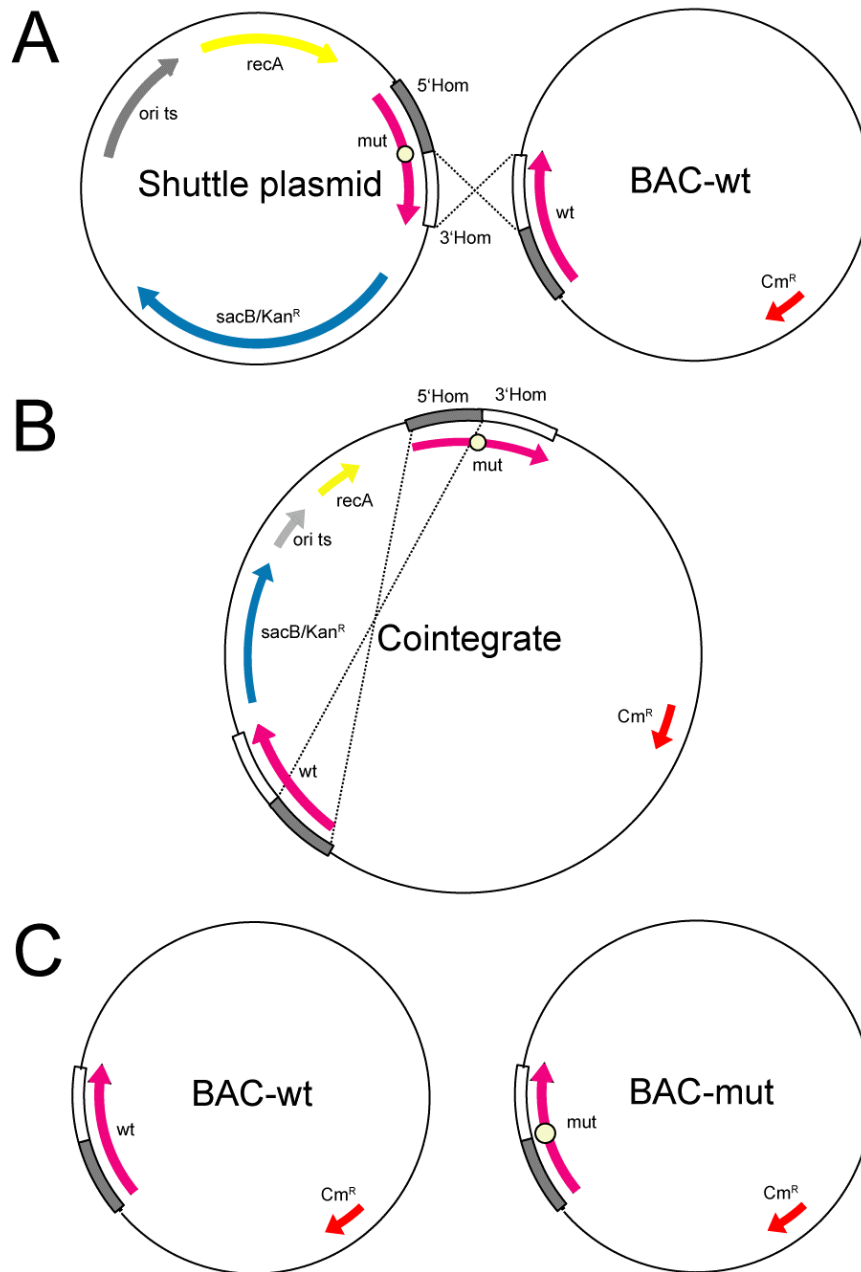


Figure 11: BAC-mutagenesis with shuttle plasmids. The shuttle plasmid encodes the RecA protein and a *sacB/Kan^R* fusion protein, providing kanamycin resistance and sucrose sensitivity. It only replicates at 30°C due to a temperature-sensitive mode of replication (*ori ts*). The mutated allele of the target gene carries 0.5-2 kbp of sequences flanking the mutation (*mut*; yellow circle), which are homologous to the target sequences (*wt*) on the BAC. (A) If *E. coli* carrying the BAC are transformed with the shuttle plasmid, RecA will mediate a crossing over between the shuttle plasmid and the BAC via the homologous sequences on one side of the mutation. (B) When selected for chloramphenicol (*Cm^R*) and kanamycin (*Kan^R*) resistance at 43°C, only the bacteria will survive, which carry a cointegrate, since at temperatures higher than 30°C, the shuttle plasmid cannot be replicated. (C) In an intramolecular recombination step, RecA now mediates the resolution of the cointegrate via the homologous sequences. In the presence of chloramphenicol and sucrose, only those bacteria will survive, which have resolved the cointegrate and thus lost *sacB* encoded on the shuttle plasmid (C). Recombination can occur via either of the homologous sequences, so BAC-clones with either the wildtype or mutant allele are isolated.

1.4.4.3. "En passant" mutagenesis

The requirement for a negative selection marker to tracelessly introduce mutations is circumvented by a method called "en passant" mutagenesis, based on a two step Red-recombination (Tischer et al., 2006). The recombination fragment encodes a positive selection marker and also contains a recognition site for the homing endonuclease I-SceI, which has a rare recognition sequence of 18 bp (TAG GGA TAA CAG GGT AAT) (Figure 12a). The target BAC must not contain this sequence. The sequences at the ends of the PCR-generated recombination fragment are again homologous to the target, e.g. for knock-outs just up- and downstream of an ORF (Figure 12 a-d). In this method, however, the PCR-primers are constructed in a way, that the 3' homology is also present directly downstream of the 5' homology on the linear DNA fragment, and the 5' homology is also inserted directly upstream of the 3' homology. After transformation of *redαβγ*-expressing *E. coli* the recombination fragment is inserted into the BAC, and thus for example knocks out a targeted ORF. The homing endonuclease I-SceI is then expressed *in situ* from a helper plasmid, and cuts at its recognition site introduced into the BAC. The juxtaposed 5' and 3' homologies can now recombine via Red-recombination, and the circular BAC is restored, without leaving any trace at the manipulation site. This step is driven by positive selection for the antibiotic resistance marker encoded on the BAC. By utilising two positive selection steps, this method is less prone to unwanted alterations in the BAC-cloned genome.

The introduction of large sequences, e.g. for GFP-tagging of a certain protein can also be performed with "en-passant" mutagenesis (Figure 12 e-h). Here, the positive selection marker and the I-SceI site are inserted into the GFP sequence. During construction of this insertion the positive selection marker and the I-SceI site have to be flanked by a duplication of a part of the GFP sequence, which mediates the recombination after the I-SceI cut. This construct is then amplified with primers containing the appropriate 5' overhangs and inserted into the BAC, so that after I-SceI cutting and recombination the GFP will be inserted at the desired genome position.

Introduction

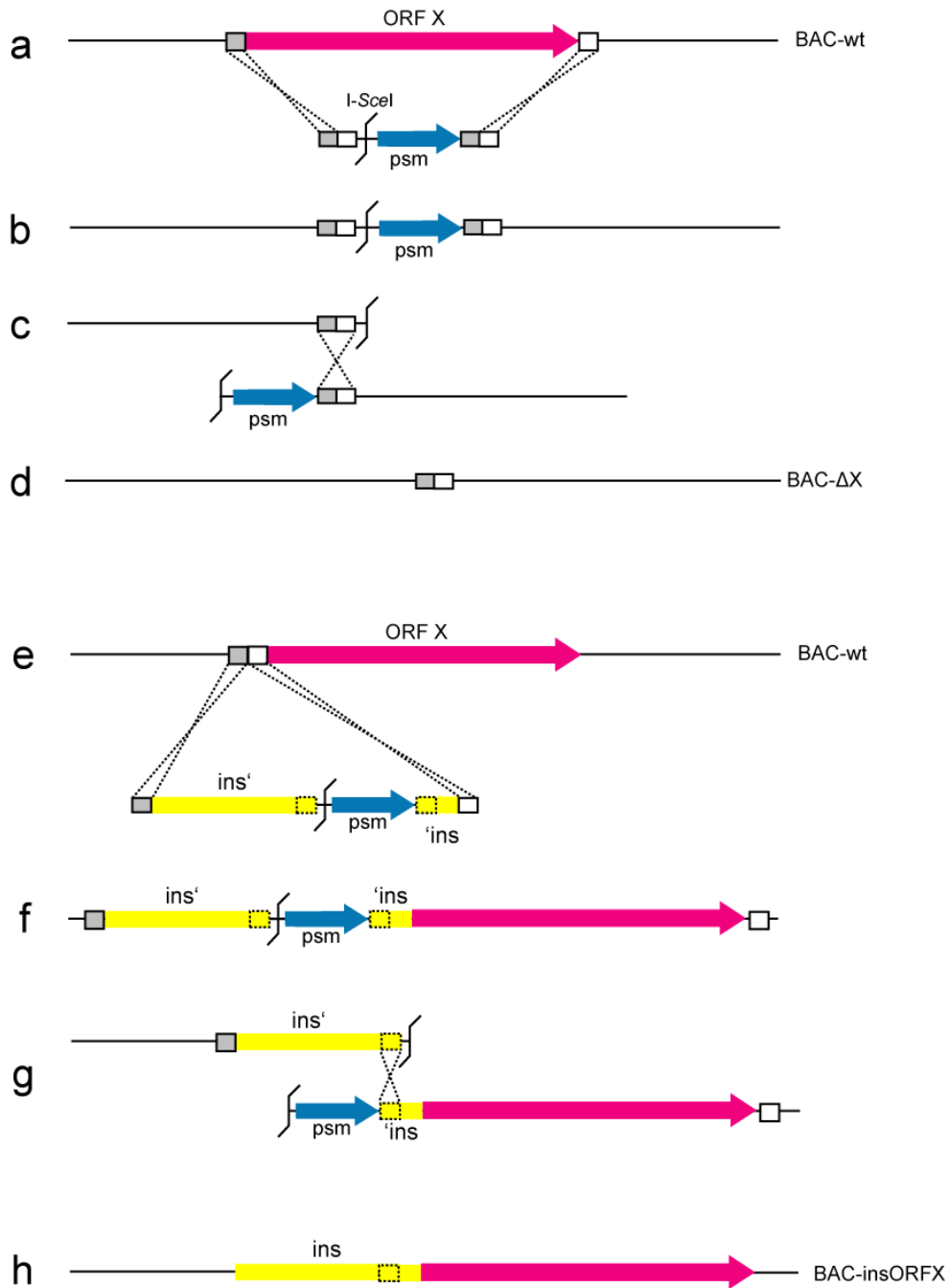


Figure 12: The "en-passant" mutagenesis. (a) For a traceless removal of an ORF X, a positive selection marker (psm) together with an I-SceI site are PCR-amplified. The primers contain 5' overhangs with sequences homologous to the 5' (grey box) and 3' region (white box) of the sequence to be targeted. The corresponding homologous sequences are duplicated and juxtaposed on the recombination fragment. (b) The fragment is inserted into the BAC-wt via Red-recombination, removing the original ORF. (c) After expression of I-SceI, the BAC is linearised. (d) Now the juxtaposed homologous sequences can recombine via a second Red-recombination step, thus reconstituting the BAC-ΔX with a traceless deletion. (e) For the introduction of foreign sequences, the positive selection marker and the I-SceI site are initially inserted into the additional sequence (ins), flanked by a duplication (dashed boxes). From this construct, the recombination fragment is PCR-amplified with primers containing 5' overhangs homologous to the 5' and 3' region of the insertion site, and introduced into the BAC via Red-recombination (f). After the I-SceI cut, the BAC-insORFX reconstitutes via the duplication (g) resulting in the traceless insertion of the foreign sequence into the BAC (h). Modified after Tischer et al. (2006).

1.4.5. HSV1-BACs

HSV1 has also been cloned as a BAC. The first HSV1-BAC clones were constructed from a set of cosmids containing overlapping fragments of the HSV1, strain 17⁺ genome (Cunningham and Davison, 1993), which were deleted for the DNA-cleavage and packaging sequences (*pac*). These cosmids were cotransfected with a plasmid containing the *E. coli* F-factor derived BAC-sequences, a homologous sequence for integration into the HSV1 genome between UL46 and UL47 and a *pac* sequence, which was flanked by *PacI* sites (Saeki et al., 1998). After cotransfection progeny virus could be harvested from the cells. The recombinant viral DNA was isolated, digested with *PacI* to remove the *pac* sequences, circularised by ligation and eventually electroporated into *E. coli*. Analyses performed with several restriction enzymes showed the integrity of the cloned viral genome. However, due to the lack of *pac* sequences this HSV1 clone was not infectious, however after re-insertion the infectivity was restored (Saeki et al., 1998). In another approach the BAC-genes and a single *pac* sequence were inserted into the UL41 (virus-host shutoff) locus on an HSV1 cosmid (Stavropoulos and Strathdee, 1998). The whole HSV1 cosmid set, again with deleted *pac* sequences was then cotransfected and recombinant virus could be isolated. After self-circularisation by ligation the DNA was electroporated into *E. coli* and BAC-clones were recovered, which turned out to be infectious. Also in this BAC, the *pac* sequence was subsequently removed.

As these first HSV1-BAC clones were cloned with the aim to construct a helper-virus free amplicon system for the transduction of cells with transgenes (Suter et al., 1999), they are not suitable for the construction of virus mutants in the context of an infectious genome, as they contain deletions in the *pac* sequences or in the UL41 ORF. Nevertheless, these studies showed the stability of the viral genome as a BAC, even after multiple passages in bacteria.

Horsburgh et al. (1999) inserted the BAC genes into the UL23 (thymidine kinase) locus of HSV1, strain F, by classical homologous recombination in eukaryotes. BAC clones were obtained by electroporating circular replication intermediates of the recombinant virus into *E. coli*. After transfection of the BAC, infection commenced and progeny virus was recovered. This HSV1-BAC was mutated using shuttle-mutagenesis (see 1.4.4.2). In the approach taken by Tanaka et al. (2003), the BAC genes were inserted into an intergenic region of HSV1, strain F, namely between UL3 and UL4. Thus, no viral gene was deleted in the resulting BAC clone. Furthermore the BAC genes were flanked with *loxP* sites, so that when cells were coinfecting with the BAC-derived virus and a recombinant adenovirus expressing Cre recombinase, the BAC sequences were specifically excised from the viral genome. This BAC

has since been used for the construction and analysis of HSV1 mutants (Tanaka et al., 2003) (Liang and Baines, 2005; Liang et al., 2004; Melancon et al., 2005).

The HSV1-BACs constructed by Horsburgh et al. (1999) and Tanaka et al. (2003) are based on HSV1, strain F, for which the full sequence is not available, thus the construction of mutants derived from these BACs requires the prior sequencing of the target genomic region, due to possible differences of the published HSV1(17⁺) sequence to the targeted HSV1(F) sequence.

1.4.6. Fluorescence tagging of HSV1 proteins

By classical mutagenesis, a number of HSV1 structural proteins have been tagged with a fluorescent protein, thus enabling the observation of the fate of a certain viral protein during the viral life-cycle by fluorescence light microscopy (Table 3). The green fluorescent protein (GFP) of the jellyfish *Aequorea victoria* is a 27 kDa protein with a β -barrel fold, in which three amino acid residues form a fluorophore by a covalent circularisation (Cody et al., 1993; Ormo et al., 1996; Prasher et al., 1992). By engineering the protein, the excitation and emission wave lengths were shifted to obtain, for example, a yellow (YFP) and a cyan (CFP) variant, furthermore the quantum yield was increased (Heim et al., 1994; Heim and Tsien, 1996). From the reef coral *Discosoma* sp. a red fluorescent protein (DsRed) was isolated, which forms a homotetramer. A variant was engineered, which exhibited fluorescence as a monomer (Campbell et al., 2002; mRFP1). This modification enabled the labelling of structural proteins with a red fluorescent tag without altering the function of the tagged protein by tetramerisation.

Whenever working with fluorescence-tagged viruses, one has to investigate whether the tagged protein has the same localisation and function as its wild type counterpart (discussed in Döhner and Sodeik, 2004). A thorough analysis of the untagged and the tagged protein by immunomicroscopic and biochemical methods is therefore indispensable. For example, when adding a tag to a capsid protein, not only fully assembled capsids are visualised, but also capsid precursors, misassembled capsids and unassembled capsid proteins. Whether the resulting fluorescent signal obtained may represent a proteolytic fragment of the fusion protein, however, can be determined by biochemical analysis.

If thoroughly analysed, herpesvirus mutants encoding structural proteins fused to fluorescent proteins tremendously helped to elucidate the function of several viral proteins during the viral life cycle. An HSV1 mutant encoding GFPVP26 (Desai and Person, 1998) showed the same intracellular behaviour upon entry as the corresponding wildtype HSV1(KOS) (Döhner et al., 2006) and was used in several other studies concerning

intracellular localisation of HSV1 capsids during assembly and egress (Desai et al., 2003; Desai et al., 2001; Desai, 2000). Using life-cell imaging and time-lapse microscopy the localisation and intracellular movements of fluorescence-labelled virion structures during entry and egress can be observed. Fluorescently labelled capsids are furthermore a valuable tool for microscopy based *in vitro* assays, such as for the reconstruction of microtubule transport of GFPVP26 labelled HSV capsids (Wolfstein et al., 2006).

| Protein (Gene) | Tag | Tag position | Reference |
|----------------|-----|--------------|------------------------------|
| VP26 (UL35) | GFP | N | (Desai and Person, 1998) |
| VP22 (UL49) | GFP | N | (Elliott and O'Hare, 1999) |
| VP13/14 (UL47) | YFP | N | (Donnelly and Elliott, 2001) |
| VP26 (UL35) | YFP | C | (Hutchinson et al., 2002) |
| VP22 (UL49) | CFP | N | (Hutchinson et al., 2002) |
| VP11/12 (UL46) | GFP | C | (Willard, 2002) |
| gB (UL27) | GFP | N | (Potel et al., 2002) |
| VP16 (UL48) | GFP | N or C | (La Boissiere et al., 2004) |
| gD (US6) | GFP | C | (Milne et al., 2005) |

Table 3: HSV1 mutants encoding fluorescence-tagged structural proteins.

1.5. Aim of the thesis

The analysis of virus-host interaction in the context of infection requires the construction of viral mutants within the full viral genome. Thereby reverse or forward genetics may be applied. In the first case the gene of interest or the whole genome is subjected to random mutagenesis, i.e. by chemical mutagenic agents or transposons, which may lead to a phenotype which is then mapped to a certain region. Otherwise a gene of interest may be specifically modified followed by the analysis of the resulting phenotype. Herpesviral mutagenesis in eukaryotes is often hampered by rare or ineffective recombination events, moreover the introduction of attenuating mutations is difficult due to the growth advantage of the wildtype precursor, and compensatory mutations in other viral genome regions can occur. Cloning herpesviruses as bacterial artificial chromosomes allows the generation of mutants in a bacterial system, by homologous recombination or random transposon mutagenesis and clonal selection. Viral mutants are then analysed after transfection in permissive eukaryotic host cells.

During this study the fully sequenced HSV1 strain 17⁺ is cloned as a bacterial artificial chromosome (BAC) with the ability to excise the *loxP* flanked BAC sequences from the viral genome by Cre-mediated site-specific recombination. The integrity of the cloned viral genome and the viral growth properties are determined. The targets for the construction of mutants will be viral proteins, involved in intracellular trafficking during entry and egress. As many assays used for studying intracellular transport are based on fluorescence microscopy *in vivo* and *in vitro*, the small capsid protein VP26 is tagged with a fluorescent protein by BAC mutagenesis, as done before in HSV1, strain KOS by classical mutagenesis (Desai and Person, 1998) or in other alphaherpesviruses as pseudorabies virus (del Rio et al., 2005; Smith et al., 2001) and bovine herpesvirus 1 (Wild et al., 2005). Moreover, the viral envelope protein gD is added a fluorescent protein label to obtain dual-coloured viruses with which the intracellular localisation of viral capsid and envelope proteins during entry, assembly and egress can be visualised. Fluorescence-tagged HSV1 mutants are characterised with regard to the integrity of the viral genome, growth properties and intracellular localisation of the tagged protein. The HSV1 strain 17⁺ BAC encoding fluorescence-tagged representative capsid and envelope proteins will be a basic construct for the further study of the life cycle of specific viral mutants.

2. Materials

2.1. Laboratory equipment

| | |
|---|--|
| Acrylamide gel electrophoresis system | Amersham, Little Chalfont, UK; Hoefer™ SE250 |
| Agarose gel electrophoresis chambers | Peqlab, Erlangen, Germany; Perfect Blue™ Mini S, Mini L, Maxi S |
| Bacteria incubators | Kendro, Rodenbach, Germany |
| Cell culture centrifuge | Eppendorf, Hamburg, Germany; 5810R |
| Cell culture incubator | Kendro, Rodenbach, Germany; Hera Cell |
| Cooling device | Biometra, Göttingen, Germany; KH3 |
| Electrophoresis power supplies | Amersham, Little Chalfont, UK; EPS300, EPS301 |
| Electroporation unit | Bio-Rad, Hercules, CA, USA; Gene Pulser Xcell |
| Gel documentation system | Alpha Innotech Corporation, San Leandro, CA, USA |
| Gradient mixer | Biocomp, Fredericton, Canada; Gradient Master™ Model 106 |
| Heating block | Omnilab, Gehrden, Germany; BT100 |
| Laminar air-flow bench for sterile work | Kendro, Rodenbach, Germany; Heraeus Hera Safe |
| Magnetic stirrers | Heidolph, Schwabach, Germany |
| Microwave oven | Sharp, Hamburg, Germany; R-330A |
| PCR cycler | Perkin Elmer, Wellesley, MA, USA; GeneAmp® PCR System 2400 Applied Biosystems, Foster City, CA, USA; GeneAmp® PCR System 9700 |
| Photometer | Eppendorf, Hamburg, Germany; BioPhotometer |
| Rocking platform | Biometra, Göttingen, Germany |
| Superspeed centrifuge | Beckman Coulter, Fullerton, CA, USA; J21-C |
| Superspeed centrifuge rotors | Beckman Coulter, Fullerton, CA, USA; JA-10, JA-20 |
| Table-top centrifuges | Eppendorf, Hamburg, Germany; 5415C, 5417R |
| Tank blotting system | Amersham, Little Chalfont, UK; TE 22 Mini Tank Transfer Unit |
| Ultracentrifuge | Beckman Coulter, Fullerton, CA, USA; L8-70 |
| Ultracentrifuge rotors | Beckman Coulter, Fullerton, CA, USA; Type19, SW28, SW40Ti, SW41Ti |
| X-ray film processor | Protec Medizintechnik GmbH, Oberstenfeld, Germany; OPTIMAX X-ray film processor |

2.2. Microscopes

For bright-field microscopy of cultured cells, an Eclipse TS microscope (Nikon, Düsseldorf, Germany) was used. Fluorescence microscopy of embedded cells was performed on an Axiovert 200M microscope (Zeiss, Oberkochen, Germany) using a 63x plan-achromatic objective (numeric aperture 1.4). To excite fluorescence, the samples were illuminated by galvanometrically monochromated light of a 150 W xenon lamp (Polychrome® IV, Till Photonics, Gräfeling, Germany).

Filter sets (all from Till Photonics, Gräfeling, Germany):

- DAPI: excitation SP 410, dichroic mirror LP 410, emission LP 420.
- GFP: excitation SP 510, dichroic mirror LP 490, emission BP 525/50
- Rhodamine: excitation SP 540 nm, dichroic mirror LP 565, emission LP 610/75
- Dualband FITC/Rhodamine filter set
- Dualband CFP/YFP filter set

Images were taken with a Till Imago® QE CCD camera and digitally acquired using the TillVision® Software, version 4.0 (Till Photonics, Gräfeling, Germany). Further image processing was performed with ImageJ 1.35j (Wayne Rasband; National Institute of Health, USA) and Adobe® Photoshop version 6 (Adobe Systems, San Jose, CA, USA).

2.3. Consumables

| | |
|---------------------------------------|-----------------------------|
| Blotting paper, Whatman® 3MM | Whatman, Maldstone, UK |
| Electroporation cuvettes | Bio-Rad, Hercules, CA, USA |
| Nitrocellulose membrane, BioTrace® NT | Pall, Pensacola, FL, USA |
| Nylon membrane, positively charged | Roche, Mannheim, Germany |
| Photometric cuvettes | Eppendorf, Hamburg, Germany |
| Ultracentrifuge tubes, Ultraclear™ | Beckman, Palo Alto, CA, USA |

Consumables not listed here were purchased from the following companies: Eppendorf, Hamburg; Sarstedt, Nümbrecht; Omnilab, Gehrden; Roth, Karlsruhe; Greiner, Frickenhausen; Neolab, Heidelberg; Brand, Wertheim (all Germany).

2.4. Kits

| | |
|--------------------------------|-----------------------------------|
| GenElute™ Plasmid Midiprep Kit | Sigma-Aldrich, Steinheim, Germany |
| MBS Mammalian Transfection Kit | Stratagene, La Jolla, CA, USA |
| NucleoBond™ BAC100 Kit | Macherey&Nagel, Düren, Germany |
| PCR DIG Probe Synthesis Kit | Roche, Mannheim, Germany |
| Qiaprep® DNA Miniprep Kit | Qiagen, Hilden, Germany |

| | |
|--|-------------------------|
| Qiaquick [®] Gel Extraction Kit | Qiagen, Hilden, Germany |
| Qiaquick [®] PCR Purification Kit | Qiagen, Hilden, Germany |

2.5. Chemicals

| | |
|---|--|
| Acetic acid | Baker, Deventer, Holland |
| Acrylamide, 30%(w/v)/Bisacrylamide, 0.8%(w/v) | Roth, Karlsruhe, Germany |
| Agar agar | Roth, Karlsruhe, Germany |
| Agarose | Roth, Karlsruhe, Germany Serva, Heidelberg, Germany |
| Agarose, low-melting point, SeaPlaque [®] | BioWhittaker, Rockland, ME, USA |
| Ammonium chloride | Roth, Karlsruhe, Germany |
| Ammonium peroxodisulfate (APS) | Roth, Karlsruhe, Germany |
| Ampicillin, sodium salt | Roth, Karlsruhe, Germany |
| Antipain | Sigma-Aldrich, Steinheim, Germany |
| <i>Aqua ad iniectabilia</i> (H ₂ O) | B. Braun, Melsungen, Germany |
| Aprotinin | Sigma-Aldrich, Steinheim, Germany |
| L-Arabinose | Roth, Karlsruhe, Germany |
| Bestatin | Sigma-Aldrich, Steinheim, Germany |
| Bicyclo(2,2,2)-1,4-diazaoctane (DABCO) | Sigma-Aldrich, Steinheim, Germany |
| Blocking reagent for Southern hybridisation (Cat. No. 1096176) | Roche, Mannheim, Germany |
| Boric acid | Merck, Darmstadt, Germany |
| Bovine serum albumine, fraction V (BSA) | Roth, Karlsruhe, Germany |
| 5-Bromo-4-chloro-indolyl-3-phosphate (BCIP) | Roth, Karlsruhe, Germany |
| 5-Bromo-4-chloro-3-indolyl-β-D-galactopyranoside (X-Gal) | Roth, Karlsruhe, Germany |
| 5-Bromo-3-indolyl-β-D-galactopyranoside (bluo-gal) | Invitrogen, Karlsruhe, Germany |
| Bromophenol blue | Roth, Karlsruhe, Germany |
| 1-Butanol | Fluka, Buchs, Switzerland |
| Calcium chloride (CaCl ₂ · 2 H ₂ O) | Sigma-Aldrich, Steinheim, Germany |
| Chloramphenicol | Sigma-Aldrich, Steinheim, Germany |
| Chloroform | Merck, Darmstadt, Germany |
| CO ₂ -independent Medium without L-glutamine (Cat. No. 18045-054) | Gibco, Paisley, UK |
| Coomassie Brilliant Blue G250 | Serva, Heidelberg, Germany |
| Coomassie Brilliant Blue R250 | Roth, Karlsruhe, Germany |
| Crystal Violet | Serva, Heidelberg, Germany |
| Cycloheximide | Sigma-Aldrich, Steinheim, Germany |
| p-Coumaric acid | Fluka, Buchs, Switzerland |

Materials

| | |
|---|-----------------------------------|
| N-N'-Dimethylformamide | Merck, Darmstadt, Germany |
| Desoxynucleotides, 10 mM each (dNTPs) | Peqlab, Erlangen, Germany |
| Dimethylsulfoxide, mol. biol. grade | Roth, Karlsruhe, Germany |
| Dipotassium hydrogenphosphate (K ₂ HPO ₄) | Merck, Darmstadt, Germany |
| Disodium hydrogenphosphate (Na ₂ HPO ₄) | Baker, Deventer, Netherlands |
| E-64 | Sigma-Aldrich, Steinheim, Germany |
| Ethanol | Baker, Deventer, Netherlands |
| Ethidium bromide | Roth, Karlsruhe, Germany |
| N,N,N',N'-Ethylenediaminetetraacetic acid (EDTA) | Roth, Karlsruhe, Germany |
| Fetal calf serum (FCS) | Gibco, Paisley, UK |
| Ficoll 400 | Sigma-Aldrich, Steinheim, Germany |
| Formaldehyde, min. 35%(w/v) | Merck, Darmstadt, Germany |
| Formamide, deionised | Roth, Karlsruhe, Germany |
| Glucose | Merck, Darmstadt, Germany |
| Glutamine, 200 mM | Seromed Biochrom, Berlin, Germany |
| Glycerol | Roth, Karlsruhe, Germany |
| Glycine | Roth, Karlsruhe, Germany |
| Glycogen for mol. biol, 20 mg/ml | Fermentas, St. Leon.-Rot, Germany |
| Hoechst 33258 | Sigma, Steinheim, Germany |
| Human IgGs, research grade (Cat. No. I-4506) | Sigma, Steinheim, Germany |
| Hydrochloric acid, 37%(w/v) (HCl) | Riedel-de-Haën, Seelze, Germany |
| Hydrogen peroxide, 30%(v/v) | Fluka, Buchs, Switzerland |
| 4-(2-Hydroxyethyl)-1-piperazineethanesulfonic acid (HEPES) | Roth, Karlsruhe, Germany |
| Immersion oil | Zeiss, Oberkochen, Germany |
| Isopropanol | Merck, Darmstadt, Germany |
| Isopropylthiogalactoside (IPTG) | Roth, Karlsruhe, Germany |
| Kanamycin sulfate | Gibco, Paisley, UK |
| Leupeptin | Sigma-Aldrich, Steinheim, Germany |
| Low fat milk powder, Sucofin [®] | TSI, Zeven, Germany |
| Luminol (5-Amino-2,3-dihydro-1,4-phthalazinidione) | Roth, Karlsruhe, Germany |
| Magnesium chloride (MgCl ₂ · 6 H ₂ O) | Roth, Karlsruhe, Germany |
| Maleic acid | Roth, Karlsruhe, Germany |
| 2-Mercaptoethanol | Roth, Karlsruhe, Germany |
| Methanol | Baker, Deventer, Netherlands |
| Minimum Essential Medium (MEM) with Earle's Balanced Salt Solution, non-essential amino acids, L-glutamine and 2.2 g/l NaHCO ₃ . (Cat. No. 04-08510) | Cytogen, Sinn, Germany |
| 2-(N-Morpholino)ethanesulfonic acid (MES) | Roth, Karlsruhe, Germany |
| Mowiol 40-88 | Sigma-Aldrich, Steinheim, Germany |

Materials

| | |
|---|-----------------------------------|
| Nitroblue tetrazolium salt (NBT) | Roth, Karlsruhe, Germany |
| o-Nitrophenyl- β -D-galactopyranoside (ONPG) | Applichem, Darmstadt, Germany |
| Nocodazole | Sigma-Aldrich, Steinheim, Germany |
| Nycodenz AG | Axis Shield PoC, Oslo, Norway |
| Paraformaldehyde | Serva, Heidelberg, Germany |
| Pepstatin | Sigma-Aldrich, Steinheim, Germany |
| Peptone | Roth, Karlsruhe, Germany |
| Phenol | Roth, Karlsruhe, Germany |
| Phenol/Chloroform/Isoamyl alcohol, volume ratio 25/24/1 | Roth, Karlsruhe, Germany |
| Phenylmethylsulfonylfluoride (PMSF) | Roth, Karlsruhe, Germany |
| Phosphate buffered saline (PBS) 10x | Gibco, Paisley, UK |
| Piperazine-1,4-bis(2-ethanesulfonic acid) (PIPES) | Roth, Karlsruhe, Germany |
| Ponceau S | Fluka, Buchs, Switzerland |
| Polyethylen glycol 4000 50%(w/v) (PEG4000) | Fermentas, St. Leon-Rot, Germany |
| Polyvinylpyrrolidone K30 | Sigma-Aldrich, Steinheim, Germany |
| Potassium chloride (KCl) | Roth, Karlsruhe, Germany |
| Potassium dihydrogenphosphate (KH_2PO_4) | Roth, Karlsruhe, Germany |
| RPMI 1640 Medium with 25 mM HEPES, L-glutamine and 2 mg/ml NaHCO_3 (Cat. No. 04-22500) | Cytogen, Sinn, Germany |
| Salmon sperm DNA, 10 mg/ml | Fermentas, St. Leon-Rot, Germany |
| Sodium acetate | Serva, Heidelberg, Germany |
| Sodium azide (NaN_3) | Roth, Karlsruhe, Germany |
| Sodium chloride (NaCl) | Merck, Darmstadt, Germany |
| Sodium citrate | Roth, Karlsruhe, Germany |
| Sodium dihydrogenphosphate (NaH_2PO_4) | Merck, Darmstadt, Germany |
| Sodium dodecylsulfate (SDS) | Roth, Karlsruhe, Germany |
| Sodium hydroxide (NaOH) | Merck, Darmstadt, Germany |
| Streptomycin sulfate | Sigma-Aldrich, Steinheim, Germany |
| Sucrose | Roth, Karlsruhe, Germany |
| 5-Sulfosalicylic acid | Merck, Darmstadt, Germany |
| Tetracycline | Sigma-Aldrich, Steinheim, Germany |
| N,N,N',N'-Tetramethylethyldiamin (TEMED) | Roth, Karlsruhe, Germany |
| Trichloroacetic acid | Roth, Karlsruhe, Germany |
| tris-(Hydroxymethyl)aminomethane (Tris) | Roth, Karlsruhe, Germany |
| Triton X-100 | Merck, Darmstadt, Germany |
| Trypsin/EDTA | Seromed Biochrom, Berlin, Germany |
| Tween 20 | Roth, Karlsruhe, Germany |
| Xylencyanol | ICN, Aurora, Ohio, USA |
| Yeast extract | Roth, Karlsruhe, Germany |

2.6. Electrophoresis standards

2.6.1. DNA standards

GeneRuler™ DNA Ladder Mix (Fermentas, St. Leon Roth, Germany)

10000, 8000, 6000, 5000, 4000, 3500, **3000**, 2500, **2000**, 1500, 1200, **1031**, 900, 800, 700, 600, **500**, 400, 300, 200, 100 (sizes in bp)

Lambda Mix Marker 19 (Fermentas, St. Leon Roth, Germany)

48502, 38416, 33498, 29946, 24508, 23994, 19397, 17053, 15004, 12220, 10086, 8614, 8271, 1503 (sizes in bp)

MassRuler™ DNA Ladder High Range (Fermentas, St. Leon Roth, Germany)

10000 (10 ng/μl), 8000 (8 ng/μl), 6000 (6 ng/μl), 5000 (5 ng/μl), 4000 (4 ng/μl), 3000 (3 ng/μl), 2500 (2.5 ng/μl), 2000 (2 ng/μl), 1500 (1.5 ng/μl)

MassRuler™ DNA Ladder Low Range (Fermentas, St. Leon Roth, Deutschland)

1031 (10 ng/μl), 900 (9 ng/μl), 800 (8 ng/μl), 700 (7 ng/μl), 600 (6 ng/μl), 500 (10 ng/μl), 400 (4 ng/μl), 300 (3 ng/μl), 200 (2 ng/μl), 100 (1 ng/μl), 80 (0.8 ng/μl) bp

2.6.2. Protein standards

Kaleidoscope Prestained Protein Marker (BioRad, Hercules, CA, USA)

250, 150, 100, 75, 50, 37, 25, 20, 15, 10 (sizes in kDa)

2.7. Enzymes

2.7.1. Restriction endonucleases

| | | |
|----------------------|------------------------|---------------------------------------|
| <i>Ascl</i> | GG ¹ CGCGCC | New England Biolabs, Ipswich, MA, USA |
| <i>BamHI</i> | G ¹ GATCC | Fermentas, St. Leon-Rot, Germany |
| <i>BglII</i> | A ¹ GATCT | Fermentas, St. Leon-Rot, Germany |
| <i>BspHI</i> | T ¹ CATGA | New England Biolabs, Ipswich, MA, USA |
| <i>BsrGI</i> | T ¹ GTACA | New England Biolabs, Ipswich, MA, USA |
| <i>BstBI</i> | TT ¹ CGAA | New England Biolabs, Ipswich, MA, USA |
| <i>Bsu15I (C1a1)</i> | AT ¹ CGAT | Fermentas, St. Leon-Rot, Germany |
| <i>DpnI</i> | GA ^{m1} TC | New England Biolabs, Ipswich, MA, USA |
| <i>EaeI</i> | Y ¹ GGCCR | New England Biolabs, Ipswich, MA, USA |

| | | |
|-----------------------|-----------|---------------------------------------|
| <i>Eco321 (EcoRV)</i> | GAT'ATC | Fermentas, St. Leon-Rot, Germany |
| <i>EcoRI</i> | G'AATTC | Fermentas, St. Leon-Rot, Germany |
| <i>HindIII</i> | A'AGCTT | Fermentas, St. Leon-Rot, Germany |
| <i>HpaI</i> | GTT'AAC | New England Biolabs, Ipswich, MA, USA |
| <i>KpnI</i> | GGTAC'C | Fermentas, St. Leon-Rot, Germany |
| <i>NcoI</i> | C'CATGG | Fermentas, St. Leon-Rot, Germany |
| <i>NdeI</i> | CA'TATG | Fermentas, St. Leon-Rot, Germany |
| <i>NheI</i> | G'CTAGC | Fermentas, St. Leon-Rot, Germany |
| <i>NotI</i> | GC'GGCCGC | Fermentas, St. Leon-Rot, Germany |
| <i>PacI</i> | TTAAT'TAA | New England Biolabs, Ipswich, MA, USA |
| <i>SbfI</i> | CCTGCA'GG | New England Biolabs, Ipswich, MA, USA |
| <i>SgrAI</i> | CR'CCGGYG | New England Biolabs, Ipswich, MA, USA |
| <i>SmaI</i> | CCC'GGG | Fermentas, St. Leon-Rot, Germany |
| <i>XbaI</i> | T'CTAGA | Fermentas, St. Leon-Rot, Germany |
| <i>XhoI</i> | C'TCGAG | Fermentas, St. Leon-Rot, Germany |

2.7.2. Other enzymes

| | |
|--|---------------------------------------|
| Calf intestine alkaline phosphatase (CIAP) | Fermentas, St. Leon-Rot, Germany |
| Klenow fragment | Fermentas, St. Leon-Rot, Germany |
| <i>Pfu</i> Polymerase | Stratagene, La Jolla, CA, USA |
| <i>Pwo</i> Polymerase | Peqlab, Erlangen, Germany |
| Ribonuclease A (RNase A) | Fermentas, St. Leon-Rot, Germany |
| T4 DNA Ligase | Fermentas, St. Leon-Rot, Germany |
| <i>Taq</i> Polymerase | New England Biolabs, Ipswich, MA, USA |

2.8. Media and solutions

If not otherwise noted, all solutions were prepared with double-distilled H₂O. Solutions not mentioned are described in the methods part.

BHK-21 cell medium

MEM supplemented with 10%(v/v) fetal calf serum

100x Denhardt's solution

1%(w/v) Ficoll 400, 1%(w/v) Polyvinylpyrrolidone K30, 1%(w/v) BSA

6x DNA loading solution

30%(w/v) glycerol, 0.25%(w/v) bromophenol blue, 0.25%(w/v) xylencyanol

DNA resuspension buffer

10 mM Tris-HCl, pH 8, 50 µg/ml RNase A

Embedding solution (Mowiol)

6 g glycerol, 2.4 g Mowiol, 6 ml H₂O, 12 ml 0.2 M Tris-HCl pH 8.5.
Prior to use add 25 mg/ml DABCO.

LB Agar

1.5%(w/v) agar-agar suspended in LB Medium, then autoclaved.

LB Medium

1%(w/v) pepton, 0.5%(w/v) yeast extract, 0.5%(w/v) NaCl, 1 mM NaOH; autoclave

MNT buffer

20 mM MES, 100 mM NaCl, 30 mM Tris-HCl, pH 7.2

NTE buffer

100 mM NaCl, 10 mM Tris-HCl, 1 mM EDTA, pH 7.4

Protease inhibitor cocktails

500x AEL: 1 mg/ml Aprotinin, 5 mg/ml E-64, 1 mg/ml Leupeptin in H₂O
500x ABP: 5 mg/ml Antipain, 1 mg/ml Bestatin, 1 mg/ml Pepstatin in methanol
250x PMSF: 40 mg/ml PMSF in isopropanol

PtK₂ cell medium

MEM supplemented with 10%(v/v) fetal calf serum

RPMI/BSA

0.1%(w/v) BSA in RPMI 1640 medium

RSB buffer (resuspension buffer)

10 mM Tris-HCl, 10 mM KCl, 1.5 mM MgCl₂, pH 7.5

6x SDS-PAGE sample buffer (Laemmli, 1970)

30%(w/v) glycerol, 6%(w/v) SDS, 0.3 M Tris-HCl, pH 6.8, bromophenol blue
Prior to use add 2-Mercaptoethanol up to 6%(v/v).

20x SSC

3 M NaCl, 0.3 M sodium citrate, pH 7

SOC Medium

2%(w/v) peptone, 0.5%(w/v) yeast extract, 8.6 mM NaCl, 2.5 mM KCl, 10 mM MgCl₂, 20 mM glucose

50x TAE

2 M Tris, 2 M acetic acid, 50 mM EDTA

5x TBE

0.44 M Tris, 0.44 M boric acid, 10 mM EDTA

TB Medium

1.3%(w/v) peptone, 2.7%(w/v) yeast extract, 0.44%(v/v) glycerol; autoclave
To 900 ml of this medium add 100 ml of a sterile solution of 0.17 M KH₂PO₄, 0.72 M K₂HPO₄.

TSM buffer

100 mM Tris-HCl, 100 mM NaCl, 5 mM MgCl₂, pH 9.5

Vero cell medium

MEM supplemented with 7.5%(v/v) fetal calf serum

2.9. Antibodies**2.9.1. Primary antibodies**

| Name | Antigen | Description | Source/Reference |
|-----------|------------------------|---|---|
| mAb LP12 | VP5 | monoclonal mouse antibody against HSV1-VP5 | (Phelan et al., 1997) kindly provided by T. Minson, University of Cambridge, UK |
| α-NC1 | VP5 | polyclonal rabbit antibody against HSV1-VP5 | (Cohen et al., 1980) kindly provided by G. Cohen & R. Eisenberg, University of Pennsylvania, USA |
| α-VP26(C) | VP26 ⁹⁵⁻¹¹² | polyclonal rabbit serum against C-terminus of VP26 (aa 95-112) | (Desai et al., 1998) kindly provided by P. Desai, Johns Hopkins University, Philadelphia, USA |
| mAb DL6 | gD | monoclonal mouse antibody against HSV1 glycoprotein D | (Eisenberg et al., 1985) kindly provided by G. Cohen & R. Eisenberg, University of Pennsylvania, USA |
| R45 | gD | polyclonal rabbit serum against HSV1-gD | (Cohen et al., 1978) kindly provided by G. Cohen & R. Eisenberg, University of Pennsylvania, USA |
| mAb JL-8 | AcGFP1 | monoclonal mouse antibody against AcGFP, EGFP, ECFP, EYFP | Clontech; Mountain View, CA, USA (Living Colors™ Cat. No. 632381) |
| α-DIG-AP | dioxygenin | Fab fragment of an anti-dioxygenin IgG antibody from sheep, conjugated to alkaline phosphatase. | Roche; Mannheim, Germany (Cat. No. 11093274910) |

2.9.2. Secondary antibodies

| Species and antigen | Conjugate | Source |
|---------------------|--|---------------------------|
| goat-α-mouse | Lissamine-rhodamine sulfonyl chloride (LRSC) | Dianova, Hamburg, Germany |
| goat-α-mouse | Fluorescein isothiocyanate (FITC) | Dianova, Hamburg, Germany |
| goat-α-rabbit | alkaline phosphatase | Dianova, Hamburg, Germany |
| goat-α-mouse | horseradish peroxidase | Dianova, Hamburg, Germany |

2.10. Oligonucleotides

With the exception of CHN20, all oligonucleotides were purchased from MWG Biotech, Ebersberg, Germany and were “High Purity Salt Free” (HPSF[®]) purified after synthesis. Primer CHN20 was obtained from Operon, Huntsville, AL, USA. Bases not annealing are indicated in italics and restriction sites are underlined. Sequences are written in 5' to 3' direction. The *loxP* sites in oligos CHNLox1 and CHNLox2c are written in bold letters.

Materials

| | |
|------------------|--|
| CHNLox1 | AGC TGC GGC CGC ATA ACT TCG TAT AAT GTA TGC TAT ACG AAG TTA TTT AAT TAA TCT AGA GGG GCT AGC G |
| CHNLox2c | AAT TCG CTA GCC CCT CTA GAT TAA TTA AAT AAC TTC GTA TAG CAT ACA TTA TAC GAA GTT ATG CGG CCG C |
| CHN01 | CGT AGT CGA GCT AGT CGA TCG TAC GAT ACG TCA G |
| CHN02 | TCG ATC GCT AGT CGA TCT ACG TCG TAG ATG CTA C |
| CHN03-500 | NNN NNN CCT GCA GGA TGC CCG GCC GAT GAT GG |
| CHN04 | NNN NNN CCT GCA GGC TCG AGT GCG GGA CGG CCA TCG GGA CCG GAG G |
| CHN05 | NNN NNC TCG AGC CGC CCC AGC ACC GTT ACC ACC GAT AG |
| CHN06-500 | NNN NNN NGG TAC CCG CCG TGC TGA CCA GCC TAC |
| CHN07N | NNN NGC TAG CTG ATG TGC TTA AAA ACT TAC TCA |
| CHN08N | NNN NGC TAG CTG ATT CCC TTT GTC AAC AGC AAT |
| CHNHomL-S | GGC CGC TCG ACA GCG ACA CAC TTG CAT CGG ATG CAG CCC GGT TAA CGT GCC GGC ACT A |
| CHNHomL-A | GGC CTA GTG CCG GCA CGT TAA CCG GGC TGC ATC CGA TGC AAG TGT GTC GCT GTC GAG C |
| CHNHomR-S | CTA GAG GCC TGG GTA ACC AGG TAT TTT GTC CAC ATA ACC GTG CGC AAA ATG TTG TG |
| CHNHomR-A | CTA GCA CAA CAT TTT GCG CAC GGT TAT GTG GAC AAA ATA CCT GGT TAC CCA GGC CT |
| CHN09 | TCG ACC ATG GTG TAC AAC |
| CHN10 | TCG AGT TGT ACA CCA TGG |
| CHN13 | CGA CAC CCC CAT ATC GCT TCC CGA CCT CCG GTC CCG ATG GCC GTC CCG CAG GCC TGG TGA TGA TGG CGG GAT C |
| CHN14 | CGC GCA TGC CAA GCG CCC GGA CGC TAT CGG TGG TAA CGG TGC TGG GGC GGT CAG AAG AAC TCG TCA AGA AGG |
| CHN17 | CAA TAG GGA CTT TCC ATT G |
| CHN20 | TAA GGC AGT TAT TGG TGC C |
| CHN21 | ATG CCC GGC CGA TGA TGG |
| CHN22 | CGC CGT GCT GAC CAG CCT AC |
| CHN33 | CAG AGC GGA CCA ATG TG |
| CHN34 | GCG ACG CTA CGT GCA AC |
| CHN43 | CCT TCG CCC CAC ACA G |
| CHN43A | CGC TAT TTG GTG GGT GGT TG |
| CHN49 | GAA CCC TTT GGT GGG TTT ACG CGG GCA CGC ACG CTC CCA TCG CGG GCG CC G GCC TGG TGA TGA TGG CGG GAT C |
| CHN50 | TGG TGT GGT CTT TTA TTG ATT AAA ACA CCC CAG AAG GAA CTC CCC GGG CC T CAG AAG AAC TCG TCA AGA AGG |
| CHN73 | CCC ACA TCC GGG AAG ACG ACC AGC CGT CCT CGC ACC AGC CCT TGT TTT ACG TGA GCA AGG GCG AGG AG |
| CHN74 | CCC AAC CCC GCA GAC CTG ACC CCC CCG CAC CCA TTA AGG GGG GGT ATC TAC TTG TAC AGC TCG TCC ATG |
| CHN77 | TTC CGC TTC CGT TCC GCA T |
| CHN78 | CTT TCC GAT GCG ATC CCG A |
| CHN79 | GTC TCC CGA GCG TCA AAA TC |
| CHN80 | GCA AGG GCC TTG TTT GTC TG |

2.11. Organisms and plasmids

2.11.1. Eukaryotic cells

BHK-21 (American Type Culture Collection, ATCC CCL-10)

Kidney fibroblast cell line from *Mesocricetus auratus* (Syrian golden hamster)

PtK₂ (ATCC CCL-56)

Epithelial kidney cell line from *Potorous tridactylis* (potoroo)

Vero (ATCC CCL-81)

Epithelial kidney cell line from *Cercopithecus aethiops* (African green monkey)

2.11.2. Viruses

Virus mutants constructed during the course of this work are described in the results section.

HSV1-wildtype strain 17⁺ (Brown et al., 1973)

kindly provided by J.H. Subak-Sharpe and M. Murphy, MRC Virology Unit, Glasgow, UK

Fully sequenced HSV1 strain (McGeoch et al., 1988; McGeoch et al., 1986; McGeoch et al., 1985; Perry and McGeoch, 1988), GenBank accession number X14112.

HSV1-wildtype strain F (ATCC VR-733)

HSV1-wildtype strain KOS (ATCC VR-1493, Smith, 1964)

kindly provided by P. Spear, Northwestern University, Chicago, IL, USA

HSV1(KOS)tk12 (Warner et al., 1998)

kindly provided by P. Spear, Northwestern University, Chicago, IL, USA

Derived from HSV1(KOS). This virus lacks the viral thymidine kinase gene (UL23) and encodes β -galactosidase under the control of the HSV1 immediate-early promoter of ICP4.

HSV1-K Δ 26Z (Desai et al., 1998)

kindly provided by P. Desai, Johns Hopkins University, Baltimore, MD, USA

Derived from HSV1(KOS). The UL35 ORF is replaced by β -galactosidase, the virus has a Δ VVP26 phenotype.

HSV1-K26GFP (Desai and Person, 1998)

kindly provided by P. Desai, Johns Hopkins University, Baltimore, MD, USA

Derived from HSV1(KOS). The UL35 ORF is replaced by an N-terminal fusion of the EGFP ORF to UL35. The phenotype is a virus which carries GFPVP26 incorporated into the capsid.

2.11.3. Bacteria

All bacterial strains used are derivatives of *Escherichia coli* K12.

***E. coli* DH5 α** (Ausubel et al., 1997)

Genotype: F⁻ Φ 80d*lacZ* Δ M15 Δ (*lacZYA-argF*)U169 *deoR recA1 endA1 hsdR17*(rk⁻, mk⁺) *phoA supE44 thi-1 gyrA96 relA1* λ^- . Used for cloning plasmids.

***E. coli* DH10B** (Grant et al., 1990)

Genotype: F⁻ Φ 80d*lacZ* Δ M15 *mcrA* Δ (*mrr-hsdRMS-mcrBC*) Δ *lacX74 deoR recA1 endA1 araD139 Δ (*ara, leu*) 7697 *galU galK rpsL*(Sm^R) *nupG* λ^- . Used for maintaining and cloning of BACs.*

***E. coli* DY380** (Lee et al., 2001)

Genotype: F⁻ Φ 80d*lacZ* Δ M15 *mcrA* Δ (*mrr-hsdRMS-mcrBC*) Δ *lacX74 deoR recA1 endA1 araD139 Δ (*ara, leu*) 7649 *galU galK rspL*(Sm^R) *nupG* [*lci857 (cro-bioA) <> tetI*]. Used for maintaining and cloning of BACs.*

Derived from strain DH10B. *E. coli* DY380 contains a defective λ prophage inserted into the bacterial genome. The recombination genes *red $\alpha\beta\gamma$* are expressed under control of the λ PL promoter. This promoter is repressed by the temperature-sensitive repressor *cI857* at 32°C and derepressed at 42°C. When bacteria containing this prophage are kept at 32°C, no recombination proteins are produced. However, after a brief heat-shock at 42°C, a sufficient amount of recombination proteins is produced.

2.11.4. Plasmids

Plasmids constructed during the course of this work are described in the results section.

Cosmid set of HSV1 (Cunningham and Davison, 1993)

kindly provided by C. Cunningham, MRC Virology Unit, Glasgow, UK

The HSV1(17⁺) genome was cloned as a set of five overlapping cosmids.

Nucleotide numbers are based on the published HSV1(17⁺) sequence; Amp^R, Kan^R.

cos 6: nt 141,221 – 29,733

cos 28: nt 24,699 – 64,405
cos14: nt 54,445 – 90,477
cos56: nt 79,442 – 115,152
cos48: nt 107,496 – 144,681

pBAD-I-SceI (Tischer et al., 2006)

kindly provided by K. Tischer & K. Osterrieder, Cornell University, Ithaca, NY, USA

Plasmid containing an expression cassette for the homing endonuclease I-SceI (recognition sequence: TAGGGATAACAGGGTAAT) under the control of an L-arabinose inducible promoter; Amp^R; Figure 13.

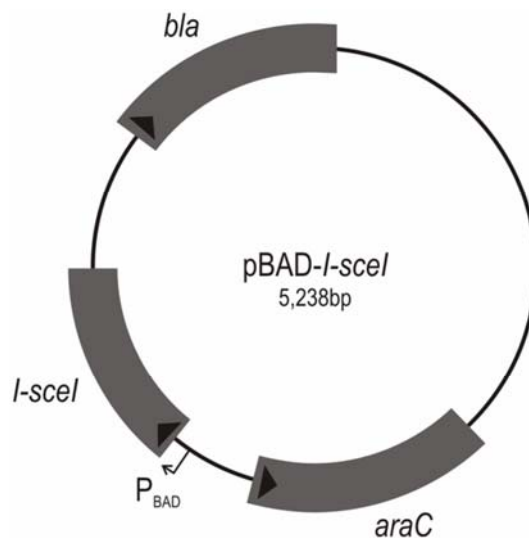


Figure 13: Plasmid map of pBAD-I-SceI. *bla*, β-lactamase (ampicillin resistance); P_{BAD}, arabinose inducible BAD promoter. (kindly provided by K. Tischer & K. Osterrieder, Cornell University, Ithaca, NY, USA)

pBlueLox (Smith and Enquist, 2000)

kindly provided by G.A. Smith, Department of Molecular Biology, Princeton University, Princeton, NJ, USA.

BAC-Vector based on pMBO131 (O'Connor et al., 1989) containing the BAC genes and a BAC replication origin, as well as a single *loxP* site and a β-galactosidase expression cassette from pSVβ*lacZ* (Clontech; San Jose, CA, USA) which expresses the gene under control of the SV40 early promoter.

pBlueLox-HomTK (Dr. Tanja Strive, Institute of Virology, Hannover Medical School)

This plasmid was constructed to insert the BAC sequences into the HSV1 genome by homologous recombination in cell culture (T. Strive, B. Sodeik & M. Messerle; personal communication; Figure 14). The kanamycin resistance gene from pEYFP-ER (Clontech, San Jose, CA, USA) was amplified with *TAT* *AGC GGC CGC* *TAC* *AGG GCG CGT CAG GTG GC*

and *AGC ATC TAG ATT AAT TAA* GTG ATG GCA GGT TGG GCG TCG CTT G, digested with *NotI* and *XbaI* and cloned into pUC18 Δ Ndelinker (Strive et al., 2002) resulting in pUC18 Δ Ndelinker-Kan. DNA sequences homologous to 2 kbp upstream and downstream of the UL23 locus were amplified from HSV1(17⁺) DNA. The 3' homology (HomA: nt 44591-46840) was amplified with GGT GGC TTG AGC CAG CGC GTC CAG and *CTA GCT AGC GTC GAC ATG CAT* GTC TTT ATC CTG GAT TAC GAC CAA TCG CC, digested with *XbaI* and *NheI* and ligated into *XbaI* and *NdeI* cut pUC18 Δ Ndelinker-Kan. The 5' homology (HomB2: nt 47561-49773) was amplified with AAA *CAT ATG TCG ACG* TAG ACG ATA TCG TCG CGC GAA CCC AGG and *AAG GGC CCT TAA TTA ACG* TGG TGC ATC AGC GTG GCG ATC ACG ATG TGC, digested with *Bsp120I* and *NdeI* and ligated into the *NotI* and *NdeI* cut product of the previous ligation resulting in pHomTK. The homology cassette was cut out from pHomTK with *SaI* and cloned into the *SaI* site of pBlueLox, yielding pblueLox-HomTK. For the insertion of BAC sequences into HSV1(17⁺), virus DNA and linearised pblueLox-HomTK were cotransfected into Vero cells. After complete CPE, cells and supernatant were harvested. Recombinant virus was identified by blue-gal staining of virus plaques to detect β -galactosidase activity (cf. chapter 3.2.5).

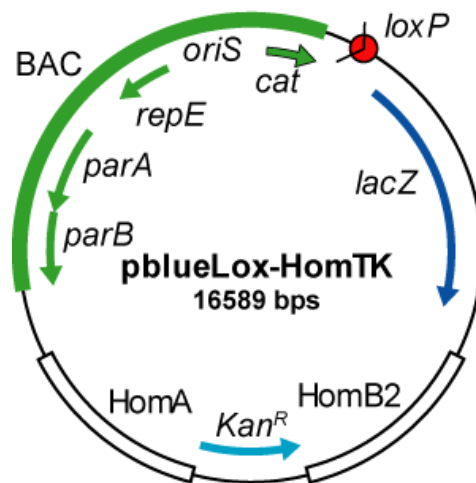


Figure 14: Map of pBlueLox-HomTK. *lacZ*, β -Galactosidase; *Kan^R*, kanamycin resistance; *cat*, chloramphenicol resistance; *parA/parB/repE/oriS*, BAC genes and BAC replication origin; *loxP*, Cre recombinase recognition site; *HomA* and *HomB2*, 2 kbp sequences homologous to sequences up- and downstream of UL23 (T. Strive, B. Sodeik & M. Messerle; personal communication).

pCreIn (Smith and Enquist, 2000)

kindly provided by G.A. Smith, Department of Molecular Biology, Princeton University, Princeton, NJ, USA
 Plasmid carrying Cre recombinase under the control of a CMV immediate early promoter. The Cre ORF carries an intron, so a functional recombinase is only synthesised in eukaryotes; Kan^R.

pCP16-HL

kindly provided by M. Messerle & E. Borst, Institute of Virology, Hannover Medical School
 modified from pCP16 (Cherepanov and Wackernagel, 1995) by Markus Wagner (Ludwig-Maximilians-Universität München, Munich, Germany). Tetracylin resistance gene flanked by two *flr* sites; Tet^R.

pEP-EGFP-in

kindly provided by K. Tischer & K. Osterrieder, Cornell University, Ithaca, NY, USA
 Template plasmid for the introduction of the enhanced green fluorescent protein (GFP) sequence into a BAC via “en passant” mutagenesis (Tischer et al., 2006). The EGFP ORF is interrupted by a kanamycin resistance cassette in apposition to a recognition site for the homing endonuclease I-SceI. Flanking the resistance gene and restriction site, 72 bp of the GFP sequence are duplicated. During “en passant” mutagenesis the BAC recombines via this duplicate by homologous recombination; Amp^R, Kan^R; Figure 15

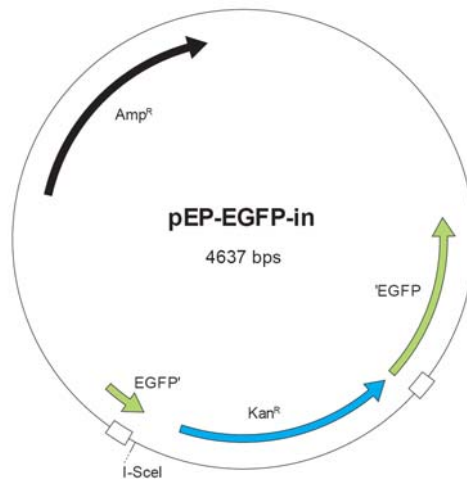


Figure 15: Plasmid map of pEP-EGFP-in. EGFP, enhanced green fluorescent protein ORF; Kan^R, kanamycin resistance; Amp^R, ampicillin resistance. The duplicate GFP sequences for recombination are indicated by white boxes.

pECFP-N1 (Clontech, San Jose, CA, USA)

Enhanced cyan fluorescent protein with N-terminal multiple cloning site; Kan^R.

pEGFP-N1 (Clontech, San Jose, CA, USA)

Enhanced green fluorescent protein with N-terminal multiple cloning site; Kan^R.

pEYFP-N1 (Clontech, San Jose, CA, USA)

Enhanced yellow fluorescent protein with N-terminal multiple cloning site; Kan^R.

pK26GFP (Desai and Person, 1998; Figure 16)

kindly provided by P. Desai, Johns Hopkins University, Baltimore, MD, USA

A 2.7 kbp *EcoRI/NotI* fragment of HSV1, strain KOS encompassing UL35 (VP26) and the C-terminal coding sequences of UL34 as well as of UL36, was cloned in pUC19 and the coding sequence of GFP was inserted into the 5' end of the UL35 ORF after codon 4, thus coding for a GFPVP26 fusion protein; Amp^R.

pKD46 (Datsenko and Wanner, 2000)

kindly provided by M. Messerle & E. Borst, Institute of Virology, Hannover Medical School

Plasmid carrying the recombination functions *redαβγ* from bacteriophage λ under the control of an L-arabinose induced promoter. It displays a temperature-sensitive mode of replication and replicates only at 30°C; Amp^R, ori^{ts}.

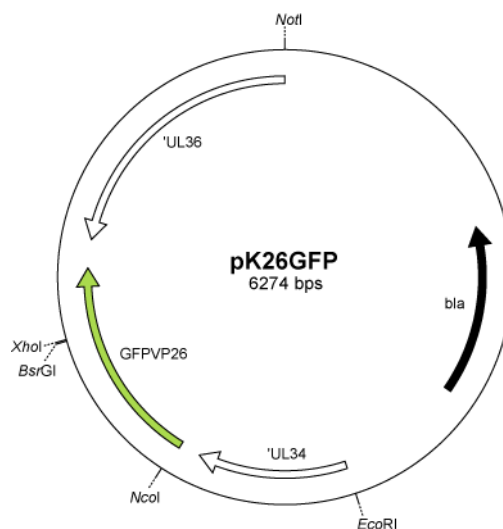


Figure 16: Plasmid map of pK26GFP. An *EcoRI/NotI* fragment of HSV1(KOS) was cloned in pUC19 and GFP was inserted at the N-terminus of VP26; bla, ampicillin resistance.

pLoCMV-VP1/3 (Figure 17)

This plasmid was constructed by Dr. Klaus Breiner in the laboratory of Prof. Ari Helenius (Swiss Federal Institute of Technology, Zürich, Switzerland; personal communication). A 12 kbp *HindIII/NheI* fragment carrying UL33 to UL36 (VP1/3) of HSV1(17⁺) was cloned into pShuttle (Stratagene, La Jolla, CA, USA) behind a CMV promoter; Kan^R.

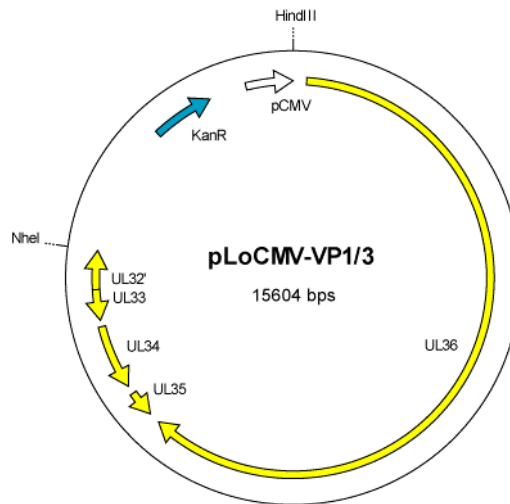


Figure 17: Plasmid map of pLoCMV-VP1/3. The ORFs UL33-UL36 of HSV1 are cloned completely, the 3' end of the UL32 ORF is truncated. pCMV, cytomegalovirus immediate early promoter; Kan^R, kanamycin resistance.

pRpsLneo (Gene Bridges, Dresden, Germany)

Template plasmid carrying a selection/counterselection cassette coding for kanamycin resistance and the *rpsL* gene for gain of streptomycin sensitivity in *E. coli* with an *rpsL* mutation. It displays a temperature-sensitive mode of replication and replicates only at 30°C; Kan^R, ori^{ts}.

pRSETB-mRFP1 (Campbell et al., 2002)

kindly provided by R. Y. Tsien, Department of Pharmacology, University of California, La Jolla, CA

Bacterial expression plasmid carrying His₆-tagged monomeric red fluorescent protein (mRFP1); Amp^R.

pST-SNR

kindly provided by M. Messerle & E. Borst, Institute of Virology, Hannover Medical School

Based on pST76-K (Posfai et al., 1997) and modified by Dr. Martin Messerle (Institute of Virology, Hannover Medical School; personal communication) this plasmid displays a temperature-sensitive mode of replication, replicates only at 30°C, and provides a fusion

protein coding for kanamycin resistance and levansucrase (sucrose sensitivity) as well as the *recA* gene; Kan^R, ori^{ts}.

pUC18 (Invitrogen, Leek, Netherlands)

Cloning plasmid, Amp^R.

pYEbac102 (Tanaka et al., 2003)

kindly provided by M. Messerle & E. Borst, Institute of Virology, Hannover Medical School

Bacterial artificial chromosome containing the HSV1, strain F genome. For cloning, the BAC sequences were inserted between UL3 and UL4 and flanked by *loxP* sites, so they are excised after expression of Cre recombinase.

3. Methods

3.1. Eukaryotic cell culture

Eukaryotic cells were grown in 10 cm dishes in Minimum essential medium containing Earle's balanced salt solution, non-essential amino acids and glutamine at 37°C and 5% CO₂. Media for BHK-21 or PtK₂ cells were supplemented with 10%(v/v) fetal calf serum (FCS), Vero cell medium contained 7.5%(v/v) FCS. The cells were passaged twice a week. After washing with PBS, 1 ml Trypsin/EDTA was added. Having detached, the cells were resuspended in medium and seeded into new culture vessels. The cells were cultured until passage 40 to 50. For long-term storage in liquid nitrogen, cells from a 10 cm dish were trypsinised, pelleted and resuspended in 2 ml of MEM with 20%(v/v) FCS and 10%(v/v) DMSO.

3.2. Virological techniques

3.2.1. Preparation of virus stocks

Virus stocks were prepared as previously described (Döhner et al., 2006; Döhner et al., 2002; Sodeik et al., 1997). All experiments were carried out with virus stocks of passage 2 or 3. BHK-21 cells were grown in 175 cm² flasks to almost confluency (1 to 2 x 10⁷ cells/flask). Prior to inoculation the cells were washed with 30 ml PBS, then 5 ml RPMI/BSA containing 0.01 pfu/cell virus were added, and the virions were allowed to attach to the cells on a slow rocking platform at room temperature for 1 h. Then, 25 ml of BHK-21 growth medium were added, and the cells were further incubated at 37°C and 5% CO₂. Dependent on the viral growth kinetics the virions were harvested from the medium when complete cytopathic effect had developed, usually within 2 to 3 days post infection.

The infected cells were detached from their substrate by knocking, cells and medium were transferred to Beckman JA-10 centrifuge rotor beakers and centrifuged at 2,000 rpm (439 x g) for 10 min at 4°C. The cell pellets were resuspended in an equal volume of MNT buffer (section 2.8) and kept at 4°C for few days or were aliquoted, snap-frozen in liquid nitrogen and stored for up to 2 years at -80°C. The supernatants were transferred to Beckman Type 19 rotor beakers and centrifuged at 12,000 rpm (13,531 x g) for 1.5 h at 4°C. The pellets (referred to as medium pellets) were carefully resuspended in a small volume of MNT buffer and either aliquoted, snap-frozen in liquid nitrogen and stored at -80°C, or further purified by density-gradient ultracentrifugation. For this purpose, the medium pellet suspensions were layered onto a linear 10-40%(w/v) gradient of Nycodenz in MNT buffer and centrifuged at 20,000 rpm (52,931 x g) for 105 min in a Beckman SW28 rotor at 4°C.

Virus was harvested as a light scattering band from the middle of the gradient, aliquoted, snap-frozen in liquid nitrogen and long-term stored at -80°C .

3.2.2. Plaque titration

The titers of viral preparations were determined as previously described (Döhner et al., 2002). Vero cells were seeded in 6-well plates with about 3 to 5×10^5 cells per well and grown at 37°C and 5% CO_2 for 20 h to almost confluency. The virus sample to be titered was diluted in a 10-fold dilution series in RPMI/BSA. Prior to inoculation, the cells were washed with 2 ml per well RPMI/BSA, then 500 μl per well of the virus dilution was added onto the cells in duplicates or triplicates and the cells were gently rocked at room temperature for 1 h. The inoculum was aspirated, and 2 ml per well Vero medium containing 20 $\mu\text{g/ml}$ purified human IgGs were added. The amount of HSV1-antibodies in such a human IgG preparation is sufficient to neutralise virions, which have been released into the medium. Thus, viral spread can only occur from cell to cell, resulting in plaque formation derived from the infection of a single cell. After 3 days at 37°C and 5% CO_2 when plaques were readily visible by eye, the medium was removed, and 1 ml per well 9.25% (w/v) formaldehyde in PBS were added for 10 min to fix the cells. Alternatively, the cells were fixed with 1 ml per well of -20°C absolute methanol for 2-3 min. The fixative was then removed and the cell lawn was stained with 0.1% crystal violet (stock solution: 5% [w/v] crystal violet in ethanol). Plaques were counted and the viral titer was calculated by multiplying the double mean plaque number of the duplicates or triplicates with the dilution factor. The infectivity is described as the number of plaque forming units (pfu) per ml.

3.2.3. Real time detection PCR of viral genomes

The amounts of viral genomes in HSV1 preparations were determined by a quantitative real time detection PCR which was developed by Dr. D. Petzold (Institute of Virology, Hannover Medical School) and performed by Sabine Hübner (Institute of Virology, Hannover Medical School). (Döhner et al., 2006)

3.2.4. Determination of viral growth kinetics

Viral growth kinetics were determined on BHK-21 cells by a single-cycle approach (Harland and Brown, 1998). BHK-21 cells were plated in 10 cm dishes in a 1:2 dilution and grown to almost confluency which accounts to app. 6 to 8×10^6 cells per dish. The cells were washed with 10 ml PBS then 2 ml RPMI/BSA containing 5 pfu/cell of the virus to be assayed

were added and shaken at room temperature for 1 h. The inoculum was removed and 10 ml BHK-21 medium were added after washing the cells with 10 ml RPMI/BSA. In 3 h intervals up to 36 h p.i., 250 µl medium samples were taken and replaced by 250 µl of fresh medium. The medium samples were snap-frozen in liquid nitrogen and stored at -80°C until their titer was determined.

3.2.5. Plaque purification

Vero cells were seeded into 6-well plates with about 4 to 6 x 10⁵ cells per well and grown at 37°C and 5% CO₂ over night. When the cells were confluent, they were washed with 2 ml per well RPMI/BSA and inoculated with 1 ml per well of RPMI/BSA with a dilution of the virus sample to be purified. After 1 h at room temperature on a rocking platform, the inoculum was aspirated and replaced by 2 ml per well Vero medium with 20 µg/ml human IgG. After 2 to 3 days at 37°C, 5% CO₂ plaques became visible.

To identify plaques which expressed β-galactosidase, the cells were stained with blue-gal. 2%(w/v) low-melting-point agarose were dissolved by cooking, cooled down to 37°C and then mixed with an equal volume of 37°C warm 2x MEM with non-essential amino acids, penicillin/streptomycin, 15%(v/v) FCS, 4 mM glutamine and 0.6 mg/ml blue-gal. The IgG-containing Vero medium was sucked off the cells and replaced with 2 ml of substrate agarose. The agarose was left to harden at 4°C in the fridge, then overlaid with 1 ml of Vero medium with 20 µg/ml human IgG and returned to 37°C, 5% CO₂ for 2 to 3 days.

Cells infected with β-galactosidase harbouring virus were stained blue. Using a cut blue pipette tip, the plaque was punched out from the cell lawn and eluted overnight in 200 µl of Vero medium. In the next purification round, a dilution series was set up from the eluted cells of the plaque and the procedure was repeated, until the number of unstained plaques became less than 1%.

3.2.6. Isolation of viral DNA

Viral DNA was prepared from HSV1-infected BHK-21 cells, the by-product of a virus stock preparation. 3 ml of a cell suspension, usually containing 1 to 2 x 10⁸ cells, were mixed with 3 ml 1%(v/v) Triton X-100 in RSB buffer, vortexed and incubated on ice for 10 min to lyse the cells. Nuclei were pelleted from the lysate in an Eppendorf 5810R centrifuge for 10 min at 4,000 rpm and 4°C. The nuclei pellet was resuspended in 6 ml of 0.5% Triton X-100 in RSB and again centrifuged. The supernatants were pooled and capsids were pelleted from the cytoplasmic lysate in a Beckman SW40Ti rotor at 30,000 rpm (113,652 x g) for 90 min at 4°C. The pellet was soaked overnight at 4°C in 800 µl of NTE buffer and then resuspended

to homogeneity. To solubilize the capsids and release the viral DNA, 200 μ l of 5x SDS/EDTA solution (12.5%[w/v] SDS, 50 mM EDTA in NTE buffer) were added, carefully mixed by inversion and incubated at 37°C for 10 min. The lysate was extracted twice with 1 ml phenol/chloroform/isoamyl alcohol by inverting 50 times and centrifuging in a table-top centrifuge for 5 min at 14,000 rpm. The DNA was precipitated from the aqueous phase by adding 800 μ l isopropanol and centrifuging 15 min at 14,000 rpm in a table-top centrifuge. The DNA pellet was washed with 1 ml 70%(v/v) ethanol, dried and resuspended in 100 μ l 10 mM Tris-HCl, pH 8, 50 μ g/ml RNase A at 4°C overnight. Viral DNA preparations were stored at 4°C to prevent shearing by ice crystal formation.

3.2.7. Isolation of small nuclear DNA ("Hirt-extraction")

Following the protocol of Hirt (1967), small nuclear DNA was extracted from the nuclei of cells infected with HSV1, thus isolating viral DNA and DNA replication intermediates. Vero cells in a confluent 10 cm dish were washed with 10 ml PBS and then inoculated with 2 ml RPMI/BSA containing HSV1 with an MOI of 20 pfu/cell. After 1 h rocking at room temperature, 8 ml of Vero medium were added, and the cells were incubated for 1 h at 37°C, 5% CO₂.

The cells were removed from their substrate by trypsinisation, resuspended with 9 ml Vero medium and pelleted at 300 x g for 5 min. The cell pellet was washed with 5 ml Vero medium, pelleted again, then washed with 5 ml PBS and pelleted. The cell pellet was carefully resuspended in 500 μ l 20 mM EDTA, pH 8 and transferred to a 2 ml reaction tube. To lyse the cells and nuclei, 500 μ l 1.2%(w/v) SDS were added and carefully mixed by inverting. 660 μ l of 5 M NaCl were added and the mixture was incubated for 4 h at 4°C to precipitate the cellular DNA. The precipitate was pelleted at 14,000 rpm for 30 min at 4°C, and the supernatant was extracted with Phenol/Chloroform. The aqueous phase containing the viral DNA was transferred to a fresh 2 ml reaction tube, 20 μ g glycogen were added as a carrier and the DNA was precipitated with 0.8 volumes of isopropanol. The pellet resulting after 20 min centrifugation at 14,000 rpm was washed with 1 ml 70%(w/v) ethanol overnight at room temperature and centrifuged at 13,000 rpm for 15 min the following day. After the ethanol had been removed, the pellet was dried and dissolved in 100 μ l of warmed 10 mM Tris-Cl, 1 mM EDTA, pH 8.5.

3.2.8. Virus entry experiments

3.2.8.1. Quantitative viral gene expression assay with β -Galactosidase

HSV1 mutants encoding β -galactosidase under the control of an immediate early promoter provide a quantitative measure for the expression of nuclear-imported viral DNA, for which efficient nuclear targeting of capsids is a prerequisite (Mabit et al., 2002; Warner et al., 1998). Thus, the effect of reagents influencing viral or cellular functions during entry can be quantified biochemically.

The day before, PtK₂ cells were seeded in 24-well plates at a density of 5×10^4 cells per well and grown at 37°C, 5% CO₂. By approximation, the cell density doubles over night. For each condition to be tested, 2 x 4 wells were seeded in parallel on two different plates to independently determine β -galactosidase expression with O-nitrophenyl- β -D-galactopyranoside (ONPG), and the corresponding cell density with crystal violet. The experiments were performed on a 37°C water bath. When the influence of inhibitors was to be tested, the cells were incubated in CO₂ independent medium with 0.2%(w/v) BSA containing the inhibitor for 1 h at 37°C. To prepare the cells for virus binding, they were washed with cold CO₂ independent medium/0.2%(w/v) BSA and kept on ice for 15 min. Then 0.2 ml of CO₂ independent medium/0.2%(w/v) BSA containing a β -galactosidase-expressing virus at an MOI of 10-20 pfu/cell and the inhibitor were added, and the virus was allowed to bind to the cells by 2 h rocking on ice. The cells were washed three times with CO₂ independent medium/0.2%(w/v) BSA and then incubated at 37°C for 4 h.

To monitor β -galactosidase expression, the cells were lysed and the conversion of ONPG to o-nitrophenol was measured photometrically. The cells were washed with PBS, then lysed with 0.5 ml per well of 1 mg/ml BSA, 0.5%(w/v) Triton X-100, protease inhibitors for 15 min at 37°C. To assay the amount of β -galactosidase expressed, 200 μ l per well of ONPG-substrate solution were added to the lysates (Stock solution: 4 mg/ml ONPG in 0.1 M Na-phosphate buffer, pH 7.5; add 1/7 volume PBS before use). After 3 h incubation at room temperature the absorption of the solution in the wells was measured photometrically at a wavelength of 420 nm.

The cell viability was measured by crystal violet staining. The cells were washed with PBS, then fixed for 20 min with 1 ml per well of 3%(w/v) paraformaldehyde in PBS. Then, the fixative was replaced with 0.5 ml per well PBS and 0.5 ml per well 0.025%(w/v) crystal violet in H₂O (Stock solution 5% [w/v] crystal violet in ethanol) were added to stain the cells for 10 min. After overnight drying, the crystal violet was dissolved in 0.5 ml per well of dried, absolute ethanol and the absorption of the wells was measured at 595 nm wavelength.

3.2.8.2. Monitoring virus entry by fluorescence microscopy

Fluorescence tagged HSV1 proteins were observed by fluorescence light microscopy. Additionally cellular and viral structures were labelled with specific primary antibodies and secondary antibodies carrying a fluorophor. Cells were plated on glass coverslips, infected and fixed. The day before 5×10^4 PtK₂ cells per well were seeded on glass coverslips in 24-well plates. Inoculation and inhibitor treatment was performed according to the β -galactosidase expression based assay (cf. section 3.2.8.1). Usually, the inoculation was performed at an MOI of 20 pfu/cell. For description of microscopy, cf. section 3.6, page 73.

3.3. Molecular biological techniques

Unless otherwise stated, most molecular biological techniques were based on standard methods as described in Ausubel et al. (1997) and Mülhardt (2002).

3.3.1. Growth and culture of bacteria

E. coli were grown on LB-agar plates (section 2.8) or in liquid culture. The growth temperature depended on the bacterial strain and the type of plasmid. For plasmid and BAC preparations LB-medium (section 2.8) was used; for the generation of electrocompetent cells, bacteria were grown in TB-medium. When casting LB-agar plates containing antibiotics, the boiled liquid agar was cooled down to 45°C prior to adding the antibiotics. For blue/white screening of bacteria on plates, 60 μ g/ml X-Gal and 0.1 mM IPTG were added to the agar.

3.3.2. Preparation of plasmids and BACs

Plasmid Mini preparations were prepared from 2-5 ml overnight cultures using the Qiaprep[®] Spin Miniprep Kit, Midi preparations from 50-100 ml overnight cultures using the GenElute[™] HP Plasmid Midiprep Kit and Maxi preparations of BACs were prepared from 500 ml overnight cultures with the NucleoBond[™] BAC 100 Kit. BAC-DNA preparations were stored at 4°C to prevent shearing by ice crystals. In each case the preparations were based on an alkaline lysis approach and performed according to the manufacturer's instructions.

For screening large numbers of plasmids by Mini preparations and for all BAC Mini preparations, the bacterial lysates were not purified over silica columns, but the DNA was directly precipitated by isopropanol. The solutions S1, S2 and S3 were derived from the NucleoBond[™] BAC 100 Kit. Overnight cultures of *E. coli* harbouring plasmids (2-5 ml) or BACs (10 ml) were centrifuged at 4,000 rpm for 15 min to pellet the bacteria. The bacterial

pellet was resuspended in 200 µl of solution S1 and transferred to a 2 ml tube. 300 µl of solution S2 were added, the solution was inverted six times and the cells were lysed for 5 min at room temperature. Then 300 µl solution S3 were added, the solution was inverted six times and then further incubated on ice for 10 min. The precipitate was pelleted at 14,000 rpm for 15 min, and the supernatant was transferred to a fresh 2 ml tube using a cut blue pipette tip. The DNA was precipitated with 900 µl isopropanol and pelleted at 14,000 rpm for 15 min. The DNA pellet was washed with 1 ml 70%(v/v) ethanol, dried and resuspended in 50 µl of DNA resuspension buffer (section 2.8).

3.3.3. DNA sequencing

Sequencing of plasmids and PCR products was carried out by Heidi Pommer from the Institute of Virology, Hannover Medical School, or by SEQLAB GmbH Göttingen, Germany.

3.3.4. Gel extraction of DNA

DNA was extracted from agarose gels using the Qiaquick® Gel Extraction Kit according to the manufacturer's instructions.

3.3.5. Cleaning of DNA from enzymatic reactions

After enzymatic reactions DNA was cleaned using the Qiaquick® PCR Purification Kit according to the manufacturer's instructions.

3.3.6. Agarose gel electrophoresis of DNA

For separation of DNA fragments in the PerfectBlue™ Mini S gel system 30 ml gels of 1-2%(w/v) agarose in 1x TAE buffer were used. Electrophoresis was performed at a constant voltage of 180 V for 15-20 min. In the PerfectBlue™ Maxi S gel system 250 ml gels of 0.5-0.8%(w/v) agarose in 0.5x TBE were run at a constant voltage of 70 V for 16 h or at 65 V for 18 h. Ethidium bromide at a concentration of 0.5 µg/ml was added to the agarose prior to casting the gel. After electrophoresis, the gels were sometimes restained by soaking in 0.5 µg/ml ethidium bromide for 30 min and destaining in H₂O for 30 min.

3.3.7. Polyacrylamide gel electrophoresis of DNA

DNA fragments smaller than 200 bp were separated by acrylamide gel electrophoresis. For this purpose the Hoefer™ SE250 system was used. Gels were cast in 0.5x TBE buffer

with a concentration of 20%(w/v) acrylamide and electrophoresis was performed at a constant current of 25 mA per gel under cooling for 45 to 60 min. After electrophoresis the gel was stained by soaking in 0.5 µg/ml ethidium bromide for 30 min and destaining in H₂O for 30 min.

3.3.8. Treatment of of BACs and viral DNA with restriction enzymes

For restriction analyses of HSV1-BACs, BAC-DNA was prepared from 5 ml overnight culture per gel lane as described above. BAC-DNA in a volume of 25 µl was digested with 20 U of restriction enzyme in a total volume of 30 µl for 4-5 h at 37°C. For digestions of viral DNA, 2 µg of DNA were diluted with H₂O to 25 µl. The restriction fragments were separated on 0.5-0.8%(w/v) agarose in 0.5x TBE buffer using the Maxi S or Mini L gel electrophoresis system.

3.3.9. Treatment of plasmids with restriction enzyme

1-2 µg of plasmid DNA were digested in a total volume of 10-20 µl using 2-5 U of enzyme and the reaction buffer supplied by the manufacturer. The reaction was allowed to proceed for 1-2 h at the appropriate temperature. The DNA fragments were separated on 1 to 2%(w/v) agarose in 1x TAE buffer using the Mini S gel electrophoresis system.

3.3.10. Polymerase chain reaction (PCR)

PCR was used for preparation of DNA fragments for cloning and directed mutagenesis as well as for diagnostic purposes. The reactions were carried out in thin-walled 200 µl round-capped reaction tubes in a temperature cycler. Each PCR reaction commenced with a 5 min denaturation step at 95°C followed by 30 cycles of 1 min denaturation at 94°C, 1 min primer annealing at the appropriate temperature (see below) and 1-4 min (see below) at 72°C for elongation. After the cycles the polymerase reaction was completed at 72°C for 10 min.

The annealing temperature in the PCR reaction depended on the melting temperature T_m of the annealing bases of the oligonucleotide primers, which was calculated to $T_m[°C] = 81.5 + 16.6 \times \log_{10} [I^+] + 0.4 \times (\%G+C) - 600/N$, with N being the number of annealing nucleotides and $[I^+]$ the molarity of monovalent cations in the reaction mixture (Müller, 2001). Both T_m values of the primers should not differ too much, ideally the appropriate annealing temperature in the PCR reaction should be 5°C below the T_m of both primers. The elongation time depended on the polymerase used and the length of the PCR product, and was arbitrarily set to 1 min per 1000 bp of product. Desoxynucleotides were added at a

concentration of 200 μM of each dATP, dCTP, dGTP and dTTP. Oligonucleotide primers had a concentration of 0.6-0.8 μM . 2.5 U of PCR polymerase were added. In the case of *Pfu* and *Taq* polymerase, the enzyme was added after the initial denaturation step, *Pwo* polymerase was added on ice prior to cycling. With sterile, double-distilled H_2O or *aqua ad iniectionabilia* the reaction mix was filled up to its final volume. The DNA polymerases were used in the buffer systems supplied by the manufacturers and the reactions were performed in a total volume of 50 or 100 μl . Due to the high GC-content of HSV1-DNA (68%) (McGeoch et al., 1988; McGeoch et al., 1986; McGeoch et al., 1985; Perry and McGeoch, 1988), dimethyl sulfoxide was added in concentrations up to 10%(v/v) to allow specific amplification. In some cases also the Mg^{2+} concentration had to be optimised.

The nature of the template depended on the application of the PCR. For cloning purposes, purified viral or plasmid DNA was used at an amount of 5 ng (plasmids) to 100 ng (viral DNA) per reaction. BAC-containing bacterial colonies were screened for the presence of correct sequences by direct colony PCR. Colony material was resuspended in 10 μl of sterile H_2O , boiled at 95°C for 5 min, then centrifuged at 14,000 rpm for 5 min. The supernatant was used as PCR template.

3.3.11. Dephosphorylation of DNA

The 5' ends of linear DNA were dephosphorylated with 0.5 U calf intestine alkaline phosphatase (CIAP) for 30 min at 37°C in the reaction buffer supplied by the manufacturer. The enzyme was inactivated by heating at 85°C for 10 min and the DNA was cleaned with a DNA purification kit.

3.3.12. Filling of recessed DNA ends

DNA with recessed 3' ends was filled using 5 U of the Klenow fragment of *E. coli* DNA Polymerase I in the presence of 50 μM of each dATP, dCTP, dGTP, dTTP. The reaction was carried out in the reaction buffer supplied by the manufacturer at 37°C for 30 min. The enzyme was inactivated by heating at 70°C for 10 min, and the DNA was cleaned with a DNA purification kit.

3.3.13. Ligation

3.3.13.1. Cloning of PCR products and DNA fragments

DNA ligations were performed with T4 DNA Ligase in a total volume of 20 μl . Before the ligation of DNA into cloning vectors, the target plasmid and the insert DNA were either

digested with restriction enzymes that provided compatible ("sticky") ends, or the DNAs were ligated blunt-ended. In a "sticky-end" ligation 20 ng of vector DNA were incubated with a 3-fold molar excess of insert DNA or with H₂O as control in the presence of 5 U T4 DNA ligase, and the provided ligase buffer at room temperature for 1-2 h. In "blunt-end" ligations, the insert was present in up to 20-fold molar excess, 5%(w/v) Polyethylen glycol 4000 (PEG4000) were added, and the reaction occurred overnight at 16°C. The ligation reaction was inactivated by heating at 65°C for 10 min. In the case of "blunt-end" ligations, the PEG4000 was removed by extracting the mixture with chloroform.

3.3.13.2. Linker ligation

Single-stranded oligonucleotide linkers had to be annealed before they could be ligated into a vector. Therefore 10 µg of each oligonucleotide together with 10 mM MgCl₂ were mixed with water to a total volume of 100 µl and boiled for 3 min at 100°C. The mixture cooled down very slowly by letting the reaction tube swim in a beaker with boiling water, which was placed in a 4°C cold room. The linker solution was diluted 10-fold and 100-fold and 1 µl of each dilution was used as insert in ligation reactions with 20 ng of cut, phosphorylated vector.

3.3.14. Southern blotting

DNA probes for Southern hybridisation were labelled with digoxigenin (DIG)-coupled desoxynucleotides in a PCR reaction according to the manufacturer's instructions. A PCR reaction was set up using primers specific for the DNA probe to be synthesised. DIG-labelled desoxynucleotides were contained in the reaction mixture and thus incorporated into the probe. Transfer of DNA to positively charged nylon membranes and detection of hybridised probes was carried out as recommended in the DIG Application Manual for Filter Hybridization (2003; Roche, Mannheim, Germany, pp.88-96/119-123)

After separation of DNA fragments on agarose gels, the gel was soaked 30 min in 0.25 M HCl to depurinate, and thus fragment the DNA. By this treatment, fragments formerly larger than 5 kbp migrate out of the gel more efficiently. Then the DNA was denatured by 30 min soaking in 0.5 M NaOH, 1.5 M NaCl, and finally the gel was soaked in 0.5 M Tris-HCl, 1.5 M NaCl, pH 7 for 30 min. The DNA was blotted overnight onto positively charged nylon membrane by capillary transfer with 20xSSC buffer. After transfer, the membrane was incubated for 30 min at 42°C in prehybridisation solution (5x SSC, 5x Denhardt's solution, 1% [w/v] SDS, 50% [v/v] formamide, 0.1 mg/ml sheared single-stranded salmon sperm DNA). Then 5 µl of a denatured DIG-labelled DNA-probe were added, and the membrane was further incubated for 6 h at 42°C. The membrane was washed twice for 5 min with low

stringency buffer (2xSSC, 0.1%[w/v]SDS), then twice for 15 min with high stringency buffer (0.5xSSC, 0.1%[w/v] SDS) heated to 65°C. The membrane was dried between Whatman-Paper sheets and stored at 4°C.

For detection the membrane was washed for 2 min in washing buffer (0.15 M maleic acid, 0.1 M NaCl, pH 7.5, 0.3%[v/v] Tween 20) then incubated for 30 min in 1x blocking solution (Roche, Mannheim, Germany) in washing buffer. For 30 min the membrane was shaken with 20 ml of a 1:3000 dilution of an α -DIG antibody coupled to alkaline phosphatase in 1x blocking solution followed by 2x 15 min washing with washing buffer. The alkaline phosphatase was detected by a colour reaction with nitroblue tetrazolium salt (NBT) and 5-Bromo-4-chloro-indolyl-3-phosphate (BCIP). The membrane with bound α -DIG antibodies was equilibrated 3 min with TSM buffer and stained in the dark with 0.165 μ g/ml BCIP, 0.305 μ g/ml NBT in TSM. The colour reaction was stopped by washing with water.

3.3.15. Transformation of bacteria

E. coli were transformed by electroporation. For the preparation of electrocompetent cells, 2 ml of LB medium with or without antibiotics were inoculated with a fresh *E. coli* colony and shaken overnight at the appropriate temperature. The next day, 100 ml of TB medium (section 2.8) were inoculated with 100 μ l of the overnight culture and shaken until the OD₆₀₀ reached 2. Then the bacterial suspensions were chilled on ice and pelleted at 4,000 rpm for 15 min at 4°C. The bacterial pellets were resuspended in 50 ml of ice-cold sterile water and repelleted. After 3 to 4 washing steps, the pellet was resuspended in 15 ml of ice-cold sterile 10%(v/v) glycerol and again pelleted. The last pellet was resuspended in an equal amount of ice-cold sterile 10%(v/v) glycerol, aliquoted on ice in 50 μ l and either used immediately or snap frozen in liquid nitrogen and stored at -80°C.

To reduce their salt content, the DNA solutions were microdialysed in some cases prior to transformation. 10-20 μ l were pipetted onto a nitrocellulose filter disc of 47 mm diameter and 0.025 μ m pore size floating on H₂O and left standing for 20 min. The droplet was carefully pipetted from the filter disc and used for transformation. DNA to be transformed was mixed with 50 μ l of electrocompetent bacteria, which had been thawed on ice. The suspension was pipetted into a pre-chilled electroporation cuvette with an electrode distance of 2 mm, and pulsed in an electroporation unit with 2.5 kV, 200 Ω , 25 μ F. Immediately, 1 ml of SOC medium (section 2.8) were poured into the cuvette, and the bacterial suspension was shaken for 1 h at 37°C or 30°C. Depending on the efficiency of transformation and the origin of the transformed DNA, different amounts of the bacteria were then plated onto the appropriate agar plates and incubated.

3.4. BAC mutagenesis

3.4.1. Red-Recombination

The recombination enzymes *redαβγ* from bacteriophage λ allow the directed mutagenesis of BACs by homologous recombination of linear DNA fragments into the BAC using selection for an antibiotic resistance encoded on the DNA insert (Court et al., 2002; Datsenko and Wanner, 2000; Muyrers et al., 2000; Muyrers et al., 1999; Zhang et al., 1998). The homologous sequences are very short (25-50 bp), thus the recombination fragments can be generated by PCR with 5' overhangs encoding the homologous sequence. Either the recombination functions were encoded on the plasmid pKD46 (Datsenko and Wanner, 2000) and were induced by the addition of L-arabinose to the bacterial culture, or were available in the bacterial genome as a prophage and activated by heat shock (see 3.4.2).

E. coli DH10B carrying the BAC to be modified were made electrocompetent and transformed with 2 ng pKD46. After 1 h recovery in SOC at 30°C, 50 μ l were plated onto LB plates with 17 μ g/ml chloramphenicol and 50 μ g/ml ampicillin, and grown overnight at 30°C. On the next day, 2 ml of LB with antibiotics were inoculated with a colony and shaken at 30°C overnight. The induction of *redαβγ* occurred prior to the preparation of electrocompetent cells: 100 ml LB medium with appropriate antibiotics were inoculated with 100 μ l of starter culture and shaken at 30°C. At an OD₆₀₀ of 0.2 L-arabinose was added to a final concentration of 0.1% (w/v). The bacteria were harvested at an OD₆₀₀ of 0.5-0.8 and made electrocompetent as described above.

The recombination fragment was obtained as a restriction fragment, or was constructed by PCR using primers that amplify an antibiotic resistance cassette from the template plasmid pRpsLneo (Gene Bridges GmbH, Dresden, Germany). The proof-reading polymerase *Pwo* was used for this purpose. After PCR, the reaction mixture was digested for 1 h with 20 U of *DpnI*, thereby destroying the template plasmid, which was methylated by the bacterial host. *E. coli* DH10B carrying the BAC and pKD46 with induced *redαβγ* were transformed with up to 5 μ g of the linear recombination fragment. The complete transformation mixture was plated onto LB agar plates containing 17 μ g/ml chloramphenicol and the antibiotic to be selected for and incubated for 2 days. Clones were analysed by restriction analysis of BAC-DNA after mini preparation.

When using the *rpsLneo* selection cassette, the recombinant clones were selected for kanamycin resistance with 30 μ g/ml kanamycin. The *rpsL* gene encoded on the cassette was responsible for the antibiotic effect of streptomycin and mutated in *E. coli* DH10B thus conferring streptomycin resistance to this strain. Provided *in trans*, *rpsL* rendered the cells

streptomycin sensitive again, so with a second *redaβy* recombination the *rpsLneo* cassette was replaced from the BAC with a sequence of choice, now selecting for the regaining of streptomycin resistance. For this second recombination step in *E. coli* DH10B carrying the BAC+*rpsLneo*, *redaβy* from pKD46 was induced at an OD₆₀₀ of 0.5-0.8 with 0.1%(w/v) L-arabinose for only 15 min. Then the cells were harvested and made electrocompetent. After transformation with the recombination fragment to replace *rpsLneo* only 10-20 µl of the transformation mixture were plated on LB agar containing 17 µg/ml chloramphenicol and 50 µg/ml streptomycin. A mock transformation with H₂O served as control.

3.4.2. "En-passant" mutagenesis

The "en passant" method of BACs is based on a two step Red-recombination (Tischer et al., 2006). Here, the recombination functions are provided by a defective λ phage in *E. coli* DY380 (Lee et al., 2001) and are induced by heat shock.

For the first recombination step, the cells were made electrocompetent and the recombination enzymes were induced. A 2 ml overnight culture of *E. coli* DY380 containing the BAC was grown at 32°C in the presence of 17 µg/ml chloramphenicol. The next day 5-200 ml LB medium with 17 µg/ml chloramphenicol were inoculated 1:20 to 1:50 with the overnight culture and shaken at 32°C to an OD₆₀₀ of 0.5-0.7. To induce *redaβy* the culture was transferred to a 42°C water bath shaker and incubated for 15 min, then placed in an ice water bath and chilled for 20 min. Then the cells were made electrocompetent as described above. The recombination fragment was amplified from the template plasmid, digested with *DpnI*, and electroporated into the electrocompetent and induced bacteria. After the electric pulse the cells were incubated in 1 ml SOC medium at 32°C and then plated onto LB agar containing antibiotics selecting for the BAC (17 µg/ml chloramphenicol) and for the selection marker provided on the template plasmid (kanamycin, 30 µg/ml). Clones obtained after 24 h growth at 32°C were analysed by restriction analyses.

Positive clones were transformed with 100 ng pBAD-I-SceI and grown on LB agar with 17 µg/ml chloramphenicol, 30 µg/ml kanamycin and 100 µg/ml ampicillin. A colony was picked and grown over night at 32°C in 2 ml of LB containing the appropriate antibiotics. The next day 2 ml of LB containing 17 µg/ml chloramphenicol and 100 µg/ml ampicillin (no kanamycin) were inoculated with 100 µl of overnight culture and shaken for 2-4 h at 32°C. Then 2 ml of 32°C warm LB containing 1%(w/v) arabinose, 17 µg/ml chloramphenicol and 100 µg/ml ampicillin were added to induce the expression of I-SceI from pBAD-I-SceI, and the bacteria were further shaken for 1 h at 32°C. The culture was transferred to a 42°C water bath shaker, incubated for 30 min to induce *redaβy* expression, and then returned to shaking at 32°C for another 1-4 h. 100 µl of the original culture as well as 1:10 and 1:100 dilutions

were plated on LB-agar plates with 17 µg/ml chloramphenicol, 100 µg/ml ampicillin and 1% arabinose and incubated at 32°C for 24-48 h. The clones were replica-picked to monitor the loss of the selection marker provided on the recombination fragment, and further analysed by restriction analyses.

3.4.3. Shuttle mutagenesis

Another method for the directed mutagenesis of BACs is a two-step method also called "shuttle mutagenesis". The mutated sequence is flanked by 500-2000 bp of sequences homologous to the target site on the BAC and cloned into the vector pST-SNR (based on pST76K (Posfai et al., 1997), modified by M. Messerle, personal communication) for the shuttle plasmid.

E. coli DH10B carrying the BAC were transformed with the shuttle plasmid and grown on LB agar with 17 µg/ml chloramphenicol and 30 µg/ml kanamycin at 30°C. The BAC and the shuttle plasmid now grew in parallel in the cells. Occasionally, the *recA* encoded on the shuttle plasmid promoted a recombination event between the homologous sequences on the BAC and the shuttle plasmid, leading to the formation of a cointegrate. Cointegrates were selected for by streaking the colonies onto LB agar with 17 µg/ml chloramphenicol and 30 µg/ml kanamycin and incubating at 43°C. The temperature-sensitive replication of the shuttle plasmid did not allow plasmid replication at this temperature, so the kanamycin resistance was only present in bacteria, which contained a cointegrate. The *sacB* gene on the shuttle plasmid encodes the enzyme levansucrase which converts sucrose into the toxic polysaccharide levan. The cointegrate-bearing bacteria were grown on 17 µg/ml chloramphenicol at 37°C. Occasionally, *recA* promoted an intramolecular recombination between homologous sequences of the BAC part and the shuttle plasmid sequences. Thereby the shuttle plasmid was excised from the cointegrate, and eventually lost from the bacteria due to the lacking selection pressure for kanamycin resistance. These clones were selected for by growing on LB agar with 17 µg/ml chloramphenicol and 5%(w/v) sucrose at 30°C. Like for the *rpsLneo* replacement, unspecific recombination may also lead to sucrose resistance so a thorough restriction analysis was necessary.

3.5. Transfection of eukaryotic cells

Transfection of Vero cells with BAC-DNA was performed with the MBS Mammalian Transfection Kit based on a modified calcium phosphate transfection. Vero cells were seeded in 6 cm culture dishes the day before at a dilution of 1:5. 2 µg of BAC-DNA were dissolved in 450 µl sterile H₂O in a 5-ml BD Falcon polystyrene round bottom tube (BD

Biosciences, Heidelberg, Germany; Cat. No. 352054). 50 µl of solution I (2.5 M CaCl₂) and 500 µl of solution II (2x *N,N*-bis[2-*hydroxyethyl*]-2-aminoethane-sulfonic acid buffered saline, pH 6.95) were added, and the tube was flicked carefully for mixing. The transfection mixture was left standing for 20 min at room temperature. The cells were washed twice with PBS, then 5 ml MEM (without FCS) containing 6%(v/v) solution III (modified bovine serum) were added. After incubation, 500 µl of the transfection mixture were added dropwise onto the cells followed by incubation at 37°C, 5% CO₂ for 3 h. The cells were then washed three times with PBS, overlaid with Vero medium and incubated for several days at 37°C, 5% CO₂.

3.6. Light microscopy

PtK₂ cells were grown on sterile clean glass coverslips in 24-well plates. If no immunofluorescent labelling was performed, permeabilisation was not necessary and the coverslips were mounted after fixation. For the PFA/Triton fixation, the cells were washed with PBS and then fixed for 20 min with 3%(w/v) paraformaldehyde (PFA) in PBS. After three washes with PBS, residual PFA was inactivated by a 10 min incubation with 50 mM NH₄Cl in PBS. For immunolabelling, the cells were washed again three times with PBS and then permeabilized with 0.1%(v/v) Triton X-100 in PBS for 5 min. The coverslips were blocked with 0.5%(w/v) BSA in PBS for 30 min then washed for 5 min with PBS. The sequential incubation with primary and secondary antibodies occurred for 30 min, each incubation followed by three 5 min washes with PBS. The nuclei were stained with 1 µg/ml Hoechst 33258 for 2 min. The coverslips were briefly rinsed with H₂O and embedded on microscope slides with Mowiol solution, containing 25 mg/ml DABCO. The microscope slides were stored at 4°C.

3.7. SDS-PAGE and Western-blotting

Proteins were separated on acrylamide gels by discontinuous SDS-PAGE (Laemmli, 1970) in the Hoefer™ SE 260 gel system. The separation gels contained an acrylamide gradient of 10-20%(w/v) in 0.375 M Tris-HCl, pH 8.8 and 0.1%(w/v) SDS; the stacking gels contained 4%(w/v) acrylamide in 0.125 M Tris-HCl, pH 6.8 and 0.1%(w/v) SDS. The samples were boiled for 5 min at 95°C in 1x SDS-sample buffer, and then centrifuged at 14,000 rpm for 5 min. Electrophoresis was carried out in running buffer (25 mM Tris pH 8.3, 192 mM glycine, 0.1%[w/v] SDS) at a constant current of 25 mA per gel for 45-60 min under water cooling.

For Western-blotting, the gel was layered onto a sheet of wet nitrocellulose membrane and placed between two sheets of Whatman paper soaked in transfer buffer (48

Methods

mM Tris, 380 mM glycine, 0.1%[w/v] SDS, 10% methanol) on each side. Tank blotting occurred in transfer buffer for 1.5 h at a constant current of 400 mA under cooling or at 40 mA for 16 h without cooling. The transferred proteins were stained for 10 min by shaking in Ponceau S staining solution (0.3%[w/v] trichloroacetic acid, 0.3%[w/v] 5-sulfosalicylic acid, 0.2%[w/v] Ponceau S). For immunoassays the membrane was blocked by 1 h of shaking in blocking solution (5%[w/v] low-fat milk powder, 0.2%[v/v] Tween 20 in PBS). Then the primary antibody in blocking solution was added and incubated by shaking for 2 h. After three 10 min washing steps with 0.1%(v/v) Tween 20 in PBS the membrane was incubated for 1 h with a dilution of a secondary antibody in blocking solution. For detection of alkaline phosphatase-labelled secondary antibodies, the membrane was washed three times for 10 min with 0.2%(v/v) Tween 20 in PBS, equilibrated twice for 10 min with TSM and stained in the dark with 0.165 µg/ml BCIP, 0.305 µg/ml NBT in TSM. The colour reaction was stopped by washing with water. Chemiluminescence was performed when using horseradish peroxidase-labelled secondary antibodies. The membrane was washed three times for 10 min with 0.2%(v/v) Tween 20 in PBS, then fresh prepared substrate solution (1.25 mM luminol, 0.2 mM p-coumaric acid, 0.01%(v/v) H₂O₂, 100 mM Tris-HCl, pH 8.5) was pipetted onto the membrane and incubated for 5 min. The substrate was removed, the wet membrane was placed between plastic sheets and exposed to chemiluminescence film (Hyperfilm, Amersham, Buckinghamshire, UK) for different amounts of time.

4. Results

Using homologous recombination in Vero cells, BAC genes were inserted into the UL23 locus of HSV1(17⁺) and the circularised genome was transferred into *E. coli* for establishment of the BAC. This BAC was modified by the insertion of a Cre recombinase expression cassette to excise the *loxP* flanked BAC sequences from the virus genome upon transfection. After characterisation of the BAC, the viral capsid protein VP26 and the envelope protein gD were tagged with a fluorescent protein by mutagenesis of the HSV1-BAC.

4.1. Cloning of HSV1(17⁺) as a BAC

4.1.1. Transfer of BAC genes into HSV1

For the cloning of HSV1 as a bacterial artificial chromosome, the BAC sequences were inserted into the thymidine kinase (UL23) locus by homologous recombination in Vero cells (Figure 18). The resulting virus HSV1-BAC had a Δ UL23 phenotype; originally this strategy was chosen to allow acyclovir selection during the purification of the recombinant BAC-virus (Horsburgh et al., 1999; T. Strive, M. Messerle & B. Sodeik, personal communication). However, in the end HSV1-BAC plaques were identified by β -galactosidase expression.

The BAC-sequences together with a eukaryotic β -galactosidase expression cassette and a single *loxP* site were provided on pblueLox (Smith and Enquist, 2000). Dr. Tanja Strive (Institute of Virology, Hannover Medical School) had flanked these genes with 2 kbp of sequences homologous to the upstream and downstream regions of UL23 for the recombination plasmid pblueLox-HomTK. The 5' homology comprised nt 44591-46840 of the HSV1(17⁺) genome, and the 3' homology nt 47561-49773. In previous attempts, no recombinants were obtained with homologous sequences of 0.5 kbp, or if the 2 kbp homologies were directly adjacent to each other, probably due to steric hindrance. After cotransfection of HSV1(17⁺) DNA and pblueLox-HomTK into Vero cells, some β -galactosidase-positive plaques were obtained (Cotransfection samples CT27, CT28, CT29, CT30.1 and CT30.2).

Results

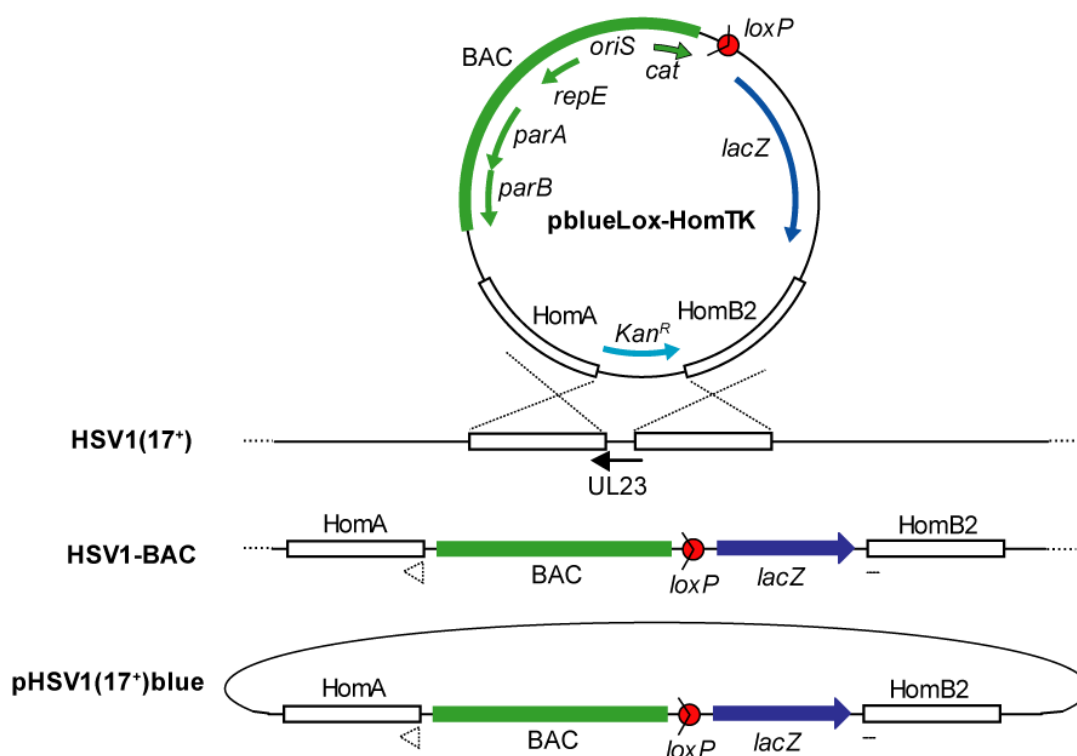


Figure 18: BAC-cloning strategy. Sequences spanning 2 kbp homologous to the UL23 gene locus and up- and downstream regions were cloned into pblueLox, resulting in pblueLox-HomTK which was linearised and cotransfected with HSV1(17⁺)-DNA into Vero cells. By homologous recombination, the BAC genes, a *lacZ* expression cassette and a *loxP* site were introduced into the viral genome. The recombinant HSV1-BAC was plaque purified and used to inoculate Vero cells for the isolation of circular replication intermediates. *E. coli* DH10B were transformed with the extracts and selected for chloramphenicol resistance. The BAC pHSV1(17⁺)blue was then isolated from the bacteria. *cat*, chloramphenicol resistance; HomA/HomB2, 5' and 3' homology of UL23; Kan^R, kanamycin resistance; *lacZ*, β-galactosidase; *oriS*, BAC origin of replication; *repE*, *parA* and *parB*, BAC replication and partitioning genes. (Strategy by T. Strive, M. Messerle & B. Sodeik; personal communication)

I plaque purified the BAC-virus from the mixture of wild-type and recombinant BAC-virus twice (Figure 19). Occasionally, some β-galactosidase-positive plaques exhibited a syncytial phenotype, which is unusual for HSV1(17⁺) of lower passage number, so these were not further purified. After passage of plaque 30.1-21, 30.1-22 and 30.1-23, almost all plaques were positive for β-galactosidase, so these three recombinants were amplified in BHK-21 cells. Recombinants 30.1-22 and 30.1-23 contained the BAC-encoded chloramphenicol resistance gene shown by PCR with primers CHN01 and CHN02 (Figure 20). Vero cells were infected with clone 30.1-23 for the preparation of a Hirt extract (Hirt, 1967). Three chloramphenicol resistant clones were obtained after electroporation of the extract into *E. coli* DH10B, and analysed by restriction digests with *Bgl*III and *Hind*III (Figure 21). The restriction patterns were consistent with the calculated fragment sizes. The UL and US regions of the HSV1 genome were arranged antiparallel in the BAC clones 1 and 3, according to a 19.9 kbp *Hind*III fragment, whereas clone 2 had a parallel orientation.

Results

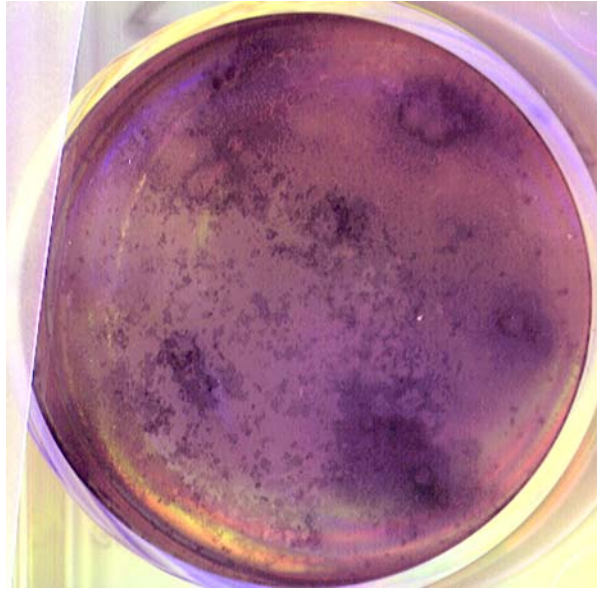


Figure 19: Recombinant BAC-virus formed β -galactosidase-positive plaques. Recombinant BAC-virus was plaque-purified under selection for β -galactosidase. Vero cells in 6-well plates were inoculated with a dilution of a purified plaque or HSV1(KOS)tk12 as control (not shown). After 1 h virus binding in RPMI/BSA at RT the cells were grown at 37°C and 5% CO₂ in Vero medium containing 20 μ g/ml human IgG for 3 d. To stain the plaques, the medium was removed and replaced with 1% LMP-Agarose in Vero medium containing 0.3 mg/ml blu-gal and the cells were incubated at 37°C and 5% CO₂ for further 3 d. Cells expressing β -galactosidase were stained blue, as shown here at an 1:100 dilution of plaque 30.1-122 (Cotransfection 30.1, plaque purified three times).

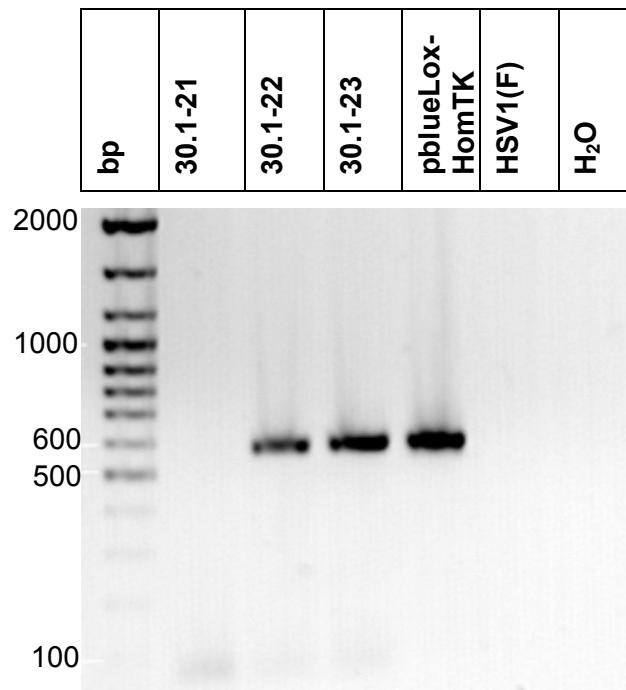


Figure 20: Purified plaques 30.1-22 and 30.1-23 contained BAC-sequences. 1% Agarose gel with diagnostic PCR products specific for chloramphenicol acetyl transferase. To check for the presence of BAC-sequences in β -galactosidase-positive virus samples, a PCR with primers CHN01 and CHN02 was carried out. As template, virions of HSVBAC 30.1-21, 30.1-22 and 30.1-23 were used; pblueLox-HomTK served as positive, HSV1(F) as negative control. Expected product size: 583 bp

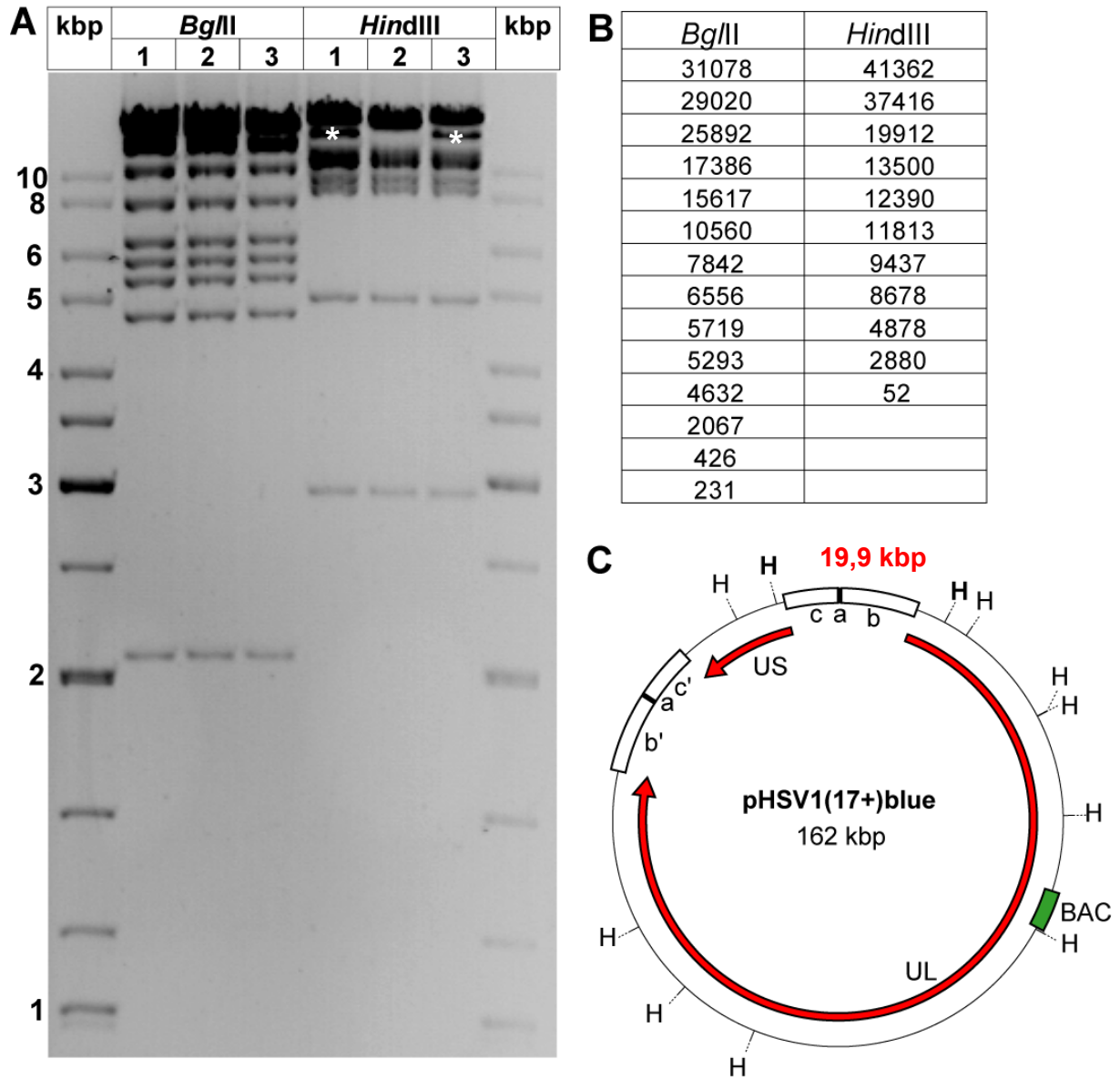


Figure 21: Characterisation of pHSV1(17⁺)blue clones by restriction digests. (A) Three chloramphenicol-resistant clones (1, 2, 3) were obtained after electroporation of *E. coli* DH10B with a Hirt extract of HSVBAC 30.1-23 infected cells. The clones were grown in liquid culture, BAC-DNA was prepared and subjected to *Bgl*II or *Hind*III restriction digest, respectively. The samples were separated on 0.8% agarose in 0.5x TBE. A 19.9 kbp *Hind*III fragment indicated an antiparallel orientation of the UL and US sequence in clones 1 and 3 (*), whereas clone 2 was oriented parallel. (B) Predicted fragment sizes of a pHSV1(17⁺)blue clone with antiparallel UL/US configuration after digestion with *Bgl*II or *Hind*III. (C) Map of pHSV1(17⁺)blue with indicated *Hind*III sites and the 19.9 kbp fragment indicating the antiparallel UL/US configuration.

4.1.2. Analysis of the BAC-cloned HSV1 genome

The BAC clones were named pHSV1(17⁺)blue (cf. Figure 18) and further characterised by restriction digestions with *EcoRI*, *BamHI* and *NotI* in comparison to purified HSV1(17⁺) DNA (Figure 22). After BAC insertion, a 2.4 kbp *EcoRI* fragment in HSV1(17⁺) was lost whereas in pHSV1(17⁺)blue novel *EcoRI* fragments at 7.1 and 4.7 kbp appeared. Furthermore, due to the circular topology of a BAC, the 3' terminal *EcoRI* fragment of linear HSV1-DNA, which formed a diffuse band at app. 5.6 kbp, is not present anymore. However, the 17.9 kbp fragment formed by circularisation of viral DNA was not resolved from neighboring bands in the used gel system. A restriction fragment spanning the connection between long and short region will be referred to as "joint fragment" in further analyses.

In *BamHI* digests, the BAC insertion was indicated by the loss of a 3.6 kbp fragment and the emergence of novel fragments at 12.0 and 1.1 kbp (Figure 22). According to the published sequence, a 8753 bp and a 3594 bp fragment should be obtained, however, a predicted *BamHI* site between the *loxP* site and the *lacZ* expression cassette was missing. In contrast to *EcoRI*, a novel joint fragment is detected at around 6 kbp. Interestingly, in the three pHSV1(17⁺)blue clones as well as in wild type HSV1(17⁺) DNA its fragment size was heterogeneous. This may reflect a heterogeneous number of the 400 bp *a*-sequences cloned in the respective BAC, as these occur in varying numbers of direct repeats in HSV1 DNA (Wadsworth et al., 1975; Wagner and Summers, 1978). Furthermore the *a*-sequence itself contains varying numbers of direct repeats (Mocarski et al., 1980; Mocarski and Roizman, 1982), which might describe the weak diffuse bands at 6 kbp instead of a single discrete band in the HSV1(17⁺) lane (Figure 23). The 3' terminal *BamHI* fragment of linear virus DNA at 3 kbp was not present in circular BAC-DNA. Two *BamHI* fragments of 2294 and 2291 bp were not resolved in HSV1(17⁺)-DNA, their common band intensity was higher than the 2.1 kbp band below. However, in the three pHSV1(17⁺)blue clones, a double band at 2.1 kbp was clearly visible and the relative intensity of the former 2294/2291 bp doublet was reduced. One explanation could be the loss of the palindromic *oriL* HSV1 replication origin, which is part of the 2291 bp *BamHI* fragment. Upon BAC cloning of HSV1(17⁺), also a 1953 bp *BamHI* fragment was reduced in size (Figure 22). This contained one copy of *oriS* (Figure 23), which also contains palindromic sequences.

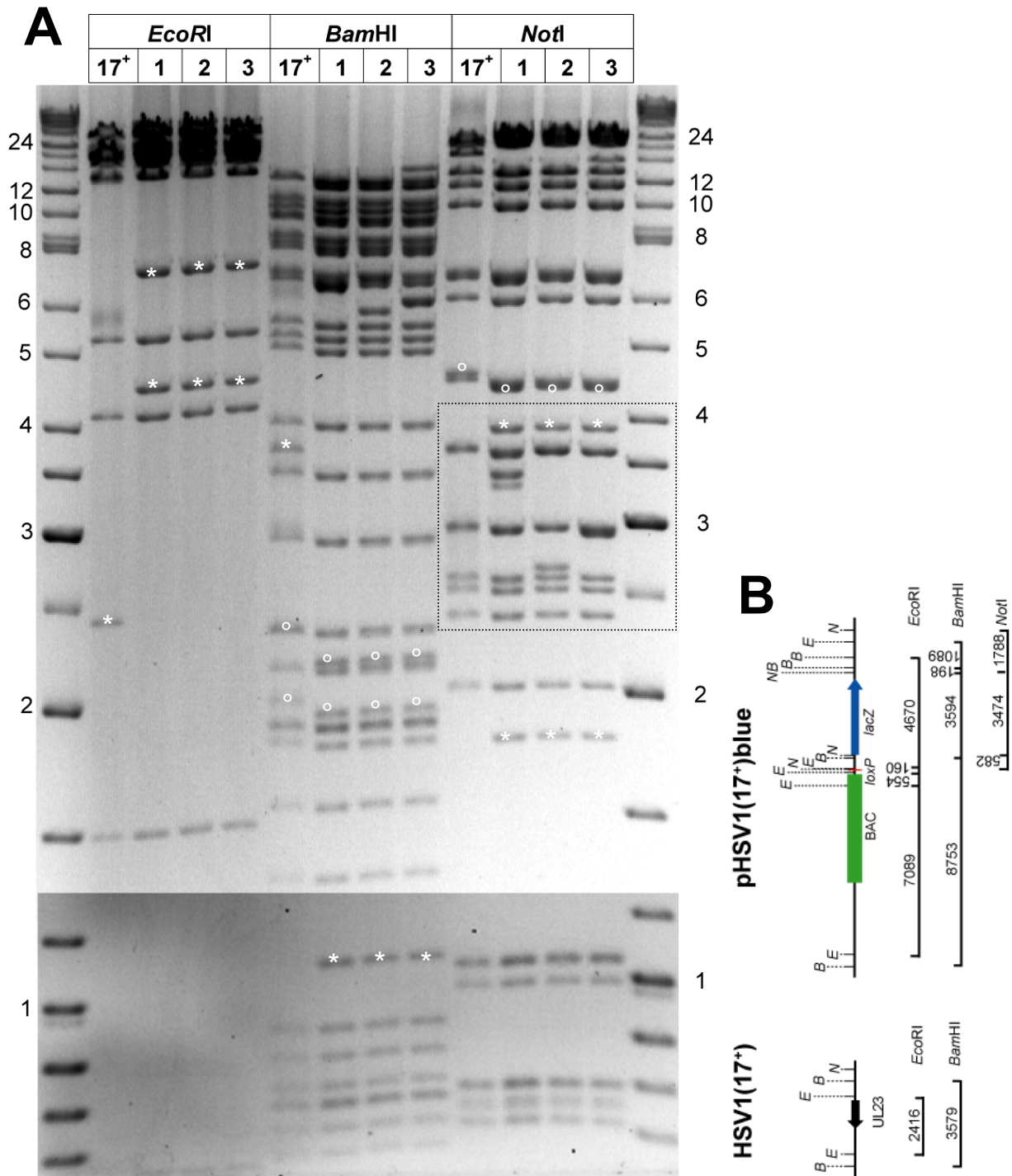


Figure 22: Characterisation of pHSV1(17⁺)blue clones by restriction digests. (A) Three BAC clones of pHSV1(17⁺)blue (lanes 1-3) and HSV1(17⁺) DNA (lane 17⁺) were digested with *EcoRI*, *BamHI* or *NotI*. The samples were separated on 0.6% agarose gel in 0.5x TBE. Restriction fragments resulting from the BAC insertion are marked with asterisks (*), alterations potentially associated with changes in viral replication origins (oriS, oriL) are marked with circles (o). The dashed box is shown enlarged in Figure 23C. (B) Schematic representation of the UL23 region and the predicted restriction fragments of *EcoRI* (E), *BamHI* (B) and *NotI* (N) digests with their respective sizes in bp. Note, that some predicted fragments were not observed, probably due to erroneous sequence data of the BAC insert. The *BamHI* site between the predicted 8753 bp and 3595 bp fragment is missing as well as the *NotI* site between the 3474 bp and the 582 bp fragment. Furthermore, the predicted sequence is app. 200 bp longer than the obtained restriction fragments; a *NotI* fragment is running at 3.8-3.9 kbp instead of 4056 bp. The predicted 4670 bp *BamHI* fragment also migrates at app. 4.4-4.5 kbp.

Results

The BAC insertion was also analysed by *NotI* restriction digests (Figure 22). Novel fragments appeared at 3.8 kbp and 1.8 kbp, whereas a 15.7 kbp band vanished. Like for *Bam*HI, a predicted *NotI* site was missing between the *loxP* site and the *lacZ* expression cassette, thus the expected fragments of 3474 bp and 582 bp were not observed. The loss of *oriL* was accompanied by a size reduction of a 4.5 kbp fragment near to a 4.4 kbp band. The genome termini of linear HSV1-DNA were not recovered as distinct bands, since they were either present in only 50% of the isolated genomes, due to genome isomerisation, or they overlapped with other bands of a similar size. The joint fragments in BAC-DNA had different sizes in the three clones (Figure 23). A predicted *NotI* restriction site between the 2918 bp joining fragment and a neighboring 339 bp fragment might be missing, as no 339 bp band can be observed after BAC or HSV1(17⁺) digestion (data not shown). Therefore the joint fragment containing a single *a*-sequence was assumed to have a size of 3.3 kbp, according to the published sequence. However, the varying number of *a*-sequences and the number of direct repeats within most likely caused the aberrations detected after *NotI* and *Bam*HI digestion. A *NotI* joint fragment carrying two adjacent *a*-sequences would also have a size of app. 3.3 kbp. During BAC cloning the variability of the number of *a*-sequences and their internal direct repeats is probably reduced.

The *oriL* contains a 140 bp palindromic sequence, and the instability of this region in *E. coli* after cloning has been described previously (Weller et al., 1985). In *E. coli* strain SURE the palindrome sequences are stably maintained (Hardwicke and Schaffer, 1995). For a previously published BAC of HSV1 strain F (Tanaka et al., 2003) it was proposed that *oriL* was stably cloned after performing a PCR specific for this region. PCR products at the expected size of 550 bp for HSV1(F) DNA as well as after amplification of a virus derived from the HSV1(F)-BAC, pYEbac102 were obtained. However, the region of the gel for a possible PCR product of about 410 bp after deletion of *oriL* was not shown. A similar PCR with the same outcome was performed for *oriS*, which also contains palindromes and secondary structure elements (Tanaka et al., 2003). Here, these regions in pHSV1(17⁺)blue were amplified with primers CHN77 and CHN78 (Figure 24), which were also used by Tanaka et al. (2003). This revealed no changes in the *oriS* amplicate size between HSV1(17⁺) and the BAC pHSV1(17⁺)blueLox, a variant of pHSV1(17⁺)blue (Figure 28). Thus other subtle changes may have led to the reduction of the 1953 bp *Bam*HI fragment. However, after PCR analysis of the *oriL* region with primers CHN79 and CHN80, a band at the expected size of 550 bp was neither observed in HSV1(17⁺) and pHSV1(17⁺)blueLox nor in HSV1(F) and pYEbac102 (Figure 24). A product of about 410-420 bp suggests that the palindromic sequence may have a secondary structure that could not be amplified with the reaction conditions used. The state of *oriL* could therefore not be assessed by PCR.

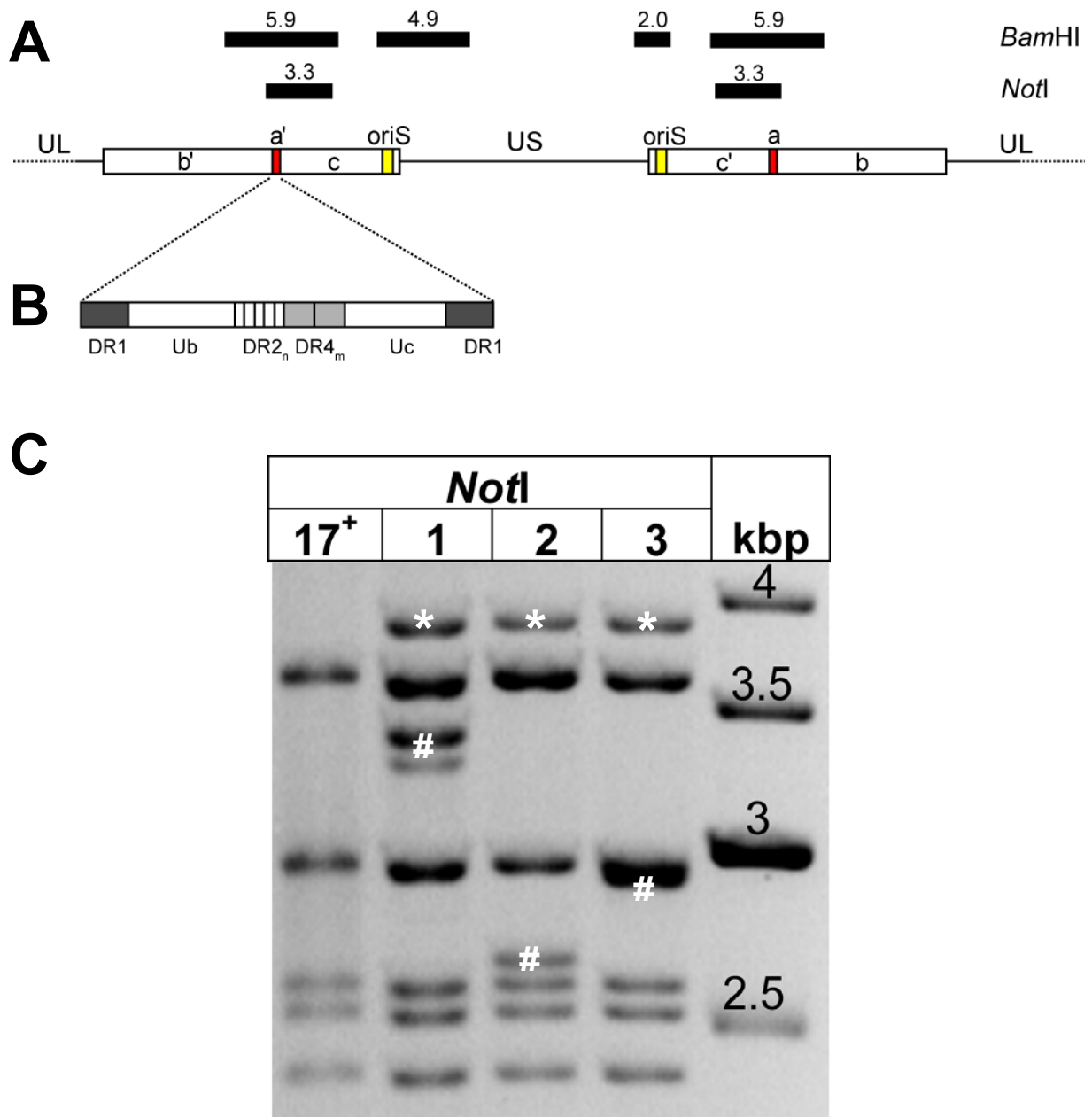


Figure 23: Characterisation of the terminal region in different HSV1-BACs. (A) During HSV1-DNA replication and in BACs, the viral genomes are circular covalently closed. Thus, the repeats flanking the unique long and unique short regions are arranged symmetrically. The *a*-sequence can occur in multiple direct repeats (only one copy shown), and therefore restriction fragments (black bars; size in kbp) spanning the joint region of the *b*- and *c*-repeat vary in size. (B) Furthermore the *a*-sequence itself contains unique sequences (Ub and Uc) as well as direct repeats at the ends (DR1), and varying numbers of the direct repeats DR2 and DR4. (C) Insert of Figure 22. Three pHSV1(17⁺) blue clones (lanes 1-3) were digested with *NotI* and compared comparison to a digest of HSV1(17⁺) DNA (lane 17⁺). The samples were separated on 0.6% agarose gel in 0.5x TBE. The joint fragments containing the *a*-sequence (#) and the BAC-derived fragments (*) are indicated.

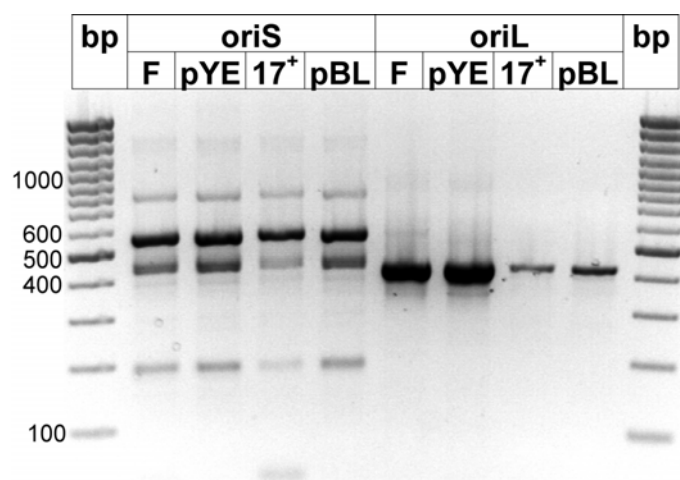


Figure 24: Characterisation of HSV1 replication origins. For analysing oriS and oriL in wildtype HSV1- DNA and BAC-DNA, DNA preparations were subjected to PCR amplification with primers specific for oriS (CHN77 and CHN78) or oriL (CHN79 and CHN80) and analysed by 2% agarose gel electrophoresis. F: HSV1(F), pYE: pYE102bac (strain F BAC), 17⁺: HSV1(17⁺), pBL: pHSV1(17⁺)blueLox (Figure 28). The expected amplificate sizes are 551 bp for oriS and 560 bp for oriL. Note that after amplification of pYE102bac and pHSV1(17⁺)blueLox as well as of HSV1(F)-DNA or HSV1(17⁺)-DNA, no oriL fragment of the expected size was obtained. No differences in oriS amplification were observed with all four templates.

DNA was prepared from HSV1(F) and of pYEbac102, the HSV1(F)-BAC. After restriction digestion with *Bam*HI or *Kpn*I several differences in the band patterns were observed between HSV1(F) and HSV1(17⁺) showing interstrain sequence polymorphisms (Figure 25A). However, both a 1.9 kbp *Kpn*I as well as a 2.3 kbp *Bam*HI fragment which are predicted to contain *oriL* according to the published HSV1(17⁺) sequence (Figure 25B), showed a size reduction of approximately 150 bp in their respective BAC clones. After Southern blotting, these fragments hybridised to a *oriL* specific probe, that was obtained by amplifying the *oriL* region in the presence of DIG-labelled oligonucleotides (Figure 25D).

Altogether the data indicate, that the HSV1 genome was successfully cloned as a BAC, but that the 140 bp palindrome of *oriL* was deleted in *E. coli* during this process. The genome configuration is fixed in a BAC, so clones with a parallel or antiparallel orientation of the UL and US region were recovered. Moreover, due to topology reasons, instead of a single joint between the long and short region, this junction was present twice in a BAC. Restriction fragments spanning over the junctions were obtained in variable size after digestion of BACs, possibly reflecting the variable number of *a*-sequences and the repetitive sequences therein. For further experiments, clone pHSV1(17⁺)blue[1] was chosen.

4.1.3. Characterisation of the BAC-derived virus

After transfection of pHSV1(17⁺)blue into Vero cells, plaques developed within 2-3 days and all cells developed full cytopathic effect within 2 further days. The resulting virus vHSV1(17⁺)blue was passaged twice in BHK-21 cells prior to the production of a working stock. Virus-DNA was isolated from infected cells and analysed by restriction digests with *Bgl*III, *Hind*III and *Eco*RV which revealed, that the insertion of BAC-sequences into the HSV1 genome (Figure 26) was maintained during passaging.

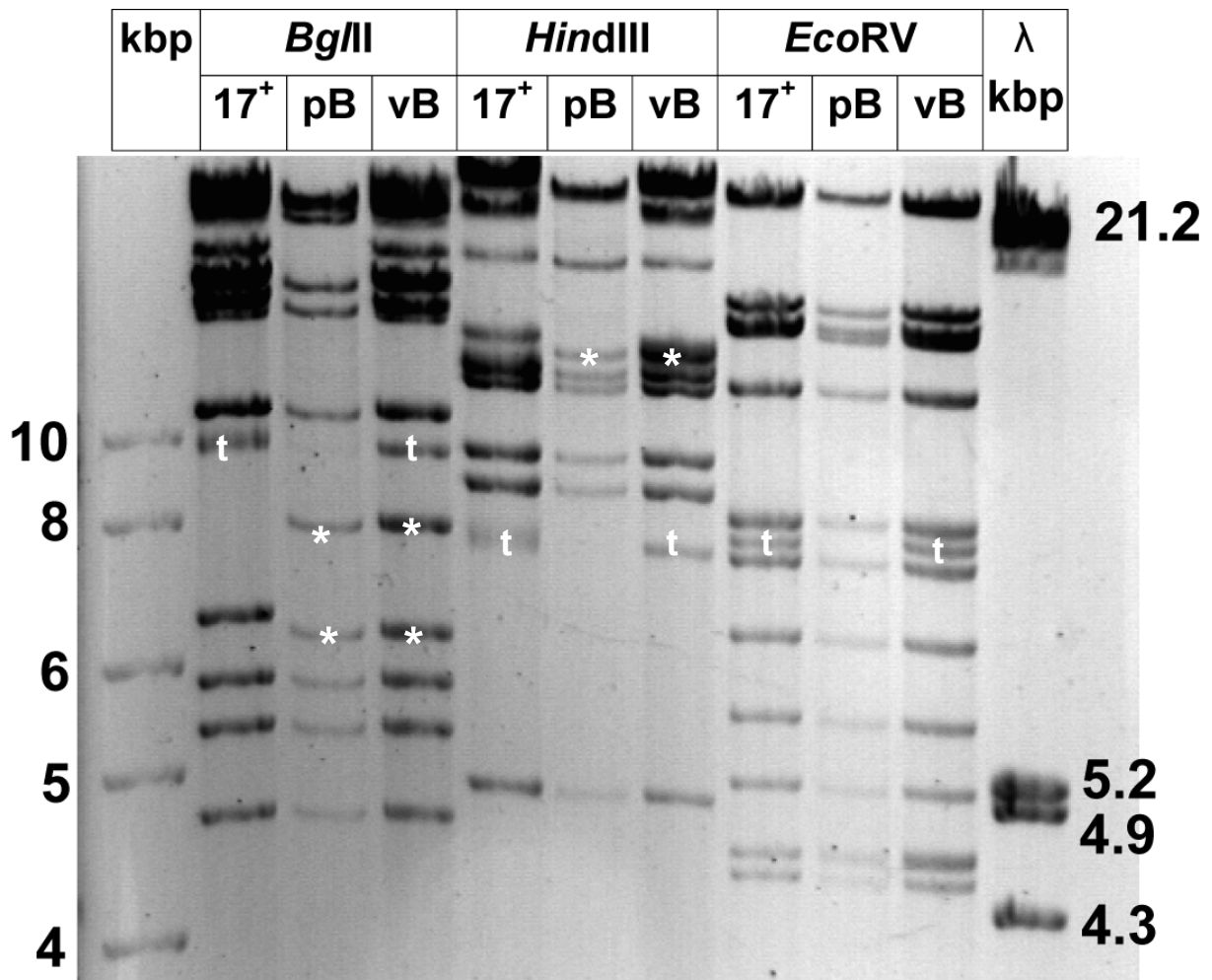


Figure 26: The BAC sequences have been stably inserted into the HSV1 genome. After transfection of pHSV1(17⁺)blue into Vero cells, vHSV1(17⁺)blue is recovered. DNA of HSV1(17⁺) (17⁺), pHSV1(17⁺)blue (pB) and vHSV1(17⁺)blue (vB) was digested with *Bgl*III, *Hind*III or *Eco*RV and separated over 0.5% agarose in 0.5x TBE. (*) BAC insertion; (t) linear DNA genome termini; λ: *Eco*RI/*Hind*III digested λ-DNA.

Results

The β -galactosidase expression cassette encoded by vHSV1(17⁺)blue, which was the marker for the enrichment of the recombinant BAC-virus is used to measure early viral gene expression (Mabit et al., 2002; Marozin et al., 2004). As efficient nuclear targeting is a prerequisite for genome release at the nuclear pore, this allows the biochemical study of the influence of reagents interfering with intracellular trafficking.

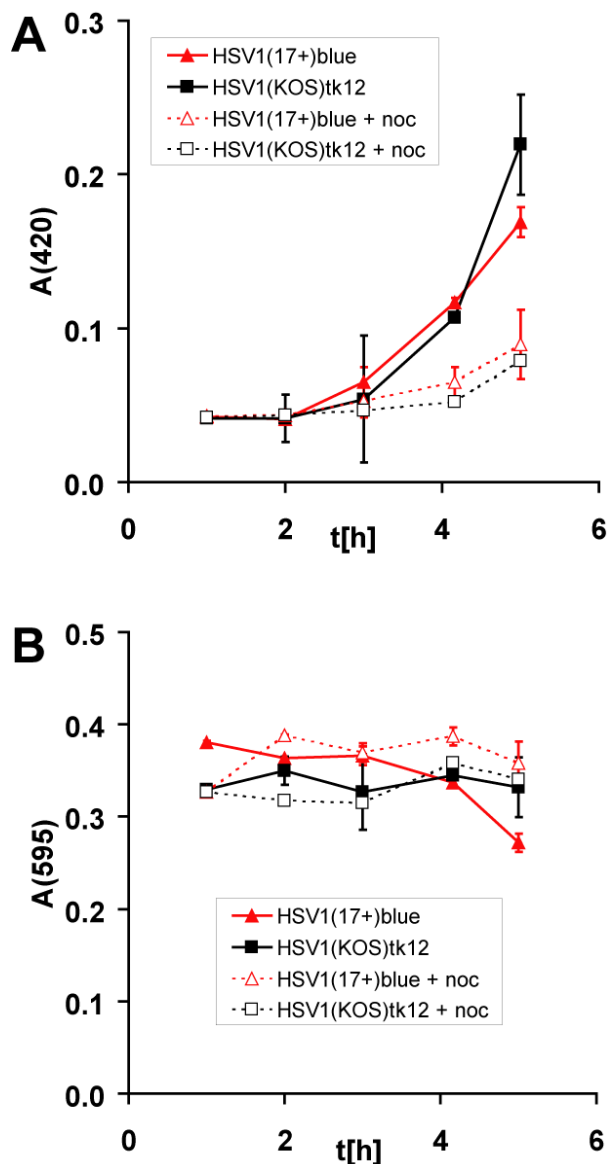


Figure 27: Time course of β -galactosidase expression of vHSV1(17⁺)blue. PtK₂ cells in 24 well plates preincubated for 1 h at 37°C with or without 20 μ M nocodazole (noc) were inoculated with 10 pfu/cell HSV1(KOS)tk12 or vHSV1(17⁺)blue and incubated at 37°C with or without nocodazole for the time indicated on the x-axis. (A) The amount of β -galactosidase was photometrically measured after substrate addition at 420 nm, as indicated on the y-axis. Each timepoint and condition was measured in four independent wells. (B) The cell density was quantified after crystal violet staining.

When the microtubule network was disrupted by the drug nocodazole, the β -galactosidase expression was significantly reduced in cells infected with HSV1(KOS)tk12 (Warner et al., 1998) or vHSV1(17⁺)blue (Figure 27A). Five hours after infection, the amount of β -galactosidase produced was higher in cells infected with HSV1(KOS)tk12 than with vHSV1(17⁺)blue. This may reflect the reduced number of cells at this timepoint (see Figure 27B). vHSV1(17⁺)blue expressed β -galactosidase under control of an SV40 early promoter, whereas in HSV1(KOS)tk12 expression was driven by the immediate early promoter of HSV1-ICP4. Thus, the difference in expression level could also reflect different promoter activity.

4.1.4. Construction of a self-excisable BAC

The insertion of BAC genes into herpesviruses can lead to their attenuation as observed for MCMV and PRV; therefore, herpesviral BACs were constructed which allow the removal of BAC sequences after transfection into eukaryotic cells (Wagner et al., 1999; Smith and Enquist, 2000). In the case of PRV, the BAC sequences were flanked by *loxP* sites and later excised by site-specific recombination catalysed by Cre recombinase (Smith and Enquist, 2000). By providing a eucaryotic Cre expression cassette on the BAC itself, the BAC-sequences are "self-excised" after transfection.

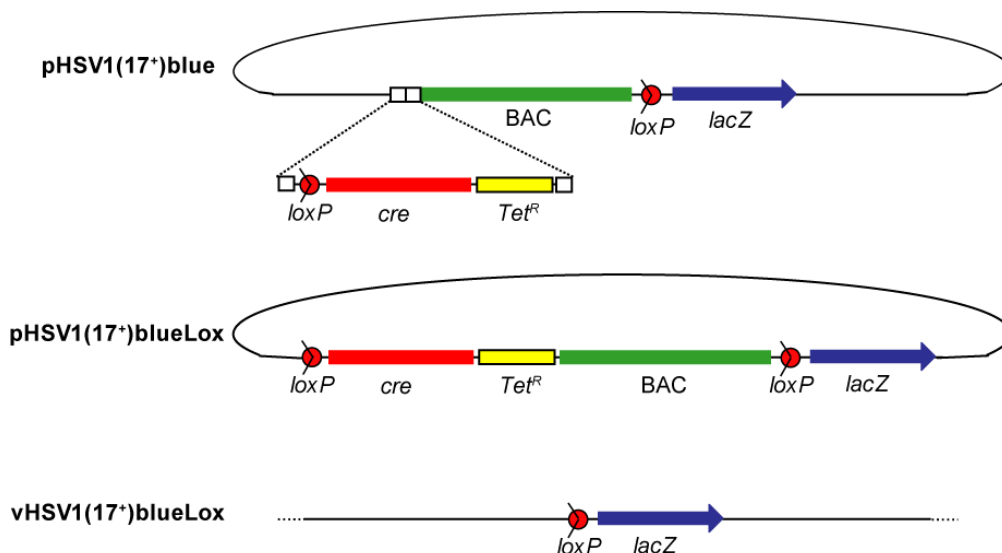


Figure 28: Construction of pHSV1(17⁺)blueLox. A 5402 bp fragment encoding a *loxP* site (red), a CMV-promoted Cre expression cassette carrying an intron (*cre*; red), and a tetracyclin resistance (*Tet^R*; yellow) were flanked with 50 bp of sequences homologous to the 5' end of the BAC sequences on pHSV1(17⁺)blue (white boxes). By Red-recombination, the fragment was introduced into pHSV1(17⁺)blue under selection for tetracyclin resistance. After transfection of eukaryotic cells, Cre recombinase was transcribed and the intron was spliced out. The recombinase then excised the sequences flanked by the *loxP* sites, and the resulting vHSV1(17⁺)blueLox only contained a single *loxP* site and the β -galactosidase expression cassette (*lacZ*).

Results

A single *loxP* site was provided on pHSV1(17⁺)blue downstream of the BAC sequences. The second *loxP* site and a Cre expression cassette were inserted into pHSV1(17⁺)blue upstream of the BAC-sequences by Red recombination of a linear DNA fragment under selection for tetracyclin resistance (Figure 28).

The recombination fragment was constructed in a pUC18 vector (Figure 29). A double-stranded DNA-linker encoding a *loxP* site was obtained by annealing oligos CHN-Lox1 and CHN-Lox2 and then cloned into *EcoRI/HindIII* digested pUC18 giving pUC18LoxP. An expression cassette for Cre under the control of a CMV immediate early promoter was provided on pCreIn. An intron was previously introduced into the Cre gene, so it is ensured that the recombinase is only translated in eukaryotes after mRNA splicing (Smith and Enquist, 2000). The cassette was cut from pCreIn (Smith and Enquist, 2000) with *PacI*, and cloned into the *PacI* site of pUC18LoxP resulting in pUC18LC. Sequences for the Red-mediated insertion, which are homologous to the 5' end of the BAC-cassette on pHSV1(17⁺)blue were provided by 50 bp DNA-linkers, obtained by annealing the oligonucleotides CHNHomL-S and CHNHomL-A or CHNHomR-S and CHNHomR-A, respectively. The linkers were cloned into the *NotI* and *NheI* sites of pUC18LC for pUC18LCH. The insertion of the Cre cassette into pHSV1(17⁺)blue was selected for via a tetracyclin resistance provided on the recombination fragment. The resistance cassette was amplified from pCP16-HL (Cherepanov and Wackernagel, 1995) with oligos CHN07N and CHN08N, digested with *NheI* and cloned into the compatible *XbaI* site on pUC18LCH yielding pUC18LCTH.

E. coli DH10B containing pHSV1(17⁺)blue were transformed with pKD46 (Datsenko and Wanner, 2000), and the expression of the Red enzymes was induced with L-arabinose. The recombination fragment was cut out from pUC18LCTH with *NotI* and *NheI*, gel purified and transferred into the prepared bacteria. Clones which exhibited chloramphenicol and tetracyclin resistance, but were sensitive to ampicillin, were screened by a *MunI* digest. Six out of ten clones had a correct *MunI* digestion pattern when compared to pHSV1(17⁺)blue (not shown) and were named pHSV1(17⁺)blueLox. Clone 1 was chosen for further experiments.

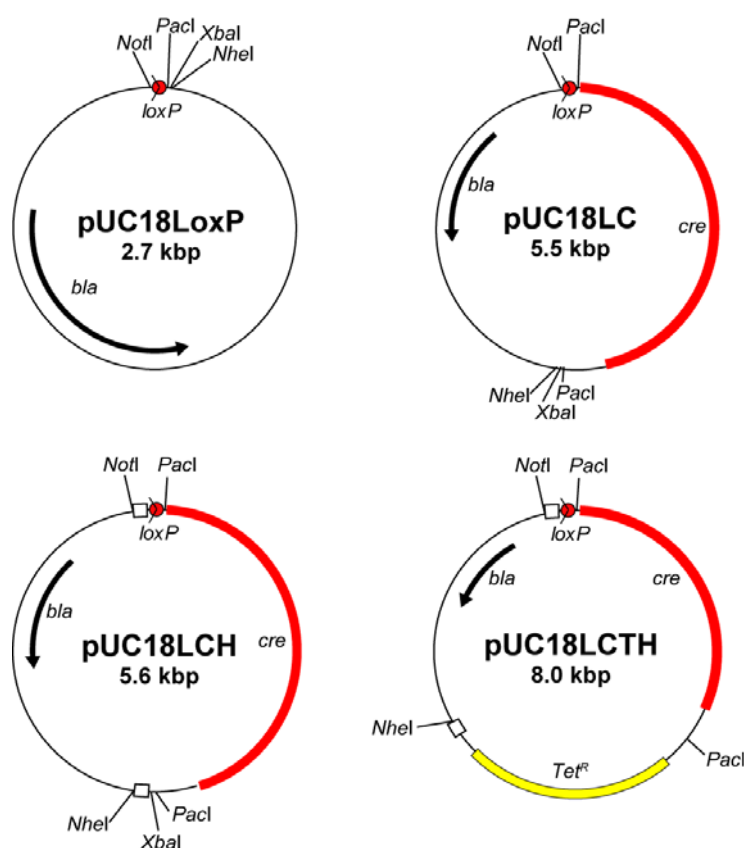


Figure 29: Construction of pUC18LCTH. Schematic representation. The targeting construct for the insertion of Cre recombinase and a second *loxP* site into pHSV1(17⁺)blue was constructed in pUC18. A *loxP* linker with *NotI*, *PacI*, *XbaI* and *NheI* restriction sites was cloned into pUC18. The Cre expression cassette (red) was cloned into the *PacI* site. For recombination, 50 bp of sequences homologous to the 5' end of the BAC genes (white boxes) were inserted into the *NotI* and *NheI* sites, respectively, and finally, a tetracyclin selection marker (yellow) was cloned into the remaining *XbaI* site. The fragment was cut out of pUC18LCTH with *NotI* and *NheI* for Red-recombination.

Restriction analyses with *EcoRI*, *BamHI*, *HindIII*, *NotI*, *EcoRV* and *BglII* revealed, that the viral backbone was not changed during Red-recombination, with the exception of the Cre insertion (Figure 30). After transfection of pHSV1(17⁺)blueLox into Vero cells, plaques developed after 1 d, and the cells developed full cytopathic effects after three further days. vHSV1(17⁺)blueLox was passaged twice in BHK-21 cells and viral DNA was prepared from infected cells. When digested with *BglII*, no BAC derived restriction fragments were observed in vHSV1(17⁺)blueLox-DNA (Figure 31), indicating that Cre had removed the sequences between the *loxP* sites efficiently. The β -galactosidase cassette was maintained in vHSV1(17⁺)blueLox. Also by Southern blotting using a BAC-specific probe, the excision was monitored, as no signal was obtained after probing a membrane onto which separated *BglII* restriction fragments of vHSV1(17⁺)blueLox were transferred (Figure 32).

Results

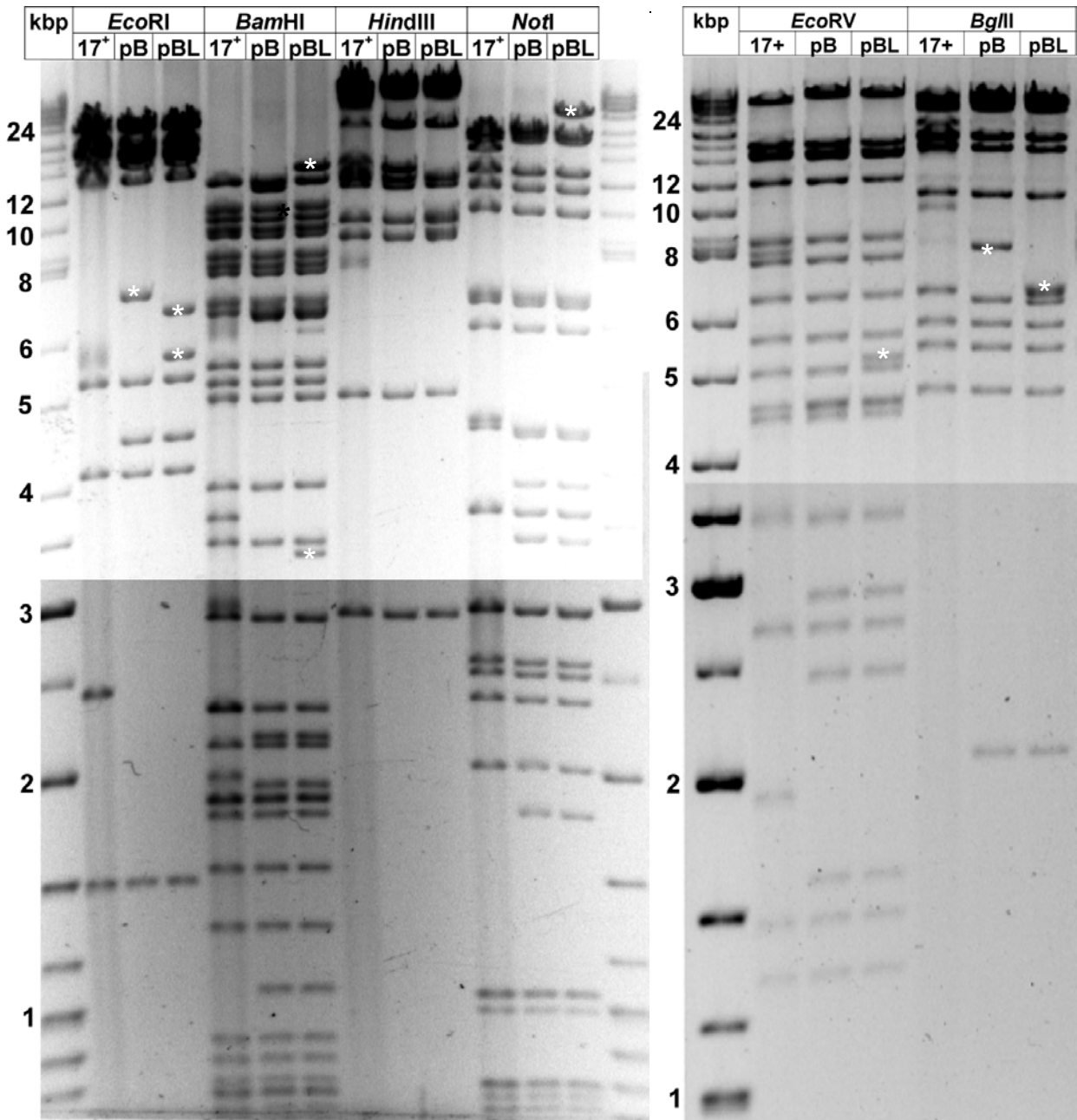


Figure 30: The insertion of Cre-recombinase into pHSV1(17+)blue did not alter the virus backbone. HSV1(17⁺) DNA (17+), pHSV1(17⁺)blue (pB) and pHSV1(17⁺)blueLox (pBL) were digested with *EcoRI*, *BamHI*, *HindIII*, *NotI*, *EcoRV* or *BglII* and separated over 0.6% agarose. Band pattern changes due to the 5.2 kbp insertion of Cre recombinase are indicated (*).

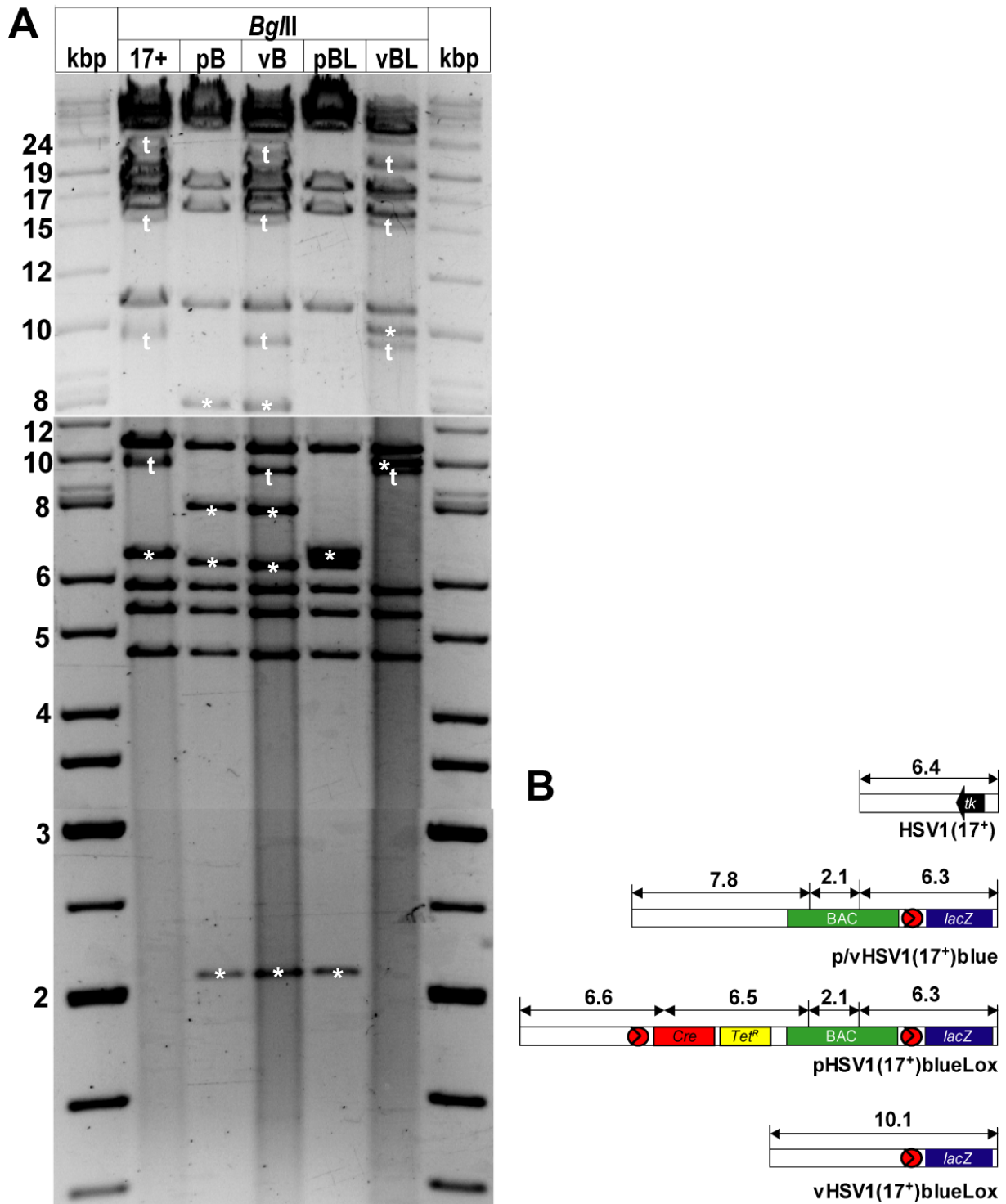


Figure 31: Cre mediated recombination works. (A) HSV1(17⁺)-DNA (17+), pHSV1(17⁺)blue (pB) vHSV1(17⁺)blue-DNA (vB) (pBL), pHSV1(17⁺)blueLox (pBL) and vHSV1(17⁺)blueLox-DNA (vBL) were digested with *Bgl*II and separated over 0.5% agarose. (t) linear DNA genome termini; (*)fragments specific for the BAC and Cre insertion. (B) Schematic representation of the UL23 region of HSV1. The *Bgl*II restriction fragments are indicated.

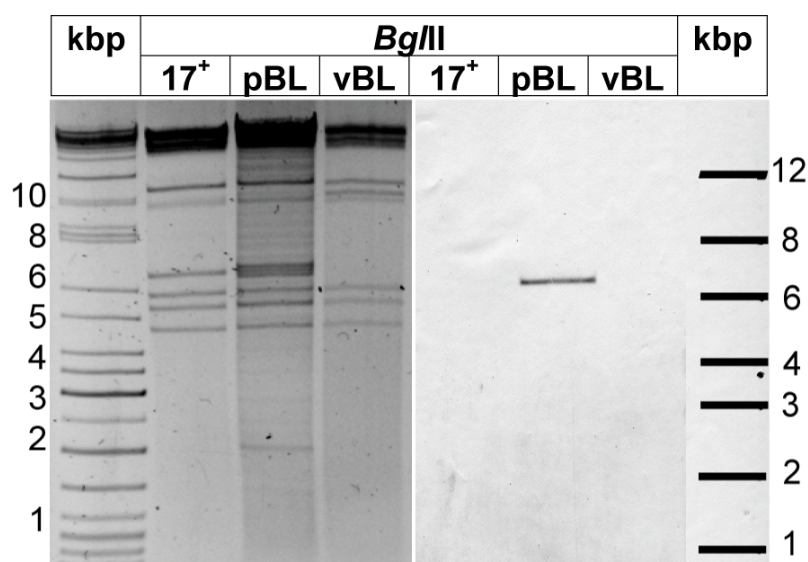


Figure 32: Cre mediated recombination works. HSV1(17⁺) DNA (17⁺), pHSV1(17⁺)blueLox (pBL) and vHSV1(17⁺)blueLox DNA (vBL) were digested with *Bgl*II, separated over 0.6% agarose (gel to the left, ethidium bromide stain) and blotted onto positively charged nylon membrane. The membrane was probed with a DIG-labelled probe specific for chloramphenicol acetyl transferase, which was generated by PCR using primers CHN01 and CHN02. After incubation with an F_{ab} fragment of an anti-DIG antibody coupled to alkaline phosphatase bands were visualised with NBT and BCIP.

4.1.5. Characterisation of BAC-derived viruses

To compare the growth kinetics of the BAC-viruses with wildtype HSV1(17⁺), BHK-21 cells were infected at an MOI of 5 pfu/cell for a single cycle growth kinetic. Samples were taken from the supernatant at different timepoints and their plaque titer was determined. Compared to wildtype, vHSV1(17⁺)blue produced a tenfold lower titer and the amplification was delayed for about six hours. The kinetic of vHSV1(17⁺)blueLox was comparable to wildtype and the titer was lower about fivefold (Figure 33). This trend was observed in three independent growth experiments (data not shown). So although vHSV1(17⁺)blueLox was attenuated compared to wildtype, the excision of BAC sequences by Cre recombination was beneficial. The HSV1 mutant HSV1(KOS)tk12 (Warner et al., 1998) contains a β -galactosidase expression cassette under the control of the HSV1 ICP4 immediate early promoter instead of UL23, making this mutant, which was derived from the wildtype strain KOS, thymidine kinase negative. However, when compared to HSV1(KOS), no significant growth defect was observed in tissue culture (Figure 34).

Results

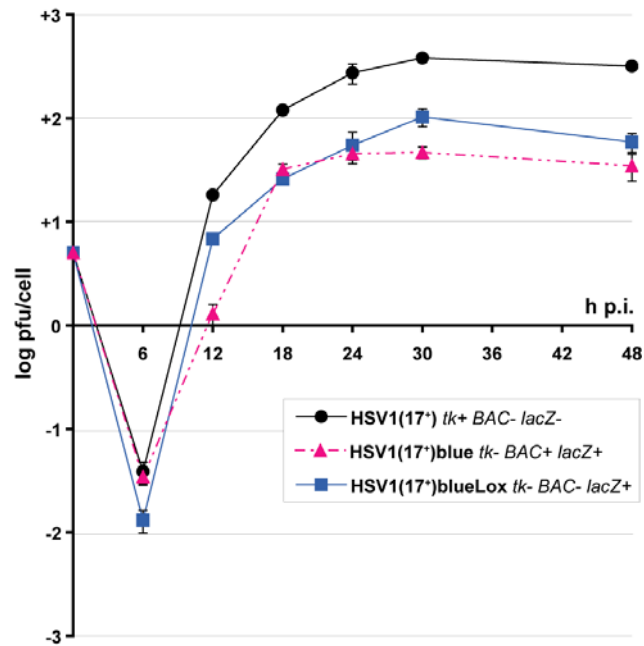


Figure 33: Growth curves of HSV1 (17⁺), vHSV1(17⁺)blue and vHSV1(17⁺)blueLox. BHK cells were infected at an MOI of 5 pfu/cell. Samples were taken from the supernatant at the indicated time points p.i. and plaque titrated in triplicates on Vero cells. Replication of vHSV1(17⁺)blue was delayed compared to wildtype and titers were reduced by a factor of ten. The excision of BAC-genes by Cre recombinase in vHSV1(17⁺)blueLox increased replication kinetics and titer. *tk*, thymidine kinase; *lacZ*, β -galactosidase

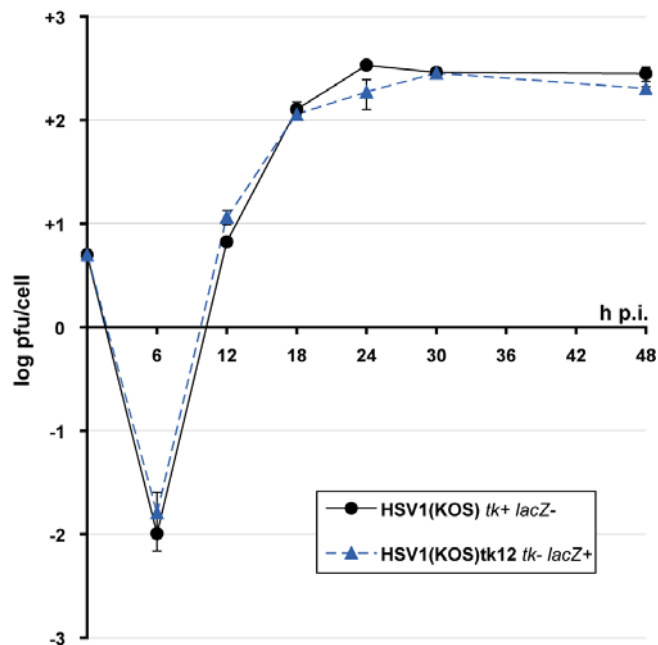


Figure 34: Growth curves of HSV1(KOS) and the thymidine kinase negative mutant HSV1(KOS)tk12. BHK cells were infected at an MOI of 5 pfu/cell. Samples were taken from the supernatant at the indicated time points p.i. and plaque titrated in triplicates. Replication of HSV1(KOS)tk12 is virtually identical to its corresponding wildtype HSV1(KOS). *tk*, thymidine kinase; *lacZ*, β -galactosidase

Results

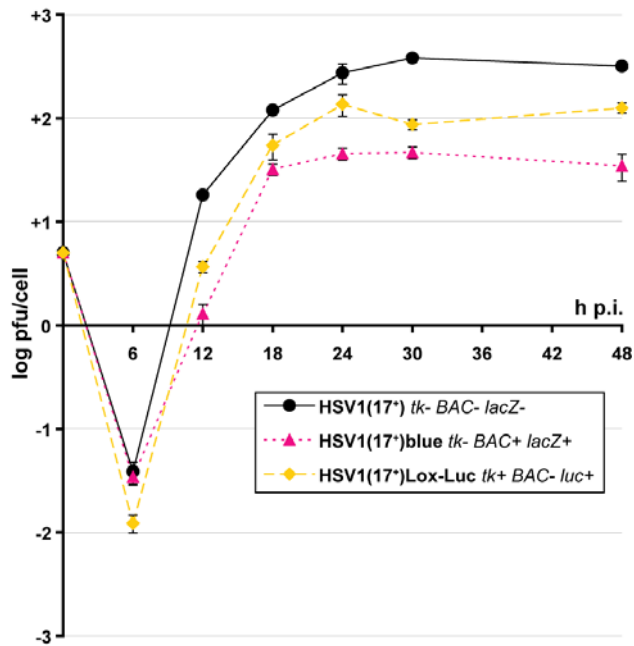


Figure 35: Growth curve of a HSV1(17⁺)-BAC repaired for thymidine kinase. BHK cells were infected at an MOI of 5 pfu/cell. Samples were taken from the supernatant at the indicated time points p.i. and plaque titrated in triplicates. Replication of vHSV1(17⁺)Lox-Luc is improved compared to vHSV1(17⁺)blue, but reduced compared to wildtype. *tk*, thymidine kinase; *lacZ*, β -galactosidase; *luc*, luciferase

The deleted thymidine kinase locus in pHSV1(17⁺)blue was repaired, and the BAC sequences together with a Cre expression cassette were flanked with *loxP* sites in the BAC variant pHSV1(17⁺)Lox (N. Mütter & M. Messerle; Institute of Virology, Hannover Medical School, personal communication). Thus after transfection of pHSV1(17⁺)Lox into permissive cells, the resulting vHSV1(17⁺)Lox was thymidine kinase positive (N. Mütter & M. Messerle; Institute of Virology, Hannover Medical School, personal communication) and did not contain any additional sequences with the exception of a single *loxP* site. A luciferase expression cassette was inserted between UL55 and UL56 for pHSV1(17⁺)Lox-Luc (kindly provided by N. Mütter & M. Messerle; Institute of Virology, Hannover Medical School). When compared to HSV1(17⁺) and vHSV1(17⁺)blue, vHSV1(17⁺)Lox-Luc showed an intermediate virus production with an increased titer and growth kinetics when compared to vHSV1(17⁺)blue. The slight growth defect compared to HSV1(17⁺) wildtype may be explained with the insertion of the luciferase transgene.

Overall, a second *loxP* site together with an expression cassette for Cre recombinase were inserted by Red recombination. After transfection into eukaryotic cells, Cre recombinase efficiently excised the BAC and Cre sequences from the viral genome, resulting in a growth advantage of vHSV1(17⁺)blueLox compared to vHSV1(17⁺)blue. The remaining attenuation compared to HSV1(17⁺) was probably not solely caused by the deletion of thymidine kinase and the insertion of β -galactosidase, since the virus mutant

HSV1(KOS)tk12 which has a very similar genotype was not attenuated in cell culture compared to HSV1(KOS) (Figure 34). The BAC plasmid pHSV1(17⁺)blueLox is the basis for the construction of HSV1 mutants.

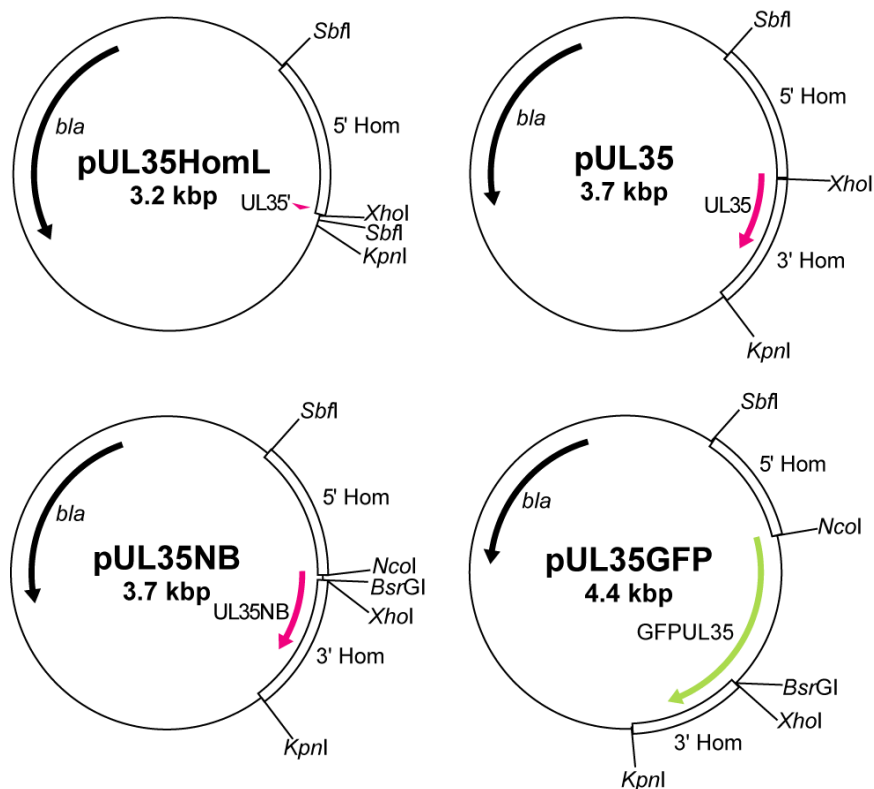
4.2. Tagging of VP26 with a fluorescent protein

The first target for a modification in pHSV1(17⁺)blueLox was the small capsid protein VP26 encoded by the UL35 open reading frame. It contains 112 amino acids and has an apparent molecular weight of about 12 kDa (Davison et al., 1992; McNabb and Courtney, 1992). The hexons, but not the pentons of the HSV1 capsids are decorated with six copies of VP26 by an interaction with the N-terminus of the major capsid protein VP5 (Desai et al., 2003; Zhou et al., 1995). In the HSV1 mutant HSV1-K26GFP, the green fluorescent protein (GFP) was inserted into the N-terminus of VP26 in HSV1, strain KOS (Desai and Person, 1998). The tagged protein is incorporated into the virus particle making this virus a valuable tool for studying intracellular trafficking of HSV1 capsids in fixed samples or, the biggest advantage, in live cells by video or time-lapse microscopy. Other alphaherpesvirus were tagged at VP26 with GFP or the monomeric red fluorescent protein mRFP1 (del Rio et al., 2005; Smith et al., 2001; Wild et al., 2005). GFPVP26-labelled HSV1 capsids were used for the reconstitution of capsid transport along microtubules *in vitro* (Wolfstein et al., 2006). For further analyses of the intracellular trafficking of GFP-tagged HSV1 capsids, further mutations can help elucidating the role of other HSV1 proteins. However, the described HSV1-K26GFP was constructed in HSV1, strain KOS, whose full sequence is not published.

4.2.1. Fluorescence-tagged VP26 by Red recombination

To allow the use of GFPVP26-tagged HSV1 for studying viral mutants generated by BAC-mutagenesis, the fluorescence label was reconstructed in pHSV1(17⁺)blueLox. The GFP derivatives cyan fluorescent protein (CFP; Heim et al., 1994) and yellow fluorescent protein (YFP; Ormo et al., 1996) as well as the *Discosoma* sp. DsRed derived monomeric red fluorescent protein (mRFP1; Campbell et al., 2002)) were chosen as alternative fluorescence tags.

Results



| | | | | | | | | | | | | | | | | | | |
|-------------------------|-----|-----|-----|-----|-----|-----|-----|-----|-----|-----|-----|-----|-----|-----|-----|-----|-----|-----|
| HSV1 (17 ⁺) | ATG | GCC | GTC | CCG | CAA | TTT | CAC | CGC | | | | | | | | | | |
| | M | A | V | P | Q | F | H | R | | | | | | | | | | |
| | | | | | | | | | | | | | | | | | | |
| | | | | | | | | | | | | | | | | | | |
| pUL35 | ATG | GCC | GTC | CCG | CAC | TCG | AGC | CGC | | | | | | | | | | |
| | M | A | V | P | H | S | S | R | | | | | | | | | | |
| | | | | | | | | | | | | | | | | | | |
| | | | | | | | | | | | | | | | | | | |
| pUL35NB | ATG | GCC | GTC | CCG | CAC | TCG | ACC | ATG | GTG | TAC | AAC | TCG | AGC | CGC | | | | |
| | M | A | V | P | H | S | T | M | V | Y | N | S | S | R | | | | |
| | | | | | | | | | | | | | | | | | | |
| | | | | | | | | | | | | | | | | | | |
| pUL35GFP | ATG | GCC | GTC | CCG | CAC | TCG | ACC | ATG | GTG | AGC | ... | GAG | CTG | TAC | AAC | TCG | AGC | CGC |
| | M | A | V | P | H | S | T | M | V | S | ... | E | L | Y | N | S | S | R |
| | | | | | | | | | | | | | | | | | | |
| | | | | | | | | | | | | | | | | | | |
| pUL35RFP | ATG | GCC | GTC | CCG | CAC | TCG | ACC | ATG | GAT | CCG | ... | ACC | GGG | TAC | AAC | TCG | AGC | CGC |
| | M | A | V | P | H | S | T | M | D | P | ... | T | G | Y | N | S | S | R |
| | | | | | | | | | | | | | | | | | | |
| | | | | | | | | | | | | | | | | | | |

Figure 36: Construction of fluorescence tagged VP26. 554 bp upstream of the insertion site were amplified from HSV1(17⁺)-DNA and cloned into pUC18. Then, 533 bp downstream of the insertion site were amplified with primers CHN05 and CHN06-500 and cloned into the product of the previous ligation. The resulting plasmid pUL35 contains the entire VP26 ORF. Due to the *XhoI* site insertion in pUL35, codons 4 to 6 of VP26 were changed from Gln-Phe-His to His-Ser-Ser. To insert the fluorescent protein sequences, a DNA linker providing a *NcoI* and a *BsrGI* site was inserted into the *XhoI* site of pUL35 for pUL35NB. For pUL35GFP, the GFP sequence was cut from pEGFP-N1 with *NcoI* and *BsrGI* and cloned into pUL35NB. The strategy was based on the construction of a GFPVP26 fusion protein described in Desai and Person (1998).

Results

A GFPVP26 fusion protein was constructed as described before (Desai and Person, 1998; Figure 36). First, an *Xho*I site was inserted between codons 4 and 6 of VP26 by PCR. Therefore, 554 bp upstream of the insertion site were amplified from HSV1(17⁺)-DNA with primers CHN03-500 and CHN04, digested with *Sbf*I and cloned into pUC18. Then, 533 bp downstream of the insertion site were amplified from HSV1(17⁺)-DNA with primers CHN05 and CHN06-500, digested with *Kpn*I and *Xho*I and cloned into the correctly oriented product of the previous ligation. The resulting plasmid pUL35 contained the complete VP26 ORF with adjacent UL34 and UL36 sequences. Due to the *Xho*I site insertion in pUL35, codons 4 to 6 of VP26 were changed from Gln-Phe-His to His-Ser-Ser. To insert the sequences of CFP, GFP or YFP, a DNA linker providing a *Nco*I and a *Bsr*GI site was obtained by annealing the oligonucleotides CHN09 and CHN10 and inserted into the *Xho*I site of pUL35 for pUL35NB. The fluorescent protein sequences were cut from pECFP-N1, pEGFP-N1 or pEYFP-N1 (all from Clontech, Mountain View, CA, USA) with *Nco*I and *Bsr*GI and cloned into pUL35NB for pUL35CFP, pUL35GFP and pUL35YFP, respectively. In these constructs, the FP-tagged VP26 ORF starts with the first four original codons, followed by the additional codons derived from the *Xho*I site insertion, then the FP sequence which ends prior to codon eight of VP26 (Figure 36). The FP insertion site was flanked on both sites with approximately 0.5 kbp. For pUL35RFP, the mRFP1 coding sequence was excised from pRESET-B-mRFP1 (Campbell et al., 2002) with *Bam*HI and *Sgr*AI, treated with Klenow polymerase and ligated blunt-ended into *Nco*I/*Bsr*GI cut pUL35NB which was also Klenow-treated.

To transfer the fluorescence-tagged VP26 constructs into pHSV1(17⁺)blueLox a two step Red-recombination procedure was used (Figure 37). In the first step, an *rpsLneo* selection/counterselection cassette was amplified from pRpsL-neo (Gene Bridges GmbH, Dresden, Germany) with primers CHN13 and CHN14, which carry 50 nt of 5' overhangs homologous to 50 bp upstream and downstream of the FP insertion site in VP26. The *rpsLneo*-cassette was introduced into pHSV1(17⁺)blueLox by Red-recombination induced from pKD46 under selection for the kanamycin resistance encoded on the cassette.

Results

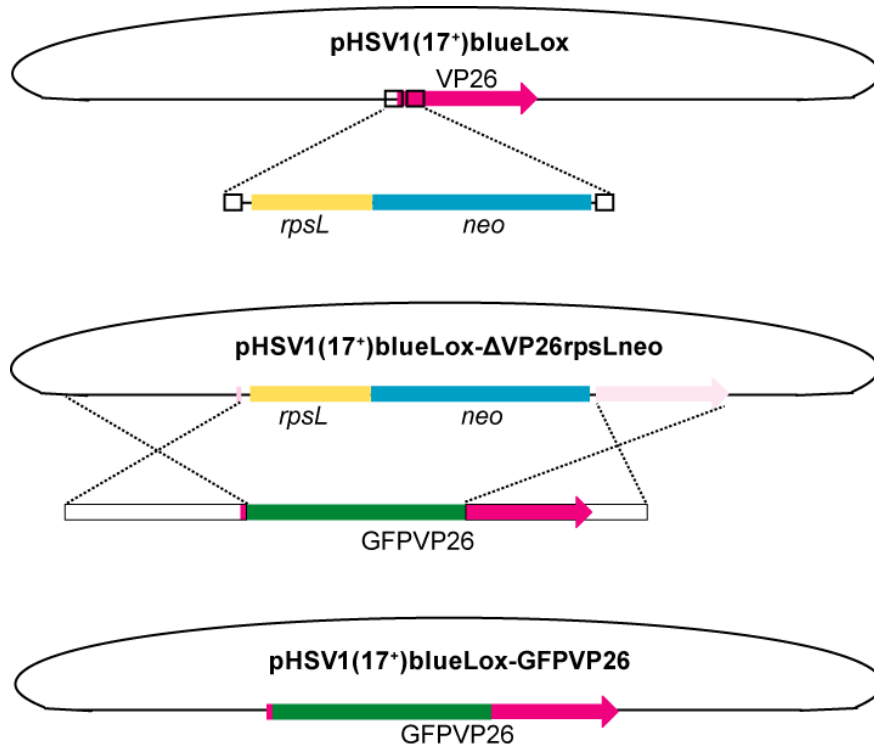


Figure 37: Transfer of fluorescence tagged VP26 into pHSV1(17⁺)blueLox. For the insertion of GFPVP26 into pHSV1(17⁺)blueLox an *rpsLneo* cassette was amplified with primers carrying 50 nt overhangs homologous to the sequences flanking the GFP insertion site and introduced into the BAC by Red-recombination under kanamycin selection. Thereby the VP26 (UL35) ORF was disrupted in the BAC pHSV1(17⁺)blueLox-ΔVP26rpsLneo. The cassette was replaced by a second Red-recombination with a GFPVP26 construct with 500 bp of homologous sequences flanking the GFP, which was present on pUL35GFP. This recombination occurred under streptomycin counterselection.

Three clones of pHSV1(17⁺)blueLox-ΔVP26rpsLneo were recovered. Clone 1 was analysed by restriction digestions, showing the expected bandshifts in the *EcoRI*, *EcoRV*, *BamHI* and *NotI* patterns due to the 1.3 kbp insertion, and an additional fragment after digestion with *BspHI*, due to an additional restriction site on the cassette. No changes were observed in other restriction fragments (Figure 38). The VP26 ORF was disrupted by the insertion and translation stopped after seven codons. Nevertheless, like for HSV1-KΔVP26Z (Desai et al., 1998), this BAC led to the recovery of viable virus after transfection into Vero cells. Plaques developed after two days and six days after transfection all cells were cytopathic and detached. After separation of capsid proteins of vHSV1(17⁺)blueLox-ΔVP26rpsLneo in SDS-polyacrylamide gel electrophoresis, no VP26 signal was detected by Western blotting (Figure 52, page 114).

Results

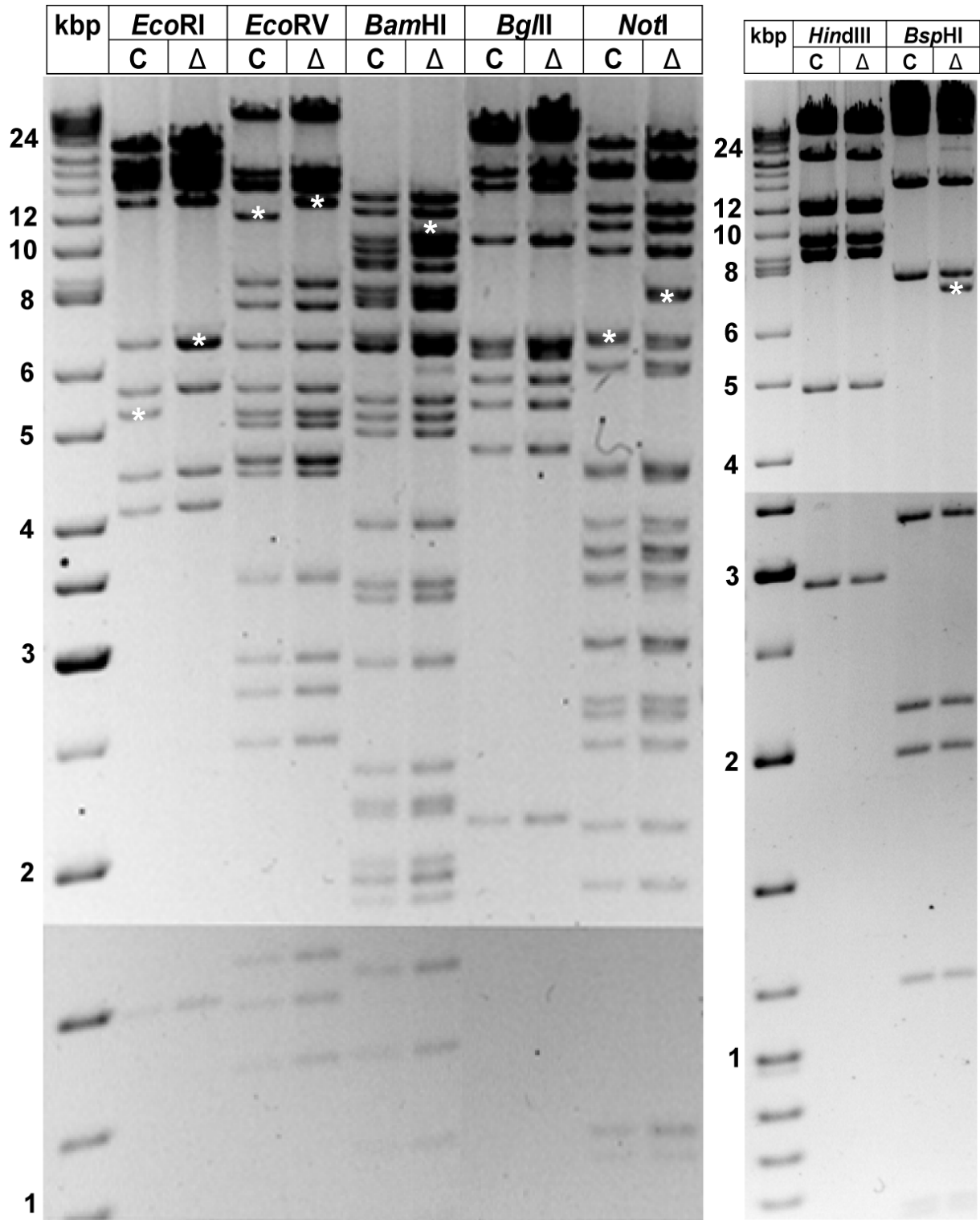


Figure 38: Characterisation of pHSV1(17⁺)blueLox-ΔVP26rpsLneo. pHSV1(17⁺)blueLox-ΔVP26rpsLneo (lane Δ) was digested with *EcoRI*, *EcoRV*, *BamHI*, *BglII*, *NotI*, *HindIII* or *BspHI* in comparison to pHSV1(17⁺)blueLox (lane C). The samples were separated on a 0.6% agarose gel in 0.5x TBE. Changes in the fragment pattern resulting from the *rpsLneo* insertion into VP26 are marked (*).

Results

Additional to the kanamycin resistance, the *rpsL* protein dominantly represses *in trans* the mutation in the ribosomal protein S12 (*rpsL*) of *E. coli* DH10B, which confers streptomycin resistance (Finken et al., 1993). Thus, *E. coli* DH10B harbouring pHSV1(17⁺)blueLox-ΔVP26rpsLneo became streptomycin-sensitive.

In the second step of reconstructing FP-tagged VP26 derivatives in the BAC, the *rpsLneo* cassette was replaced by Red-recombination with the FP-VP26 constructs described above, thereby restoring the streptomycin resistance of *E. coli* DH10B, which was selected for during this procedure. The recombination fragments for Red recombination into pHSV1(17⁺)blueLox-ΔVP26rpsLneo were amplified from pUL35CFP, pUL35GFP or pUL35YFP with primers CHN21 and CHN22, and *E. coli* DH10B harbouring pHSV1(17⁺)blueLox-ΔVP26rpsLneo were transformed with the PCR product. For this second Red recombination, the 500 bp of homologous sequences were preferred over 50 bp to ensure a more specific exchange of *rpsLneo*. Even after a mock transfection with water, many streptomycin-resistant colonies were obtained, indicating that the clones gained streptomycin-resistance by the loss of the *rpsLneo* cassette by unspecific recombination or by an inactivation of *rpsL*. Therefore, all clones were screened by colony PCR with primers CHN03-500 and CHN06-500 for the specific replacement of the *rpsLneo* cassette with the FP-VP26 construct. Clones with a positive PCR signal at 1.7 kbp were chosen for further restriction analysis. Surprisingly, of 9 clones transfected, only the clone pHSV1(17⁺)blueLox-CFPVP26[7B] led to the development of plaques and a complete cytopathic effect after transfection into Vero cells, thereby exhibiting nuclear punctate fluorescence (not shown). On the other hand, all other clones which were positive for the FP insertion as detected by PCR were not infectious after transfection or strongly attenuated. However, they showed a punctate nuclear fluorescence pattern (Figure 39). A subsequent sequencing of the BAC-clones GFPVP26[6A], CFPVP26[7B] and YFPVP26[9C] in the region preceding the FP insertion demonstrated, that the fluorescent proteins were inserted correctly (Figure 40).

For analysis of the repetitive regions between the long and the short genome part, all FP-VP26 clones were digested with *NotI* (Figure 41). The *NotI* joint fragments at around 3.3 kbp showed a strong heterogeneity. It is, however, unclear whether genomic alterations in this region were the sole cause for the complete loss of infectivity of some FP-VP26 BAC-clones. The exceptional clone vHSV1(17⁺)blueLox-CFPVP26[7B] was infectious as stated above, showed a similar growth kinetic compared to vHSV1(17⁺)blueLox but reached reduced titers (Figure 42). Nevertheless, vHSV1(17⁺)blueLox-ΔVP26rpsLneo was more attenuated, was amplified with slower kinetics and reached tenfold lower titers compared to vHSV1(17⁺)blueLox (Figure 42).

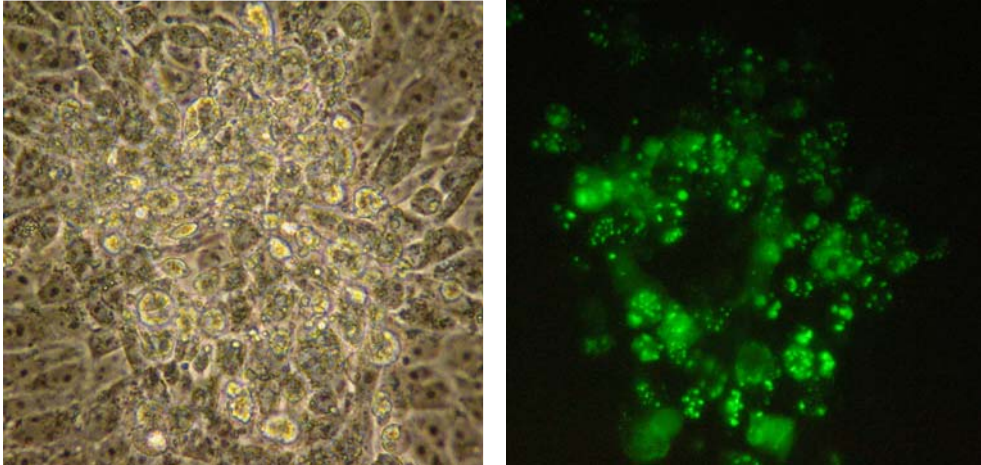


Figure 39: Attenuated phenotype of GFPVP26 clone 6A. 4 d after transfection of Vero cells with pHSV1(17⁺)blueLox-GFPVP26[6A], only small plaques had developed which did not increase in size during further incubation. In many cells, the GFP fluorescence was localised to nuclear puncta, comparable to infection with HSV1-K26GFP.

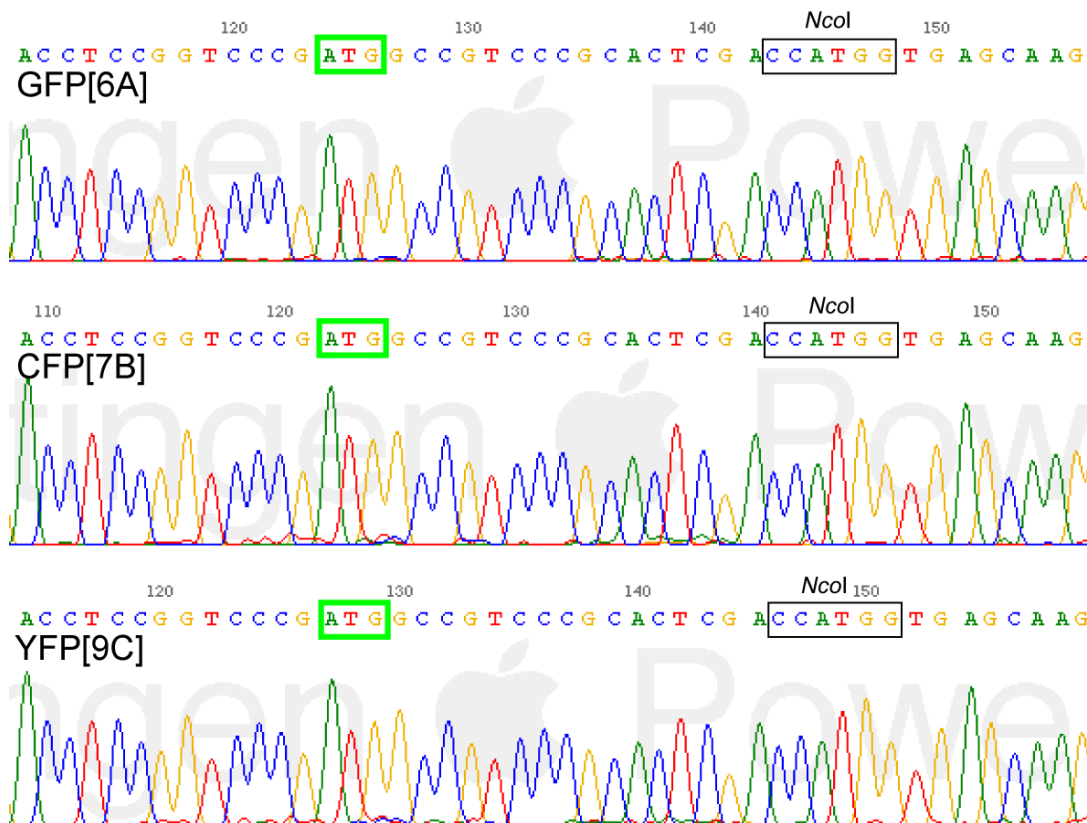


Figure 40: Sequences of BAC clones GFPVP26[6A], CFPVP26[7B] and YFPVP26[9C]. Sequencing results obtained with primer CHN43. The sequences at the site of the FP insertion into VP26 were identical in all three clones and were consistent with the cloning strategy (cf. Figure 36). The start ATG of FP-VP26 (green box) and the *NcoI* site after which the fluorescent protein sequence was inserted (black box) are indicated.

Results

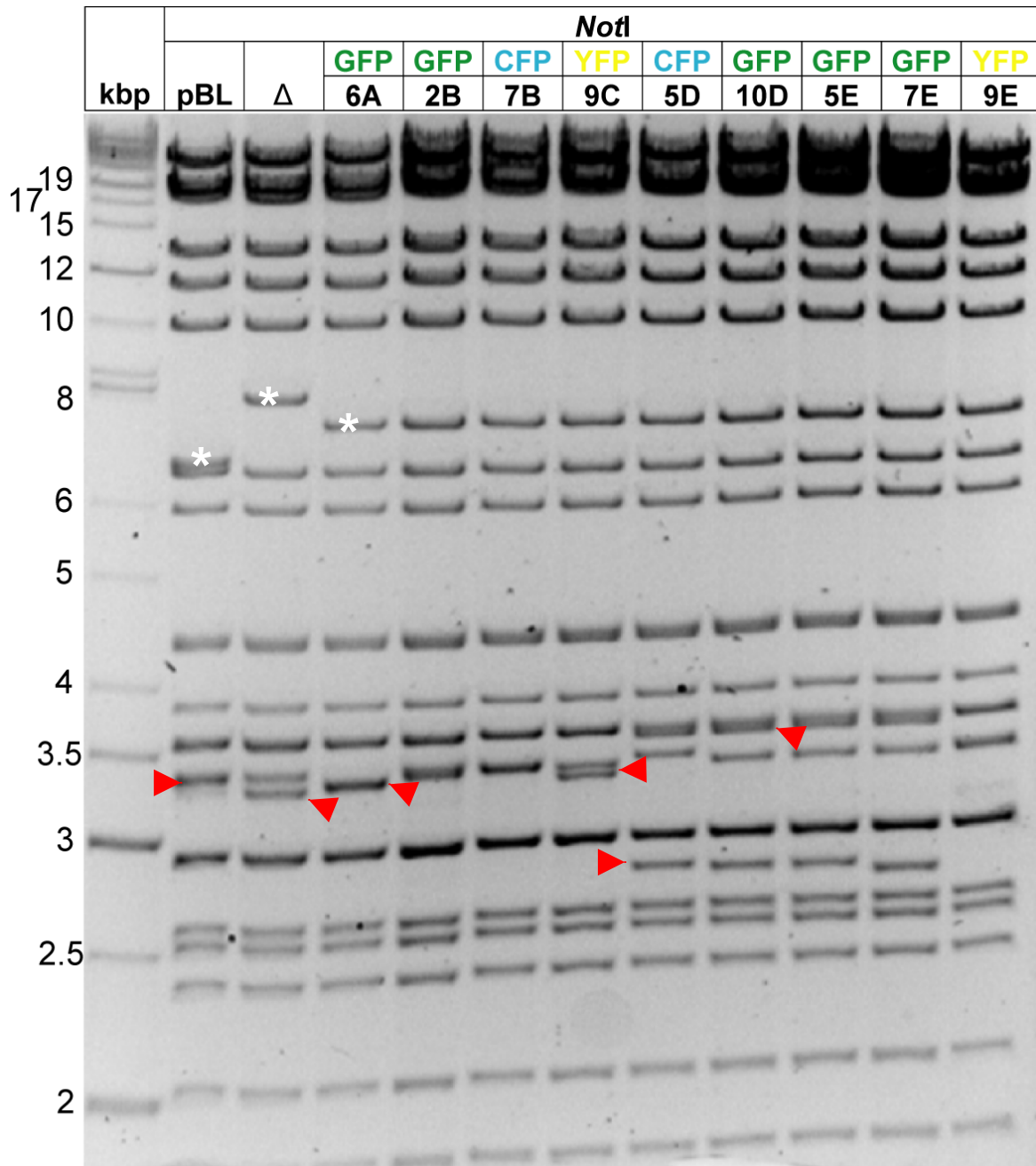


Figure 41: The terminal repeats became unstable upon Red recombination. Streptomycin-resistant BAC clones, which were PCR positive for the insertion of a FP-VP26 were digested with *NotI* and separated over 0.65% agarose in 0.5x TBE. pHSV1(17⁺)blueLox (pBL) and pHSV1(17⁺)blueLox-ΔVP26rpsLneo (Δ) served as control. Bandshifts resulting from the *rpsLneo* or FP insertion, respectively, are marked (*) as well as bands which represent joint fragments with changing size (red arrowheads).

Results

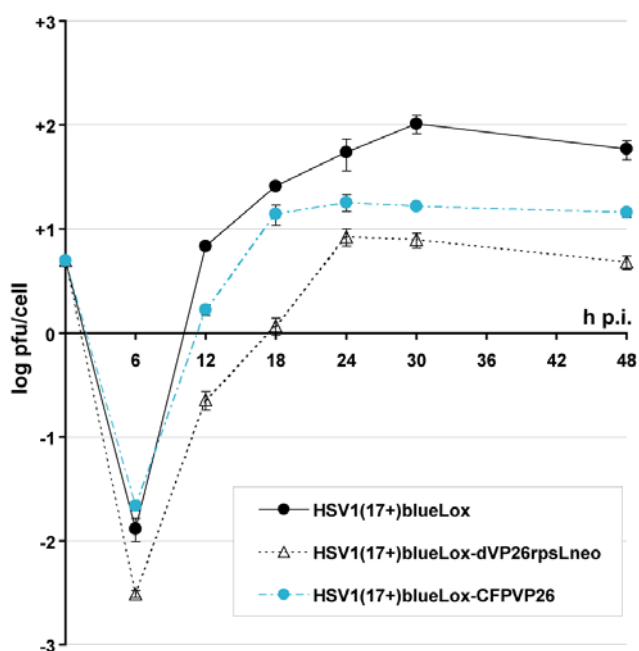


Figure 42: Growth curve of CFPVP26 expressing HSV1. BHK cells were infected at an MOI of 5 pfu/cell. Samples were taken from the supernatant at the indicated time points p.i. and plaque titrated in triplicates. The replication of vHSV1(17⁺)blueLox-CFPVP26[7B] was attenuated in titer compared to vHSV1(17⁺)blueLox, but with faster kinetics and higher titer than of vHSV1(17⁺)blueLox-ΔVP26rpsLneo.

4.2.2. Construction of a HSV1-GFPVP26 virus by shuttle mutagenesis

The Red-recombination probably had a deleterious effect on the terminal repeat sequences of HSV1. The GFPVP26 constructs were therefore cut from pUL35GFP and cloned into the *Sma*I site of pST-SNR for a mutagenesis approach based on RecA-mediated shuttle mutagenesis. After the formation and resolution of cointegrates, the sucrose-resistant clones were screened by digestion with *Not*I, and clones with correct restriction patterns were identified (not shown). A more detailed restriction analysis with *Eco*RI, *Hind*III, *Bgl*II, *Not*I and *As*I revealed that with the exception of the GFP insertion, no major changes had taken place in clone pHSV1(17⁺)blueLox-GFPVP26[20] (Figure 43). After transfection of GFPVP26[20] into Vero cells, fluorescent cells were observed after one day and small plaques developed after four days. Seven days after transfection the plaques were large, but most of the cell lawn was neither showing any cytopathic effect nor fluorescence. Clone GFPVP26[33], which was identified in a second screening round, had the same phenotype after transfection into Vero cells. After transfection of GFPVP26[33] into BHK-21 cells a more pronounced cytopathic effect was observed, but after harvesting the cells to determine the titer by plaque assay on Vero cells, only very small plaques developed after three days compared to HSV1-K26GFP. In summary, the phenotypes of the GFPVP26 BAC-clones obtained by shuttle mutagenesis were very similar to those constructed by Red recombination, with the exception of clone CFPVP26[7B].

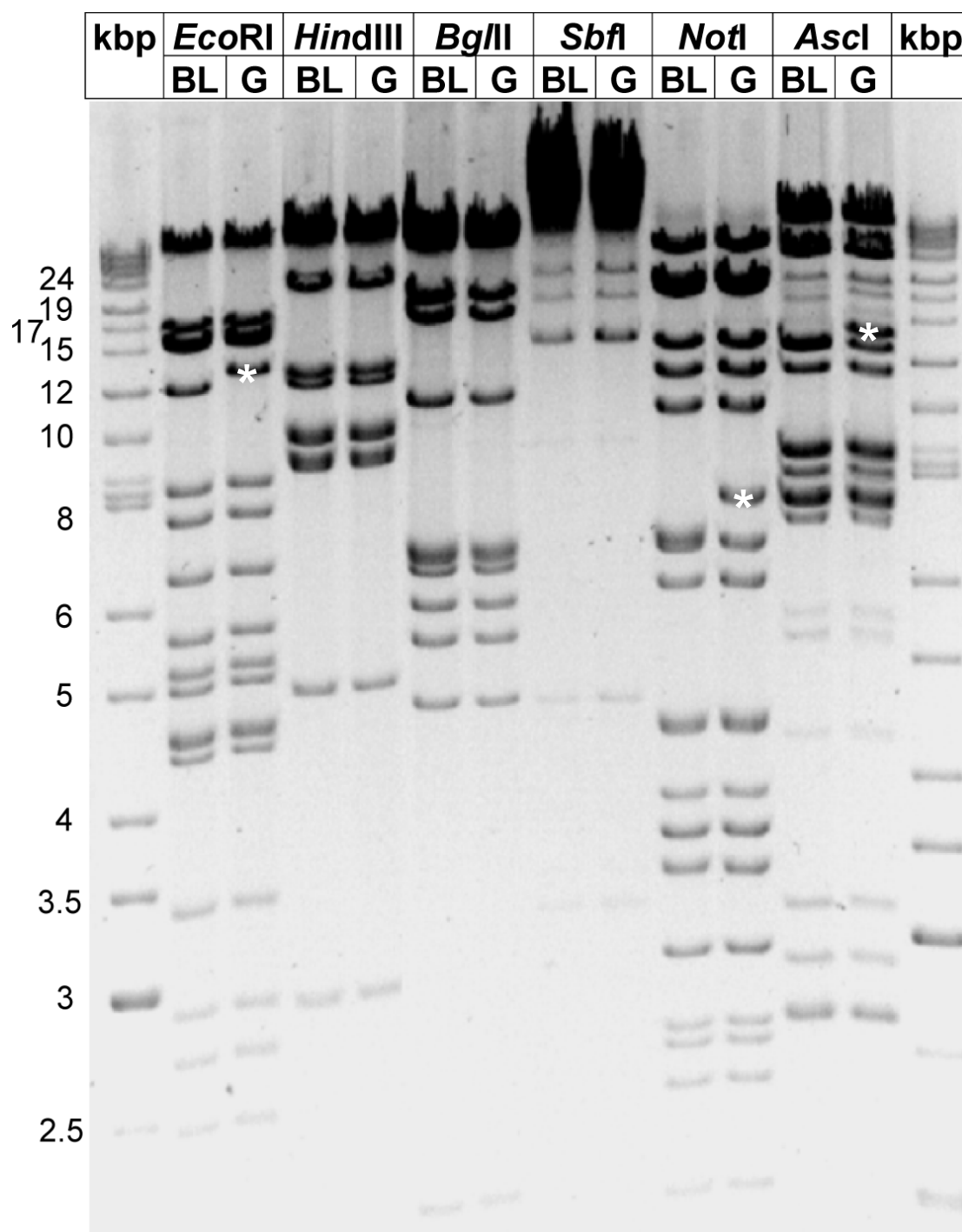


Figure 43: Characterisation of a HSV1-GFPVP26 BAC-clone obtained by shuttle mutagenesis. pHSV1(17⁺)blueLox-GFPVP26[20] (lane G) which was obtained by shuttle mutagenesis was digested with *EcoRI*, *HindIII*, *BglII*, *SbfI*, *NotI*, or *AscI* and separated over 0.6% agarose in 0.5x TBE. pHSV1(17⁺)blueLox (BL) served as control. Bands shifts indicating the GFP insertion, are marked (*).

4.2.3. Marker rescue of BAC-derived GFPVP26 viruses

The cause for the complete loss of infectivity or the strong attenuation of the FP-VP26 BACs was not revealed by restriction analysis or sequencing of FP-VP26 in the BAC context. With marker rescue experiments, the position of possible subtle mutations in FP-VP26 modified BACs was narrowed down. The set of the five HSV1(17⁺) cosmids (Cunningham and Davison, 1993) was linearised with *PacI*, and each of them was cotransfected together with pHSV1(17⁺)blueLox-GFPVP26[33] into BHK-21 cells; pHSV1(17⁺)blueLox-CFPVP26(7B) served as control. Cos14 (HSV1 nucleotides 54445-90478) rescued the attenuation, however, most cytopathic cells were not fluorescent, most probably due to the wildtype VP26 present on Cos14, which was also transferred into the recombinant virus (Figure 44). Since the other cosmids did not rescue, potential lethal mutations in the terminal repeat sequences and other genome regions of HSV1 could be excluded. A 16.6 kbp *NheI/PacI* fragment of Cos14 spanning UL35 (VP26), UL36 (VP1-3) and UL37 and a 12 kbp *NheI/HindIII* fragment encoding UL33-UL36 also rescued the attenuation of GFPVP26[33]. Thus, the mutation with the highest impact for the attenuation of pHSV1(17⁺)blueLox-GFPVP26[33] was mapped to the region of UL33-UL36 (Figure 44).

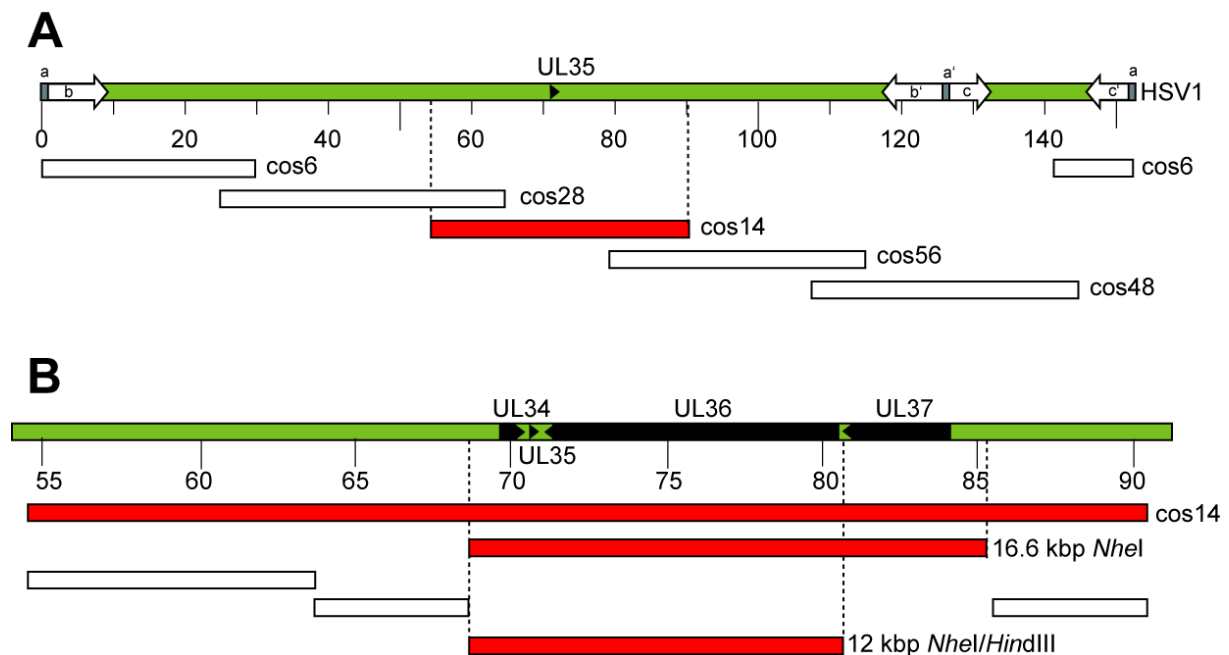


Figure 44: Marker rescue of pHSV1(17⁺)blueLox-GFPVP26[33]. (A) Position of the VP26 ORF in the HSV1 genome. The sequences spanned by a set of five HSV1 cosmids are depicted as boxes. Cosmid 14 (red box) rescued the attenuated phenotype of BAC clone GFPVP26[33] albeit with a loss of fluorescence. (B) Fragments of Cosmid 14 were used for rescue. A 16.6 kbp *NheI* and a 12 kbp *NheI/HindIII* fragment (red boxes) also rescued the attenuation. The numbers indicate the position on the HSV1 genome in kbp.

4.2.4. Construction of a GFPVP26 virus by complementation

To force the insertion of a FP-tagged VP26 into the HSV1 genome, a deletion mutant for UL35 (VP26) and the adjacent essential membrane protein UL34 was constructed. UL34 is required for budding of newly synthesised capsids through the inner nuclear membrane (Reynolds et al., 2001). This virus was then rescued with a DNA fragment encoding UL34 and FP-VP26. After cotransfection into eukaryotes, replication-competent virus would only be recovered after rescue with the UL34/VP26 fragment. The rescue fragments were constructed in pLoCMV-VP1-3 which contains the 12 kbp *NheI/HindIII* fragment of HSV1 encoding UL33-UL36 (Figure 45). The *HpaI/BstBI* fragment which encompasses the wildtype VP26 was replaced with the respective fragment from pUL35CFP, -GFP, -RFP or -YFP. The UL34/VP26 deletion was constructed in pHSV1(17⁺)blue, which does not excise the BAC sequences after transfection into eukaryotes, so that after successful introduction of FP-VP26 in eukaryotes the virus could have been retransferred into *E. coli*. The ORFs UL34 and VP26 were deleted by Red recombination using the *rpsLneo* cassette which was amplified from pRpsL-neo with CHN49 and CHN50. The correct deletion in pHSV1(17⁺)blue- Δ UL34/35 was confirmed by restriction analysis with *EcoRV*, *EcoRI*, *HindIII*, *BglII* and *NotI* (Figure 46). After cotransfection with *HindIII*-linearised pLoCMV-VP1-3 derivatives, only wildtype-VP26 and CFPVP26 gave rise to a cytopathic effect and, in case of CFPVP26, fluorescence, whereas GFPVP26 and YFPVP26 showed only little fluorescent plaques, which were barely growing over time. After rescue of Δ UL34/35 with RFPVP26 large red fluorescent plaques developed, however, after passaging a lysate of the infected cells, there was no longer fluorescence associated with cytopathic cells.

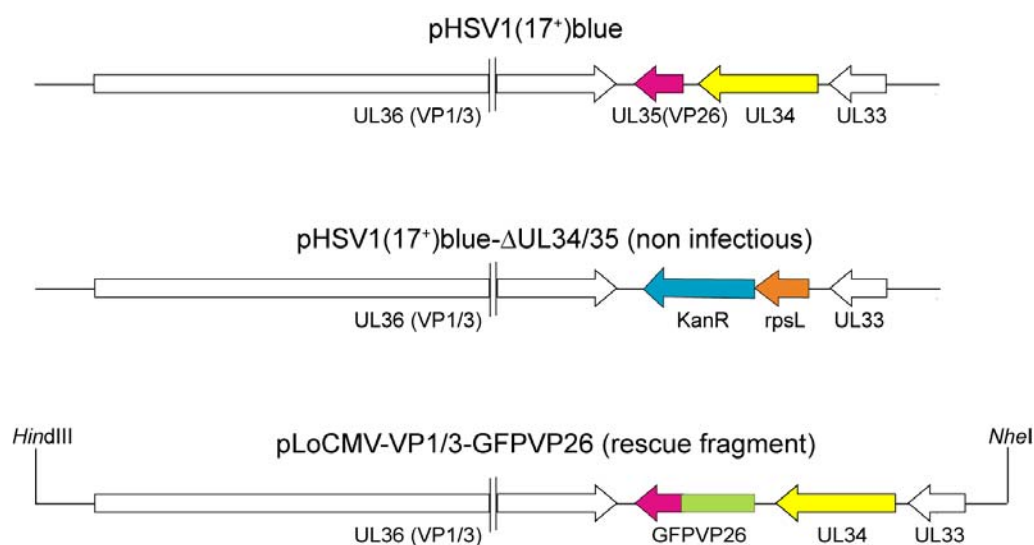


Figure 45: Introduction of FP-VP26 into HSV1 by rescue of a lethal mutant. By deletion of UL34 and VP26 a non-infectious BAC clone was obtained. This was transfected together with a 12 kbp *NheI/HindIII* rescue fragment, in which the VP26 ORF was replaced by a GFPVP26 sequence, into eucaryotic cells. Homologous recombination could then lead to the reconstitution of an infectious genome, coding for the GFP fusion protein.

Results

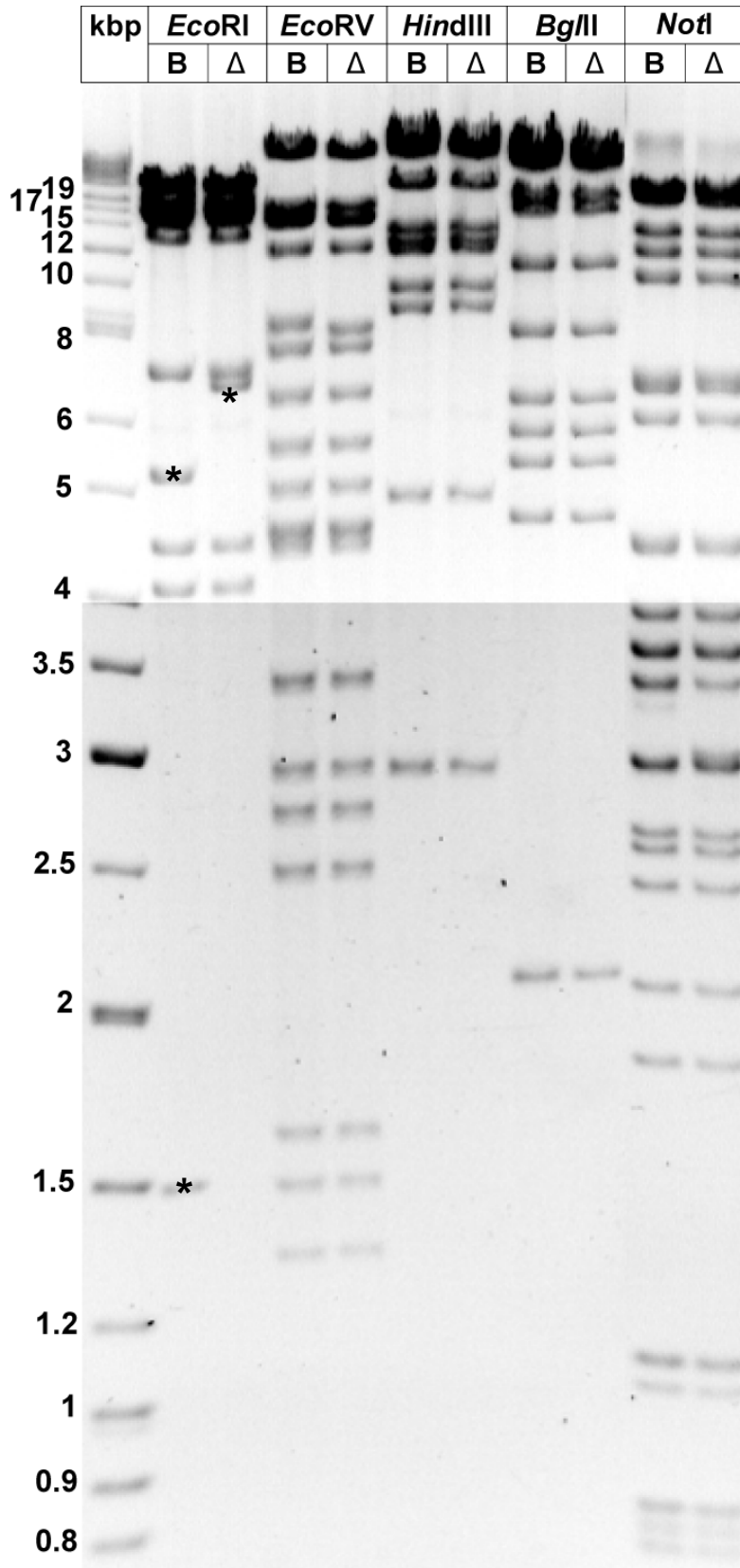


Figure 46: Characterisation of pHSV1(17⁺)blue-ΔUL34/35. pHSV1(17⁺)blue-ΔUL34/35 (lane Δ) was digested with *EcoRI*, *EcoRV*, *HindIII*, *BglII*, *SbfI* or *NotI* comparison to pHSV1(17⁺)blue (lane B). The samples were separated on 0.6% agarose gel in 0.5x TBE. Changes in the fragment pattern resulting from the deletion of UL34 and VP26 by *rpsLneo* are marked (*).

Taken together the results suggested that the FP-VP26 fusion constructs had an inhibitory effect on the growth of HSV1 mutants constructed to express these proteins instead of wildtype VP26 despite the fact that this protein is not essential for growth (Desai et al., 1998) and that the BAC-generated mutant pHSV1(17⁺)blueLox-ΔVP26rpsLneo was infectious.

4.2.5. Without four N-terminal VP26 residues, FP-VP26 is viable

The GFPVP26 virus HSV1-K26GFP was originally obtained by homologous recombination in Vero cells infected with HSV1(KOS) after cotransfection of pK26GFP (Desai and Person, 1998). This plasmid contains the 2.7 kbp *EcoRI/NotI* fragment of HSV1(KOS) with the GFP sequence inserted at the N-terminus of VP26 as described above. However, sequencing of pK26GFP revealed, that in contrast to the published procedure the first 4 original codons (Met-Ala-Val-Pro) of VP26 were missing on pK26GFP (Figure 47). In addition, 53 bases upstream of VP26 are missing. The deletion begun 49 base pairs after the stop codon of UL34 and ended at the start of the UL35 (VP26) ORF. These alterations were also observed after sequencing viral DNA of HSV1-K26GFP and were probably acquired during cloning of pK26GFP. Thus, the translation of the GFPVP26 fusion protein in HSV1-K26GFP starts with the ATG provided by the GFP sequence, three additional upstream codons introduced by the cloning of the fusion protein (His-Ser-Thr, cf. Figure 36) are also not translated. Sequencing also revealed, that besides the abovementioned deletions no further differences in DNA sequence between HSV1(17⁺) and HSV1(KOS) were observed in the flanking regions of the genome.

To test whether the fusion construct in pK26GFP lacking the four N-terminal amino acids of VP26 was functional after transfer into pHSV1(17⁺)blueLox, a fragment was amplified from this plasmid using primers CHN21 and CHN22 and used for the Red-recombination mediated replacement of *rpsLneo* in pHSV1(17⁺)blueLox-ΔVP26rpsLneo. Moreover, the GFP sequence was cut out from pK26GFP with *NcoI* and *BsrGI* and replaced by mRFP1 for pK26RFP as described above for pUL35RFP. After recombination of both GFPVP26 and RFPVP26 into the BAC, 18 streptomycin-resistant clones of each recombination were screened by *NotI* digestion (not shown). Clones GFPVP26(9) and RFPVP26(13) were further characterised by restriction digests with *EcoRI*, *EcoRV*, *BamHI*, *HindIII*, *BglII* and *NotI* (Figure 48 and Figure 49) showing no major alteration except the fluorescent protein sequence insertion. Indeed, after transfection of both pHSV1(17⁺)blueLox-GFPVP26[9] or -RFPVP26[13], fluorescent plaques developed, and the cells developed full cytopathic effects after six days.

Results

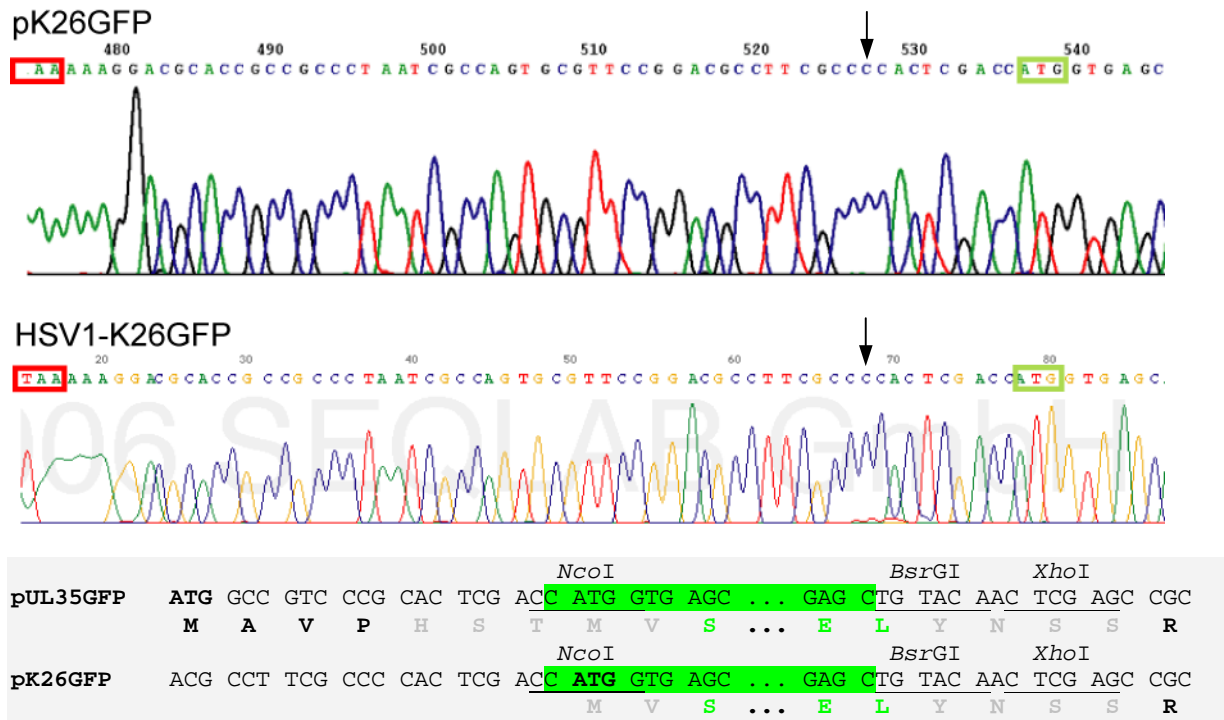


Figure 47: Sequences of pK26GFP and of HSV1-K26GFP. Sequencing results obtained with primer CHN33 (pK26GFP) and CHN43A (HSV1-K26GFP). Compared to the published wildtype sequence which is also present on pUL35 (cf. Figure 36), 53 bp are missing in pK26GFP and HSV1-K26GFP 49 bp downstream of the stop codon of UL34 (red box; arrow at start of deletion). Four original N-terminal VP26 codons were deleted, so the GFPVP26 fusion protein starts directly with the ATG of the GFP sequence (green box).

Results

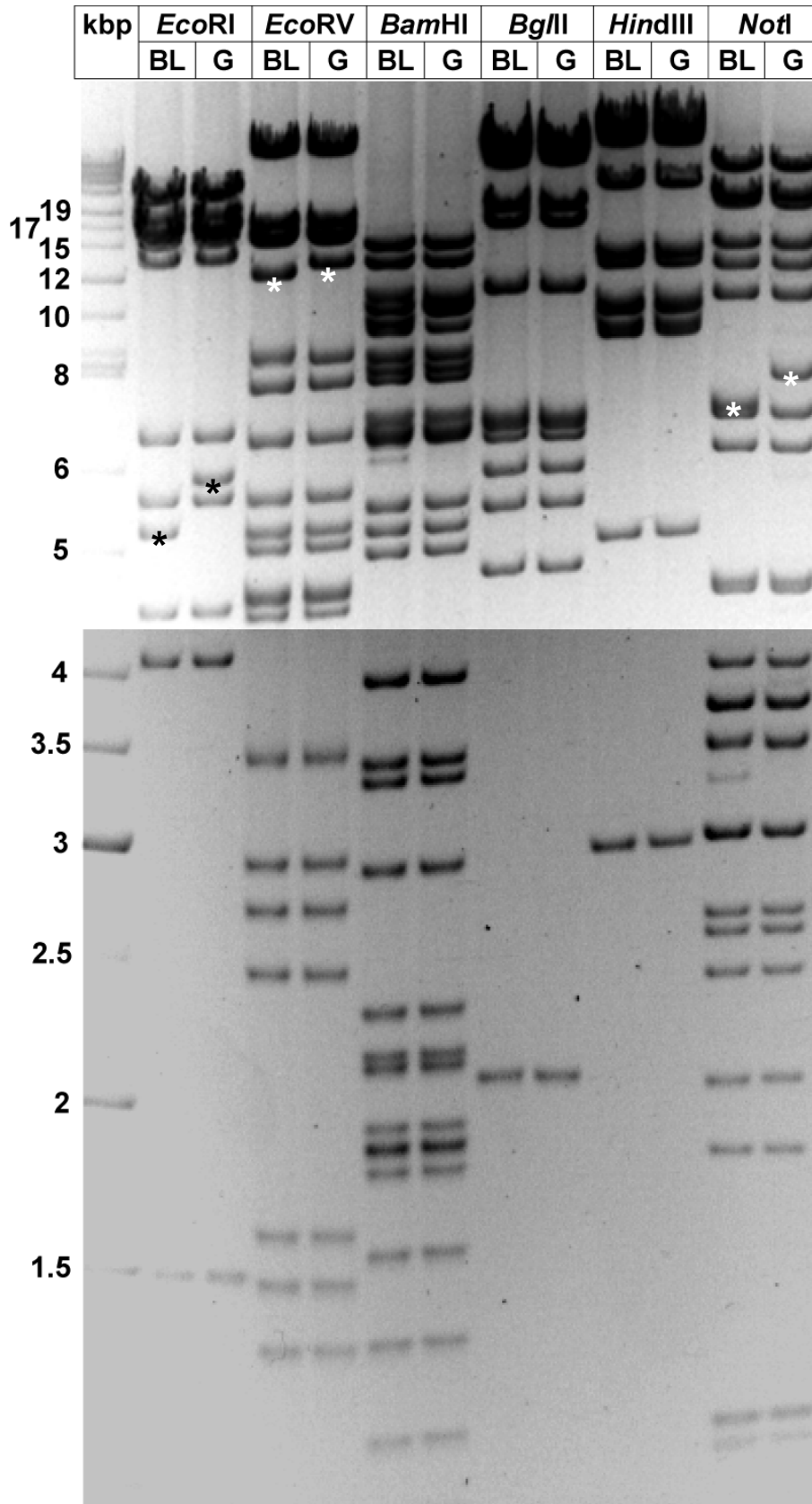


Figure 48: Characterisation of pHSV1(17⁺)blueLox-GFPVP26[9]. pHSV1(17⁺)blueLox-GFPVP26(9) (lane G) was digested with *EcoRI*, *EcoRV*, *BamHI*, *BglII*, *HindIII*, or *NotI* comparison to pHSV1(17⁺)blueLox (lane BL). The samples were separated on 0.6% agarose gel in 0.5x TBE. Changes in the fragment pattern resulting from the GFP insertion are marked (*).

Results

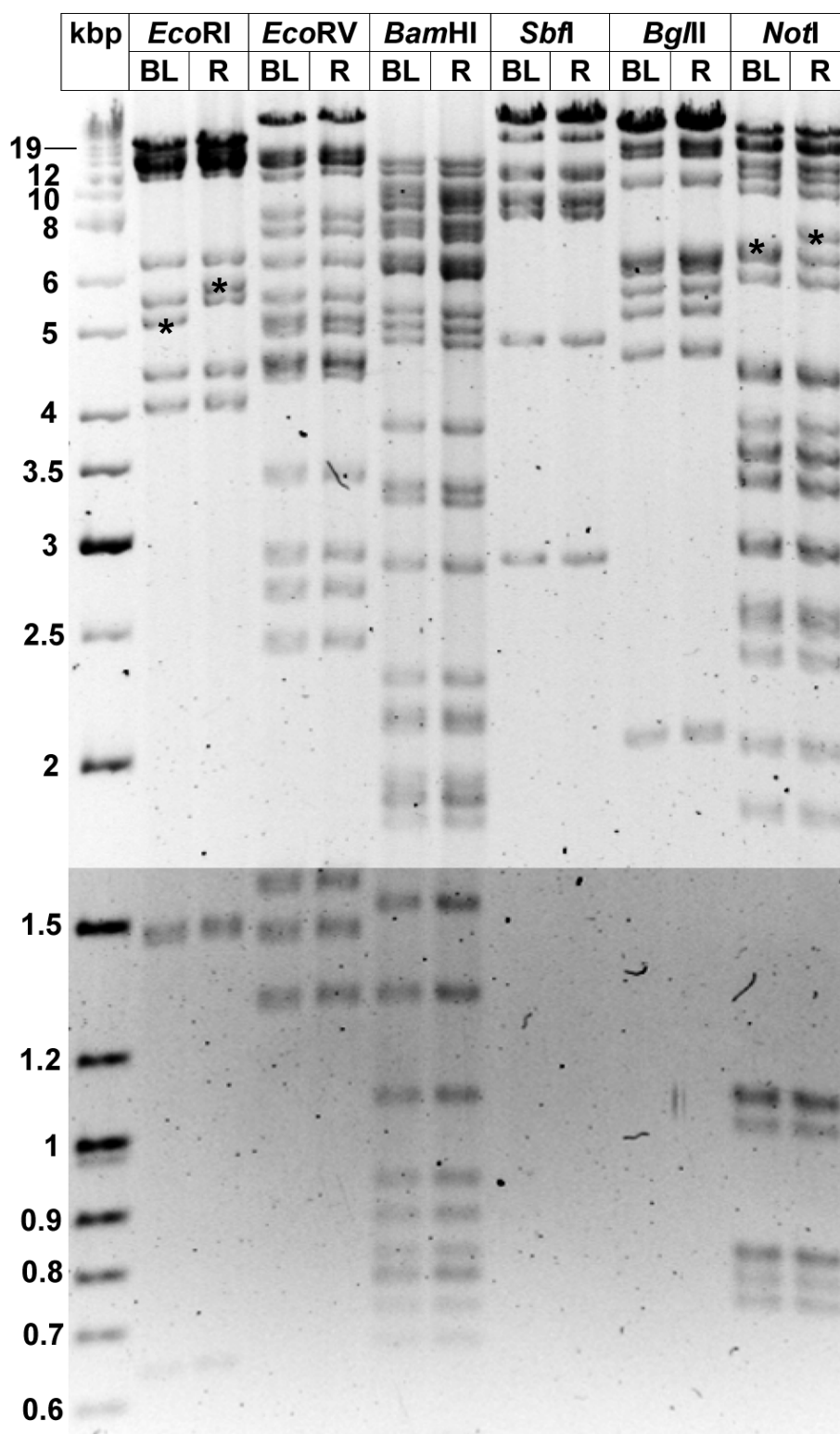


Figure 49: Characterisation of pHSV1(17⁺)blueLox-RFPVP26(13). pHSV1(17⁺)blueLox-RFPVP26(13) (lane R) was digested with *EcoRI*, *EcoRV*, *BamHI*, *SbfI*, *BglII* or *NotI* comparison to pHSV1(17⁺)blueLox (lane BL). The samples were separated on 0.6% agarose gel in 0.5x TBE. Changes in the fragment pattern resulting from the RFP insertion are marked (*).

4.2.6. Growth of HSV1 with GFP/RFP-labelled or deleted VP26

The viruses were passaged twice from the infected cells and used for the preparation of virus stock. In single cycle growth experiments vHSV1(17⁺)blueLox-GFPVP26[9] as well as -RFPVP26[13] reached a fivefold reduced titer compared to vHSV1(17⁺)blueLox, however, the kinetics of vHSV1(17⁺)blueLox-GFPVP26[9] were delayed for about 6 six hours compared to -RFPVP26[13] (Figure 50). Both viruses grew to higher titers than vHSV1(17⁺)blueLox-ΔVP26rpsLneo. Interestingly, for the vHSV1(17⁺)blueLox-GFPVP26[9] the drop of infectivity in the supernatant 6 h after inoculation was not as pronounced as for the other viruses analysed (Figure 50). These results were repeated in an independent experiment (not shown). The growth curves of the previously constructed HSV1-KΔ26Z and HSV1-K26GFP (Desai et al., 1998; Desai and Person, 1998) were also assessed in a single cycle growth experiment (Figure 51). The introduction of GFPVP26 into HSV1(KOS) led to reduction of the titers which was comparable to the attenuation observed for vHSV1(17⁺)blueLox-GFPVP26[9]. The VP26 deletion mutant HSV1-KΔ26Z grew to the same titers as HSV1-K26GFP with almost equal kinetics, which is in strong contrast to the attenuated phenotype of vHSV1(17⁺)blueLox-ΔVP26rpsLneo.

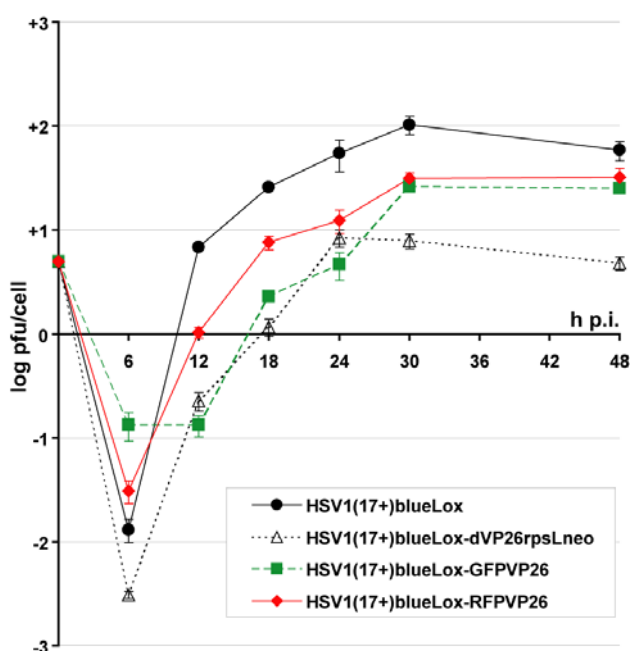


Figure 50: Growth curves of HSV1-BAC based VP26 mutants. BHK cells were infected at an MOI of 5 pfu/cell. Samples were taken from the supernatant at the indicated time points p.i. and plaque titrated in triplicates. The replication of vHSV1(17⁺)blueLox-GFPVP26[9] and -RFPVP26[13] was attenuated in titer compared to vHSV1(17⁺)blueLox, but with faster kinetics and higher titer than of vHSV1(17⁺)blueLox-ΔVP26rpsLneo.

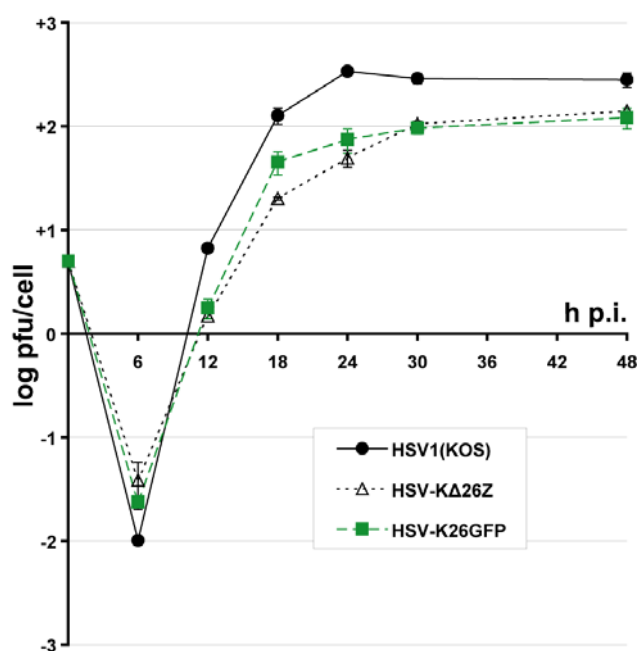


Figure 51: Growth kinetics of previous VP26 mutants. BHK cells were infected at an MOI of 5 pfu/cell. Samples were taken from the supernatant at the indicated time points p.i. and plaque titrated in triplicates. Viruses testes were a VP26 deletion mutant (HSV1-KΔ26Z; Desai et al., 1998) and a virus expressing GFPVP26 (HSV1-K26GFP; Desai and Person, 1998) compared to HSV1(KOS) wildtype, on which the mutants were based.

4.2.7. GFPVP26 and RFPVP26 viruses express only the fusion protein

Virions were pelleted from the medium of cells infected with the BAC-derived VP26 mutants and subjected to SDS-PAGE (Figure 52). In Western blots with a VP26-specific antiserum, a single band at about 14 kDa was observed for HSV1(17⁺), on the other hand there was no signal for vHSV1(17⁺)blueLox-ΔVP26rpsLneo. The GFPVP26 and RFPVP26 fusion constructs have a calculated molecular weight of 38.3 kDa and 37.4 kDa, respectively. Consistent with that, the bands at around 37 kDa in vHSV1(17⁺)blueLox-GFPVP26 and -RFPVP26 represented the fusion proteins (Figure 52). Smaller bands at lower molecular most likely indicate proteolytic degradation. The signal of the major capsid protein VP5 at app. 150 kDa served as loading control, the bands appearing at 100 kDa and 85 kDa were possible degradation products of VP5. When the same membrane was probed with a monoclonal antibody directed against GFP, a signal only appeared at the position of the GFPVP26 fusion protein around 37 kDa and thus no free GFP was present in the virions. The antibody did not cross-react with mRFP1. Due to a lack of an antibody this analysis was not repeated for mRFP1.

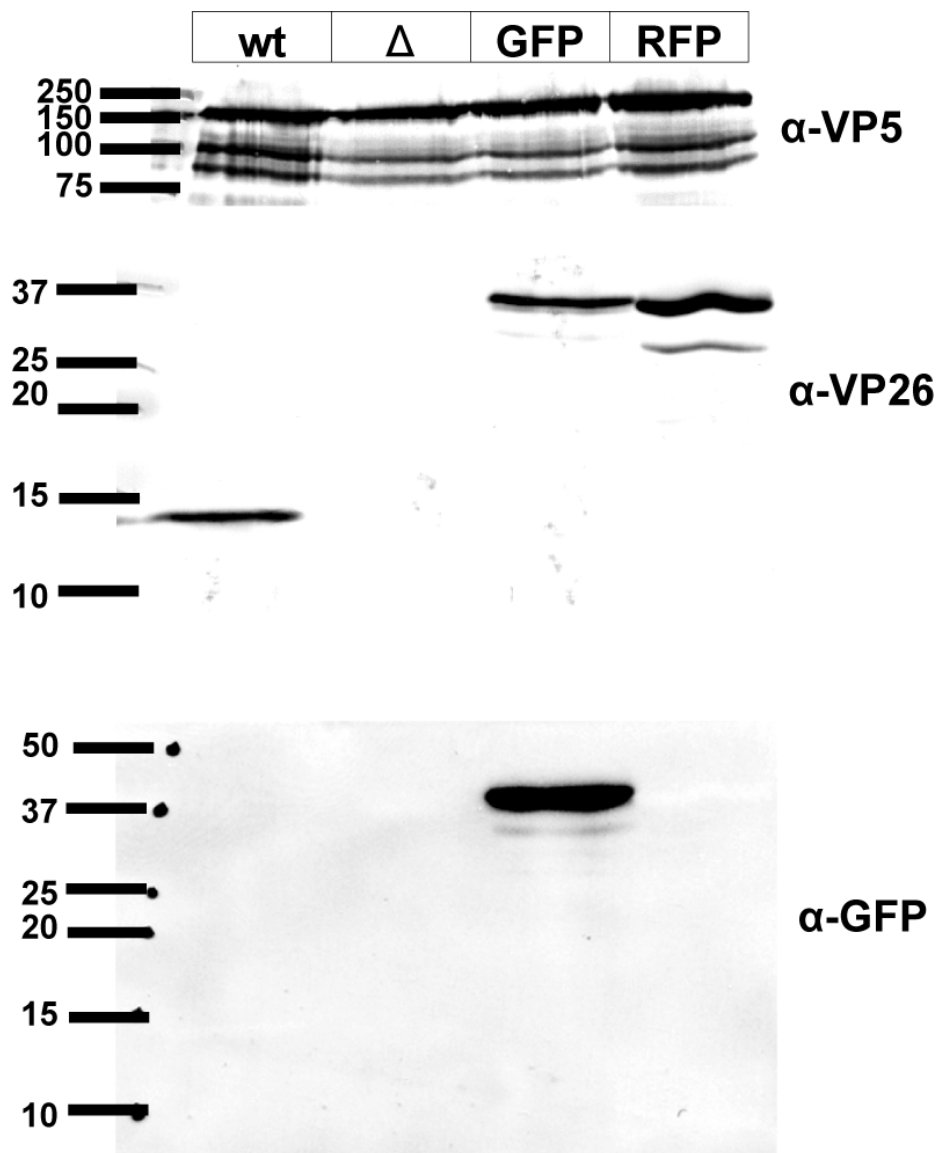


Figure 52: Western blot analysis of VP26 mutants. Virions were pelleted from the medium of cells infected with HSV1(17⁺) (wt), vHSV1(17⁺)blueLox- Δ VP26rpsLneo (Δ), vHSV1(17⁺)blueLox-GFPVP26 (GFP) and -RFPVP26 (RFP) and solubilized in SDS-PAGE sample buffer. After separation on a 10-20% gradient SDS-PAGE gel, the proteins were transferred to nitrocellulose and probed with antisera specific for VP5 and VP26. No VP26 signal was obtained with vHSV1(17⁺)blueLox- Δ VP26rpsLneo whereas vHSV1(17⁺)blueLox-GFPVP26 (GFP) and -RFPVP26 (RFP) express a FP-VP26 fusion protein with higher molecular weight. VP5 served as loading control. All GFP is incorporated as GFPVP26 fusion protein. The sizes of the marker bands are indicated in kDa.

4.2.8. Cell entry of vHSV1(17⁺)blueLox-GFPVP26

In immunofluorescence experiments, the subcellular localisation of the fluorescently labelled VP26 during virus entry was examined. Vero cells were inoculated with gradient purified vHSV1(17⁺)blueLox-GFPVP26 in the presence of cycloheximide to inhibit protein synthesis and thus prevent the formation of progeny virions. The capsids were labelled with the monoclonal mouse antibody (mAb) LP12 which is specific for the major capsid protein VP5.

15 min after infection (p.i.), a punctate GFPVP26 pattern was randomly distributed over the entire cell which often colocalised with VP5, suggesting that GFPVP26 remained associated with the capsids during cell entry (Figure 53). However, many GFPVP26 puncta did not colocalise with the mAb LP12 labelling. On the other hand, some capsids as detected by the VP5 antibody did not exhibit GFP fluorescence. A dissociation of GFPVP26 from the cytosolic capsids upon entry would result in its diffusion within the entire cytosol. Thus, it was unlikely that the puncta, which were not labelled by the VP5 antibody, represented free GFPVP26.

Three hours p.i. most capsids were located at the nucleus and were labelled stronger by the VP5 antibody than 15 min p.i. (Figure 54). Almost all capsids at the nucleus also contained GFPVP26. The labelling intensity of the VP5 antibody and the GFPVP26 fluorescence were heterogeneous and sometimes reciprocal. This may be explained by a reduced accessibility of VP5 if the capsids were covered with GFPVP26. In the cell periphery, the VP5 antibody labelling efficiency was less pronounced than at the nucleus and similar to the labelling intensity at 15 min p.i., whereas the GFPVP26 signal intensity seemed independent of its subcellular localisation.

Thus, capsids of vHSV1(17⁺)blueLox-GFPVP26 were efficiently transported to the nucleus, and GFPVP26 remained bound to the capsids during the cytosolic passage. Nevertheless, the VP5 epitope for mAb LP12 was more accessible on capsids located at the nucleus. The peripheral GFPVP26 structures that were not labelled by the VP5 antibody could reflect an association of GFPVP26 to structures without capsids or capsids with masked LP12 epitopes.

Infected cells showed a strong punctate labelling of a gD antibody which was randomly distributed over the entire cell at 15 min p.i. (Figure 55). The number of puncta positive for gD outnumbered the GFPVP26 signals, and colocalisation was rarely observed. Furthermore, clustered gD-labelled structures were also present. The low degree of colocalisation could be explained by a separation of viral envelope and capsid by fusion at the plasma membrane, an entry pathway, by which Vero cells are predominantly infected (Nicola and Straus, 2004; Sodeik et al., 1997). Nevertheless, the virus preparation contained

a large number of gD-positive particles without capsid, which could consist of defective viral particles, membrane vesicles containing viral glycoproteins and possibly tegument proteins (Döhner et al., 2006).

After 3 h p.i., most gD was found in the cell periphery, where it appeared in clusters, whereas GFPVP26 mainly localised to the nucleus (Figure 56). Virtually no gD signal was detected on GFPVP26 structures at the nuclear envelope. In the periphery, GFPVP26 often colocalised with gD, suggesting that these structures represented endocytosed virions or virions bound to the plasma membrane.

The efficiency of capsid transport to the nucleus during cell entry is strongly dependent on the quality of the virus preparation (Döhner et al., 2006). This has to be taken into account, because vHSV1(17⁺)blueLox-GFPVP26 was less efficiently replicated than wildtype, and possibly less efficiently assembled. The high number of gD-positive, but GFPVP26-negative structures early after inoculation as well as the peripheral gD clusters and the high amount of peripheral GFPVP26 at 3 h p.i. were an indication of a rather medium to poor quality of the inoculum used in these experiments. However, the genome/pfu ratio of the preparation which was used in these experiments was 25 genomes/pfu without prior DNase treatment of the virions. For HSV1-K26GFP a ratio in this range coincided with a low protein/pfu ratio and efficient nuclear targeting (Döhner et al., 2006). So the entry behaviour of vHSV1(17⁺)blueLox-GFPVP26 was not consistent with these previous observations.

Nevertheless, the GFPVP26 fusion protein is an excellent marker to localise viral capsids (Desai and Person, 1998; Döhner et al., 2006; Wolfstein et al., 2006), and vHSV1(17⁺)blueLox-GFPVP26 had a similar behavior during entry (this thesis) as the HSV1(KOS) mutant HSV1-K26GFP (Desai and Person, 1998).

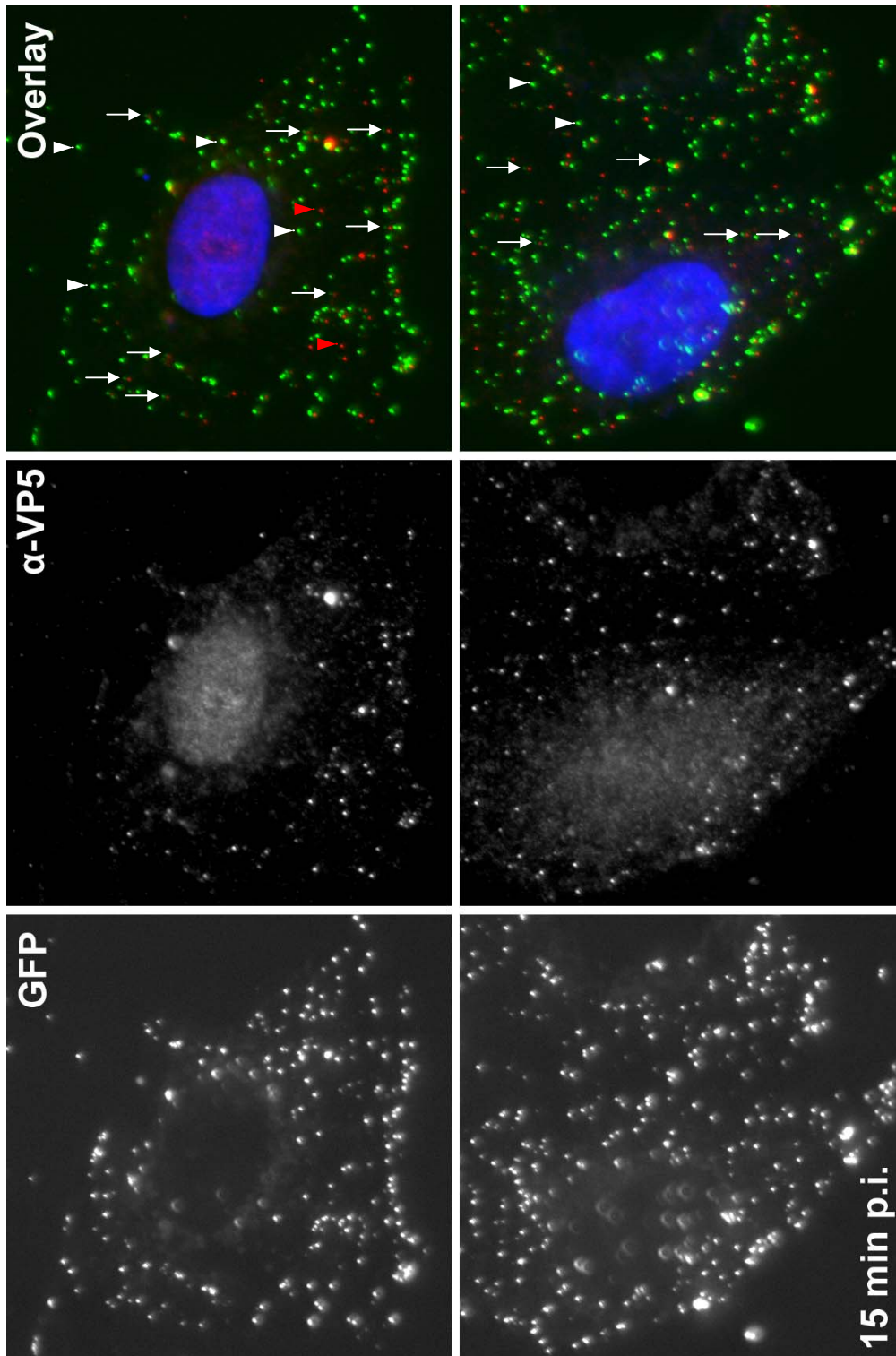


Figure 53: Subcellular localisation of GFPVP26 and capsids 15 min after infection with vHSV1(17⁺)blueLox-GFPVP26. A bright punctate GFP signal was randomly distributed over the entire cell which in some cases colocalised with VP5 (white arrows). Colocalisation was identified as a close apposition of GFPVP26 and VP5 signal due to a constant optical offset. Many GFPVP26 structures were not labelled by the VP5 antibody LP12 (white arrowheads) and some capsids did not show GFP fluorescence (red arrowheads). Vero cells were infected at an MOI of 20 pfu/cell for 15 min in the presence of cycloheximide, fixed with 3% paraformaldehyde, permeabilized with 0.1% Triton X-100 and labelled with mAb LP12 followed by an LRSC goat α -mouse antibody. The nuclei were stained with Hoechst 33258.

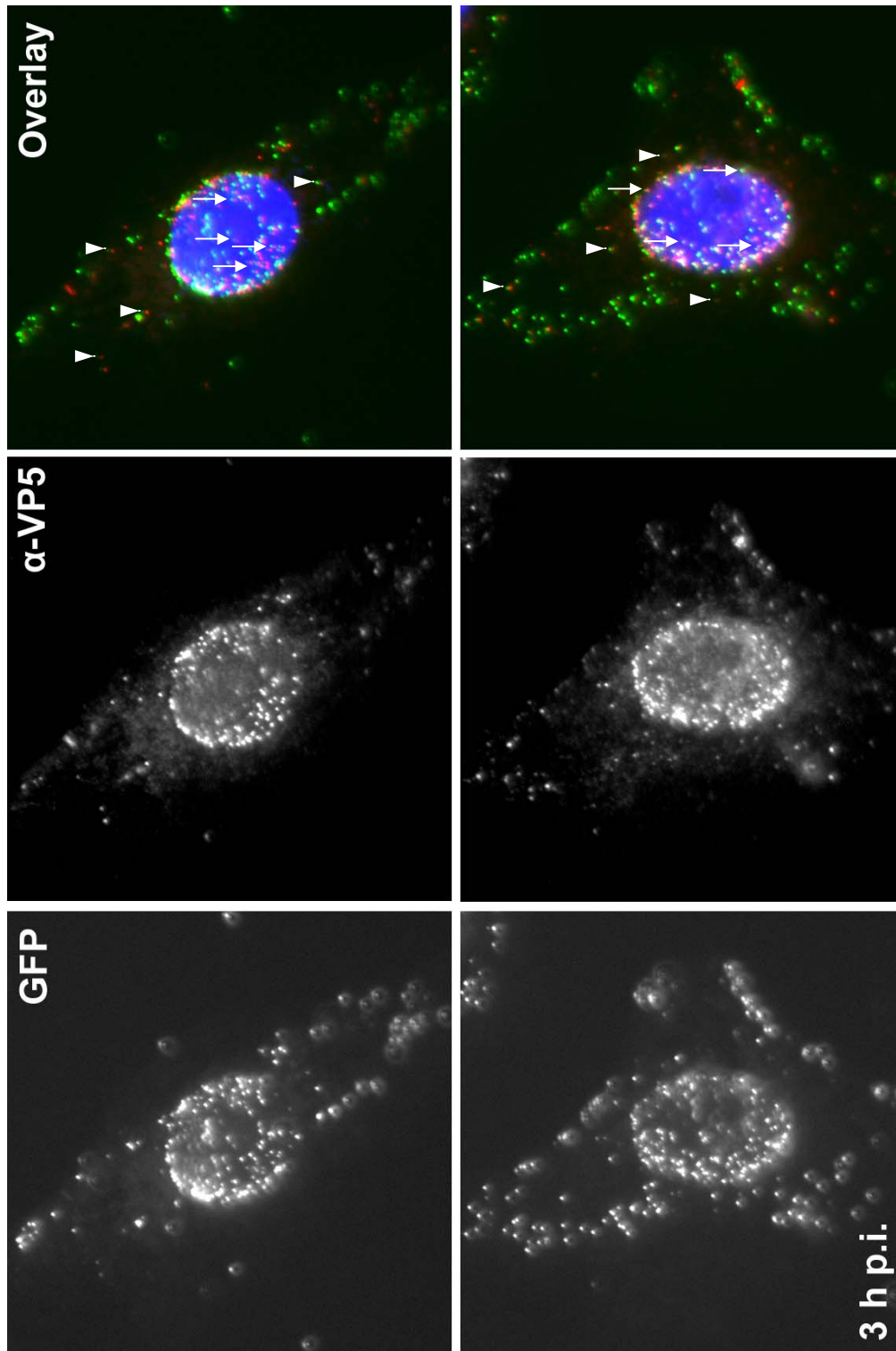


Figure 54: Subcellular localisation of GFPVP26 and capsids 3 h after infection with vHSV1(17⁺)blueLox-GFPVP26. The incoming capsids were efficiently targeted to the nucleus. Most GFPVP26- and VP5-positive particles were localised at the nucleus with a high degree of colocalisation (white arrows). Peripheral GFP signal also colocalised with VP5 in some cases (white arrowheads). Vero cells were infected at an MOI of 20 pfu/cell for 3 h in the presence of cycloheximide, fixed with 3% paraformaldehyde, permeabilized with 0.1% Triton X-100 and labelled with mAb LP12 followed by an LRSC goat α -mouse antibody. The nuclei were stained with Hoechst 33258.

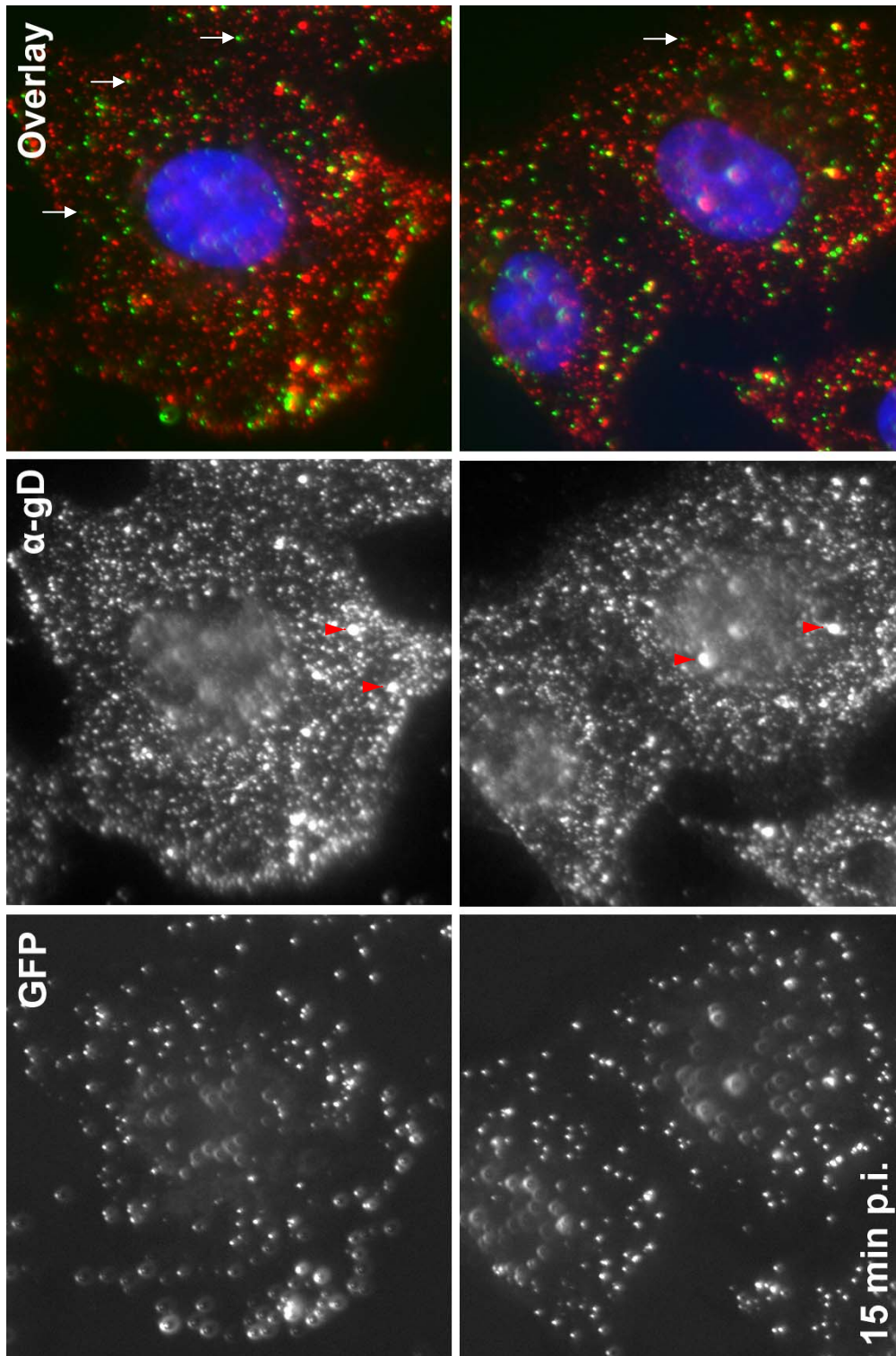


Figure 55: Subcellular localisation of GFPVP26 and glycoprotein D 15 min after infection with vHSV1(17⁺)blueLox-GFPVP26. Most GFPVP26 signals did not colocalise with gD 15 min after infection. The glycoprotein labelling was distributed over the entire cell, sometimes forming clusters (red arrowheads). The number of gD labelled spots was higher than the amount of GFPVP26 signals. In some cases peripheral GFPVP26 colocalised with gD (white arrows). Vero cells were infected at an MOI of 20 pfu/cell for 15 min the presence of cycloheximide, fixed with 3% paraformaldehyde, permeabilized with 0.1% Triton X-100 and labelled with mAb DL6 followed by an LRSC goat α -mouse antibody. The nuclei were stained with Hoechst 33258.

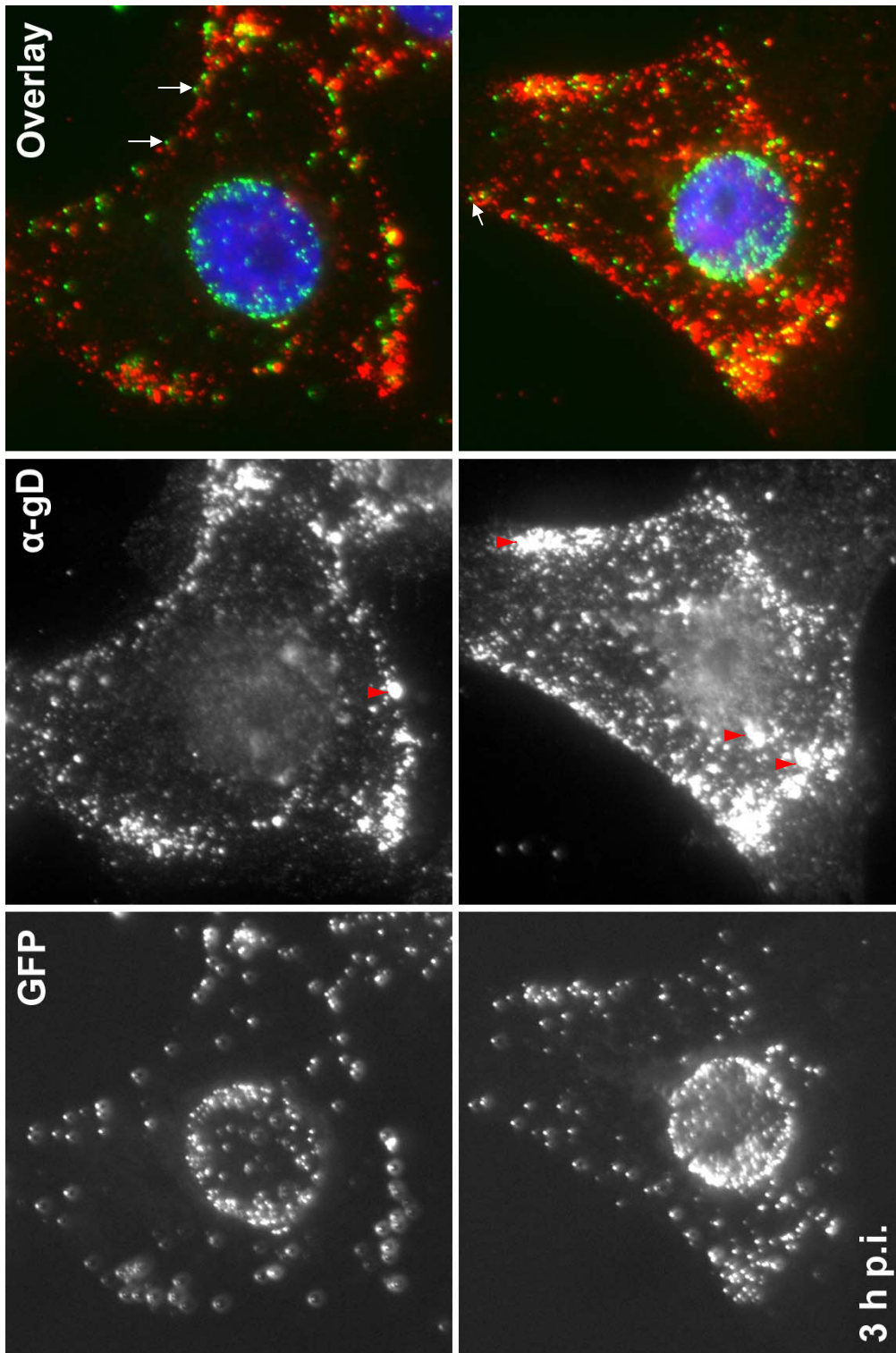


Figure 56: Subcellular localisation of GFPVP26 and glycoprotein D 3 h after infection with vHSV1(17⁺)blueLox-GFPVP26. Most capsids were efficiently targeted to the nucleus, where they did not colocalise with gD, whereas the glycoprotein staining was relocated to the cell margins and intracellular clusters (red arrowheads). In some cases peripheral GFPVP26 colocalised with gD (white arrows) Vero cells were infected at an MOI of 20 pfu/cell for 3 h the presence of cycloheximide, fixed with 3% paraformaldehyde, permeabilized with 0.1% Triton X-100 and labelled with mAb DL6 followed by an LRSC goat α -mouse antibody. The nuclei were stained with Hoechst 33258.

4.2.9. Cell entry of vHSV1(17⁺)blueLox-RFPVP26

When Vero cells were inoculated with gradient purified vHSV1(17⁺)blueLox-RFPVP26 in the presence of cycloheximide, punctate RFPVP26 signals were randomly distributed over the entire cell at 15 min p.i. which sometimes colocalised with a VP5 antibody labelling (Figure 57). However, like for the GFPVP26 virus, many RFPVP26 positive particles were not labelled for VP5 and the overall VP5 labelling intensity was weak.

At three hours p.i., particles labelled with a VP5 antibody were localised almost exclusively at the nucleus with a higher labelling intensity than at 15 min p.i. (Figure 58). In contrast, peripheral capsids were labelled to a lower extent. At the nucleus, almost all capsids exhibited RFPVP26 fluorescence, whereas not all nuclear RFPVP26 particles were labelled with the VP5 antibody. Peripheral RFPVP26 particles were mostly negative for VP5 labelling. These structures could represent capsids in which the LP12 epitopes were masked by RFPVP26, or viral structures which contained RFPVP26, but no capsid. Thus, also for RFPVP26, the VP5 epitope of mAb LP12 was more accessible at nuclear located capsids.

The punctate antibody labelling for glycoprotein D mostly colocalised with RFPVP26 at 15 min p.i., but also RFPVP26-positive structures without a labelling with a gD antibody were observed (Figure 59). Similar to the GFPVP26 virus, the number of gD puncta was higher than of RFPVP26 particles, however, as more particles were positive for both RFPVP26 and gD, it must be assumed, that many virions were bound to the plasma membrane or were endocytosed.

Nevertheless, the glycoprotein staining was clearly separate from the RFPVP26 labelled capsids at 3 h p.i. (Figure 60) and gD aggregates accumulated in the cell periphery. Capsids at the nucleus did not contain glycoprotein, and only some peripheral capsids were gD-positive.

The preparation quality was not optimal, because the vHSV1(17⁺)blueLox-RFPVP26 preparation contained a large amount of gD-containing particles and aggregates which were both RFPVP26 negative. The genome/pfu ratio of the preparation which was used in these experiments was 25 genomes/pfu without prior DNase treatment of the virions. So similar to vHSV1(17⁺)blueLox-GFPVP26, a coherence of genome/pfu ratio and entry efficiency (Döhner et al., 2006) was not observed for vHSV1(17⁺)blueLox-RFPVP26.

In summary, RFPVP26, like GFPVP26, provided a useful marker to localise capsids. Like for vHSV1(17⁺)blueLox-GFPVP26, the impairment in growth compared to wildtype, requires special attention during growth and preparation of this virus mutant to obtain inocula of sufficient quality for efficient nuclear targeting after entry.

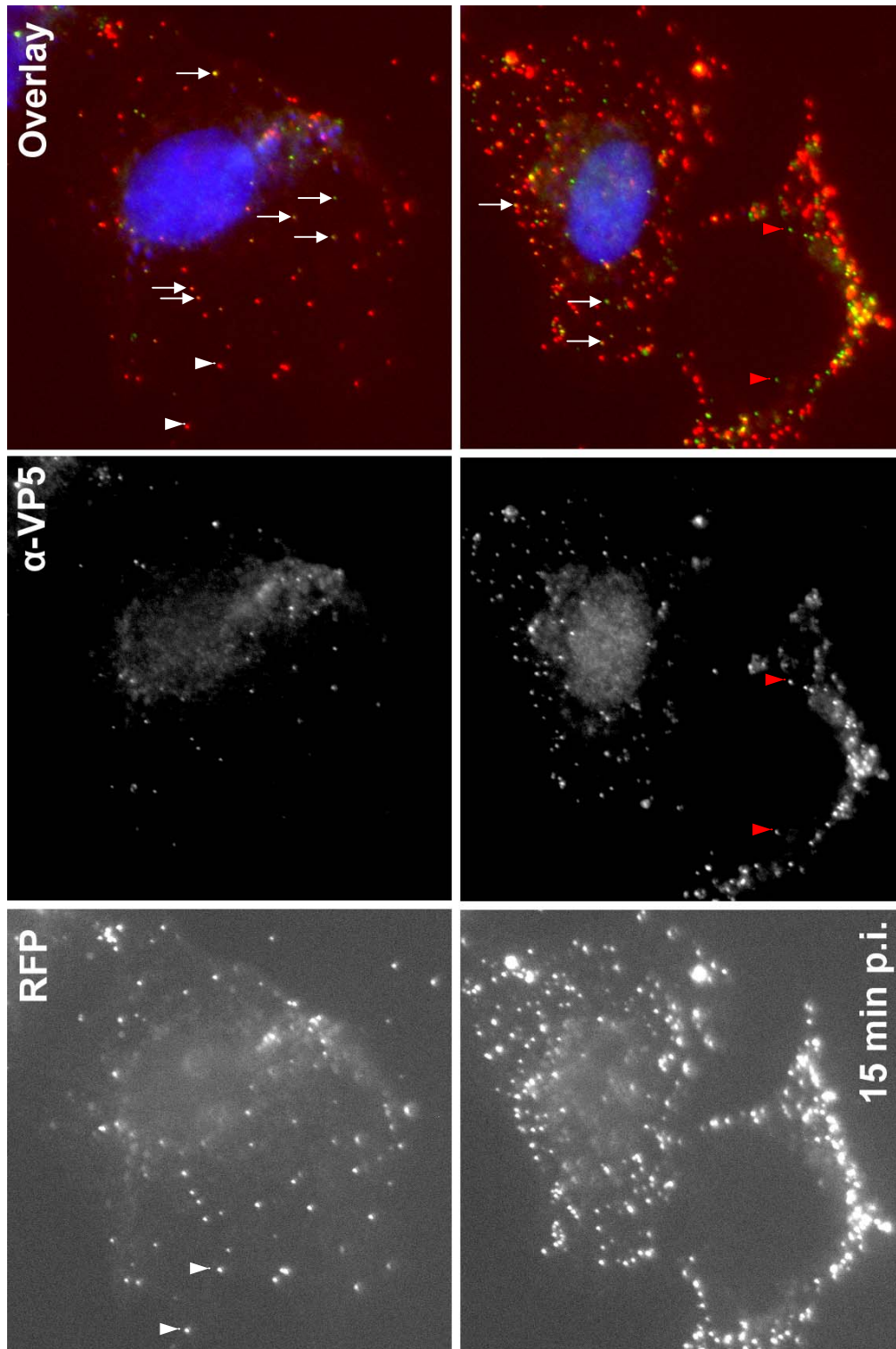


Figure 57: Subcellular localisation of RFPVP26 and capsids 15 min after infection with vHSV1(17⁺)blueLox-RFPVP26. A bright dotted RFP signal was randomly distributed over the entire cell which in some cases colocalised with the VP5 signal (white arrows). Many RFPVP26 particles were not labelled by the VP5 antibody LP12 (white arrowheads) and some capsids did not show RFP fluorescence (red arrowheads). Vero cells were infected at an MOI of 20 pfu/cell for 15 min in the presence of cycloheximide, fixed with 3% paraformaldehyde, permeabilized with 0.1% Triton X-100 and labelled with mAb LP12 followed by an FITC goat α -mouse antibody. The nuclei were stained with Hoechst 33258.

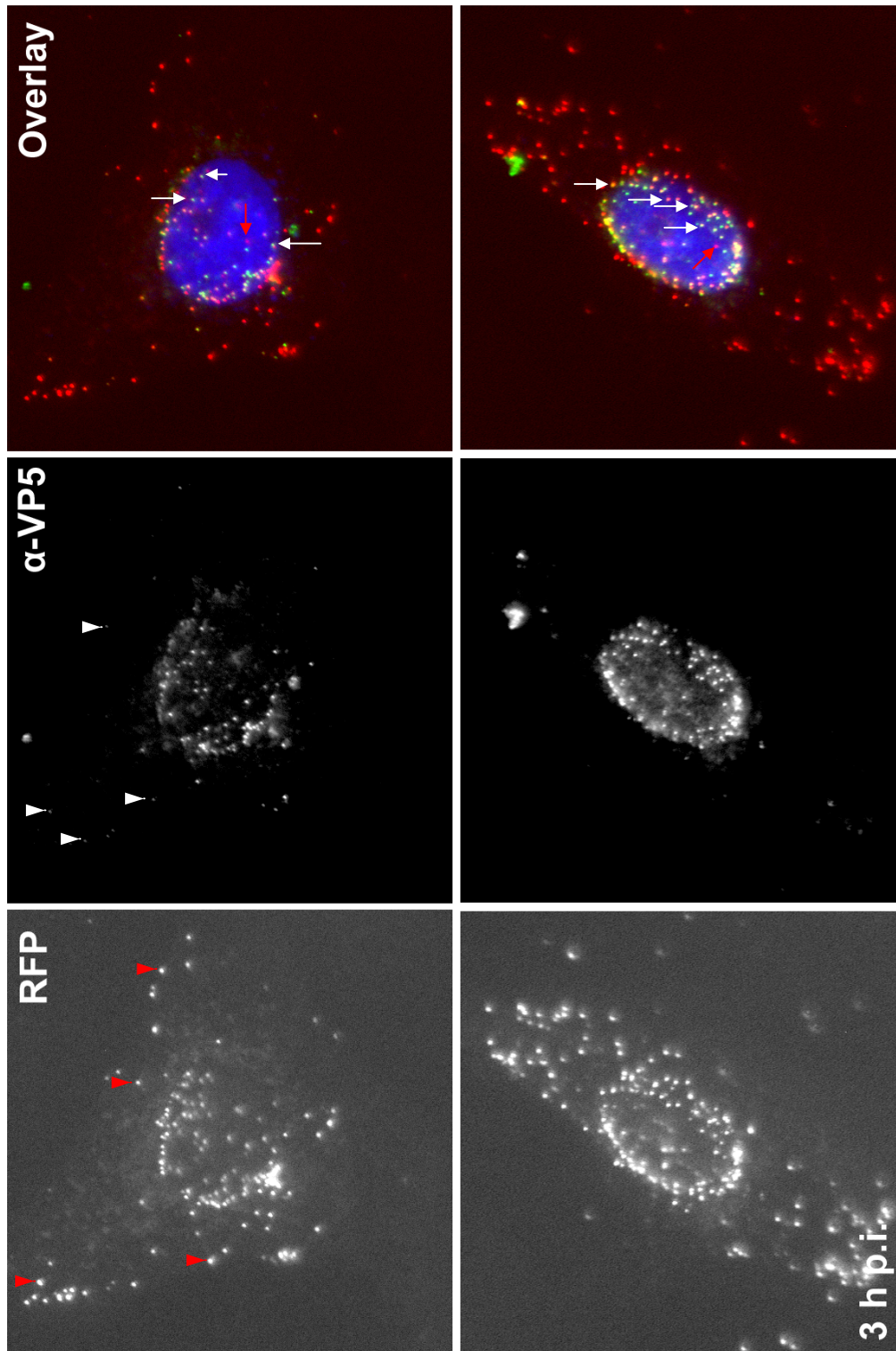


Figure 58: Subcellular localisation of RFPVP26 and capsids 3 h after infection with vHSV1(17⁺)blueLox-RFPVP26. The incoming capsids were efficiently targeted to the nucleus, where most bright VP5 signals were localised with a high amount of colocalisation with RFP (white arrows). Some RFPVP26 particles at the nucleus was not labelled with a VP5 antibody (red arrows). Most of the peripheral RFP particles did not colocalise with VP5 antibody labelling (red arrowheads) and only weak peripheral VP5 signals colocalised with RFP (white arrowheads). Vero cells were infected at an MOI of 20 pfu/cell for 3 h in the presence of cycloheximide, fixed with 3% paraformaldehyde, permeabilized with 0.1% Triton X-100 and labelled with mAb LP12 followed by an FITC goat α -mouse antibody. The nuclei were stained with Hoechst 33258.

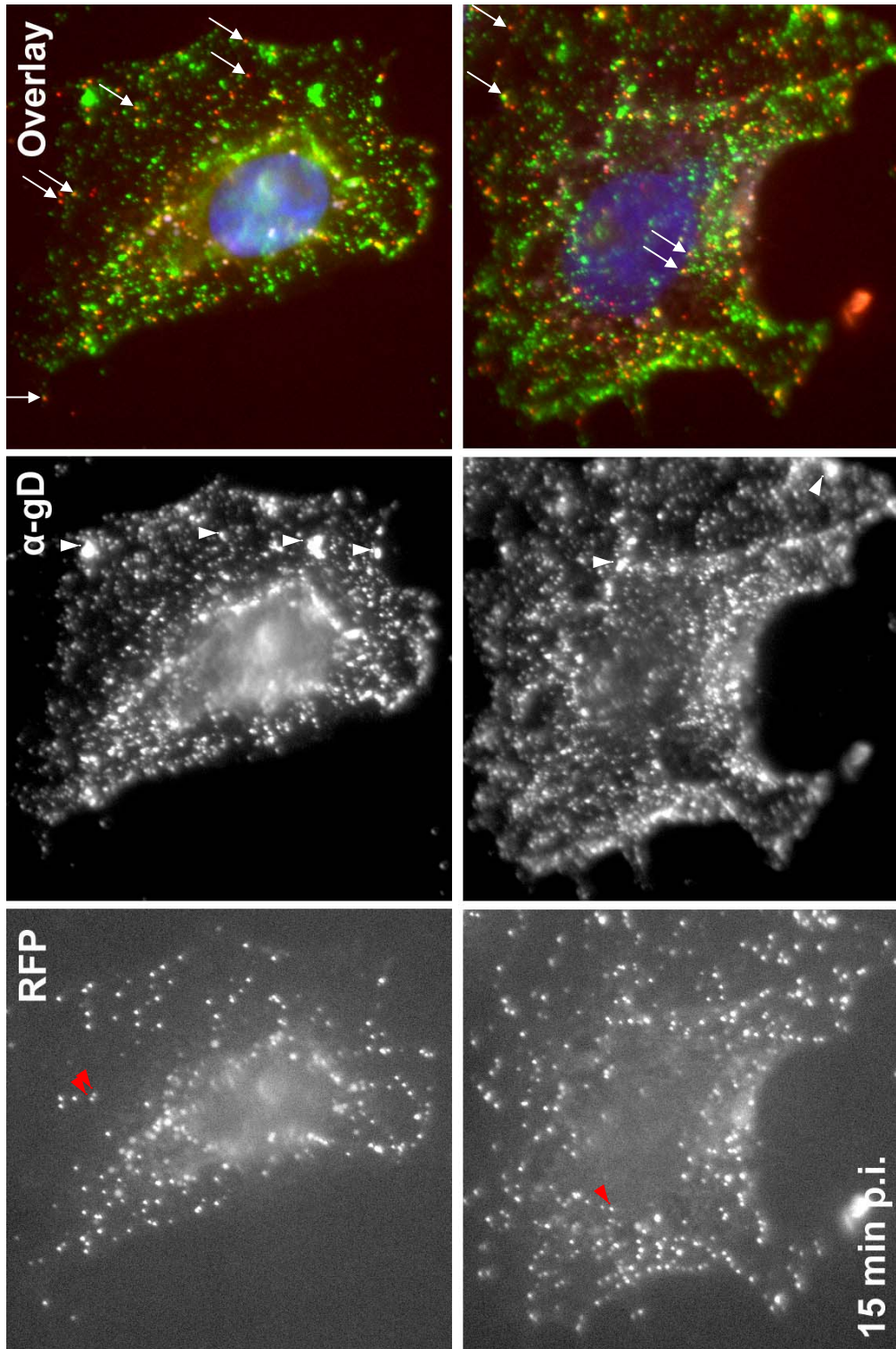


Figure 59: Subcellular localisation of RFPVP26 and glycoprotein D 15 min after infection with vHSV1(17⁺)blueLox-RFPVP26. Many RFPVP26 particles still colocalised with gD 15 min after infection (white arrows). Predominantly, a widespread glycoprotein staining without RFP signal was distributed over the entire cell sometimes in aggregates (white arrowheads). Also RFPVP26 labelled structures without gD labelling (red arrowheads) were observed. Vero cells were infected at an MOI of 20 pfu/cell for 15 min in the presence of cycloheximide, fixed with 3% paraformaldehyde, permeabilized with 0.1% Triton X-100 and labelled with mAb DL6 followed by an FITC goat α -mouse antibody. The nuclei were stained with Hoechst 33258.

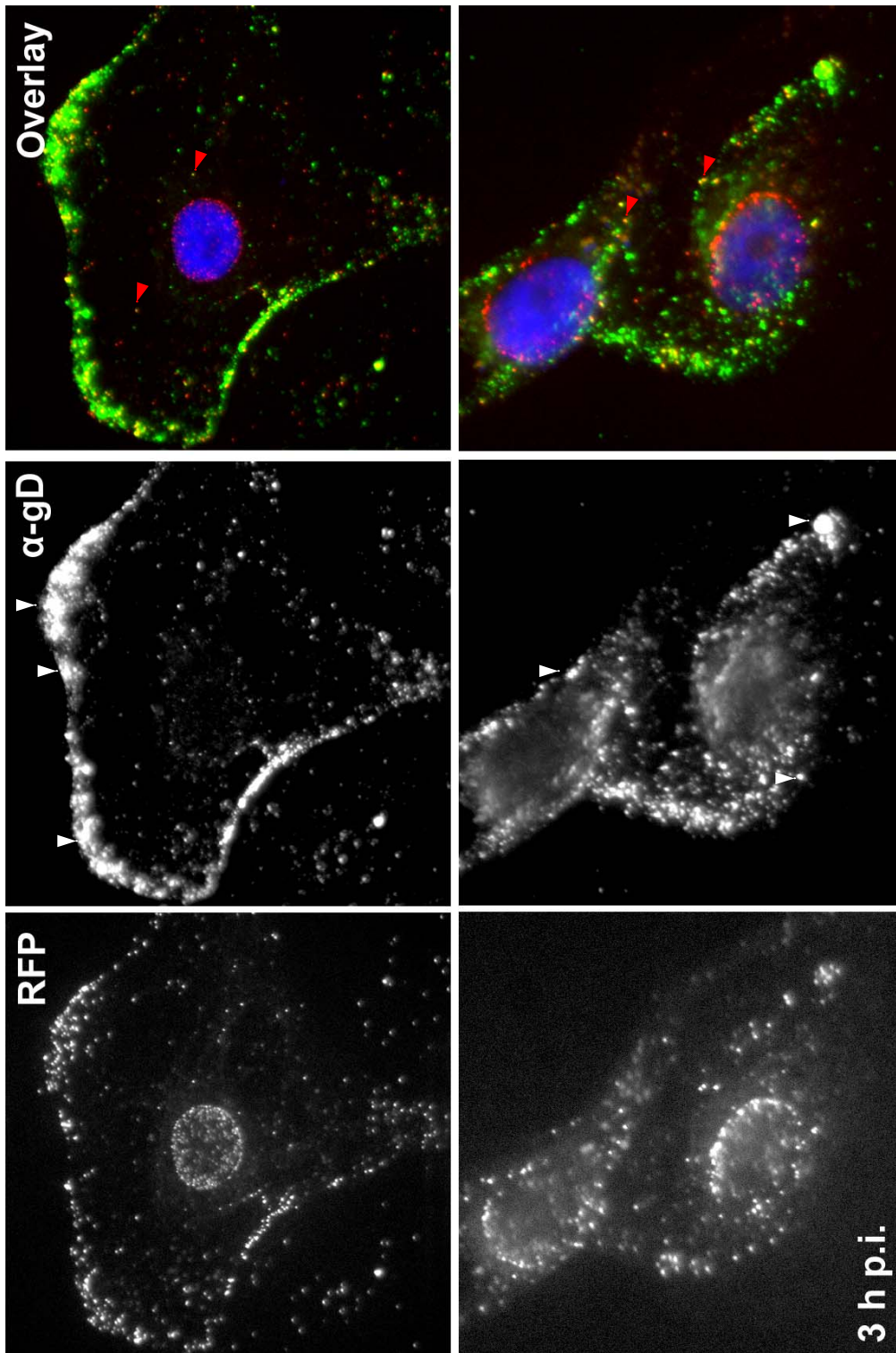


Figure 60: Subcellular localisation of RFPVP26 and glycoprotein D 3 h after infection with vHSV1(17⁺)blueLox-RFPVP26. Large numbers of capsids were efficiently targeted to the nucleus, where they did not colocalise with gD, whereas the glycoprotein staining was relocalised to the cell margins and intracellular aggregates (white arrowheads) did not colocalise with gD 15 min after infection. Some RFP signals still colocalised with gD (red arrowheads), however nuclear localised RFPVP26 was not labelled for envelope. Vero cells were infected at an MOI of 20 pfu/cell for 3 h in the presence of cycloheximide, fixed with 3% paraformaldehyde, permeabilized with 0.1% Triton X-100 and labelled with mAb DL6 followed by an FITC goat α -mouse antibody. The nuclei were stained with Hoechst 33258.

4.3. Tagging of HSV1-gD with a fluorescent protein

4.3.1. Fluorescence-tagged gD by en passant mutagenesis

After the addition of a fluorescence tag to the capsid protein VP26, an envelope protein of HSV1 was additionally tagged. After labelling the glycoprotein gB (UL27) with GFP at the N-terminal ectodomain (Potel et al., 2002), the resulting virus was attenuated 5-fold in plaque size and 100-fold in titers. However, a GFP tag was successfully attached to the cytosolic C-terminus of the envelope protein gD (US) without attenuating the virus (Milne et al., 2005).

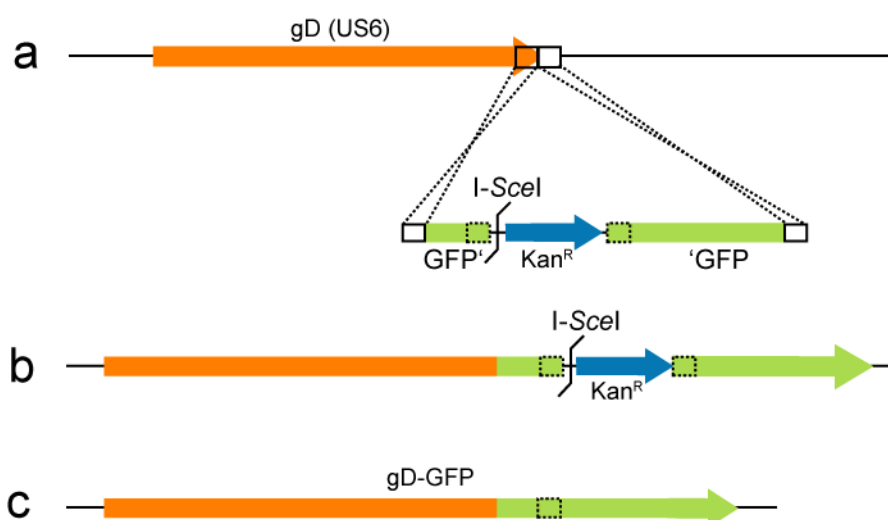


Figure 61: Mutagenesis strategy for gD-GFP. The GFP sequence was directly added to the 3' end of the gD (US6) ORF for a C-terminal fusion protein. (a) For en passant mutagenesis, a GFP cassette with an inserted kanamycin resistance, an I-SceI site and a GFP sequence duplication (dashed box) was amplified from pEP-EGFP-in with primers CHN73 and CHN74 which carried 5' overhangs homologous to 50 bp upstream and downstream of the original gD stop codon. (b) By a first Red recombination step the cassette was introduced into pHSV1(17⁺)blueLox-RFPVP26 under selection for kanamycin resistance. (c) The BAC was cut *in situ* with I-SceI expressed from pBAD-I-SceI and recircularised via the GFP sequence duplication in a second Red recombination step.

To tag gD in pHSV1(17⁺)blueLox-RFPVP26 with GFP, I used the two step Red-recombination procedure by Tischer et al. (2006) also called "en passant" mutagenesis (Figure 61). The GFP insertion construct was amplified from pEP-EGFP-in (kindly provided by K. Tischer & K. Osterrieder, Cornell University, Ithaca, NJ, USA) with primers CHN73 and CHN74 and introduced into pHSV1(17⁺)blueLox-RFPVP26 by Red recombination and selection for kanamycin resistance. The mutagenesis was performed in the *E. coli* strain DY380 (Lee et al., 2001) in which *redαβγ* are expressed from a prophage upon temperature

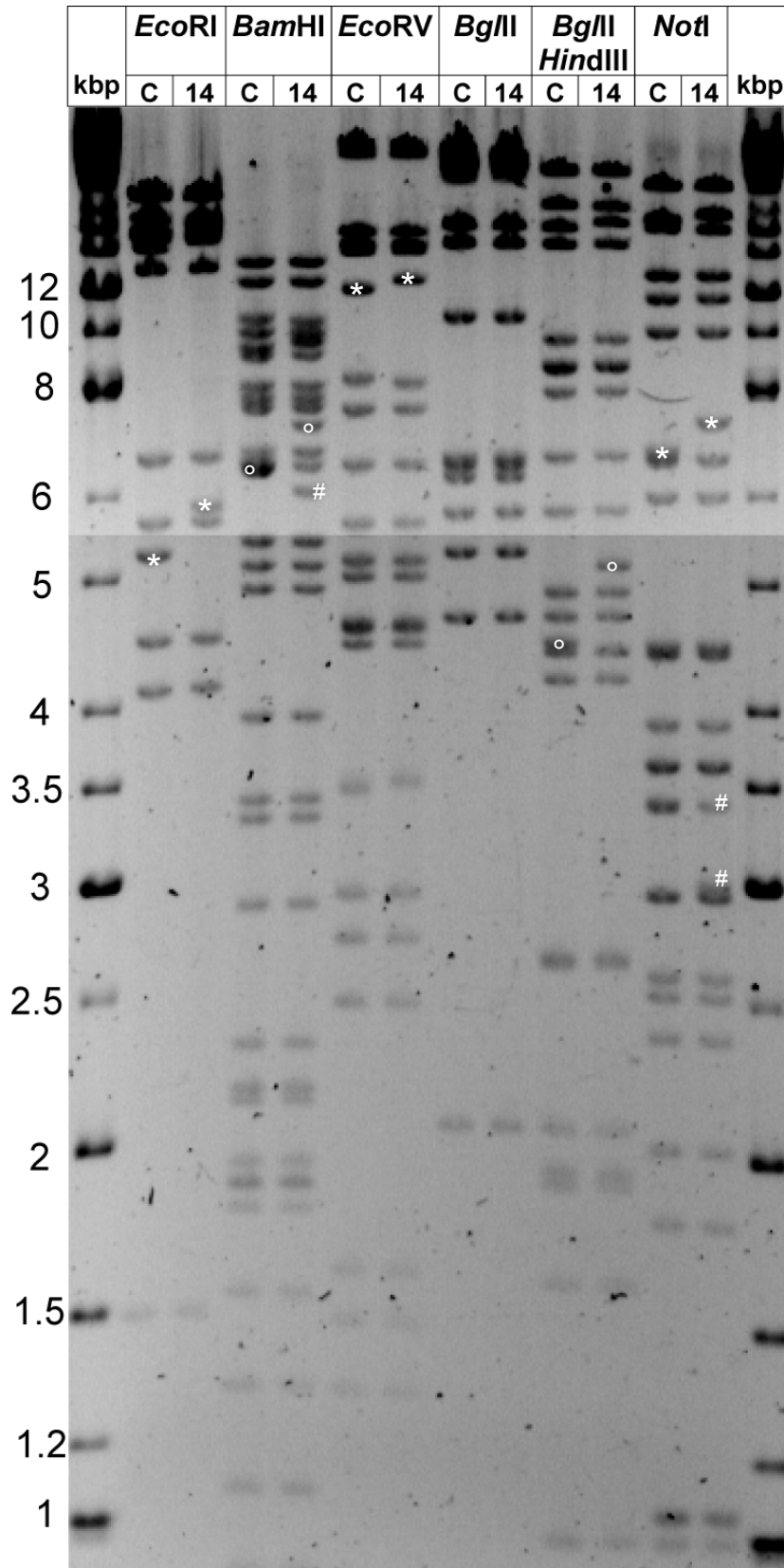


Figure 62: Characterisation of a RFPVP26-gDGFp containing HSV1-BAC. vHSV1(17+)blueLox-RFPVP26-gDGFp[14.1] was digested with the indicated enzymes in comparison to pHSV1(17+)blueLox (C). The alterations in the restriction patterns caused by the RFP tagging of VP26 (*) and of gD with GFP (°) are indicated. A joint fragment was reduced in size by about 400 bp (#).

induction, so no helper plasmid such as pKD46 was required. The fragment was inserted efficiently; of 20 kanamycin-resistant clones analysed, 12 had the fragment inserted correctly as shown by *Hind*III digests (data not shown). Positive clones were transformed with pBAD-I-SceI (Tischer et al., 2006) which contains an arabinose-inducible expression cassette for the endonuclease I-SceI. I-SceI and *red $\alpha\beta\gamma$* expression were induced by addition of L-arabinose and heat-shock, respectively. During the Red-mediated reconstitution of the BAC, the kanamycin resistance was excised from the GFP sequence, and the gD-GFP fusion was provided in frame (cf. Figure 61). Clones which grew in the presence of chloramphenicol, ampicillin and L-arabinose were replica-picked on kanamycin-containing plates. Of 20 clones analysed, clone pHSV1(17⁺)blueLox-RFPVP26-gDGFP[14.1] was kanamycin-sensitive and thus subjected to restriction digests (Figure 62), which demonstrated the insertion of GFP into gD. This clone had a 400 bp deletion in its terminal repeats as shown by bandshifts in *Bam*HI and *Not*I fragments spanning the joint regions of the HSV1 genome. Thus, an *a*-sequence was probably lost during mutagenesis. However, the resulting fragments were consistent with the presence of a single *a*-sequence in the joining region, so this clone was further characterised.

4.3.2. Characterisation of vHSV1(17⁺)blueLox-RFPVP26-gDGFP

After transfection into Vero cells, fluorescence and cytopathic effects were observed after two days. Thereby the RFPVP26 fluorescence was mostly nuclear and showed a punctate pattern in most cells, whereas the gDGFP fluorescence was cytoplasmic and excluded from the nuclei. Occasionally gDGFP was particularly present in the perinuclear region, possibly representing gDGFP located in the Golgi apparatus. Six days after transfection, the cells had developed full cytopathic effects and were harvested to prepare a virus stock.

Western blotting of lysates of cells infected with vHSV1(17⁺)blueLox-RFPVP26-gDGFP revealed that the molecular weight of gD, which was around 60 kDa in vHSV1(17⁺)blueLox and vHSV1(17⁺)blueLox-RFPVP26 infected cells, had shifted to higher molecular weight, consistent with the addition of GFP (27 kDa) (Figure 63). A faint band at the original gD position could indicate a fragment of gDGFP, or cross reactivity of the gD antibody with a cellular protein. When blotted against GFP, the bulk of the signal was at the same position as the gD signal. However, there appeared some weaker fragments with lower molecular weights, which most likely were proteolytic fragments derived from gDGFP. Like for vHSV1(17⁺)blueLox-RFPVP26, a VP26 antibody labelled a band consistent with the expected molecular weight of the RFPVP26 fusion protein at around 37 kDa, as well as a

Results

proteolytic fragment (cf. also Figure 52). In summary, the envelope protein gD of HSV1 was specifically tagged with GFP at its C-terminus by BAC-mutagenesis.

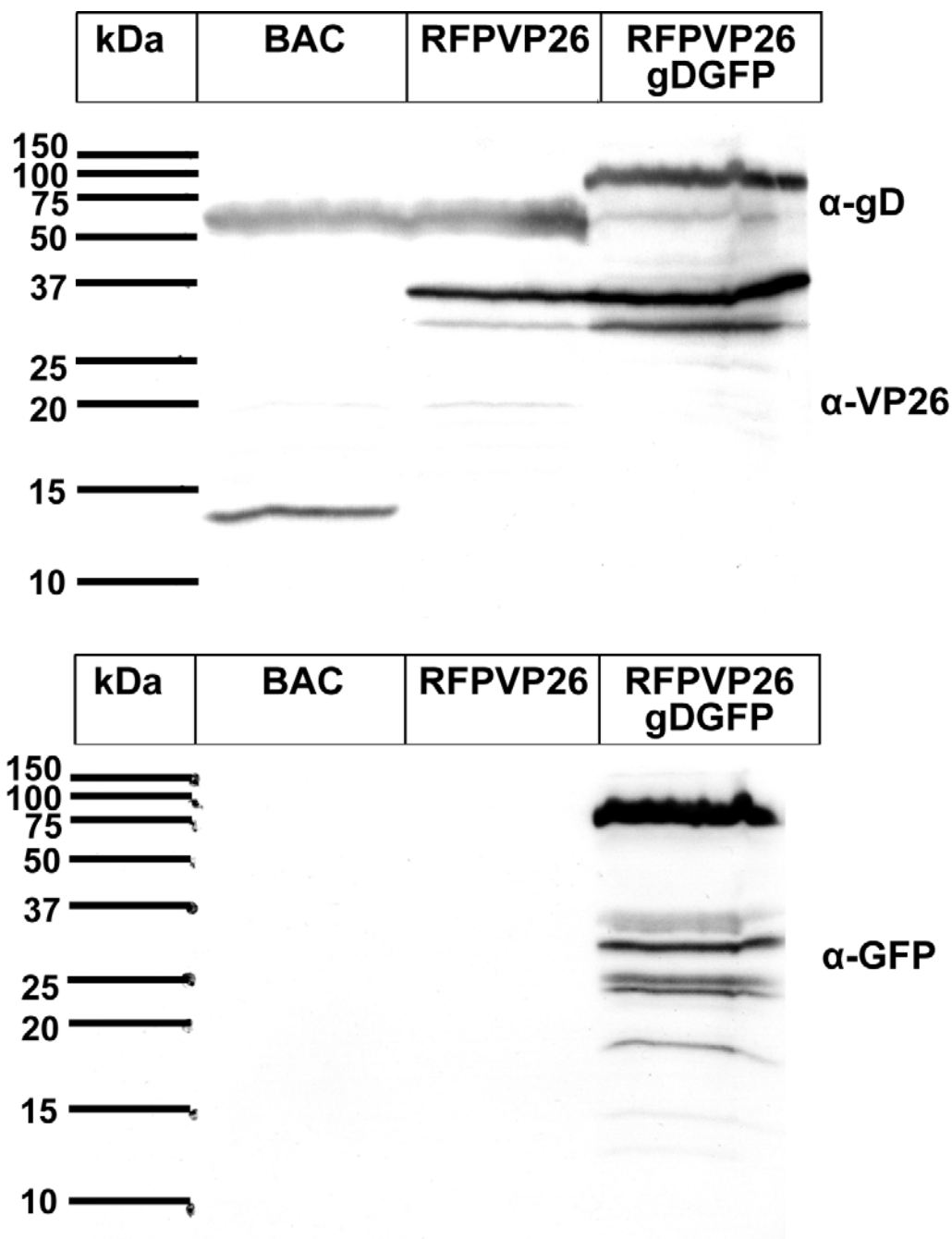


Figure 63: Protein characterisation of HSV1-RFPVP26-gDGFP. Cells infected with vHSV1(17⁺)blueLox (BAC), -RFPVP26 or -RFPVP26-gDGFP were lysed in SDS-PAGE sample buffer and subjected to 15% SDS-PAGE. The proteins were transferred to nitrocellulose and probed with antibodies specific for the envelope protein gD, the capsid protein VP26 or GFP. vHSV1(17⁺)blueLox-RFPVP26-gDGFP expressed a gDGFP fusion protein, however, also some GFP containing fragments were detected. The sizes of the marker bands are indicated in kDa on the left.

4.3.3. Subcellular localisation of RFPVP26 and gDGFP in an infected cell

In a plaque assay on Vero cells, the plaque size of vHSV1(17⁺)blueLox-RFPVP26-gDGFP[14.1] was comparable to vHSV1(17⁺)blueLox-RFPVP26 (not shown). In a developing plaque, the localisation of RFPVP26 changed as the infection progressed (Figure 64). In peripheral cells of the plaque, RFPVP26 showed a diffuse nuclear localisation, whereas towards the centre of a plaque, there was a concentric zone in which the nuclei exhibited a punctate fluorescent pattern. In the middle of a plaque, i.e. where infection was most advanced, the RFPVP26 fluorescence was cytoplasmic. For gDGFP, a cytoplasmic localisation was similar throughout the entire plaque. However, the signal was strongest in the centre of the plaque, whereas in the plaque periphery, and in the middle of the plaque where infection was most advanced and the cells had probably already detached, the signal was reduced.

To further analyse the subcellular localisation of RFPVP26 and gDGFP during infection, Vero cells were infected at an MOI of 0.5 pfu/cell, and fixed at different timepoints. Six hours p.i., the RFPVP26 fluorescence was almost exclusively nuclear in a dot-like pattern or in bright clusters (Figure 65). The small number of peripheral particles could have represented viral capsids from the inoculum or newly synthesised capsids which had egressed from the nucleus. The gDGFP fluorescence covered the entire cytoplasm, but the distribution was spotted rather than diffuse, and the signal was strongest in a perinuclear region which most likely represented the Golgi apparatus. In some cells the nuclear envelope was also labelled by gDGFP. There was virtually no colocalisation between RFPVP26 and gDGFP.

Later in infection after 18 h, the cells started to round up, and developed long ribbon-like or filamentous protrusions (Figure 66). The majority of RFPVP26 was present as intranuclear or perinuclear clusters. However, in the cell periphery and occasionally at the cell margins, a large number of individual RFPVP26 dots was detected, which sometimes colocalised with gDGFP. These structures most likely represented capsids which had left the nucleus, and in some cases underwent secondary envelopment. The overall signal intensity of gDGFP had increased and the perinuclear signal was very bright. In perinuclear regions, there was a strong overlap of RFPVP26 and gDGFP.

Taken together, these results suggested, that after different fluorescent labelling of two HSV1 proteins representative for capsid or envelope, the subcellular localisation of different viral structures could be monitored during the course of infection.

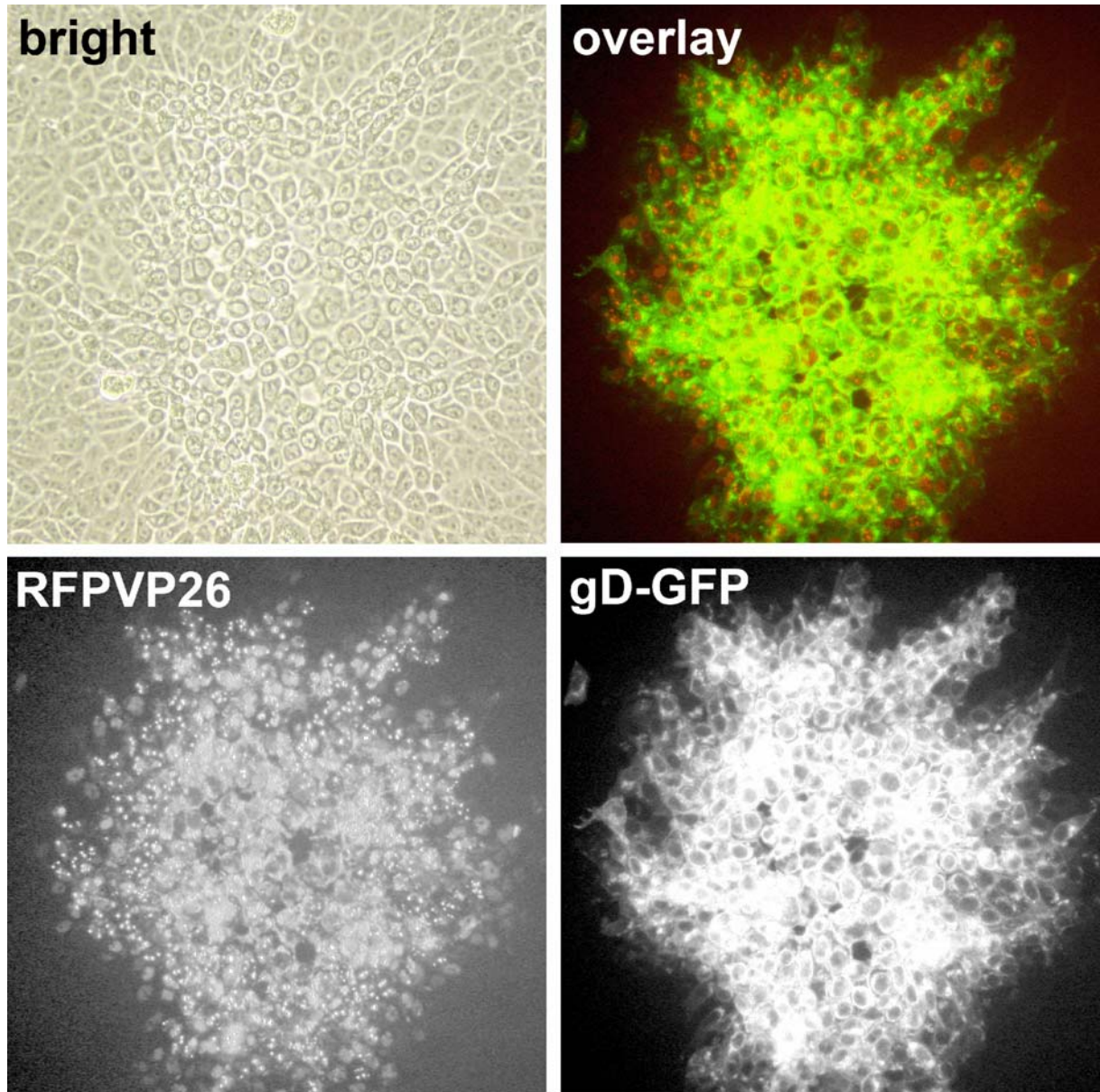


Figure 64: HSV1 plaques expressing RFPVP26 and gDGFP. In infected Vero cells, the GFP-tagged gD localised to the cytoplasm, and was excluded from nuclei, whereas RFPVP26 showed a diffuse nuclear background with bright puncta. Vero cells were infected for 2 days with an extract of cells transfected with pHSV1(17⁺)blueLox-RFPVP26-gDGFP[14.1] and grown in the presence of 20 µg/ml human IgGs to allow plaque formation, but prevent viral spread.

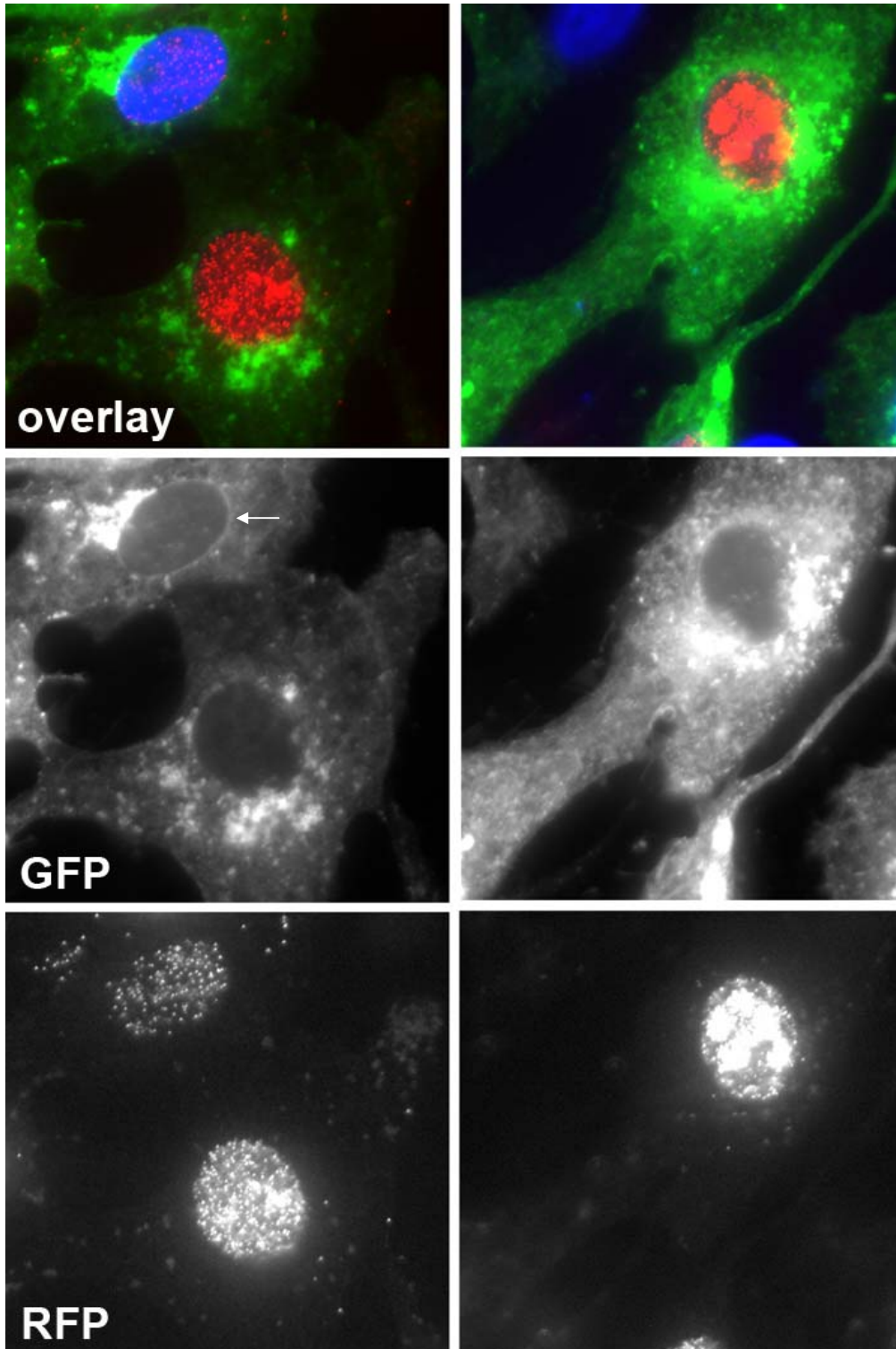


Figure 65: Subcellular localisation of RFPVP26 and gDGFP 6 h p.i. gDGFP was cytoplasmic and more accumulated in a perinuclear region, most likely the Golgi apparatus. The nuclear envelope was also labelled (arrow). RFPVP26 was almost exclusively nuclear, the peripheral puncta most likely represented capsids from the inoculum. Vero cells were infected at an MOI of 0.5 pfu/cell for 6 h and fixed with 3% paraformaldehyde. The nuclei were stained with Hoechst 33258.

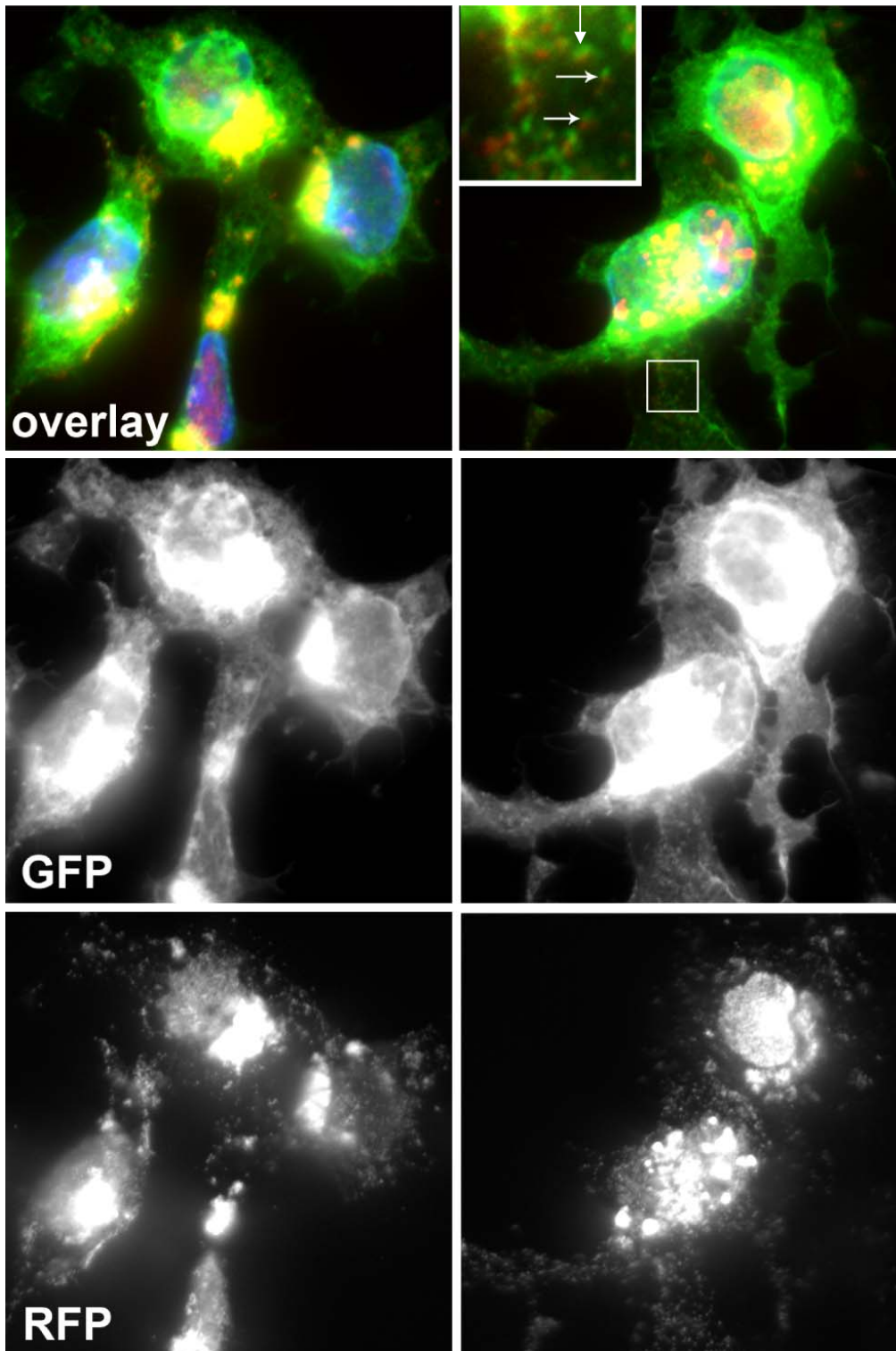


Figure 66: Subcellular localisation of RFPVP26 and gDGFP 18 h p.i. Late in infection, the cells had rounded up. The gDGFP signal accumulated in a perinuclear region. RFPVP26 formed intranuclear or perinuclear clusters. In the cell periphery, several puncta, possibly individual capsids, were observed. Many RFPVP26-positive structures colocalised with gDGFP and thus most likely represented complete virions (white arrows in insert) Vero cells were infected at an MOI of 0.5 pfu/cell for 18 h and fixed with 3% paraformaldehyde. The nuclei were stained with Hoechst 33258. The enlarged insert was image-processed differently.

5. Discussion

The cloning of herpesviruses as bacterial artificial chromosomes in *E. coli* made the fast construction of virus mutants by clonal selection and amplification in prokaryotes feasible and, in contrast to methods based on recombination in eukaryotes, allowed the fast introduction of strongly attenuating or even lethal mutations without the need of a complementing cell line (Adler et al., 2003; Wagner et al., 2002). HSV1 has been cloned as a BAC before, however, the BAC-vectors were constructed in a way that made them replication-incompetent without a helpervirus or they were constructed using the HSV1 strain F, whose sequence is not fully published (Horsburgh et al., 1999; Saeki et al., 1998; Stavropoulos and Strathdee, 1998; Tanaka et al., 2003). Therefore, the aim of this thesis was the cloning of the fully sequenced HSV1 strain 17⁺ (McGeoch et al., 1988; McGeoch et al., 1986; McGeoch et al., 1985; Perry and McGeoch, 1988) as a bacterial artificial chromosome, which is able to replicate without a helpervirus. Furthermore, fluorescent protein labels were added to viral proteins to allow the cell biological characterisation of the HSV1 life cycle in living cells as well as to study the kinetics of certain stages of the viral life cycle in biochemical assays. Moreover, the experiments of this thesis revealed the potential as well as pitfalls of HSV1 BAC-mutagenesis.

5.1. BAC-Cloning of HSV1

5.1.1. The need for HSV1 mutants

The human herpesvirus HSV1 is a prominent pathogen, whose normally mild course of infection in healthy, immunocompetent individuals can turn into a life-threatening condition in immunocompromised patients or in the rare case of an HSV1 encephalitis. On the other hand, the natural neurotropism of HSV1 allows the usage of this virus for the treatment of diseases of the central nervous system, either by the specific destruction of malignant tissue or by expression of a beneficial transgene. In basic research, viruses such as HSV1 are an important tool to analyse of host functions by investigating the life cycle of the virus. As all viruses depend on the cell for replication and propagation, they exploit almost every cellular pathway. Thus, the study of virus-host interactions can lead to new insights into cellular functions, like gene expression control, intracellular trafficking or protein processing. Therefore, the construction of HSV1 mutants carrying mutations in viral proteins or gene sequences which are responsible for host interaction is an indispensable experimental approach in the analysis of viral as well as cellular functions.

5.1.2. Cloning the genome of HSV1

To clone HSV1 as a BAC, genes needed for the replication and maintenance of the genome in *E. coli* ("BAC-genes") had to be introduced into the viral genome. Preparatory works on this issue were carried out by Dr. Tanja Strive (laboratory of Beate Sodeik, Institute of Virology, Hannover Medical School). To the BAC-genes provided on the plasmid pblueLox (Smith and Enquist, 2000) a *loxP* site and a β -galactosidase expression cassette under the control of an SV40 early promoter were added. Dr. Strive flanked these genes with 2 kbp of sequences homologous to regions upstream and downstream of the viral thymidine kinase UL23, which was thereby destroyed during recombination (T. Strive, B. Sodeik & M. Messerle; personal communication). Thymidine kinase is a non-essential virus protein in cell culture (Roizman and Knipe, 2001), but essential for virus replication in differentiated, non-dividing cells such as neurons, in which the virus cannot exploit the cellular nucleotide metabolism, because they do not longer replicate their chromosomal DNA. During screening for recombinants, the thymidine kinase deletion would have allowed the usage of acyclovir, which has to be converted by thymidine kinase into the viral DNA-polymerase inhibitor. However, by staining the cells infected by cotransfection with the β -galactosidase substrate blueo-gal, Dr. Strive obtained viral plaques which were positive for the insertion of BAC-genes (T. Strive, B. Sodeik & M. Messerle; personal communication).

At this point I took over the project, and plaque purified the recombinant virus. After enrichment, the amount of plaques not expressing β -galactosidase was reduced to less than 1%. Two of three purified virus clones were contained the BAC-genes as shown by PCR. The negative clone may have arisen from a loss of the BAC-genes during recombination or from a contamination with the β -galactosidase-positive virus mutant HSV1(KOS)tk12 (Warner et al., 1998) which served as a positive control in the blueo-gal staining.

Vero cells were then infected at a high MOI with the recombinant virus to isolate circular replication intermediates. These consist of covalently closed circular virus DNA and had thus already the topology of a BAC. The circular nuclear DNAs were isolated early after infection when the viral genomes have been injected into the nucleus of the inoculated cell. It is discussed controversially, whether incoming viral DNA becomes circular after disposal into the nucleus (cf. chapter 1.3.3). Nevertheless, after isolating small nuclear DNA molecules by a Hirt-Extract (Hirt, 1967) and transforming *E. coli* three chloramphenicol-resistant colonies were obtained which suggested, that at least a certain fraction of virus genomes had circularised. BAC-DNA was isolated from these clones and after digestion with restriction enzymes the presence of the HSV1 genome in these BAC-plasmids, which were named pHSV1(17⁺)blue, was confirmed.

5.1.3. Characterisation of the BAC pHSV1(17⁺)blue

DNA replication of HSV1 in infected host cells involves several recombination events during which viral DNA strands recombine via the terminal repeat regions, so that branched structures appear and genome regions undergo inversion (Wilkinson and Weller, 2003). This explains why in virions the linear viral genome occurs in four isomeric arrangements with regard to the relative orientation of the unique long (UL) and unique short (US) sequences. Therefore, DNA fragments of digests with some restriction endonucleases only occur in a half or a quarter of the isolated genomes, if their recognition sequences are at the termini of the UL and the US regions. In a BAC, the genome configuration is invariant during replication in *E. coli*; indeed, in two of the three obtained pHSV1(17⁺)blue clones the UL and US region were oriented antiparallel, and parallel in another. For topology reasons, only these two genome configurations can be distinguished in the circular form.

Restriction enzyme digestions with several rare cutting enzymes revealed that the HSV1 genome was completely cloned in pHSV1(17⁺)blue, as they were almost no unexpected differences in the restriction fragment sizes between isolated HSV1(17⁺) wildtype DNA and pHSV1(17⁺)blue. The changes caused by the insertion of the BAC-genes were observed. However, the published sequence between the BAC-genes and the β -galactosidase expression cassette is apparently erroneous, as some restriction sites are missing and some obtained restriction fragments were app. 200 bp smaller than expected. Although this may not be critical with regard to virus function or BAC replication, it may require additional resequencing of this region to avoid misinterpretations in the future..

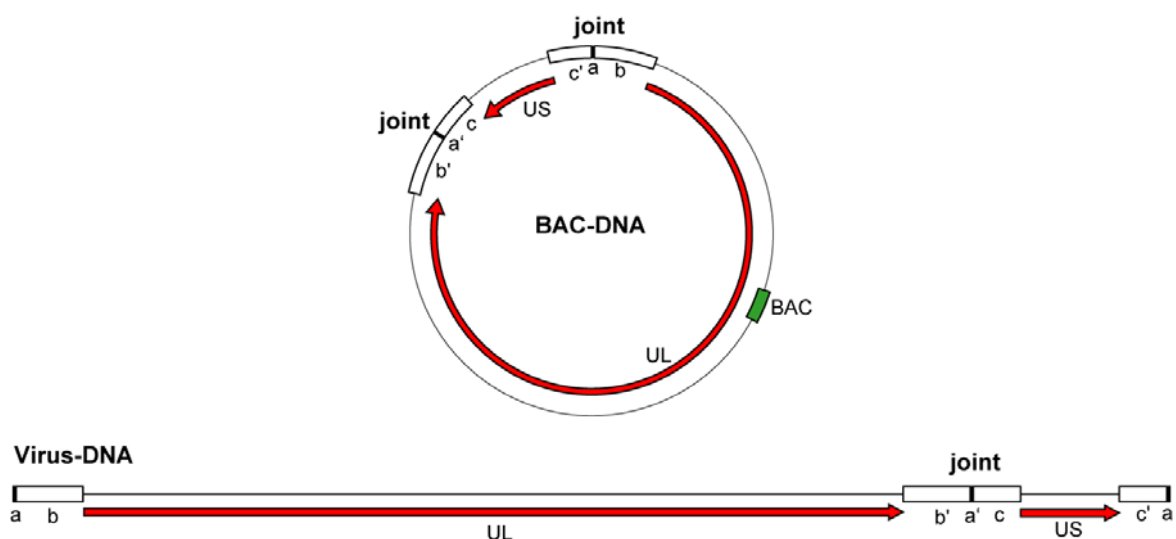


Figure 67: Topology of BAC-DNA and virus-DNA. Due to circularisation, BAC-DNA contains two joints between the long and short genome region.

Further differences in the restriction pattern between HSV1(17⁺) wildtype DNA and pHSV1(17⁺)blue were reflected by the fact that BAC-DNA is circular whereas viral DNA is linear. The long and short sequence in virus DNA are joined once whereas the joint occurs twice in the BAC when the viral genome has circularised over the genome termini. In restriction analyses the terminal genome fragments will be missing whereas the fragments spanning the joint are doubled in BAC-cloned virus herpesvirus genome (Figure 67).

5.1.4. The terminal *a*-sequences in pHSV1(17⁺)blue

During analysis of the joint region, restriction fragments of *Bam*HI and *Not*I a heterogeneity was observed between the three pHSV1(17⁺)blue clones. These fragments contain the viral *a*-sequences, which in viral DNA are located at the genome termini and the joint between the long and short region. They occur as several direct repeats and contain internal direct repeats with changing number themselves (Roizman and Knipe, 2001). So terminal restriction fragments as well as joint restriction fragments after digestions of viral DNA exhibit a sometimes cloudy signal on agarose gels and no distinct band. In contrast, the number of *a*-sequences and the repeats therein are more stable when they are cloned in a BAC, and therefore the different size of restriction fragments containing *a*-sequences in the three pHSV1(17⁺)blue clones can almost be expected. However they were still subject to some bandshifts as observed in several *Not*I digests of BACs derived from pHSV1(17⁺)blue clone 1. So also in *E. coli* these highly repetitive sequences are not completely stable. Clone pHSV1(17⁺)blue[1] carries *Not*I joint fragments with a size consistent with the presence of two *a*-sequences, whereas in clones 2 and 3 a single *a*-sequence or deleted forms occurred. Whether this leads to changes in viral pathogenesis has to be tested in animal infection models in the future. The *a*-sequences contain the packaging signals for cleavage and encapsidation of concatemeric viral DNA (Deiss and Frenkel, 1986; Hodge and Stow, 2001), thus a complete loss of the *a*-sequences during BAC-cloning would have been lethal for the virus.

5.1.5. The viral replication origins in pHSV1(17⁺)blue

Replication of HSV1-DNA initiates with binding of the origin-binding-protein UL9 to one or more origins which results in opening of the DNA double strand and the installation of replication forks (Wilkinson and Weller, 2003). After digesting the three pHSV1(17⁺)blue clones with *Bam*HI or *Not*I, the restriction fragments containing the viral replication origin *ori*L between the ORFs UL29 and UL30 were reduced by about 150 bp in size compared to the corresponding fragments of digested HSV1(17⁺) wildtype DNA. It has therefore to be

assumed that the 144 bp palindromic *oriL* sequence was lost during replication in *E. coli*. This sequence has been reported to be unstable in *E. coli* (Cunningham and Davison, 1993; Weller et al., 1985). Moreover, a *Bam*HI fragment containing a copy of the duplicate origin *oriS* was reduced in size about 50 bp in all three pHSV1(17⁺)blue clones. This origin contains an imperfect 45 bp palindrome and is present twice in the genome on the *c*-sequences flanking the US region as inverted repeats. To assess the structure of the origins, a PCR specific for either *oriL* or *oriS* was performed with the same primers as used for the analysis of a HSV1-BAC of strain F (Tanaka et al., 2003). However, after amplification of wildtype HSV1(17⁺) and HSV1(F) DNA no *oriL* amplificate of the expected size was obtained, and for virus as well as BAC-DNA the *oriL* region was amplified without the palindrome resulting in a PCR product with a size of 150 bp reduced compared to the expected size. Probably due to the secondary structure of *oriL*, PCR is not the method of choice and in the analysis by Tanaka et al. (2003) the part of the gel, where an amplificate negative for *oriL* would appear, was not shown. In this thesis, Southern blotting confirmed the loss of the *oriL* sequence in BAC-cloned HSV1 genomes for the BACs derived from HSV1(17⁺) and HSV1(F).

The *oriS* region was amplified from viral as well as from BAC-DNA of strains 17⁺ and F at the correct size, and no products appeared at positions reduced by 50 bp as deduced from the restriction bands. Therefore *oriS* seems to be unaltered after BAC cloning and the reduction of the 1953 bp *Bam*HI fragment size had other reasons which have to be approached by sequencing this fragment.

In other previously cloned HSV1-BACs, *oriL* was also deleted. The HSV1(F)-BAC of Horsburgh et al. (1999) did not carry an *oriL* as shown by Southern blotting, where only a band of reduced size was obtained, whereas probing a digest of Cosmid28 (Cunningham and Davison, 1993) led to hybridisation with a band of the same length and of a band which runs 100-200 bp higher, probably reflecting both the deleted and undeleted form of *oriL*. *Bam*HI digests of the replication-incompetent HSV1(17⁺)-BAC by Stavropoulos and Strathdee (1998) revealed the same bandshift caused by the loss of *oriL* as was observed for pHSV1(17⁺)blue and the HSV1(F)-BAC by Tanaka et al. (2003). Surprisingly, in the replication-incompetent HSV1(17⁺)-BAC by Saeki et al. (1998) the *Kpn*I fragment containing *oriL* was at the correct position. All HSV1-BACs described were prepared in *E. coli* strain DH10B. Perhaps Saeki et al. (1998) used a different substrain of *E. coli* DH10B.

In a yeast vector, *oriL* was stably cloned (Weller et al., 1985) and in *E. coli* the stability of *oriL* in was strongly increased if the *E. coli* strain SURE (Hardwicke and Schaffer, 1995). Although *oriL* is not essential *in vitro*, viruses that carry point mutations in *oriL* that abrogate the DNA replication initiation function show reduced titers when isolated from corneally infected mice. Moreover, mortality and reactivation from latency were reduced (Balliet and

Schaffer, 2006). However, it is not possible to clone HSV1-BACs with complete *oriL* in *E. coli* SURE, because this strain already contains an F-plasmid. Moreover, *E. coli* SURE carries the *Tn5* transposon which confers kanamycin-resistance, a selection marker on which most BAC-mutagenesis protocols are based. So in order to repair *oriL* in HSV1-BACs, it would be necessary to cotransfect a viral DNA fragment with an intact *oriL* together with BAC-DNA into eukaryotic cells and isolate repaired clones. Nevertheless, this approach would have all the disadvantages of mutagenesis by recombination in eukaryotes.

5.1.6. Reconstitution of virus from pHSV1(17⁺)blue

After cloning or mutagenesis of a BAC, the virus was reconstituted after transfection of the BAC into permissive eukaryotic cells. Cytopathic effects arose 1-2 d after transfection, the cells rounded up and plaques were formed. The efficiency of reconstitution could be calculated by the number of transfected BACs per cell needed for plaque formation. Usually 1 µg of BAC-DNA was used to transfect 2×10^6 cells. 1 µg BAC-DNA (app. 160 kbp) corresponds to 9.5×10^{-15} mol which corresponds to 5.7×10^9 BAC molecules. So app. 2800 genomes were transfected per cell. In many cases the development of cytopathic effects started from 5-10 single plaques, so the reconstitution efficiency was very low. This could have been due to a low transfection efficiency caused by the large size of BACs or impurities in the DNA preparation. Nevertheless, this was an example of the much greater potency of a virion as a vehicle for the productive deposition of a viral genome into the host cell nucleus than any transfection protocol.

The virus vHSV1(17⁺)blue was reconstituted from pHSV1(17⁺)blue. The BAC-genes were stably inserted as determined by isolation of viral DNA from the reconstituted virus and the subsequent restriction analysis. However same as other herpesviruses which have been cloned as a BAC (Messerle et al., 1997; Smith and Enquist, 1999), vHSV1(17⁺)blue was attenuated compared to its corresponding wildtype HSV1(17⁺). The titers obtained in a single-cycle growth curve were reduced and the time for reaching a saturated titer was enhanced. This attenuation could be have been the result of the deletion of the thymidine kinase gene, however, this gene is not essential in cell culture and no attenuation was associated with the thymidine kinase negative virus HSV1(KOS)tk12 (Warner et al., 1998; this thesis). The insertion of BAC genes and β-galactosidase enhances the size of the viral genome from 152 kbp to 162 kbp. Therefore it may be possible that packaging of the genome may not occur as efficient as in wild-type viruses due to steric hindrance, simply because the capsids become "jam-packed".

The β-galactosidase cassette in pHSV1(17⁺)blue under the control of the SV40 early promoter (Schumperli et al., 1982; Wildeman, 1988), provides a tool for measuring the

successful delivery of the viral genome into the nucleoplasm. Comparable to HSV1(KOS)tk12 in which the β -galactosidase gene is expressed from the immediate-early promoter of HSV1-ICP4, vHSV1(17⁺)blue infection leads to an increase in β -galactosidase production in infected cells which was raising over time, but was reduced after depolymerisation of the microtubule network. This allows a rapid biochemical analysis of the efficiency of transport to the nucleus and DNA-release at the nuclear pore for mutants derived from this BAC or in the presence of pharmacological inhibitors (Mabit et al., 2002; Marozin et al., 2004).

5.1.7. Construction of the self-excisable BAC pHSV1(17⁺)blueLox

To decrease the size of the BAC-derived viral genome, the BAC genes in pHSV1(17⁺)blue were flanked with *loxP* sites, and furthermore, an expression cassette for Cre recombinase was introduced between them. A single *loxP* site was already contained on pHSV1(17⁺)blue and the introduction of the second site together with Cre recombinase was performed by Red recombination to obtain the extended BAC pHSV1(17⁺)blueLox. This mutagenesis step was closely monitored by restriction analyses which revealed no changes of the viral genome during exposure to the recombination enzymes Exo (*red α*), Bet (*red β*) and Gam (*red γ*). Although Exo requires linear dsDNA as a substrate for its exonuclease activity, BACs with nicks or double-strand breaks could be targeted by the recombination system. After transfection into eukaryotes, Cre was expressed from pHSV1(17⁺)blueLox and catalysed a site-specific recombination between the two *loxP* sites resulting in excision of both the BAC and the Cre genes. The resulting vHSV1(17⁺)blueLox was slightly improved in titer and growth kinetics compared to vHSV1(17⁺)blue, but still grew less efficient than HSV1(KOS)tk12, in which thymidine kinase is also replaced by a β -galactosidase expression cassette. The genome size of vHSV1(17⁺)blueLox is 156 kbp, and thus only slightly larger than that of wildtype. In HSV1(KOS)tk12 the β -galactosidase expression cassette was inserted into the thymidine kinase gene UL23 between a *SacI* and *SphI* site, so only 58 bp were removed (Warner et al., 1998). The increase in genome size by about 3.5 kbp, however, did not influence growth of this mutant.

Recently, in pHSV1(17⁺)blue, the initial HSV1-BAC without a Cre/Lox self-excision system, the β -galactosidase cassette and the deleted thymidine kinase locus were repaired. Thereafter, the BAC regions were flanked with *loxP* sites and a Cre recombinase expression cassette was inserted (N. Mütter & M. Messerle, Institute of Virology, Hannover Medical School; personal communication). This BAC pHSV1(17⁺)Lox was added a luciferase expression cassette between UL55 and UL56. The resulting virus reached higher titers compared to vHSV1(17⁺)blue and grew similar to vHSV1(17⁺)blueLox. Thus, in this BAC the

Cre-mediated excision of BAC-sequences was also beneficial, although the maximal titers were not as high as for HSV1(17⁺) wildtype, either. Possibly, the insertion of the luciferase transgene led to this residual attenuation. Analysis of vHSV1(17⁺)Lox growth without a transgene and comparison to HSV1(17⁺) wildtype can reveal whether the BAC-cloning process *per se* impaired the virus at certain stages of its life cycle.

5.1.8. Conclusion

HSV1(17⁺) has been cloned as the BAC pHSV1(17⁺)blue in *E. coli* DH10B. Thereby the HSV1 replication origin *oriL* was deleted due to a general instability of this region in *E. coli*. To overcome an attenuation of the viral replication efficiency by the introduction of BAC sequences, a Cre recombinase expression cassette was introduced and the BAC sequences were flanked with *loxP* sites so that both Cre and BAC sequences were excised from the genome after transfection into eukaryotes. The resulting BAC pHSV1(17⁺)blueLox grew more efficient than pHSV1(17⁺)blue, but possibly due to the introduction of β -galactosidase and the deletion of thymidine kinase titers are still reduced compared to wildtype HSV1(17⁺). Since the introduction of Cre-recombinase by Red-recombination was efficient and did not perturb the HSV1 genome, this method is very suitable for further mutageneses.

5.2. HSV1 encoding a fluorescence-tagged VP26

5.2.1. Adding a fluorescent tag to VP26

By recombination in Vero cells (Desai and Person, 1998) generated a HSV1(KOS), mutant in which the small capsid protein VP26 was replaced by an N-terminal fusion of GFP to VP26 (HSV1-K26GFP). The fusion construct was described as having an insertion of the GFP coding sequence into the N-terminus of VP26 after codon 4. In HSV1-K26GFP, the GFPVP26 fusion protein remained associated with virus capsids during infection (Döhner et al., 2006). In contrast to wild-type VP26, GFPVP26 does not decorate all six VP5 copies per hexon, due to the size of the fusion protein, in which the GFP tag has the double size as the tagged protein (P. Desai, personal communication). VP26 and VP5 interact via amino acids 50 to 112 of VP26 (Desai et al., 2003). This interaction may have an influence on the ATP-dependent maturation of several VP5 hexon epitopes, as they are not recognised on capsids derived from HSV1-K Δ 26Z and HSV1-K26GFP by some monoclonal antibodies (Döhner et al., 2006, and references therein).

In the HSV1-BAC generated in this thesis, VP26 was labelled with CFP, GFP and YFP via the detour of a VP26 deletion mutant. The VP26 ORF was disrupted by the insertion of

an *rpsLneo* selection/countersélection cassette by Red-recombination which served as placeholder for the fluorescent protein insertion. Translation stopped 10 residues after the original VP26 ATG and the rest of the protein was not produced. As VP26 is not essential for infection in cell culture, vHSV1(17⁺)blueLox-ΔVP26*rpsLneo* was infectious. However, HSV1-KΔ26Z, a deletion mutant of VP26 (Desai et al., 1998), only showed a minor attenuation in growth kinetics and titer compared to HSV1(KOS), whereas the titer of vHSV1(17⁺)blueLox-ΔVP26*rpsLneo* was reduced by more than the factor 10. HSV1-KΔ26Z was generated by homologous recombination in Vero cells by replacing codons 10 to 102 of VP26 with a cassette coding for β-galactosidase (Desai et al., 1998). The minor attenuation observed for HSV1-KΔ26Z compared to vHSV1(17⁺)blueLox-ΔVP26*rpsLneo* could reflect compensatory mutations during recombination. During plaque purification to enrich HSV1-KΔ26Z these were probably selected due to their growth advantage. The BAC derived vHSV1(17⁺)blueLox-ΔVP26*rpsLneo* is of clonal origin and the time to acquire mutations was probably not sufficient.

In a second Red-recombination step, the *rpsLneo* cassette was replaced with the FP-VP26 constructs. Although after transfection single fluorescent cells were obtained, only the CFPVP26 clone 7B developed plaques and full cytopathic effects within few days, whereas all other clones which were positive for the insertion of the fusion construct gave no rise to plaques after transfection or very slow plaque growth. The sequence of CFPVP26(7B) in the region upstream of the CFP insertion was the same as for GFPVP26(6A) and YFPVP26(9C), so either the nature of the fluorescent protein or mutations in other parts of the genome led to this attenuation.

The terminal *a*-sequences were thought to be involved in the attenuation, as *NotI* joint restriction fragments were drastically changing in size between the different identified FP-VP26 clones. But also after RecA-mediated recombination using shuttle plasmids, a GFPVP26-bearing virus exhibited the same phenotype, although there were no differences in the restriction patterns compared to pHSV1(17⁺)blueLox, except of the GFP insertion. A region of 12 kbp spanning the ORFs UL33 to UL36 was identified by marker rescue to carry the most influential mutation which led to attenuation, whereas DNA-fragments spanning the terminal repeat regions could not rescue the attenuation of a GFPVP26-BAC. Attempts to force the insertion of GFPVP26 by construction of a lethal UL34/VP26 double knockout and the rescue of this mutant with UL34/GFPVP26, UL34/RFPVP26 and UL34/YFPVP26 constructs failed. However, UL34/CFPVP26 could rescue ΔUL34/VP26, as did wildtype UL34/VP26. Thus, the nature of the FP-VP26 fusion protein itself was detrimental to virus growth.

HSV1-K26GFP is infectious and not strongly attenuated (Desai and Person, 1998). Sequencing of VP26 in this mutant as well as in the recombination plasmid pK26GFP used for transferring the fusion construct into HSV1(KOS) revealed that the codons for four N-terminal residues of VP26 as well as several bases upstream of the VP26 ORF were deleted, so expression of GFPVP26 starts directly with the first methionine of GFP. This deletion, which was not described originally, was non-intentional and possibly occurred during cloning of pK26GFP. As the surrounding regions showed sequence similarity between HSV1(KOS) and HSV1(17⁺), pK26GFP was further modified to pK26RFP and both were used for replacement of the *rpsLneo* cassette in pHSV1(17⁺)blueLox-ΔVP26*rpsLneo*. The resulting BACs with the GFPVP26 or RFPVP26 insertion were infectious and showed only a slight attenuation compared to the starting BAC pHSV1(17⁺)blueLox, which was similar to the attenuation of HSV1-K26GFP compared to the corresponding wildtype HSV1(KOS). So four N-terminal residues of VP26 have a strong inhibitory effect on virus growth, if they are present in an FP-VP26 fusion protein.

The VP26 homologues of other alphaherpesviruses were tagged with GFP or mRFP1 without major attenuation. For the construction of pseudorabies virus (PrV) GFPVP26 (Smith et al., 2001) and RFPVP26 (del Rio et al., 2005) the fluorescent protein was inserted between codons two and three of VP26. In bovine herpesvirus 1 (BHV1) GFPVP26 (Wild et al., 2005) the fusion protein starts directly with the GFP sequence. Between these three species VP26 shows strong homology only in the C-terminal half, whereas the N-termini are more divergent (Figure 68). There is no common N-terminal sequence with homology to the four HSV1-VP26 residues MAVP; in BHV1, the peptide MSAP has some similarity.

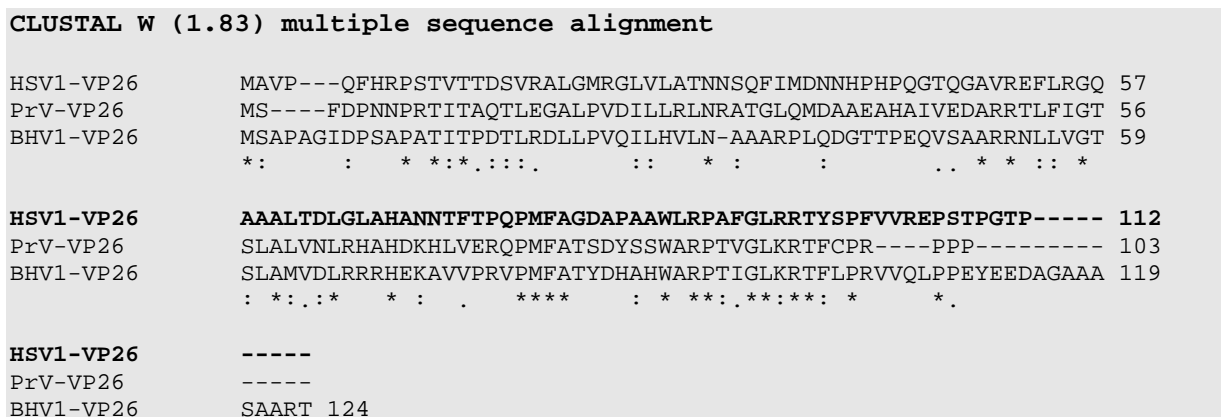


Figure 68: Multiple sequence alignment of alphaherpesvirus VP26 homologues. The VP26 sequences of the alphaherpesviruses herpes simplex virus (HSV1), pseudorabies virus (PrV; Klupp et al., 2004) and bovine herpesvirus 1 (BHV1; Schwyzer et al., unpublished; GenBank accession number AJ004801) were aligned using the CLUSTAL W (1.83) software. A region spanning residues 77-100 has the highest grade of conservation between the three species.

In contrast to HSV1, the betaherpesvirus CMV VP26 homologue (small capsid protein, SCP) is essential as a knockout was not viable (Borst et al., 2001). A GFP fusion to the VP26 homologue of human or mouse CMV gave rise to fluorescent nuclear puncta, but was also not viable (Borst et al., 2001). For HCMV, the GFP was inserted after codon 8, for MCMV after codon 4. The N-terminal eight residues of HSV1 and CMV VP26 homologues are not conserved (Figure 69), so the inhibition by the N-terminal peptide may be non-sequence-specific.

```

CLUSTAL W (1.83) multiple sequence alignment

HSV1-VP26      MAVPQFHRPSTVTTDSVRALGMRGLVLATNNSQFIMDNNHPHPQGTQGAVREFLRGQAAA 60
HCMV-SCP       -MSNTAPGPTVANKRDEKHRHVNVVLELPTE--ISEATHP-----VLATMLS-KYTR 49
                *:.... . : : :** .. * : .** .: :* : :

HSV1-VP26      LTDLGLAHANNFTFTPQPMFAGDAPAAWLRPAFGLRRTYSPFVVREPSTPGTP 112
HCMV-SCP       MSSL-----FNDKCAFK----LDLLR-MVAVSRTRR----- 75
                :.:*      * . : *      ** ..: **

```

Figure 69: Multiple sequence alignment of VP26 homologues of HSV1 and HCMV. The VP26 sequences of the alphaherpesviruses herpes simplex virus (HSV1), and of the homologous SCP of human cytomegalovirus (HCMV, Davison et al., 2003) were aligned using the CLUSTAL W (1.83) software.

The nature of the inhibition is not clear. In HSV1, VP26 interacts with VP5 via the 62 C-terminal residues 50-112 (Desai et al., 2003), which were not affected by the insertion of a fluorescent protein. Cells transfected with the attenuated BACs GFPVP26(6A) and YFPVP26(9C) exhibited nuclear fluorescent puncta, similar to cells transfected with CFPVP26(7B) or infected with HSV1-K26GFP. An interaction between VP5 and VP26 is sufficient for this nuclear localisation of VP26 (Desai et al., 2003). Although no or low cytopathic effects were associated with the attenuated BAC mutants, the interaction of the VP26 fusion proteins with VP5 was thus probably not impaired, so other steps during virus assembly or spread to neighboring cells were distorted. Transient overexpression of FP-VP26 constructs with in eucaryotic cells prior to inoculation with HSV1 may reveal an inhibitory effect of the fusion protein on virus entry and establishment of infection. To elucidate the effect of the four-amino-acid-peptide of HSV1-VP26 one could N-terminally add these to GFP, transfect cells prior to inoculation with HSV1 and monitor the course of infection in the presence of the overexpressed peptide-GFP fusion. In another approach the effect could be assessed by the incorporation of a synthetic peptide into cells prior to infection. These experiments may even lead to the development of an antiviral peptide assembly inhibitor.

5.2.2. Characterisation of GFPVP26 and RFPVP26 tagged viruses

As shown by SDS-PAGE and Western-blotting the fluorescent VP26 bearing viruses expressed only the fusion protein and no free GFP was associated with virions expressing GFPVP26. Due to a lack of an mRFP1 antibody, the presence of free mRFP1 could not be determined. To test whether this GFP- or RFP-tagged capsids were a suitable tool for the study of intracellular trafficking of HSV1, gradient purified virus stocks were prepared and analysed for their entry behaviour in Vero cells. Because several monoclonal antibodies against VP5 hexon epitopes did not detect capsids of HSV1-K26GFP or HSV1-K Δ 26Z in immunofluorescence microscopy (Döhner et al., 2006). VP26 is suggested to have a role in the formation of these epitopes. The mouse mAb LP12 against VP5 labelled capsids of HSV1-K26GFP and HSV1-K Δ 26Z and therefore it was used in this study for detecting incoming capsids of vHSV1(17⁺)blueLox-GFPVP26 and -RFPVP26.

After entry, GFPVP26 and RFPVP26 colocalised with capsids in many cases. However, the labelling by the VP5 antibody mAb LP12 was stronger for nuclear localised capsids than for peripheral capsids. Therefore it can be assumed, that GFPVP26 or RFPVP26 interfered with binding to its epitopes and that capsids at the nucleus were detected more easily by the antibody due to a dissociation or a conformational change of GFPVP26 or RFPVP26 which also led to the decrease in autofluorescence. Nevertheless, most capsids of vHSV1(17⁺)blueLox-GFPVP26 and -RFPVP26 were efficiently transported to the nucleus within 3 h, and the fluorescence-labelled VP26 was a useful marker for capsid localisation as shown by the predominant colocalisation with a VP5 antibody. However, a significant amount of GFPVP26/RFPVP26 as well as of VP5 antibody labelling was still peripheral after three hours.

Immunolabelling for the HSV1 membrane protein gD demonstrated, that a large amount of glycoprotein-containing subviral particles without capsid was contained in the virus preparations. However, during passage to the nucleus, glycoprotein and GFPVP26/RFPVP26 capsid signal have separated in both viruses and no glycoprotein was detected at nuclear capsids.

The quality of a virus preparation is critical for the efficiency of transport of incoming capsids to the nucleus (Döhner et al., 2006). Virus preparations of a high grade are characterised by efficient capsid transport and low genome/pfu and protein/pfu ratios. In a virus preparation of high quality it was observed that the glycoprotein signal decreased three hours after inoculation (Döhner et al., 2006). The immunofluorescence data suggested, that the quality of the preparations of vHSV1(17⁺)blueLox-GFPVP26 and -RFPVP26 used in this experiment was not optimal. The genome/pfu ratios of these preparations were determined by quantitative real time detection PCR of the inocula. The values which were obtained were

low and thus should indicate a good preparation quality (Döhner et al., 2006). However, the efficiencies of transport to the nucleus of the used vHSV1(17⁺)blueLox-GFPVP26 and -RFPVP26 preparations did not match to this parameters. So either the real time detection PCR protocol was not as quantitative for HSV1(17⁺) derived mutants as for HSV1(KOS) or HSV1(F). This is unlikely, because between the two wildtype strains HSV1(KOS) or HSV1(F) the coincidence between genome/pfu ratio to entry efficiency was almost equal. vHSV1(17⁺)blueLox-GFPVP26 and -RFPVP26 could secrete a higher proportion of particles without DNA, compared to the viruses tested in Döhner et al. (2006). A determination of the particle/pfu ratio by electron microscopy or protein analysis will provide more insight for the characterisation of the inocula.

5.2.3. Conclusion

The construction of FP-labelled VP26 mutants of pHSV1(17⁺)blueLox by BAC-mutagenesis was technically accomplished by two strategies. The Red-recombination mediated insertion and replacement of an *rpsLneo* selection/counterselection cassette via a Δ VP26 intermediate as well as the *recA* recombination based construction of a GFPVP26-BAC using a shuttle plasmid led to several BAC-clones which were positive for the correct insertion of the FP-VP26 fusion protein as revealed by restriction analysis and sequencing. However, the construction of the fusion protein as initially performed, resulted in a strong attenuation of the obtained mutants or a complete loss of infectivity. The previous assumption, that a perturbation of repetitive regions in the virus genome by the action of recombination enzymes was the reason for this unexpected phenotype was abandoned, when an intact HSV1 DNA fragment spanning the repetitive regions was not able to rescue an attenuated GFPVP26-BAC clone, whereas a DNA fragment containing the wildtype VP26 sequence was able to do so. Surprisingly, the insertion of a CFPVP26 fusion either by Red-recombination, or the rescue of a Δ UL34/VP26 BAC with a UL34/CFPVP26 construct by homologous recombination in Vero cells led to the production of an infectious fluorescent virus with only weak attenuation. The intrinsic properties of CFPVP26 itself may be the cause for the attenuation of its GFPVP26 and YFPVP26 derivatives.

The previously constructed HSV1-K26GFP (Desai and Person, 1998) did not carry four original VP26 residues at the N-terminus of the GFPVP26 fusion protein and the insertion of FP-VP26 constructs without this peptide into the HSV1-BAC led to the recovery of viable virus, so at least for GFPVP26 and RFPVP26 this peptide might be the cause for the attenuation. Coherent with this, the BAC-derived GFPVP26 and RFPVP26 containing viruses without the N-terminal VP26 residues were growing with only a slight attenuation comparable to HSV1-K26GFP. They can be used for the analysis of HSV1 entry and provide a marker for

the localisation of capsids. The efficiency of nuclear targeting during entry could, nevertheless, benefit from a good quality of the virus preparation, which is dependent on a well-maintained cell culture, low MOI for inoculation, the time point of harvesting and thorough purification of the virions.

5.3. Dual coloured HSV1 virions

5.3.1. Adding a fluorescent tag to glycoprotein D

For the study of entry and assembly in live cells the continuous monitoring of capsid and envelope structures can provide important information. For studying entry by live cell imaging of incoming virions, the localisation of the envelope relative to the capsid will be dependent on the mode of entry. When fusing with the plasma membrane, both structures separate early and the capsid alone is transported within the cell. After endocytosis, envelope and capsid colocalise in an endocytic vesicle during transport and both signals separate at a later timepoint after viral fusion with the endosomal membrane. During assembly and egress the simultaneous visualisation of capsid and envelope can reveal the compartment of the cell where secondary budding occurs and which subviral species are transported inside the cell during egress.

The viral envelope protein gD was added a GFP tag directly to the C-terminus, so the fluorophore was localised inside the virion or facing the cytosol, respectively. The construction of the BAC-mutant by "en passant" mutagenesis gave rise to the clone pHSV1(17⁺)blueLox-RFPVP26-gDGFP expressing both RFPVP26 and gDGFP after transfection into eucaryotic cells as shown by Western-blotting. In a developing plaque both proteins localised to different compartments and the plaque size of the double-labelled mutant was not smaller compared to the single labelled RFPVP26 virus. Modification of the 30 amino acid cytosolic C-terminal tail of gD has no influence on fusion and entry capacity of gD (Browne et al., 2003), so the GFP addition should not interfere with cell entry. During assembly of alphaherpesviruses, glycoproteins are preassembled with outer tegument at patches of the secondary budding organelle (Mettenleiter, 2004). However, among the herpesviruses the roles of the glycoproteins during assembly and entry are not conserved, so interactions of glycoproteins with host receptors or viral proteins are specific for each virus species. HSV1-gH interacts with the tegument protein VP16 (Gross et al., 2003; Kamen et al., 2005), nevertheless it is not essential for egress (Browne et al., 1996; Forrester et al., 1992). HSV1-gE and gD have an essential, but redundant role during egress (Farnsworth et al., 2003), and interacts via its cytosolic C-terminus with the tegument protein VP22 (Chi et al.,

2005). As the gD-GFP virus was growing well, the addition of GFP directly to the C-terminus of gD had no major influence on virus egress.

5.3.2. Intracellular localisation of RFPVP26 and gDGFP

In a developing plaque, the localisation of gDGFP was strictly cytoplasmic, whereas the localisation of RFPVP26 was dependent on the progress of infection and changed from a nuclear to a cytoplasmic labelling. Early in infection, after six hours, RFPVP26 was only found in the nucleus in a dense punctate pattern or in aggregates. Both possibly represented areas of capsid assembly or single intranuclear capsids. Interestingly, no diffuse RFPVP26 signal was observed, suggesting that the protein was targeted to the nucleus almost quantitatively, possibly after an interaction with VP5 in the cytosol, or the 39 kDa RFPVP26 was sequestered in the nucleus after diffusion through the nuclear pores (discussed in (Desai et al., 2003)). However, the strict nuclear localisation of RFPVP26 early in infection contradicts a diffusion-controlled accumulation, as one would expect a stronger cytosolic RFPVP26 signal. These data support the assumption that RFPVP26 has an intracellular behaviour similar to wildtype VP26.

The GFP-tagged glycoprotein D exhibited a strictly cytoplasmic localisation in infected cells which covered the whole cell area, and in some cells also the nuclear envelope was stained. Early in infection the signal was most pronounced in a perinuclear region, which most likely represented the Golgi apparatus. The bright perinuclear signal was irregularly scattered in most cells which is consistent with the observation that the Golgi apparatus becomes fragmented during HSV1 infection (Campadelli et al., 1993).

16 h after infection the localisation of RFPVP26 has dramatically changed. The intranuclear signal was concentrated into large aggregates which were also observed in the perinuclear cytoplasm, moreover, the cytoplasm was filled with dotted RFPVP26 signals which were likely capsids during egress. Indeed, some colocalised with gDGFP in the cell periphery. RFPVP26 dots at the cell margins could represent virions in the process of release from the host cell. The localisation of gD was unchanged and very strong in a perinuclear region, thereby strongly colocalising with RFPVP26, so one could either assume that these perinuclear region comprises a major secondary budding region like the trans-Golgi network (Granzow et al., 2001; Turcotte et al., 2005), or the large excess of viral protein produced during infection leads to the formation of aggregates which are degraded in proteasomes in the perinuclear region (Gordon, 2002). Additional immunofluorescence labelling with antibodies directed against specific cellular structures as well as ultrastructural analyses can help to determine, whether assembly and egress of vHSV1(17⁺)blueLox-RFPVP26-gDGFP occur comparable to wildtype.

Capsid and envelope components of HSV1 can now be separately monitored also in live cells. A big potential of the dual-labelled vHSV1(17⁺)blueLox-RFPVP26-gDGFP lies in the study of axonal transport of progeny capsids by video or time-lapse microscopy of infected neurons. The differently labelled capsid and envelope structures allow the distinction between “naked” capsids, vesicles with viral glycoproteins, or virions in vesicles. But also in the analysis of entry, the dual-labelled virus can provide important information. A distinction between fusion at the plasma membrane and endocytosis in different cell types, would be possible; and most importantly, in live-cell-imaging the possibly different intracellular dynamics of cytosolic capsids or endocytic virions can be analysed.

5.4. Outlook

HSV1(17⁺) was successfully cloned as a BAC, and established protocols for mutagenesis were applied for insertion and modification of sequences in the viral genome (Table 4). For the study of virus-host interactions during infection and studies regarding the interactions in the large HSV1 proteome, pHSV1(17⁺)blueLox and its fluorescence-labelled derivatives provide powerful tools. However, for pathogenesis studies in animals or the analysis of the viral life-cycle in replication-incompetent cells, e.g. neurons, further modifications are necessary. The thymidine kinase locus was repaired in pHSV1(17⁺)Lox by mutagenesis of pHSV1(17⁺)blue (N. Mütter & M. Messerle, Institute of Virology, Hannover Medical School; personal communication). The instability of *oriL* in *E. coli* has also to be considered. Unless no bacterial strains are available which allow the maintenance of BACs as well as of a stable HSV1-*oriL*, this sensitive region may be only repaired by recombination in eukaryotes.

| BAC | Phenotype of the resulting virus |
|---|---|
| pHSV1(17 ⁺)blue | Δ UL23, <i>BAC</i> ⁺ , <i>lacZ</i> ⁺ ; titer reduced 10 fold compared to HSV1(17 ⁺) |
| pHSV1(17 ⁺)blueLox | Δ UL23, <i>BAC</i> ⁻ , <i>lacZ</i> ⁺ ; grows faster than vHSV1(17 ⁺)blue |
| pHSV1(17 ⁺)blueLox- Δ VP26rpsLneo | Δ UL23, <i>BAC</i> ⁻ , <i>lacZ</i> ⁺ , Δ VP26; titer reduced 10-fold |
| pHSV1(17 ⁺)blueLox-GFPVP26[6A] pHSV1(17 ⁺)blueLox-CFPVP26[7B] pHSV1(17 ⁺)blueLox-YFPVP26[9C] pHSV1(17 ⁺)blueLox-GFPVP26[20]/[33] | Δ UL23, <i>BAC</i> ⁻ , <i>lacZ</i> ⁺ , FP-VP26. Except clone CFPVP26[7B], the resulting viruses are not viable or strongly attenuated. The FP-VP26 fusion proteins contain the first four original VP26 residues at the N-terminus. |
| pHSV1(17 ⁺)blueLox- Δ UL34/35 | Δ UL23, <i>BAC</i> ⁻ , <i>lacZ</i> ⁺ , Δ VP26, Δ UL34; not viable due to deletion of the essential membrane protein UL34 |
| pHSV1(17 ⁺)blueLox-GFPVP26[9] pHSV1(17 ⁺)blueLox-RFPVP26[13] | Δ UL23, <i>BAC</i> ⁻ , <i>lacZ</i> ⁺ , FP-VP26; only slightly attenuated. Both viruses express an FP-VP26 fusion protein and incoming capsids are efficiently transported to the nucleus of infected cells, thereby retaining the fluorescent protein label. |
| pHSV1(17 ⁺)blueLox-RFPVP26-gDGFP[14.1] | Δ UL23, <i>BAC</i> ⁻ , <i>lacZ</i> ⁺ , RFPVP26, gDGFP. Dual coloured virus with fluorescence label at representative capsid and envelope protein. |

Table 4: Bacterial artificial chromosomes of HSV1 described in this thesis.

The behaviour of fluorescence-labelled VP26 and gD has to be further characterised to ensure that they preserved the function of their wildtype counterparts. The data obtained so far suggest, that both proteins are functional as FP-fusion proteins and that their modification only slightly attenuated HSV1. However, as was the case for FP-VP26, unexpected phenotypes and inconsistent properties of similar fluorescence tags, have to be taken into account. Some HSV1 mutants had a replication phenotype which was reflected in reduced titers and slower growth kinetics. Especially for entry experiments the quality of the inoculum is crucial and the preparation of virions from these mutants requests special care, not to misinterpret entry phenotypes with phenomena caused by inferior preparation quality.

The usefulness of HSV1(17⁺)-BAC pHSV1(17⁺)blueLox and its derivatives will be shown in the construction and analysis of a large range of virus mutants which on one hand will elucidate the complex biology of this large DNA-virus and its interplay with the multitude of cellular pathways. Still, HSV1 is an important pathogen which provides a risk to patients in several clinical manifestations, so mutagenesis-based studies also may help in the treatment of the disease as well as in the development of vaccines. The conversion of the human pathogen HSV1 into a gene therapy vector or a selective agent for the destruction of malignant tissue is a promising field of medical research which will benefit from the insights obtained by basic research of HSV1-cell interaction based on specific virus mutants: a viral genome does not necessarily need to encode a threat.

6. Literature

- Adler, H., Messerle, M. and Koszinowski, U.H. (2003) Cloning of herpesviral genomes as bacterial artificial chromosomes. *Rev Med Virol*, **13**, 111-121.
- Adler, H., Messerle, M., Wagner, M. and Koszinowski, U.H. (2000) Cloning and mutagenesis of the murine gammaherpesvirus 68 genome as an infectious bacterial artificial chromosome. *J Virol*, **74**, 6964-6974.
- Arii, J., Hushur, O., Kato, K., Kawaguchi, Y., Tohya, Y. and Akashi, H. (2006) Construction of an infectious clone of canine herpesvirus genome as a bacterial artificial chromosome. *Microbes Infect*.
- Ausubel, F.M., Brent, R., Kingston, R.E., Moore, D.D., Seidman, J.G., Smith, J.A. and Struhl, K. (eds.). (1997) *Short protocols in molecular biology, 3rd edition*. John Wiley & Sons, Inc., New York, Chichester, Weinheim, Brisbane, Singapore, Toronto.
- Balliet, J.W. and Schaffer, P.A. (2006) Point Mutations in Herpes Simplex Virus Type 1 oriL, but Not in oriS, Reduce Pathogenesis during Acute Infection of Mice and Impair Reactivation from Latency. *J Virol*, **80**, 440-450.
- Benboudjema, L., Mulvey, M., Gao, Y., Pimplikar, S.W. and Mohr, I. (2003) Association of the herpes simplex virus type 1 Us11 gene product with the cellular kinesin light-chain-related protein PAT1 results in the redistribution of both polypeptides. *J Virol*, **77**, 9192-9203.
- Bloom, D.C. (2004) HSV LAT and neuronal survival. *Int Rev Immunol*, **23**, 187-198.
- Borst, E.M., Hahn, G., Koszinowski, U.H. and Messerle, M. (1999) Cloning of the human cytomegalovirus (HCMV) genome as an infectious bacterial artificial chromosome in *Escherichia coli*: a new approach for construction of HCMV mutants. *J Virol*, **73**, 8320-8329.
- Borst, E.M., Mathys, S., Wagner, M., Muranyi, W. and Messerle, M. (2001) Genetic evidence of an essential role for cytomegalovirus small capsid protein in viral growth. *J Virol*, **75**, 1450-1458.
- Borst, E.M., Posfai, G., Pogoda, F. and Messerle, M. (2004) Mutagenesis of Herpesvirus BACs by Allele Replacement. In Zhao, S. and Stodolsky, M. (eds.), *Methods in Molecular Biology, vol. 256: Bacterial Artificial Chromosomes, Volume 2: Functional Studies*. Humana Press, Totowa, NJ, USA, pp. 269-279.
- Brown, S.M., Ritchie, D.A. and Subak-Sharpe, J.H. (1973) Genetic studies with herpes simplex virus type 1. The isolation of temperature-sensitive mutants, their arrangement into complementation groups and recombination analysis leading to a linkage map. *J Gen Virol*, **18**, 329-346.
- Browne, H., Bell, S., Minson, T. and Wilson, D.W. (1996) An endoplasmic reticulum-retained herpes simplex virus glycoprotein H is absent from secreted virions: evidence for reenvolopment during egress. *J Virol*, **70**, 4311-4316.
- Browne, H., Bruun, B., Whiteley, A. and Minson, T. (2003) Analysis of the role of the membrane-spanning and cytoplasmic tail domains of herpes simplex virus type 1 glycoprotein D in membrane fusion. *J Gen Virol*, **84**, 1085-1089.
- Brune, W., Messerle, M. and Koszinowski, U.H. (2000) Forward with BACs: new tools for herpesvirus genomics. *Trends Genet*, **16**, 254-259.
- Campadelli, G., Brandimarti, R., Di Lazzaro, C., Ward, P.L., Roizman, B. and Torrisi, M.R. (1993) Fragmentation and dispersal of Golgi proteins and redistribution of glycoproteins and

- glycolipids processed through the Golgi apparatus after infection with herpes simplex virus 1. *Proc Natl Acad Sci U S A*, **90**, 2798-2802.
- Campbell, R.E., Tour, O., Palmer, A.E., Steinbach, P.A., Baird, G.S., Zacharias, D.A. and Tsien, R.Y. (2002) A monomeric red fluorescent protein. *Proc Natl Acad Sci U S A*, **99**, 7877-7882.
- Chang, W.L. and Barry, P.A. (2003) Cloning of the full-length rhesus cytomegalovirus genome as an infectious and self-excisable bacterial artificial chromosome for analysis of viral pathogenesis. *J Virol*, **77**, 5073-5083.
- Cherepanov, P.P. and Wackernagel, W. (1995) Gene disruption in *Escherichia coli*: TcR and KmR cassettes with the option of Flp-catalyzed excision of the antibiotic-resistance determinant. *Gene*, **158**, 9-14.
- Chi, J.H., Harley, C.A., Mukhopadhyay, A. and Wilson, D.W. (2005) The cytoplasmic tail of herpes simplex virus envelope glycoprotein D binds to the tegument protein VP22 and to capsids. *J Gen Virol*, **86**, 253-261.
- Cleator, M.C. and Klapper, P.E. (2004a) Herpes Simplex. In Zuckerman, A.J., Banatvala, J.E., Pattison, J.R., Griffiths, P.D. and Schoub, B.D. (eds.), *Principles and Practice of Clinical Virology, 5th Edition*. John Wiley & Sons.
- Cleator, M.C. and Klapper, P.E. (2004b) The Herpesviridae. In *Principles and Practice of Clinical Virology, 5th Edition*. John Wiley & Sons Ltd.
- Cody, C.W., Prasher, D.C., Westler, W.M., Prendergast, F.G. and Ward, W.W. (1993) Chemical structure of the hexapeptide chromophore of the *Aequorea* green-fluorescent protein. *Biochemistry*, **32**, 1212-1218.
- Cohen, G., Katze, M., Hydrean-Stern, C. and Eisenberg, R. (1978) Type-Common CP-1 antigen of herpes-simplex-virus is associated with a 59,000-molecular-weight envelope glycoprotein. *J. Virol*, **27**, 172-181.
- Cohen, G.H., Ponce de Leon, M., Diggelmann, H., Lawrence, W.C., Vernon, S.K. and Eisenberg, R.J. (1980) Structural analysis of the capsid polypeptides of herpes simplex virus types 1 and 2. *J Virol*, **34**, 521-531.
- Cohen, J.I. and Seidel, K.E. (1993) Generation of varicella-zoster virus (VZV) and viral mutants from cosmid DNAs: VZV thymidylate synthetase is not essential for replication in vitro. *Proc Natl Acad Sci U S A*, **90**, 7376-7380.
- Court, D.L., Sawitzke, J.A. and Thomason, L.C. (2002) Genetic engineering using homologous recombination. *Annu Rev Genet*, **36**, 361-388.
- Craig, A.G., Nizetic, D., Hoheisel, J.D., Zehetner, G. and Lehrach, H. (1990) Ordering of cosmid clones covering the herpes simplex virus type I (HSV-I) genome: a test case for fingerprinting by hybridisation. *Nucleic Acids Res*, **18**, 2653-2660.
- Cunningham, C. and Davison, A.J. (1993) A cosmid-based system for constructing mutants of herpes simplex virus type 1. *Virology*, **197**, 116-124.
- Datsenko, K.A. and Wanner, B.L. (2000) One-step inactivation of chromosomal genes in *Escherichia coli* K-12 using PCR products. *Proc Natl Acad Sci U S A*, **97**, 6640-6645.
- Davison, A.J., Dolan, A., Akter, P., Addison, C., Dargan, D.J., Alcendor, D.J., McGeoch, D.J. and Hayward, G.S. (2003) The human cytomegalovirus genome revisited: comparison with the chimpanzee cytomegalovirus genome. *J Gen Virol*, **84**, 17-28.
- Davison, A.J., Trus, B.L., Cheng, N., Steven, A.C., Watson, M.S., Cunningham, C., Le Deuff, R.M. and Renault, T. (2005) A novel class of herpesvirus with bivalve hosts. *J Gen Virol*, **86**, 41-53.

- Davison, M.D., Rixon, F.J. and Davison, A.J. (1992) Identification of genes encoding two capsid proteins (VP24 and VP26) of herpes simplex virus type 1. *J Gen Virol*, **73** (Pt 10), 2709-2713.
- Decman, V., Freeman, M.L., Kinchington, P.R. and Hendricks, R.L. (2005a) Immune control of HSV-1 latency. *Viral Immunol*, **18**, 466-473.
- Decman, V., Kinchington, P.R., Harvey, S.A. and Hendricks, R.L. (2005b) Gamma interferon can block herpes simplex virus type 1 reactivation from latency, even in the presence of late gene expression. *J Virol*, **79**, 10339-10347.
- Deiss, L.P. and Frenkel, N. (1986) Herpes simplex virus amplicon: cleavage of concatemeric DNA is linked to packaging and involves amplification of the terminally reiterated a sequence. *J Virol*, **57**, 933-941.
- del Rio, T., Ch'ng, T.H., Flood, E.A., Gross, S.P. and Enquist, L.W. (2005) Heterogeneity of a fluorescent tegument component in single pseudorabies virus virions and enveloped axonal assemblies. *J Virol*, **79**, 3903-3919.
- Delecluse, H.J., Hilsendegen, T., Pich, D., Zeidler, R. and Hammerschmidt, W. (1998) Propagation and recovery of intact, infectious Epstein-Barr virus from prokaryotic to human cells. *Proc Natl Acad Sci U S A*, **95**, 8245-8250.
- Desai, P., Akpa, J.C. and Person, S. (2003) Residues of VP26 of herpes simplex virus type 1 that are required for its interaction with capsids. *J Virol*, **77**, 391-404.
- Desai, P., DeLuca, N.A. and Person, S. (1998) Herpes simplex virus type 1 VP26 is not essential for replication in cell culture but influences production of infectious virus in the nervous system of infected mice. *Virology*, **247**, 115-124.
- Desai, P. and Person, S. (1998) Incorporation of the green fluorescent protein into the herpes simplex virus type 1 capsid. *J Virol*, **72**, 7563-7568.
- Desai, P., Sexton, G.L., McCaffery, J.M. and Person, S. (2001) A null mutation in the gene encoding the herpes simplex virus type 1 UL37 polypeptide abrogates virus maturation. *J Virol*, **75**, 10259-10271.
- Desai, P.J. (2000) A null mutation in the UL36 gene of herpes simplex virus type 1 results in accumulation of unenveloped DNA-filled capsids in the cytoplasm of infected cells. *J Virol*, **74**, 11608-11618.
- Diefenbach, R.J., Miranda-Saksena, M., Diefenbach, E., Holland, D.J., Boadle, R.A., Armati, P.J. and Cunningham, A.L. (2002) Herpes Simplex Virus Tegument Protein US11 Interacts with Conventional Kinesin Heavy Chain. *J Virol*, **76**, 3282-3291.
- Döhner, K., Radtke, K., Schmidt, S. and Sodeik, B. (2006) The eclipse phase of herpes simplex virus type 1 infection: efficient dynein-mediated nuclear targeting in the absence of the small capsid protein VP26. *submitted to Journal of Virology*.
- Döhner, K. and Sodeik, B. (2004) The role of the cytoskeleton during viral infection. *Curr Top Microbiol Immunol*, **285**, 67-108.
- Döhner, K., Wolfstein, A., Prank, U., Echeverri, C., Dujardin, D., Vallee, R. and Sodeik, B. (2002) Function of dynein and dynactin in herpes simplex virus capsid transport. *Mol Biol Cell*, **13**, 2795-2809.
- Domi, A. and Moss, B. (2002) Cloning the vaccinia virus genome as a bacterial artificial chromosome in *Escherichia coli* and recovery of infectious virus in mammalian cells. *Proc Natl Acad Sci U S A*, **99**, 12415-12420.
- Domi, A. and Moss, B. (2005) Engineering of a vaccinia virus bacterial artificial chromosome in *Escherichia coli* by bacteriophage lambda-based recombination. *Nat Methods*, **2**, 95-97.

- Donnelly, M. and Elliott, G. (2001) Fluorescent tagging of herpes simplex virus tegument protein VP13/14 in virus infection. *J Virol*, **75**, 2575-2583.
- Douglas, M.W., Diefenbach, R.J., Homa, F.L., Miranda-Saksena, M., Rixon, F.J., Vittone, V., Byth, K. and Cunningham, A.L. (2004) Herpes simplex virus type 1 capsid protein VP26 interacts with dynein light chains RP3 and Tctex1 and plays a role in retrograde cellular transport. *J Biol Chem*.
- Eisenberg, R.J., Long, D., Ponce de Leon, M., Matthews, J.T., Spear, P.G., Gibson, M.G., Lasky, L.A., Berman, P., Golub, E. and Cohen, G.H. (1985) Localization of epitopes of herpes simplex virus type 1 glycoprotein D. *J Virol*, **53**, 634-644.
- Elliott, G. and O'Hare, P. (1999) Live-cell analysis of a green fluorescent protein-tagged herpes simplex virus infection. *J Virol*, **73**, 4110-4119.
- Enquist, L.W., Husak, P.J., Banfield, B.W. and Smith, G.A. (1998) Infection and spread of alphaherpesviruses in the nervous system. *Adv Virus Res*, **51**, 237-347.
- Enquist, L.W., Tomishima, M.J., Gross, S. and Smith, G.A. (2002) Directional spread of an alpha-herpesvirus in the nervous system. *Vet Microbiol*, **86**, 5-16.
- Everett, R.D. and Murray, J. (2005) ND10 components relocate to sites associated with herpes simplex virus type 1 nucleoprotein complexes during virus infection. *J Virol*, **79**, 5078-5089.
- Everett, R.D., Sourvinos, G. and Orr, A. (2003) Recruitment of herpes simplex virus type 1 transcriptional regulatory protein ICP4 into foci juxtaposed to ND10 in live, infected cells. *J Virol*, **77**, 3680-3689.
- Farnsworth, A., Goldsmith, K. and Johnson, D.C. (2003) Herpes simplex virus glycoproteins gD and gE/gI serve essential but redundant functions during acquisition of the virion envelope in the cytoplasm. *J Virol*, **77**, 8481-8494.
- Finken, M., Kirschner, P., Meier, A., Wrede, A. and Bottger, E.C. (1993) Molecular basis of streptomycin resistance in *Mycobacterium tuberculosis*: alterations of the ribosomal protein S12 gene and point mutations within a functional 16S ribosomal RNA pseudoknot. *Mol Microbiol*, **9**, 1239-1246.
- Forrester, A., Farrell, H., Wilkinson, G., Kaye, J., Davis-Poynter, N. and Minson, T. (1992) Construction and properties of a mutant of herpes simplex virus type 1 with glycoprotein H coding sequences deleted. *J Virol*, **66**, 341-348.
- Foster, T.P., Rybachuk, G.V. and Kousoulas, K.G. (1998) Expression of the enhanced green fluorescent protein by herpes simplex virus type 1 (HSV-1) as an in vitro or in vivo marker for virus entry and replication. *J Virol Methods*, **75**, 151-160.
- Frenkel, N. and Roizman, B. (1971) Herpes simplex virus: genome size and redundancy studied by renaturation kinetics. *J Virol*, **8**, 591-593.
- Fuchs, W., Klupp, B.G., Granzow, H., Osterrieder, N. and Mettenleiter, T.C. (2002) The interacting UL31 and UL34 gene products of pseudorabies virus are involved in egress from the host-cell nucleus and represent components of primary enveloped but not mature virions. *J Virol*, **76**, 364-378.
- Gärtner, B. and Müller-Lantzsch, N. (2002) Herpesviren: allgemein. In Doerr, H.W. and Gerlich, W.H. (eds.), *Medizinische Virologie - Grundlagen, Diagnostik und Therapie virologischer Krankheitsbilder*. Georg Thieme Verlag, Stuttgart, New York, pp. 370-372.
- Gay, P., Le Coq, D., Steinmetz, M., Ferrari, E. and Hoch, J.A. (1983) Cloning structural gene sacB, which codes for exoenzyme levansucrase of *Bacillus subtilis*: expression of the gene in *Escherichia coli*. *J Bacteriol*, **153**, 1424-1431.

- Gibson, W. and Roizman, B. (1972) Proteins specified by herpes simplex virus. 8. Characterization and composition of multiple capsid forms of subtypes 1 and 2. *J Virol*, **10**, 1044-1052.
- Gillet, L., Daix, V., Donofrio, G., Wagner, M., Koszinowski, U.H., China, B., Ackermann, M., Markine-Goriaynoff, N. and Vanderplasschen, A. (2005) Development of bovine herpesvirus 4 as an expression vector using bacterial artificial chromosome cloning. *J Gen Virol*, **86**, 907-917.
- Goldstein, D.J. and Weller, S.K. (1988a) Herpes simplex virus type 1-induced ribonucleotide reductase activity is dispensable for virus growth and DNA synthesis: isolation and characterization of an ICP6 lacZ insertion mutant. *J Virol*, **62**, 196-205.
- Goldstein, D.J. and Weller, S.K. (1988b) An ICP6::lacZ insertional mutagen is used to demonstrate that the UL52 gene of herpes simplex virus type 1 is required for virus growth and DNA synthesis. *J Virol*, **62**, 2970-2977.
- Gordon, C. (2002) The intracellular localization of the proteasome. *Curr Top Microbiol Immunol*, **268**, 175-184.
- Grant, S.G., Jessee, J., Bloom, F.R. and Hanahan, D. (1990) Differential plasmid rescue from transgenic mouse DNAs into Escherichia coli methylation-restriction mutants. *Proc Natl Acad Sci U S A*, **87**, 4645-4649.
- Granzow, H., Klupp, B.G., Fuchs, W., Veits, J., Osterrieder, N. and Mettenleiter, T.C. (2001) Egress of alphaherpesviruses: comparative ultrastructural study. *J Virol*, **75**, 3675-3684.
- Granzow, H., Klupp, B.G. and Mettenleiter, T.C. (2005) Entry of pseudorabies virus: an immunogold-labeling study. *J Virol*, **79**, 3200-3205.
- Gray, H. (1918) *Anatomy of the Human Body*. Lea & Febiger, Philadelphia.
- Gray, W.L. and Mahalingam, R. (2005) A cosmid-based system for inserting mutations and foreign genes into the simian varicella virus genome. *J Virol Methods*, **130**, 89-94.
- Gross, S.T., Harley, C.A. and Wilson, D.W. (2003) The cytoplasmic tail of Herpes simplex virus glycoprotein H binds to the tegument protein VP16 in vitro and in vivo. *Virology*, **317**, 1-12.
- Grünewald, K., Desai, P., Winkler, D.C., Heymann, J.B., Belnap, D.M., Baumeister, W. and Steven, A.C. (2003) Three-dimensional structure of herpes simplex virus from cryo-electron tomography. *Science*, **302**, 1396-1398.
- Hardwicke, M.A. and Schaffer, P.A. (1995) Cloning and characterization of herpes simplex virus type 1 oriL: comparison of replication and protein-DNA complex formation by oriL and oriS. *J Virol*, **69**, 1377-1388.
- Harland, J. and Brown, S.M. (1998) HSV Growth, Preparation, and Assay. In Brown, S.M. and MacLean, A.R. (eds.), *Herpes Simplex Virus Protocols*. Humana Press Inc., Totowa, New Jersey, pp. 7-8.
- Heim, R., Prasher, D.C. and Tsien, R.Y. (1994) Wavelength mutations and posttranslational autooxidation of green fluorescent protein. *Proc Natl Acad Sci U S A*, **91**, 12501-12504.
- Heim, R. and Tsien, R.Y. (1996) Engineering green fluorescent protein for improved brightness, longer wavelengths and fluorescence resonance energy transfer. *Curr Biol*, **6**, 178-182.
- Hellenbrand, W., Thierfelder, W., Muller-Pebody, B., Hamouda, O. and Breuer, T. (2005) Seroprevalence of herpes simplex virus type 1 (HSV-1) and type 2 (HSV-2) in former East and West Germany, 1997-1998. *Eur J Clin Microbiol Infect Dis*, **24**, 131-135.
- Hirt, B. (1967) Selective extraction of polyoma DNA from infected mouse cell cultures. *J Mol Biol*, **26**, 365-369.

- Hodge, P.D. and Stow, N.D. (2001) Effects of mutations within the herpes simplex virus type 1 DNA encapsidation signal on packaging efficiency. *J Virol*, **75**, 8977-8986.
- Hohn, B., Koukolikova-Nicola, Z., Lindenmaier, W. and Collins, J. (1988) Cosmids. *Biotechnology*, **10**, 113-127.
- Horsburgh, B.C., Hubinette, M.M., Qiang, D., MacDonald, M.L. and Tufaro, F. (1999) Allele replacement: an application that permits rapid manipulation of herpes simplex virus type 1 genomes. *Gene Ther*, **6**, 922-930.
- Hutchinson, I., Whiteley, A., Browne, H. and Elliott, G. (2002) Sequential localization of two herpes simplex virus tegument proteins to punctate nuclear dots adjacent to ICP0 domains. *J Virol*, **76**, 10365-10373.
- Jackson, S.A. and DeLuca, N.A. (2003) Relationship of herpes simplex virus genome configuration to productive and persistent infections. *Proc Natl Acad Sci U S A*, **100**, 7871-7876.
- Kamen, D.E., Gross, S.T., Girvin, M.E. and Wilson, D.W. (2005) Structural basis for the physiological temperature dependence of the association of VP16 with the cytoplasmic tail of herpes simplex virus glycoprotein H. *J Virol*, **79**, 6134-6141.
- Kanda, T., Yajima, M., Ahsan, N., Tanaka, M. and Takada, K. (2004) Production of high-titer Epstein-Barr virus recombinants derived from Akata cells by using a bacterial artificial chromosome system. *J Virol*, **78**, 7004-7015.
- Kemble, G., Duke, G., Winter, R. and Spaete, R. (1996) Defined large-scale alterations of the human cytomegalovirus genome constructed by cotransfection of overlapping cosmids. *J Virol*, **70**, 2044-2048.
- Klupp, B.G., Hengartner, C.J., Mettenleiter, T.C. and Enquist, L.W. (2004) Complete, annotated sequence of the pseudorabies virus genome. *J Virol*, **78**, 424-440.
- La Boissiere, S., Izeta, A., Malcomber, S. and O'Hare, P. (2004) Compartmentalization of VP16 in cells infected with recombinant herpes simplex virus expressing VP16-green fluorescent protein fusion proteins. *J Virol*, **78**, 8002-8014.
- La Scola, B., Audic, S., Robert, C., Jungang, L., de Lamballerie, X., Drancourt, M., Birtles, R., Claverie, J.M. and Raoult, D. (2003) A giant virus in amoebae. *Science*, **299**, 2033.
- Laemmli, U.K. (1970) Cleavage of structural proteins during the assembly of the head of bacteriophage T4. *Nature*, **227**, 680-685.
- Lavail, J.H., Tauscher, A.N., Hicks, J.W., Harrabi, O., Melroe, G.T. and Knipe, D.M. (2005) Genetic and molecular in vivo analysis of herpes simplex virus assembly in murine visual system neurons. *J Virol*, **79**, 11142-11150.
- Lee, E.C., Yu, D., Martinez de Velasco, J., Tessarollo, L., Swing, D.A., Court, D.L., Jenkins, N.A. and Copeland, N.G. (2001) A highly efficient Escherichia coli-based chromosome engineering system adapted for recombinogenic targeting and subcloning of BAC DNA. *Genomics*, **73**, 56-65.
- Leuzinger, H., Ziegler, U., Schraner, E.M., Fraefel, C., Glauser, D.L., Heid, I., Ackermann, M., Mueller, M. and Wild, P. (2005) Herpes simplex virus 1 envelopment follows two diverse pathways. *J Virol*, **79**, 13047-13059.
- Liang, L. and Baines, J.D. (2005) Identification of an essential domain in the herpes simplex virus 1 UL34 protein that is necessary and sufficient to interact with UL31 protein. *J Virol*, **79**, 3797-3806.

- Liang, L., Tanaka, M., Kawaguchi, Y. and Baines, J.D. (2004) Cell lines that support replication of a novel herpes simplex virus 1 UL31 deletion mutant can properly target UL34 protein to the nuclear rim in the absence of UL31. *Virology*, **329**, 68-76.
- Luby-Phelps, K. (2000) Cytoarchitecture and physical properties of cytoplasm: volume, viscosity, diffusion, intracellular surface area. *Int Rev Cytol*, **192**, 189-221.
- Luxton, G.W., Haverlock, S., Coller, K.E., Antinone, S.E., Pincetic, A. and Smith, G.A. (2005) Targeting of herpesvirus capsid transport in axons is coupled to association with specific sets of tegument proteins. *Proc Natl Acad Sci U S A*, **102**, 5832-5837.
- Mabit, H., Nakano, M.Y., Prank, U., Saam, B., Döhner, K., Sodeik, B. and Greber, U.F. (2002) Intact microtubules support adenovirus and herpes simplex virus infections. *J Virol*, **76**, 9962-9971.
- Mahony, T.J., McCarthy, F.M., Gravel, J.L., West, L. and Young, P.L. (2002) Construction and manipulation of an infectious clone of the bovine herpesvirus 1 genome maintained as a bacterial artificial chromosome. *J Virol*, **76**, 6660-6668.
- Marozin, S., Prank, U. and Sodeik, B. (2004) Herpes simplex virus type 1 infection of polarized epithelial cells requires microtubules and access to receptors present at cell-cell contact sites. *J Gen Virol*, **85**, 775-786.
- McGeoch, D.J., Dalrymple, M.A., Davison, A.J., Dolan, A., Frame, M.C., McNab, D., Perry, L.J., Scott, J.E. and Taylor, P. (1988) The complete DNA sequence of the long unique region in the genome of herpes simplex virus type 1. *J Gen Virol*, **69**, 1531-1574.
- McGeoch, D.J., Dolan, A., Donald, S. and Brauer, D.H. (1986) Complete DNA sequence of the short repeat region in the genome of herpes simplex virus type 1. *Nucleic Acids Res*, **14**, 1727-1745.
- McGeoch, D.J., Dolan, A., Donald, S. and Rixon, F.J. (1985) Sequence determination and genetic content of the short unique region in the genome of herpes simplex virus type 1. *J Mol Biol*, **181**, 1-13.
- McGregor, A. and Schleiss, M.R. (2001) Molecular cloning of the guinea pig cytomegalovirus (GPCMV) genome as an infectious bacterial artificial chromosome (BAC) in *Escherichia coli*. *Mol Genet Metab*, **72**, 15-26.
- McNab, A.R., Desai, P., Person, S., Roof, L.L., Thomsen, D.R., Newcomb, W.W., Brown, J.C. and Homa, F.L. (1998) The product of the herpes simplex virus type 1 UL25 gene is required for encapsidation but not for cleavage of replicated viral DNA. *J Virol*, **72**, 1060-1070.
- McNabb, D.S. and Courtney, R.J. (1992) Identification and characterization of the herpes simplex virus type 1 virion protein encoded by the UL35 open reading frame. *J Virol*, **66**, 2653-2663.
- Melancon, J.M., Luna, R.E., Foster, T.P. and Kousoulas, K.G. (2005) Herpes simplex virus type 1 gK is required for gB-mediated virus-induced cell fusion, while neither gB and gK nor gB and UL20p function redundantly in virion de-envelopment. *J Virol*, **79**, 299-313.
- Meseda, C.A., Schmeisser, F., Pedersen, R., Woerner, A. and Weir, J.P. (2004) DNA immunization with a herpes simplex virus 2 bacterial artificial chromosome. *Virology*, **318**, 420-428.
- Messerle, M., Crnkovic, I., Hammerschmidt, W., Ziegler, H. and Koszinowski, U.H. (1997) Cloning and mutagenesis of a herpesvirus genome as an infectious bacterial artificial chromosome. *Proc Natl Acad Sci U S A*, **94**, 14759-14763.
- Mettenleiter, T.C. (2002) Herpesvirus assembly and egress. *J Virol*, **76**, 1537-1547.
- Mettenleiter, T.C. (2004) Budding events in herpesvirus morphogenesis. *Virus Res*, **106**, 167-180.

- Mettenleiter, T.C. and Minson, T. (2006) Egress of alphaherpesviruses. *J Virol*, **80**, 1610-1611; author reply 1611-1612.
- Milne, R.S., Nicola, A.V., Whitbeck, J.C., Eisenberg, R.J. and Cohen, G.H. (2005) Glycoprotein D receptor-dependent, low-pH-independent endocytic entry of herpes simplex virus type 1. *J Virol*, **79**, 6655-6663.
- Miranda-Saksena, M., Boadle, R.A., Armati, P. and Cunningham, A.L. (2002) In rat dorsal root ganglion neurons, herpes simplex virus type 1 tegument forms in the cytoplasm of the cell body. *J Virol*, **76**, 9934-9951.
- Mocarski, E.S., Post, L.E. and Roizman, B. (1980) Molecular engineering of the herpes simplex virus genome: insertion of a second L-S junction into the genome causes additional genome inversions. *Cell*, **22**, 243-255.
- Mocarski, E.S. and Roizman, B. (1982) Herpesvirus-dependent amplification and inversion of cell-associated viral thymidine kinase gene flanked by viral α sequences and linked to an origin of viral DNA replication. *Proc Natl Acad Sci U S A*, **79**, 5626-5630.
- Mohr, I. (2004) Neutralizing innate host defenses to control viral translation in HSV-1 infected cells. *Int Rev Immunol*, **23**, 199-220.
- Mülhardt, C. (2002) *Der Experimentator: Molekularbiologie/Genomics, 3. Auflage*. Spektrum Akademischer Verlag, Heidelberg, Berlin.
- Müller, H.J. (2001) *PCR - Polymerase Kettenreaktion*. Spektrum Akademischer Verlag, Heidelberg, Berlin.
- Muyrers, J.P., Zhang, Y., Benes, V., Testa, G., Ansorge, W. and Stewart, A.F. (2000) Point mutation of bacterial artificial chromosomes by ET recombination. *EMBO Rep*, **1**, 239-243.
- Muyrers, J.P., Zhang, Y., Testa, G. and Stewart, A.F. (1999) Rapid modification of bacterial artificial chromosomes by ET- recombination. *Nucleic Acids Res*, **27**, 1555-1557.
- Nagaike, K., Mori, Y., Gomi, Y., Yoshii, H., Takahashi, M., Wagner, M., Koszinowski, U. and Yamanishi, K. (2004) Cloning of the varicella-zoster virus genome as an infectious bacterial artificial chromosome in *Escherichia coli*. *Vaccine*, **22**, 4069-4074.
- Naldinho-Souto, R., Browne, H. and Minson, T. (2006) Herpes simplex virus tegument protein VP16 is a component of primary enveloped virions. *J Virol*, **80**, 2582-2584.
- Newcomb, W.W. and Brown, J.C. (1994) Induced extrusion of DNA from the capsid of herpes simplex virus type 1. *J Virol*, **68**, 433-440.
- Newcomb, W.W., Juhas, R.M., Thomsen, D.R., Homa, F.L., Burch, A.D., Weller, S.K. and Brown, J.C. (2001) The UL6 gene product forms the portal for entry of DNA into the herpes simplex virus capsid. *J Virol*, **75**, 10923-10932.
- Newcomb, W.W., Thomsen, D.R., Homa, F.L. and Brown, J.C. (2003) Assembly of the herpes simplex virus capsid: identification of soluble scaffold-portal complexes and their role in formation of portal-containing capsids. *J Virol*, **77**, 9862-9871.
- Nicola, A.V., Hou, J., Major, E.O. and Straus, S.E. (2005) Herpes simplex virus type 1 enters human epidermal keratinocytes, but not neurons, via a pH-dependent endocytic pathway. *J Virol*, **79**, 7609-7616.
- Nicola, A.V., McEvoy, A.M. and Straus, S.E. (2003) Roles for endocytosis and low pH in herpes simplex virus entry into HeLa and Chinese hamster ovary cells. *J Virol*, **77**, 5324-5332.
- Nicola, A.V. and Straus, S.E. (2004) Cellular and viral requirements for rapid endocytic entry of herpes simplex virus. *J Virol*, **78**, 7508-7517.

- O'Connor, M., Peifer, M. and Bender, W. (1989) Construction of large DNA segments in *Escherichia coli*. *Science*, **244**, 1307-1312.
- Ogasawara, M., Suzutani, T., Yoshida, I. and Azuma, M. (2001) Role of the UL25 gene product in packaging DNA into the herpes simplex virus capsid: location of UL25 product in the capsid and demonstration that it binds DNA. *J Virol*, **75**, 1427-1436.
- Ojala, P.M., Sodeik, B., Ebersold, M.W., Kutay, U. and Helenius, A. (2000) Herpes simplex virus type 1 entry into host cells: reconstitution of capsid binding and uncoating at the nuclear pore complex in vitro. *Mol Cell Biol*, **20**, 4922-4931.
- Ormo, M., Cubitt, A.B., Kallio, K., Gross, L.A., Tsien, R.Y. and Remington, S.J. (1996) Crystal structure of the *Aequorea victoria* green fluorescent protein. *Science*, **273**, 1392-1395.
- Osterrieder, N., Schumacher, D., Trapp, S., Beer, M., von Einem, J. and Tischer, K. (2003) [Establishment and use of infectious bacterial artificial chromosome (BAC) DNA clones of animal herpesviruses]. *Berl Munch Tierarztl Wochenschr*, **116**, 373-380.
- Parry, C., Bell, S., Minson, T. and Browne, H. (2005) Herpes simplex virus type 1 glycoprotein H binds to alphavbeta3 integrins. *J Gen Virol*, **86**, 7-10.
- Perdue, M.L., Cohen, J.C., Kemp, M.C., Randall, C.C. and O'Callaghan, D.J. (1975) Characterization of three species of nucleocapsids of equine herpesvirus type-1 (EHV-1). *Virology*, **64**, 187-204.
- Perez, A., Li, Q.X., Perez-Romero, P., Delassus, G., Lopez, S.R., Sutter, S., McLaren, N. and Fuller, A.O. (2005) A new class of receptor for herpes simplex virus has heptad repeat motifs that are common to membrane fusion proteins. *J Virol*, **79**, 7419-7430.
- Perez-Romero, P. and Fuller, A.O. (2005) The C terminus of the B5 receptor for herpes simplex virus contains a functional region important for infection. *J Virol*, **79**, 7431-7437.
- Perry, L.J. and McGeoch, D.J. (1988) The DNA sequences of the long repeat region and adjoining parts of the long unique region in the genome of herpes simplex virus type 1. *J Gen Virol*, **69** (Pt 11), 2831-2846.
- Pfister, K.K., Fisher, E.M., Gibbons, I.R., Hays, T.S., Holzbaur, E.L., McIntosh, J.R., Porter, M.E., Schroer, T.A., Vaughan, K.T., Witman, G.B., King, S.M. and Vallee, R.B. (2005) Cytoplasmic dynein nomenclature. *J Cell Biol*, **171**, 411-413.
- Phelan, A., Dunlop, J., Patel, A.H., Stow, N.D. and Clements, J.B. (1997) Nuclear sites of herpes simplex virus type 1 DNA replication and transcription colocalize at early times postinfection and are largely distinct from RNA processing factors. *J Virol*, **71**, 1124-1132.
- Posfai, G., Koob, M.D., Kirkpatrick, H.A. and Blattner, F.R. (1997) Versatile insertion plasmids for targeted genome manipulations in bacteria: isolation, deletion, and rescue of the pathogenicity island LEE of the *Escherichia coli* O157:H7 genome. *J Bacteriol*, **179**, 4426-4428.
- Post, L.E. and Roizman, B. (1981) A generalized technique for deletion of specific genes in large genomes: alpha gene 22 of herpes simplex virus 1 is not essential for growth. *Cell*, **25**, 227-232.
- Potel, C., Kaelin, K., Gautier, I., Lebon, P., Coppey, J. and Rozenberg, F. (2002) Incorporation of green fluorescent protein into the essential envelope glycoprotein B of herpes simplex virus type 1. *J Virol Methods*, **105**, 13-23.
- Prasher, D.C., Eckenrode, V.K., Ward, W.W., Prendergast, F.G. and Cormier, M.J. (1992) Primary structure of the *Aequorea victoria* green-fluorescent protein. *Gene*, **111**, 229-233.

- Preston, C.M. (2000) Repression of viral transcription during herpes simplex virus latency. *J Gen Virol*, **81**, 1-19.
- Rajcani, J., Andrea, V. and Ingeborg, R. (2004) Peculiarities of herpes simplex virus (HSV) transcription: an overview. *Virus Genes*, **28**, 293-310.
- Raoult, D., Audic, S., Robert, C., Abergel, C., Renesto, P., Ogata, H., La Scola, B., Suzan, M. and Claverie, J.M. (2004) The 1.2-megabase genome sequence of Mimivirus. *Science*, **306**, 1344-1350.
- Reuven, N.B., Staire, A.E., Myers, R.S. and Weller, S.K. (2003) The herpes simplex virus type 1 alkaline nuclease and single-stranded DNA binding protein mediate strand exchange in vitro. *J Virol*, **77**, 7425-7433.
- Reynolds, A.E., Ryckman, B.J., Baines, J.D., Zhou, Y., Liang, L. and Roller, R.J. (2001) U(L)31 and U(L)34 proteins of herpes simplex virus type 1 form a complex that accumulates at the nuclear rim and is required for envelopment of nucleocapsids. *J Virol*, **75**, 8803-8817.
- Roizman, B. and Knipe, D.M. (2001) Herpes simplex viruses and their replication. In Fields, B.N., Knipe, D.M., Howley, P.M. and al., e. (eds.), *Fundamental Virology, 4th edition*. Lippincott-Raven Publishers, Philadelphia, pp. 2399-2459.
- Rudolph, J., O'Callaghan, D.J. and Osterrieder, N. (2002) Cloning of the genomes of equine herpesvirus type 1 (EHV-1) strains KyA and raL11 as bacterial artificial chromosomes (BAC). *J Vet Med B Infect Dis Vet Public Health*, **49**, 31-36.
- Saeki, Y., Ichikawa, T., Saeki, A., Chiocca, E.A., Tobler, K., Ackermann, M., Breakefield, X.O. and Fraefel, C. (1998) Herpes simplex virus type 1 DNA amplified as bacterial artificial chromosome in *Escherichia coli*: rescue of replication-competent virus progeny and packaging of amplicon vectors. *Hum Gene Ther*, **9**, 2787-2794.
- Saksena, M.M., Wakisaka, H., Tijono, B., Boadle, R.A., Rixon, F., Takahashi, H. and Cunningham, A.L. (2006) Herpes simplex virus type 1 accumulation, envelopment, and exit in growth cones and varicosities in mid-distal regions of axons. *J Virol*, **80**, 3592-3606.
- Schildgen, O., Graper, S., Blumel, J. and Matz, B. (2005) Genome replication and progeny virion production of herpes simplex virus type 1 mutants with temperature-sensitive lesions in the origin-binding protein. *J Virol*, **79**, 7273-7278.
- Schrag, J.D., Prasad, B.V., Rixon, F.J. and Chiu, W. (1989) Three-dimensional structure of the HSV1 nucleocapsid. *Cell*, **56**, 651-660.
- Schumacher, D., Tischer, B.K., Fuchs, W. and Osterrieder, N. (2000) Reconstitution of Marek's disease virus serotype 1 (MDV-1) from DNA cloned as a bacterial artificial chromosome and characterization of a glycoprotein B-negative MDV-1 mutant. *J Virol*, **74**, 11088-11098.
- Schumperli, D., Howard, B.H. and Rosenberg, M. (1982) Efficient expression of *Escherichia coli* galactokinase gene in mammalian cells. *Proc Natl Acad Sci U S A*, **79**, 257-261.
- Shahin, V., Hafezi, W., Oberleithner, H., Ludwig, Y., Windoffer, B., Schillers, H. and Kuhn, J.E. (2006) The genome of HSV-1 translocates through the nuclear pore as a condensed rod-like structure. *J Cell Sci*, **119**, 23-30.
- Singer, G.P., Newcomb, W.W., Thomsen, D.R., Homa, F.L. and Brown, J.C. (2005) Identification of a region in the herpes simplex virus scaffolding protein required for interaction with the portal. *J Virol*, **79**, 132-139.
- Smith, G.A. and Enquist, L.W. (1999) Construction and transposon mutagenesis in *Escherichia coli* of a full-length infectious clone of pseudorabies virus, an alphaherpesvirus. *J Virol*, **73**, 6405-6414.

- Smith, G.A. and Enquist, L.W. (2000) A self-recombining bacterial artificial chromosome and its application for analysis of herpesvirus pathogenesis. *Proc Natl Acad Sci U S A*, **97**, 4873-4878.
- Smith, G.A. and Enquist, L.W. (2002) Break ins and break outs: viral interactions with the cytoskeleton of Mammalian cells. *Annu Rev Cell Dev Biol*, **18**, 135-161.
- Smith, G.A., Gross, S.P. and Enquist, L.W. (2001) Herpesviruses use bidirectional fast-axonal transport to spread in sensory neurons. *Proc Natl Acad Sci U S A*, **98**, 3466-3470.
- Smith, K.O. (1964) Relationship between the Envelope and the Infectivity of Herpes Simplex Virus. *Proc Soc Exp Biol Med*, **115**, 814-816.
- Sodeik, B. (2000) Mechanisms of viral transport in the cytoplasm. *Trends Microbiol*, **8**, 465-472.
- Sodeik, B. (2002) Unchain my heart, baby let me go--the entry and intracellular transport of HIV. *J Cell Biol*, **159**, 393-395.
- Sodeik, B., Ebersold, M.W. and Helenius, A. (1997) Microtubule-mediated transport of incoming herpes simplex virus 1 capsids to the nucleus. *J Cell Biol*, **136**, 1007-1021.
- Spear, P.G. (2004) Herpes simplex virus: receptors and ligands for cell entry. *Cell Microbiol*, **6**, 401-410.
- Spear, P.G., Eisenberg, R.J. and Cohen, G.H. (2000) Three classes of cell surface receptors for alphaherpesvirus entry. *Virology*, **275**, 1-8.
- Spear, P.G. and Longnecker, R. (2003) Herpesvirus entry: an update. *J Virol*, **77**, 10179-10185.
- Stavropoulos, T.A. and Strathdee, C.A. (1998) An enhanced packaging system for helper-dependent herpes simplex virus vectors. *J Virol*, **72**, 7137-7143.
- Stow, N.D. (2001) Packaging of genomic and amplicon DNA by the herpes simplex virus type 1 UL25-null mutant KUL25NS. *J Virol*, **75**, 10755-10765.
- Stow, N.D., Subak-Sharpe, J.H. and Wilkie, N.M. (1978) Physical mapping of herpes simplex virus type 1 mutations by marker rescue. *J Virol*, **28**, 182-192.
- Strang, B.L. and Stow, N.D. (2005) Circularization of the herpes simplex virus type 1 genome upon lytic infection. *J Virol*, **79**, 12487-12494.
- Strive, T., Borst, E., Messerle, M. and Radsak, K. (2002) Proteolytic processing of human cytomegalovirus glycoprotein B is dispensable for viral growth in culture. *J Virol*, **76**, 1252-1264.
- Strive, T., Hardy, C.M., French, N., Wright, J.D., Nagaraja, N. and Reubel, G.H. (2005) Development of canine herpesvirus based antifertility vaccines for foxes using bacterial artificial chromosomes. *Vaccine*.
- Suter, M., Lew, A.M., Grob, P., Adema, G.J., Ackermann, M., Shortman, K. and Fraefel, C. (1999) BAC-VAC, a novel generation of (DNA) vaccines: A bacterial artificial chromosome (BAC) containing a replication-competent, packaging- defective virus genome induces protective immunity against herpes simplex virus 1. *Proc Natl Acad Sci U S A*, **96**, 12697-12702.
- Tanaka, M., Kagawa, H., Yamanashi, Y., Sata, T. and Kawaguchi, Y. (2003) Construction of an excisable bacterial artificial chromosome containing a full-length infectious clone of herpes simplex virus type 1: viruses reconstituted from the clone exhibit wild-type properties in vitro and in vivo. *J Virol*, **77**, 1382-1391.

- Tischer, B.K., von Einem, J., Kaufer, B. and Osterrieder, N. (2006) Two-step red-mediated recombination for versatile high-efficiency markerless DNA manipulation in *Escherichia coli*. *Biotechniques*, **40**, 191-197.
- Trapp, S., Osterrieder, N., Keil, G.M. and Beer, M. (2003) Mutagenesis of a bovine herpesvirus type 1 genome cloned as an infectious bacterial artificial chromosome: analysis of glycoprotein E and G double deletion mutants. *J Gen Virol*, **84**, 301-306.
- Trus, B.L., Booy, F.P., Newcomb, W.W., Brown, J.C., Homa, F.L., Thomsen, D.R. and Steven, A.C. (1996) The herpes simplex virus procapsid: structure, conformational changes upon maturation, and roles of the triplex proteins VP19c and VP23 in assembly. *J Mol Biol*, **263**, 447-462.
- Trus, B.L., Cheng, N., Newcomb, W.W., Homa, F.L., Brown, J.C. and Steven, A.C. (2004) Structure and polymorphism of the UL6 portal protein of herpes simplex virus type 1. *J Virol*, **78**, 12668-12671.
- Turcotte, S., Letellier, J. and Lippe, R. (2005) Herpes simplex virus type 1 capsids transit by the trans-Golgi network, where viral glycoproteins accumulate independently of capsid egress. *J Virol*, **79**, 8847-8860.
- Vittone, V., Diefenbach, E., Triffett, D., Douglas, M.W., Cunningham, A.L. and Diefenbach, R.J. (2005) Determination of interactions between tegument proteins of herpes simplex virus type 1. *J Virol*, **79**, 9566-9571.
- Vrabec, J.T. and Alford, R.L. (2004) Quantitative analysis of herpes simplex virus in cranial nerve ganglia. *J Neurovirol*, **10**, 216-222.
- Wadsworth, S., Jacob, R.J. and Roizman, B. (1975) Anatomy of herpes simplex virus DNA. II. Size, composition, and arrangement of inverted terminal repetitions. *J Virol*, **15**, 1487-1497.
- Wagner, M., Jonjic, S., Koszinowski, U.H. and Messerle, M. (1999) Systematic excision of vector sequences from the BAC-cloned herpesvirus genome during virus reconstitution. *J Virol*, **73**, 7056-7060.
- Wagner, M. and Koszinowski, U. (2004) Mutagenesis of Viral BACs With Linear PCR Fragments (ET Recombination). In Zhao, S. and Stodolsky, M. (eds.), *Methods in Molecular Biology, vol. 256: Bacterial Artificial Chromosomes, Volume 2: Functional Studies*. Humana Press, Totowa, NJ, USA, pp. 257-268.
- Wagner, M., Ruzsics, Z. and Koszinowski, U.H. (2002) Herpesvirus genetics has come of age. *Trends Microbiol*, **10**, 318-324.
- Wagner, M.J. and Summers, W.C. (1978) Structure of the joint region and the termini of the DNA of herpes simplex virus type 1. *J Virol*, **27**, 374-387.
- Warner, M.S., Geraghty, R.J., Martinez, W.M., Montgomery, R.I., Whitbeck, J.C., Xu, R., Eisenberg, R.J., Cohen, G.H. and Spear, P.G. (1998) A cell surface protein with herpesvirus entry activity (HvE) confers susceptibility to infection by mutants of herpes simplex virus type 1, herpes simplex virus type 2, and pseudorabies virus. *Virology*, **246**, 179-189.
- Weir, J.P. (2001) Regulation of herpes simplex virus gene expression. *Gene*, **271**, 117-130.
- Weller, S.K., Spadaro, A., Schaffer, J.E., Murray, A.W., Maxam, A.M. and Schaffer, P.A. (1985) Cloning, sequencing, and functional analysis of oriL, a herpes simplex virus type 1 origin of DNA synthesis. *Mol Cell Biol*, **5**, 930-942.
- White, C.A., Stow, N.D., Patel, A.H., Hughes, M. and Preston, V.G. (2003a) Herpes simplex virus type 1 portal protein UL6 interacts with the putative terminase subunits UL15 and UL28. *J Virol*, **77**, 6351-6358.

Literature

- White, R.E., Calderwood, M.A. and Whitehouse, A. (2003b) Generation and precise modification of a herpesvirus saimiri bacterial artificial chromosome demonstrates that the terminal repeats are required for both virus production and episomal persistence. *J Gen Virol*, **84**, 3393-3403.
- Wild, P., Engels, M., Senn, C., Tobler, K., Ziegler, U., Schraner, E.M., Loepfe, E., Ackermann, M., Mueller, M. and Walther, P. (2005) Impairment of nuclear pores in bovine herpesvirus 1-infected MDBK cells. *J Virol*, **79**, 1071-1083.
- Wildeman, A.G. (1988) Regulation of SV40 early gene expression. *Biochem Cell Biol*, **66**, 567-577.
- Wilkinson, D.E. and Weller, S.K. (2003) The role of DNA recombination in herpes simplex virus DNA replication. *IUBMB Life*, **55**, 451-458.
- Willard, M. (2002) Rapid Directional Translocations in Virus Replication. *J Virol*, **76**, 5220-5232.
- Wingfield, P.T., Stahl, S.J., Thomsen, D.R., Homa, F.L., Booy, F.P., Trus, B.L. and Steven, A.C. (1997) Hexon-only binding of VP26 reflects differences between the hexon and penton conformations of VP5, the major capsid protein of herpes simplex virus. *J Virol*, **71**, 8955-8961.
- Wittels, M. and Spear, P.G. (1991) Penetration of cells by herpes simplex virus does not require a low pH-dependent endocytic pathway. *Virus Res*, **18**, 271-290.
- Wolfstein, A., Nagel, C.H., Radtke, K., Dohner, K., Allan, V. and Sodeik, B. (2006) The inner tegument promotes Herpes Simplex Virus transport along microtubules in vitro. *Traffic*, **7**, 1-11.
- Wutzler, P. (2002) Herpesviren: Herpes-simplex-Virus Typ 1 und 2, Varicella-Zoster-Virus. In Doerr, H.W. and Gerlich, W.H. (eds.), *Medizinische Virologie - Grundlagen, Diagnostik und Therapie virologischer Krankheitsbilder*. Georg Thieme Verlag, Stuttgart, New York, pp. 373-381.
- Yao, X.D., Matecic, M. and Elias, P. (1997) Direct repeats of the herpes simplex virus a sequence promote nonconservative homologous recombination that is not dependent on XPF/ERCC4. *J Virol*, **71**, 6842-6849.
- Yu, D., Smith, G.A., Enquist, L.W. and Shenk, T. (2002) Construction of a self-excisable bacterial artificial chromosome containing the human cytomegalovirus genome and mutagenesis of the diploid TRL/IRL13 gene. *J Virol*, **76**, 2316-2328.
- Zhang, Y., Buchholz, F., Muyrers, J.P. and Stewart, A.F. (1998) A new logic for DNA engineering using recombination in *Escherichia coli*. *Nat Genet*, **20**, 123-128.
- Zhou, F.C., Zhang, Y.J., Deng, J.H., Wang, X.P., Pan, H.Y., Hettler, E. and Gao, S.J. (2002) Efficient infection by a recombinant Kaposi's sarcoma-associated herpesvirus cloned in a bacterial artificial chromosome: application for genetic analysis. *J Virol*, **76**, 6185-6196.
- Zhou, Z.H., He, J., Jakana, J., Tatman, J.D., Rixon, F.J. and Chiu, W. (1995) Assembly of VP26 in herpes simplex virus-1 inferred from structures of wild-type and recombinant capsids. *Nat Struct Biol*, **2**, 1026-1030.

Lebenslauf

Persönliche Daten

Name: Claus-Henning Friedrich Joachim Nagel
Geburtstag: 13. Februar 1977
Geburtsort: Hannover
Familienstand: ledig

Schulbildung

1983 - 1987 Grundschule in Gestorf, Stadt Springe/Deister
1987 - 1989 Orientierungsstufe Süd, Stadt Springe/Deister
1989 - 1996 Otto-Hahn-Gymnasium, Stadt Springe/Deister
Mai 1996 Abitur

Universitäre Ausbildung

Okt. 1996 Immatrikulation zum Wintersemester 1996/97 an der
 Universität Hannover im Diplom-Studiengang Biochemie

Okt. 2000-Mrz. 2001 Studienaufenthalt bei Dr. Paul Barker am MRC Centre for Protein
 Engineering, University of Cambridge, England.

Jan. 2002 Absolvierung der Diplomprüfungen in den Fächern Biochemie,
 Organische Chemie und Pharmakologie

Feb.–Aug. 2002 Anfertigung der Diplomarbeit am Institut für Biochemie, Medizinische
 Hochschule Hannover unter der Anleitung von PD Dr. Beate Sodeik.
 Thema: „Der Zelleintritt von Herpes-Simplex-Virus Typ 1 in isolierte
 Synaptosomen - die Zusammensetzung des zytosolischen Kapsids“

Dez. 2002-Apr.2006 Anfertigung einer naturwissenschaftlichen Dissertation am
 Institut für Virologie, Medizinische Hochschule Hannover
 unter der Anleitung von PD Dr. Beate Sodeik.

Apr. 2003-Dez. 2005 Gefördert im Graduiertenkolleg 745 der Deutschen Forschungsgemeinschaft
 „Mukosale Erreger-Wirt-Interaktionen“

14.07.2006 erfolgreiche Disputation

Publikationen

Originalarbeiten

Wolfstein A, **Nagel CH**, Radtke K, Döhner K, Allan V, Sodeik B (2006) The inner tegument promotes Herpes Simplex Virus transport along microtubules in vitro. *Traffic* **7** 1-11

Übersichtsartikel

Döhner K, **Nagel CH**, Sodeik B (2005) Viral stop-and-go along microtubules: taking a ride with dynein and kinesins. *Trends Microbiol* **13** 320-7

Vorträge/Poster zum Thema dieser Arbeit auf Fachtagungen

Nagel CH, Fathollahy M, Strive T, Borst E, Messerle M, Sodeik B. "Pitfalls in BAC-mutagenesis of Herpes Simplex Virus." Poster auf der *Jahrestagung der Gesellschaft für Virologie*, Hannover 2005

Nagel CH, Strive T, Fathollahy M, Borst E, Messerle M, Sodeik B. "Fluorescent capsids of herpes simplex virus obtained by BAC-mutagenesis." Vortrag beim 3. *Workshop des Arbeitskreises "Zellbiologie von Virusinfektionen" der Gesellschaft für Virologie*, Zeilitzheim 2004

Nagel CH, Strive T, Fathollahy M, Borst E, Messerle M, Sodeik B. "Mutagenesis of herpes simplex virus cloned as a bacterial artificial chromosome." Poster auf der *Jahrestagung der Gesellschaft für Virologie*, Tübingen 2004

Erklärung zur Dissertation

Hierdurch erkläre ich, dass die Dissertation

**"Fluorescence tagging of herpes simplex virus type 1 proteins
by mutagenesis of a bacterial artificial chromosome"**

selbständig verfasst und alle benutzten Hilfsmittel sowie evtl. zur Hilfeleistung herangezogene Institutionen vollständig angegeben wurden.

Die Dissertation wurde nicht schon als Diplom- oder ähnliche Prüfungsarbeit verwendet.

Hannover, den 03.05.2006

Claus-Henning Nagel